Università degli Studi di Torino
Doctoral School of Sciences and Innovative Technologies
Ph.D. Program in Pharmaceutical and Biomolecular Science

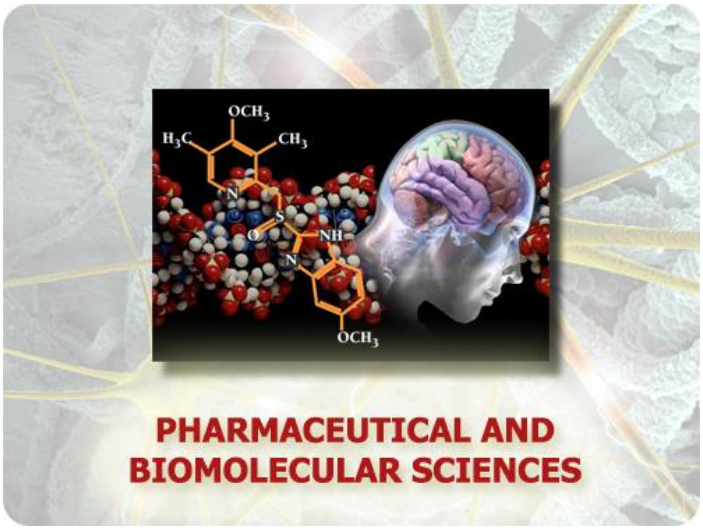

Modern analytical strategies for the study of plant raw materials and derivatives with potential biological activities

Ph.D. Candidate: **Francesca Capetti**

Supervisor: Prof. Dr. **Barbara Sgorbini**

Università degli Studi di Torino

Department of Drug Science and Technology

Ph.D. Programme in:
Pharmaceutical and Biomolecular Sciences
XXXIV Cycle

Modern analytical strategies for the study of plant raw materials and derivatives with potential biological activities

Thesis' author: **Francesca Capetti**

Supervisor**: Prof. Dr. Barbara Sgorbini**

Ph.D. Program Co-ordinator: **Prof. Dr. Roberta Cavalli**

Academic years of enrolment: **2018/19, 2019/20, 2020/21**

Code of scientific discipline: **BIO/15-Biologia Farmaceutica**

Contents

General introduction.....6

Chapter 1: Essential Oils and Analytical Strategies for their Quality Assessment 8

1.1 Introduction 8

1.2 Essential oils 9

1.2.1 Definition 9

1.2.2 Production of essential oils 9

1.3 Chemistry of essential oils and physicochemical properties of their constituents 10

1.3.1 Terpenoids 11

1.3.2 Shikimic acid derivatives 13

1.4 "Essential oil plants" 14

1.5 Quality of plant derivatives bearing essential oils 18

1.5.1 Headspace Solid-Phase Microextraction (HS-SPME) 18

1.6 Analytical strategies for the qualitative and quantitative composition of plant volatile and semi-volatile fractions and essential oils 20

1.6.1 Qualitative analysis 20

1.6.2 Quantitative analysis 21

1.6.3 Enantioselective GC 22

1.6.4 High-speed GC 22

1.7 References 23

1.8 Research projects 26

1.8.1 Adulteration of Essential Oils: A Multitask Issue for Quality Control. Three Case Studies: *Lavandula angustifolia* Mill., *Citrus limon* (L.) Osbeck and *Melaleuca alternifolia* (Maiden & Betche) Cheel 26

1.8.2 Exploiting the Versatility of Vacuum Assisted Headspace Solid-Phase Microextraction in Combination with the Selectivity of Ionic Liquids-Based GC Stationary Phases to Discriminate *Boswellia Ssp*. Resins Through Their Volatile and Semi-Volatile Fractions 45

1.8.3 A Sustainable Approach for the Reliable and Simultaneous Determination of Terpenoids and Cannabinoids in Hemp Inflorescences by Vacuum Assisted Headspace Solid-Phase Microextraction 67

2 Chapter 2: Essential Oils as Tyrosinase Inhibitors 89

2.1 Introduction 89

2.2 Tyrosinase role in melanin biosynthesis in human skin 90
2.3 Skin depigmentation agents interfering with tyrosinase activity 90
2.4 Tyrosinase inhibitors from natural products 91
2.5 The research of new bioactive compounds from plant matrices 92
2.5.1 *In vitro* assay 92
2.5.2 Fractionation 93
2.6 References 95
2.7 Research projects 97
2.7.1 Citral-Containing Essential Oils as Potential Tyrosinase Inhibitors: A Bio-Guided Fractionation Approach 97
2.7.2 Screening of 47 Essential Oils as Potential Sources of Tyrosinase Inhibitors 120
3 Chapter 3: *In vitro* Dermal Absorption Studies of Essential Oil Components 131
3.1 Introduction 131
3.2 The skin anatomy and physiology 1132
3.3 The barrier function of the skin and its permeability 134
3.4 Process of skin permeation and percutaneous absorption 134
3.5 Molecular properties influencing dermal absorption 135
3.6 How to study the percutaneous absorption of topically exposed compounds? 136
3.6.1 *In vitro* permeation studies 136
3.6.2 Experimental Equipment 137
3.6.3 *In vitro* release testing 138
3.7 Dermal absorption of essential oil constituents 138
3.8 Analytical approaches to study the dermal absorption profile of essential oils components 139
3.9 References 141
3.10 Research projects 144
3.10.1 Tea Tree (*Melaleuca Alternifolia*) Essential Oil: Evaluation of Skin Permeation and Distribution from Topical Formulations with a Solvent-Free Analytical Method 144
3.10.2 Investigation of the Dermal Absorption Profile of Tyrosinase Inhibitors Released from Topical Formulations Containing a Bioactive Mixture of Three Essential Oils: *Litsea Cubeba* (Lour.) Pers, *Pinus Mugo* Turra, *Cymbopogon Winterianus* Jowitt Ex Bor 160
Conclusions.....172
Scientific pubblications.....174
Oral contributions to congresses.....175
Poster contributions to congresses.....176

General introduction

The use of plants and their products for therapeutic, cosmetic, and nutritional purposes dates back to ancient times, and medicinal and aromatic plants (MAPs) specialised metabolites have often been the base for starting the development and optimization of pharmacologically active chemical compounds.

As embedded in the title, this doctoral thesis has been carried out following two main lines of research. The first one is the study plant derivatives as new promising active mixtures for human health. In contrast, the second one is the investigation of modern analytical strategies to assess their quality and grant their safe use in addition to comprehensively characterise the bioactive constituents and monitoring *in vitro* their interaction with the biological target.

Researching new lead compounds from raw plant materials and natural products with promising biological activities for human health is a highly challenging task. It requires different disciplines, including analytical chemistry, among others. This is because natural products differ from their pharmaceutical counterpart in that they are typically complex mixtures, with significant intrinsic variability in chemical composition even when the product is obtained from the same plant species following standardised procedures.

This thesis studies essential oils (EOs) as potential bioactive mixtures to treat hyperpigmentation disorders clinically and cosmetically. Up to date, EOs and their isolated compounds have been widely used in cosmetics, perfumes, and household products but mainly in light of their pleasant scent. A wide range of other biological activities has been ascribed to some EOs, including analgesic, antiseptic, antimicrobial, and spasmolytic properties, among others. The interest in using EOs components to treat skin-related disorders, such as hyperpigmentation, arises from the potential of EOs constituents to penetrate the skin and unfold their effect there. The distillation process (i.e., hydro or steam distillation) through which EOs are obtained implies that their constituents present low molecular weights (i.e., below 300 Daltons) and a fairly lipophilic character, both being molecular properties that favor the dermal penetration process.

Chapter 1 of this thesis describes what EOs are and highlights the possible analytical strategies for the qualitative and quantitative characterisation of EOs and the related plant material. It also reports three experimental works. The first one aims to verify different analytical approaches based on GC-MS to detect various adulterations taking *Lavandula angustifolia* Mill., *Citrus limon* (L.) Osbeck and *Melaleuca alternifolia* (Maiden & Betche) Cheel EOs as case-studies. The other two projects investigate the use of new parameters (Vacuum) in Headspace Solid-phase Microextraction (HS-SPME) to extend its application in analytical protocols that aims at defining the quality of two biologically active plant derivatives bearing EOs: *Cannabis sativa* L. inflorescences and Frankincence resins.

Chapter 2 of this manuscript describes in-depth the biochemical mechanism that leads to hyperpigmentation disorders in humans and provides two research projects to identify new skin whitening agents among EOs components. **Chapter 3** describes the theoretical aspects required to understand the dermal absorption process of exogenous compounds and the *in vitro* strategies that can be exploited to investigate the process. In addition, two research

projects are presented. The first deals with optimising a solvent-free analytical strategy based on Headspace Solid-Phase Micro-Extraction (HS-SPME) and GC-MS analysis to monitor the permeation kinetic rate, the skin layers' distribution, and the emission in the surrounding atmosphere of volatile components released from topic formulations. *Melaleuca alternifolia* (Maiden & Betche) Cheel EO (Tea tree oil) was chosen as a case study for the method optimisation due to the relevant lack of information concerning the percutaneous (dermal) absorption profile of its constituents. The second study applies the optimised analytical strategy for investigating the dermal absorption behaviour of those essential oils and their respective bioactive constituents.

1 Chapter 1:

Essential Oils and Analytical Strategies for their Quality Assessment

1.1 Introduction

The research for new led compounds from plant raw materials as well as natural products with promising biological activities for human health, irrespective of which activity it is, is an extremely challenging task that requires different disciplines, including analytical chemistry, among others. Natural products differ from their pharmaceutical counterpart (which usually operates with single compounds or a mixture of few) in that they are typically complex mixtures, with significant intrinsic variability in terms of chemical composition even when the product is obtained from the same plant species following standardised procedures. In this thesis, in parallel to the study of plant materials, and in particular of essential oils (EOs), as potential bioactive mixtures to treat skin-related disorders, modern analytical strategies to assess the quality and authenticity of EOs and the corresponding raw plant material were also investigated.

This chapter describes what EOs are and which are the analytical strategies used to characterise their chemical composition and that of the related plant material. It reports three experimental works. The first one aims at verifying different analytical approaches based on GC-MS to detect various adulterations taking *Lavandula angustifolia* Mill., *Citrus limon* (L.) Osbeck and *Melaleuca alternifolia* (Maiden & Betche) Cheel EOs as case-studies. The other two projects investigate the use of new parameters (Vacuum) in Headspace Solid-phase Microextraction (HS-SPME) to extend its application in analytical protocols that aim at defining the quality of two biologically active plant derivatives bearing EOs: *Cannabis sativa* L. inflorescences and Frankincence resins.

1.2 Essential oils

1.2.1 Definition

An essential oil (EO) is a complex mixture of volatile constituents isolated from a plant (generally from some of its parts) of known taxonomic origin by hydrodistillation, steam distillation, or dry distillation, or by a suitable mechanical process without heating [1]. The European Pharmacopoeia defines an EO as an "Odorous product, usually of complex composition, obtained from a botanically defined plant raw material by steam distillation, dry distillation, or a suitable mechanical process without heating"[2]. Similarly, an EO is defined by the International Standard Organisation (ISO), in the document ISO 9235.2 , as a "Product obtained from vegetable raw material—either by distillation with water or steam or—from the epicarp of *Citrus* fruits by a mechanical process, or—by dry distillation"[3].

An additional definition of EO was provided by Professor Dr. Gerhard Buchbauer of the Institute of Pharmaceutical Chemistry, University of Vienna. It states that "Essential oils are more or less volatile substances with more or less odorous impact, produced either by steam distillation or dry distillation or using a mechanical treatment from one single species" (25th International Symposium on Essential Oils, 1994). Altogether, these definitions highlight important characteristics of EOs: they are distillates and not extracts; they can be defined as such only if they are obtained with the suitable processes reported in the definition; finally, in the production process of an EO, it is not allowed to mix several different plant species [4].

It is important to highlight that the composition of the isolated EO, mainly when it is obtained by distillation, may vary from that of the EO present in the plant. During the distillation process, some constituents of the plant material may undergo chemical changes when in contact with steam. For example, aldehydes can be oxidized, and esters may be formed from the acids generated. The opposite reaction may occur for other compounds: esters may be hydrolysed to acids and alcohol. Some water-soluble molecules may be lost by solution in the still water, changing the chemical profile of the isolated EO [1].

Chamazulene is a clear example of thermal artefact. It is a blue bicyclic sesquiterpene, present in the steam-distilled oil of the flower heads of German chamomile, *Chamomilla recutita* (L.) Rauschert. It is the result of a complex series of chemical reactions: (i.e., dehydrogenation, dehydration, and ester hydrolysis) that lead to its formation starting from the sesquiterpene lactone matricin.

1.2.2 Production of essential oils

Only three specific isolation methods can be employed to recover EOs from specific plant materials to obtain a product compliant with the various definitions of EOs. These methods include 1) expression, 2) hydro or steam distillation, and 3) dry distillation. The latter is rarely used and will not be discussed in the following paragraphs.

1.2.2.1 Expression

Cold Expression is almost exclusive to the production of EOs from the fruit peel of different species belonging to the Rutaceae family from which the largest production of commercial EOs derives [5]. The latter include:

- *Citrus aurantium* L., bitter orange EO

- *Citrus sinensis* (L.) Osbeck, sweet orange EO
- *Citrus limon* (L.) Osbeck, bergamot EO
- *Citrus limon* (L.) Osbeck, lemon EO
- *Citrus nobilis* Lour., mandarin EO
- *Citrus paradise* Macfad, grapefruit EO

The epicarp of the fruits of these species presents lysogenic cavities containing different specialised metabolites, including volatile and semi-volatile compounds (i.e., 85–99% of the entire oil fraction) and a non-volatile residue that is mainly composed of flavonoids, coumarins, sterols, and fatty acids [6]. In the volatile fraction, hydrocarbon and derivate mono-and sesquiterpenes are the compounds most frequently reported, followed by aliphatic and olefinic C6–C12 non-terpene aldehydes, alcohols, ketones, esters, acids, along with several aromatic compounds. Hydrodistillation of *Citrus* fruit is generally not performed as it yields poor quality oils due to chemical reactions (i.e. heat and acid-initiated degradation) of some unstable fruit volatiles (i.e., mainly aliphatic aldehydes such as heptanal, octanal, nonanal) [1].

In the past and until the beginning of the twentieth century, *Citrus* EOs were obtained manually, even on an industrial scale, using the sponge method. The latter relied on squeezing by hand the peel to burst the oil glands and collecting the EO with a sponge. More sophisticated semi- industrial techniques now include the *pelatrice* process, which is based on the use of an abrasive shell against which the entire fruit is rotated, causing the bursting of the oil glands and the release of their content, and the *sfumatrice* technique, which is an automated upgrade of the sponge method. In addition, at the industrial scale *Citrus* essential oils are today obtained as a by-product of *Citrus* juice production in specific extractors that implement one of the above-mentioned techniques with the juice extraction process [5].

1.2.2.2 Steam Distillation and Hydro Distillation

Steam and hydro distillation are unquestionably the most frequently used methods for the isolation of EOs from plants [1]. The equipment employed for such sample preparation techniques is based on the circulatory distillation approach introduced by Clevenger which is reported in the European Pharmacopoeia [7]. In hydrodistillation, the plant material is placed inside a glass container (also known as still) and immersed in water. The application of a heat source allows water to boil. The plant material soaks up water during the boiling process, and EOs constituents are extracted from the plant material; they vaporise and get carried away by the stream of steam. In the condensing system, the steam and the vaporised analytes are condensed, and the different densities of EOs with respect to water allow separation and collection. In steam distillation, the only difference is that the steam is generated in a separate vessel and brought into contact with plant material through a perforated inlet to vaporise the plant's volatile molecules [5].

1.3 Chemistry of essential oils and physicochemical properties of their constituents

Plants are chemical laboratories producing countless compounds grouped into two major divisions known as primary and specialised metabolites. Primary metabolites include four subgroups: proteins, carbohydrates, nucleic acids, and lipids. These compounds are universal across the plant and animal families, and constitute the basic building blocks of

life; in other words, they are fundamental for plant life [8]. Specialised or secondary metabolites are responsible for the plant behaviour in the environment. They are biosynthesised from primary metabolites by a sequence of chemical reactions catalysed by enzymes some of which limits the pathway defining the synthesis and the amount of metabolite produced. They are non-nutritional chemical compounds exploited by the plant to establish relationships with other living organisms among and with which the plant has to live and survive. Specialised metabolites are usually classified according to their biosynthetic pathway into terpenoids, shikimates, polyketides, and alkaloids. EOs present specialised metabolites belonging to the terpenoid and shikimate classes. Irrespective of their chemical class, all EOs components share similar properties. They are fairly hydrophobic, and all have molecular weights below 300 Dalton, which grant boiling points low enough to enable their isolation from the plant materials by distillation. In other words, they are fairly volatile/ semi-volatile compounds whose degree of volatility depends on their chemistry (i.e., oxygenation, architecture of hydrocarbon backbone, saturation of carbon double bonds, etc.) [9]. They are liquid at room temperature; they are usually coloured, and their density is generally lower than that of water. They have a high refractive index, and most rotate polarised light. They are soluble in lipids and common organic solvents while very sparingly soluble in water [10].

1.3.1 Terpenoids

Terpenoids are the most abundant specialised metabolites contained in EOs. They are sometimes called "terpenes". However, this term is nowadays restricted to monoterpenoid hydrocarbons [11]. The biosynthesis of all terpenoids is dependent on the two (C_5) isoprene precursors, namely isopentenyl pyrophosphate (IPP) and dimethylallyl pyrophosphate (DMAPP), which are biosynthesized via either the methylerythritol 4-phosphate (MEP) pathway, also known as the 1-deoxy-D-xylulose5-phosphate (DXP) pathway or the mevalonate-dependent (MVA) pathway [12]. IPP and DMAPP are condensed to form the universal C10 precursors: geranylpirophosphate (GPP). The latter forms by a head-to-tail coupling mechanism of DMAPP and IPP which involves a series of reactions, including 1) ionization of DMAPP by loss of the diphosphate group to the allylic cation 2) electrophilic addition to the double bond of IPP, followed by the loss of the C2 *prorectus* proton of IPP and formation of a new *trans* (*E)* double bond.

Terpenoids are classified, according to their number of five-carbon units, as hemiterpenoids (C_5), monoterpenoids (C_{10}), sesquiterpenoids (C_{15}), diterpenoids (C_{20}), triterpenoids (C_{30}), tetraterpenoids (C_{40}), and polyterpenoids (more than 80-carbon units).

In EOs, only hemiterpenoids, monoterpenoids, sesquiterpenoids and a few diterpenoids can be found as they are compatible with the distillation process [8].

1.3.1.1 Monoterpenoid

Monoterpenes are the most representative terpenoids in EOs, encompassing over 40 000 defined structures [9]. In the following paragraphs, the limited number of monoterpenes scaffolds that gives rise to such outstanding structural diversity will be briefly described, together with the biosynthesis of some representative monoterpenes common to several EOs. Natural product molecules are always biosynthesized by reactions catalysed by enzymes and the enzymes present in any given plant will determine the terpenoids it will

produce [13]. For simplicity, in the following paragraphs, these reactions will be described in chemical terms only.

The precursor of all monoterpenoids is geranyldiphoshate (GPP), along with its isomers linalyl diphosphate (LPP) and neryl diphosphate (NPP). LPP and NPP are likely to be formed from GPP by its ionization to the allylic cation, which can thus allow a change in the attachment of the diphosphate group (to the tertiary carbon in LPP) or a change in stereochemistry at the double bond (to *Z* in NPP) [14]. These three precursors give rise to a wide range of linear monoterpenes, including hydrocarbons, alcohols, aldehydes, and esters, especially acetates. For example, the monoterpene primary alcohol **geraniol** (from which the aldehyde **geranial** is formed by dehydrogenation and oxidation) derives from GPP ionisation to the geranyl carbocation followed by its discharge by the addition of a water molecule. By the same chemical reactions, **nerol** (and eventually the corresponding aldehyde **neral**) is formed from NPP. The hydrocarbon monoterpene **β-myrcene** and the monoterpenoid tertiary alcohol **linalool** derive from the linalyl carbocation through its discharge via the loss of a proton and via the addition of a water molecule, respectively. Its acetate (i.e., **linalyl acetate**) is also frequently encountered.

NPP and LPP are thought to be precursors of the cyclic menthyl / α-terpinyl carbocation, which is formed by an intramolecular electrophilic addition reaction.

The menthyl / α-terpinyl carbocation gives rise to a wide range of mono and bicyclic monoterpenoids. When the menthyl cation is quenched by the attack of water, the alcohol **α-terpineol** is formed. Alternatively, it could lose a proton forming the cyclic monoterpene hydrocarbon **limonene,** which is the precursor of ***trans*-carveol** and ***trans*-isopiperitenol** (which in turn is the precursor of **menthol)** [13]**.** The menthyl cation can be converted into the terpinen-4-yl cation by a hydride shift allowing the formation of **α-terpinene**, **γ-terpinene**, and the **α-terpineol** isomer, **terpinen-4-ol**. A further cyclization reaction on the terpinen-4-yl cation generates the thujane skeleton, from which **sabinene** and **thujone** derive. Turning back to the menthyl / α-terpinyl cation, by folding its cationic side-chain towards the double bond, two bicyclic cations can form the bicyclic bornyl and pinyl cations. **Borneo**l would result from quenching of the bornyl cation with water, and then its oxidation could generate the ketone **camphor**. **α-Pinene** and **β-pinene** are formed by the loss of different protons from the pinyl cation. Finally, the menthyl cation, may be converted by a 1,3-hydride shift into a favourable resonance stabilized allylic cation, which allows the formation of **α-** and **β-phellandrene** by loss of a proton from the phellandryl carbocation.

***p*-Cymene**, **thymol,** and **carvacrol** are representatives of a small group of aromatic compounds produced from isoprene units rather than by the much more common routes to aromatics involving acetate or shikimate. Therefore they belong to the terpenoid class, regardless of their aromatic ring [13].

1.3.1.2 Sesquiterpenoids

The fundamental precursor of linear and cyclic sesquiterpene/sesquiterpenoids is farnesyl diphosphate (*E*-*E*-FPP) which presents a C15 structure containing three double bonds. The latter is formed by a head-to-tail coupling mechanism of geranyl diphosphate and IPP. Similarly, to geranyl pyrophosphate, in addition to *E*,*E*-FPP, also its geometric isomer *E*,*Z*-FPP occurs in nature as well as the tertiary diphosphate nerolidyl PP.

Because of the increased chain length and an additional double bond, the number of possible cyclization modes is also increased, and several mono-, bi-, and tri-cyclic structures can result. From *E,Z*-FPP, monocyclic, six-membered ring sesquiternes, and sesquiterpenoids with the bisabolane skeleton can form (i.e., **γ-bisabolene**, **β-bisabolene**, **bisabolol,** and **zingiberene**). Alternatively, other cyclization reactions occurring in *E,Z*-FPP and *E,E*-FPP lead to larger ring systems, including seven-, ten-, and 11-membered ring structures. The two ten-membered ring systems include germacryl (which is the precursor of **valeranone,** a common sesquiterpenoids in *Valeriana officinalis* EO) and *cis*-germacryl (i.e., the precursor of **cadinol** and **muurulene**) cations which form from *E,E*-FPP and *E,Z*-PP respectively. The two 11-membered systems include humulyl (i.e., the precursor of **humulene**) and *cis*-humulyl cations (i.e, the precursor of ***trans*-β-caryophyllene**), which similarly to germacryl ans *cis*-germacryl cations, differ only in the stereochemistry associated with the double bonds [13,14].

1.3.1.3 Diterpenoids

The precursor of diterpenes and diterpenoids is geranylgeranyl diphosphate (GGPP), which again is formed by adding another IPP molecule to FPP. Compared to mono and sesquiterpes/terpenoids, their presence in EOs is much less common. However, there are examples of EOs containing diterpenes/diterpenoid, such as *Rosmarinus officinalis* EO which presents **carnosol** and **carnosic acid**, and Frankincence resin EOs which contain cembrane derivatives including **serratol**, **incensole,** and **incensole acetate.**

1.3.2 Shikimic acid derivatives

Shikimic acid is an important precursor of several EOs constituents, including benzoic acid and cinnamic acid derivatives.

Shikimic acid biosynthesis starts from the carbohydrate pathway by the coupling (i.e., aldol-type condensation) of phosphoenolpyruvate (PEP) and D-erythrose 4-phosphate. Its derivatives can usually be recognized by the characteristic shikimate scaffold of a six-membered ring with either a one- or three-carbon substituent on position one and oxygenation in the third, and/or fourth, and/or fifth positions [13].

Aromatization of shikimic acid gives benzoic acid, whose derivatives can be found in different EOs. The latter include methyl benzoate, benzyl alcohol, benzaldehyde, and their derivatives. Methyl benzoate is found in ylang ylang EO, among others. Benzyl alcohol occurs in muguet, jasmine, and narcissus, and its acetate is the major component of jasmine oils, while sources of benzaldehyde include cassia and cinnamon EOs. Salicylic acid (i.e., *o*-hydroxybenzoic) forms by hydroxylation of benzoic acid, and together with its esters, it is widely distributed in nature. For instance, methyl salicylate is the major component (about 90% of the volatiles) of wintergreen. Similarly, amination of benzoic acid leads to *o*-aminobenzoic acid, which is known as anthranilic acid and whose methyl ester has a potent odour and is found in such oils as genet and bitter orange flower.

Other examples of shikimate derivatives common to some EOs are indole and 2-phenylethanol. Indole usually occurs in jasmine at a level of about 3–5%, and it significantly contributes to the EO aroma, while 2-phenylethanol accounts for one-third to three-quarters of rose oil.

The typical C6-C3 phenylpropionic acid structure of cinnamic acid derives from the combination of shikimic acid with a second PEP molecule via an addition-elimination reaction. Cinnamic acid derivatives include cinnamaldehyde, cinnamyl alcohol and its esters, estragole, anethole, and eugenol, among others. Estragole (also known as methylchavicol) and anethole form by oxygenation in the *p*-position of cinnamic acid (i.e., *p*-coumaric acid) followed by methylation of the phenol and reduction of the acid to alcohol with subsequent elimination of the alcohol. Estragole is found in a variety of EOs, mostly herb oils such as basil, fennel, clary sage, anise, and rosemary. Anethole occurs in both the *(E)*- and *(Z)*-forms and it is found in spices and herbs such as anise, fennel, lemon balm, coriander, and basil and also in flower EOs such as ylang ylang and lavender. Eugenol derives from the reduction of the side chain of ferulic acid (which in turn is formed by the hydroxilation of the *p*-coumaric acid followed by the methylation of the hydroxyl group in *meta* position) It is found in spices such as clove, cinnamon, and herbs such as bay and basil, and in flower EOs including rose, jasmine, and carnation. Isoeugenol is found in basil, cassia, clove, nutmeg, and ylang ylang. The methyl ether of eugenol, methyleugenol is also widespread in EOs, creating difficulties for the EO business due to toxicological safety issues [13].

1.4 "Essential oil plants"

All plants may biosynthesise volatile specialised metabolites that may be responsible for three main physiological processes, namely plant-plant interaction, the signalling between symbiotic organisms, and the attraction of pollinating insects [9]. However, "essential oil plants" are those species producing mixtures of volatiles of commercial interest. On a worldwide scale, the number of plant species accounts for around 300,000, of which 10% could be used as sources of essential oil [11].

"Essential oils plants" biosynthesise and accumulate volatiles in specific anatomical structures, including secretory idioblasts (i.e., secretory cells), cavities or ducts, and glandular trichomes. Secretory idioblasts are individual cells producing a mixture of volatile specialised metabolites in large quantities and retaining the product within the cell. These cells are typical in many flowers, for example, *Rosa sp*., *Viola sp*., or *Jasminum sp*. Cavities and ducts are extracellular spaces formed by two possible processes: schizogeny, where localized cell separation creates spaces, and lysogeny, where cells die to create intercellular spaces. In both cases, the peripheral epithelial cells are highly active in synthesising and secreting their product in the extracellular space. Schizogenic oil ducts are characteristic for the Apiaceae family, for example, *Carum carvi*, *Foeniculum vulgare*, or *Cuminum cyminum*, but also for Hypericaceae or Pinaceae. Lysogenic cavities are found in Rutaceae (*Citrus sp*.), Myrtaceae (e.g., *Syzygium aromaticum*), and others. Glandular trichomes generally coat the aerial parts of the plant as extensions of the epidermis from which they originate. They are classified into capitate and peltate trichomes. The former display 1) one basal cell, 2) one to several stalk cells, and 3) one or a few secretory cells at the stalk's tip synthesising mainly non-volatile or poorly volatile compounds that are directly reversed onto the surface of the trichome. Peltate trichomes have a similar structure, but the head, consisting of several secretory cells, is surmounted by a large sub-cuticular storage cavity in which the products of the secretory cells are reversed [15]. These structures are common to the Asteraceae, Lamiaceae, and Solanaceae families. For instance, plants of the Lamiaceae, comprising

species such as mint (*Mentha x piperita*), basil (*Ocimum basilicum*), lavender (*Lavandula spica*), oregano (*Origanum vulgare*), and thyme (*Thymus vulgaris*), are cultivated for their glandular trichome-produced essential oils [15]. The location of the anatomical structure producing volatile specialised metabolites defines the part of the plant used to produce the EOs. Table 1 lists important EO-bearing plants, including the common and botanical names, the family, and the plant part used to obtain the essential oil.

Table 1 Important essential oil-bearing plants, including the common and botanical names, the family, and the plant part used to obtain the essential oil [11]

Trade Name	Species	Plant Family	Used Plant Part(s)
Ambrette seed	*Hibiscus abelmoschus* L.	Malvaceae	Seed
Amyris	*Amyris balsamifera* L.	Rutaceae	Wood
Angelica root	*Angelica archangelica* L.	Apiaceae	Root
Anise seed	*Pimpinella anisum* L.	Apiaceae	Fruit
Armoise	*Artemisia herba-alba* Asso	Asteraceae	Herb
Asafoetida	*Ferula assa-foetida* L.	Apiaceae	Resin
Basil	*Ocimum basilicum* L.	Lamiaceae	Herb
Bay	*Pimenta racemosa* Moore	Myrtaceae	Leaf
Bergamot	*Citrus aurantium* L. subsp. *bergamia* (Risso et Poit.) Engl.	Rutaceae	Fruit peel
Birch tar	*Betula pendula* Roth. (syn. *Betula verrucosa* Erhart. *Betula alba sensu* H.J.Coste. non L.)	Betulaceae	Bark/wood
Buchu leaf	*Agathosma betulina* (Bergius) Pillans. *A. crenulata* (L.) Pillans	Rutaceae	Leaf
Cade	*Juniperus oxycedrus* L.	Cupressaceae	Wood
Cajuput	*Melaleuca leucandendron* L.	Myrtaceae	Leaf
Calamus	*Acorus calamus* L.	Araceae	Rhizome
Camphor	*Cinnamomum camphora* L. (Sieb.)	Lauraceae	Wood
Cananga	*Cananga odorata* Hook. f. et Thoms.	Annonaceae	Flower
Caraway	*Carum carvi* L.	Apiaceae	Seed
Cardamom	*Elettaria cardamomum* (L.) Maton	Zingiberaceae	Seed
Carrot seed	*Daucus carota* L.	Apiaceae	Seed
Cascarilla	*Croton eluteria* (L.) W.Wright	Euphorbiaceae	Bark
Cedarwood, Chinese	*Cupressus funebris* Endl.	Cupressaceae	Wood
Cedarwood, Texas	*Juniperus mexicana* Schiede	Cupressaceae	Wood
Cedarwood, Virginia	*Juniperus virginiana* L.	Cupressaceae	Wood
Celery seed	*Apium graveolens* L.	Apiaceae	Seed
Chamomile	*Matricaria recutita* L.	Asteraceae	Flower
Chamomile, Roman	*Anthemis nobilis* L.	Asteraceae	Flower
Chenopodium	*Chenopodium ambrosioides* (L.) Gray	Chenopodiaceae	Seed
Cinnamon bark, Ceylon	*Cinnamomum zeylanicum* Nees	Lauraceae	Bark
Cinnamon bark, Chinese	*Cinnamomum cassia* Blume	Lauraceae	Bark
Cinnamon leaf	*Cinnamomum zeylanicum* Nees	Lauraceae	Leaf

Trade Name	Species	Plant Family	Used Plant Part(s)
Citronella, Ceylon	*Cymbopogon nardus* (L.) W. Wats.	Poaceae	Leaf
Citronella, Java	*Cymbopogon winterianus* Jowitt.	Poaceae	Leaf
Clary sage	*Salvia sclarea* L.	Lamiaceae	Flowering herb
Clove buds	*Syzygium aromaticum* (L.) Merill et L.M. Perry	Myrtaceae	Leaf/bud
Clove leaf	*Syzygium aromaticum* (L.) Merill et L.M. Perry	Myrtaceae	Leaf
Coriander	*Coriandrum sativum* L.	Apiaceae	Fruit
Cornmint	*Mentha canadensis* L. (syn. *M. arvensis* L. f. *piperascens* Malinv. ex Holmes; *M. arvensis* L. var. *glabrata. M. haplocalyx* Briq.; *M. sachalinensis* (Briq.) Kudo)	Lamiaceae	Leaf
Cumin	*Cuminum cyminum* L.	Apiaceae	Fruit
Cypress	*Cupressus sempervirens* L. C	upressaeae	Leaf/twig
Davana	*Artemisia pallens* Wall.	Asteraceae	Flowering herb
Dill	*Anethum graveolens* L.	Apiaceae	Herb/fruit
Dill, India	*Anethum sowa* Roxb.	Apiaceae	Fruit
Elemi	*Canarium luzonicum* Miq.	Burseraceae	Resin
Eucalyptus	*Eucalyptus globulus* Labill.	Myrtaceae	Leaf
Eucalyptus, lemon-scented	*Eucalyptus citriodora* Hook.	Myrtaceae	Leaf
Fennel bitter	*Foeniculum vulgare* Mill. subsp. *vulgare* var. *vulgare*	Apiaceae	Fruit
Fennel sweet	*Foeniculum vulgare* Mill. subsp. *vulgare* var. *vulgare*	Apiaceae	Fruit
Fir needle, Canadian	*Abies balsamea* Mill.	Pinaceae	Leaf/twig
Fir needle, Siberian	*Abies sibirica* Ledeb.	Pinaceae	Leaf/twig
Gaiac	*Guaiacum officinale* L.	Zygophyllaceae	Resin
Galbanum	*Ferula galbanifl ua* Boiss. *F. rubricaulis* Boiss.	Apiaceae	Resin
Garlic	*Allium sativum* L.	Alliaceae	Bulb
Geranium	*Pelargonium* spp.	Geraniaceae	Leaf
Ginger	*Zingiber officinale* Roscoe	Zingiberaceae	Rhizome
Gingergrass	*Cymbopogon martinii* (Roxb.) H. Wats var. *sofia* Burk	Poaceae	Leaf
Grapefruit	*Citrus x paradisi* Macfad.	Rutaceae	Fruit peel
Guaiacwood	*Bulnesia sarmienti* L.	Zygophyllaceae	Wood
Gurjum	*Dipterocarpus* spp.	Dipterocarpaceae	Resin
Hop	*Humulus lupulus* L.	Cannabaceae	Flower
Hyssop	*Hyssopus offi cinalis* L.	Lamiaceae	Leaf
Juniper berry	*Juniperus communis* L.	Cupressaceae	Fruit
Laurel leaf	*Laurus nobilis* L.	Lauraceae	Leaf
Lavandin	*Lavandula angustifolia* Mill. x L. *latifolia* Medik.	Lamiaceae	Leaf
Lavender	*Lavandula angustifolia* Miller	Lamiaceae	Leaf

Trade Name	Species	Plant Family	Used Plant Part(s)
Lavender, Spike	*Lavandula latifolia* Medik.	Lamiaceae	Flower
Lemon	*Citrus limon* (L.) Burman fi l.	Rutaceae	Fruit peel
Lemongrass, Indian	*Cymbopogon fl exuosus* (Nees ex Steud.) H. Wats.	Poaceae	Leaf
Lemongrass, West Indian	*Cymbopogon citratus* (DC.) Stapf	Poaceae	Leaf
Lime distilled	*Citrus aurantiifolia* (Christm. et Panz.) Swingle	Rutaceae	Fruit
Litsea cubeba	*Litsea cubeba* C.H. Persoon	Lauraceae	Fruit/leaf
Lovage root	*Levisticum officinale* Koch	Apiaceae	Root
Mandarin	*Citrus reticulata* Blanco	Rutaceae	Fruit peel
Marjoram	*Origanum majorana* L.	Lamiaceae	Herb
Mugwort common	*Artemisia vulgaris* L.	Asteraceae	Herb
Mugwort, Roman	*Artemisia pontica* L.	Asteraceae	Herb
Myrtle	*Myrtus communis* L.	Myrtaceae	Leaf
Neroli	*Citrus aurantium* L. subsp. *aurantium*	Rutaceae	Flower
Niaouli	*Melaleuca viridiflora*	Myrtaceae	Leaf
Nutmeg	*Myristica fragrans* Houtt.	Myristicaceae	Seed
Onion	*Allium cepa* L.	Alliaceae	Bulb
Orange	*Citrus sinensis* (L.) Osbeck	Rutaceae	Fruit peel
Orange bitter	*Citrus aurantium* L.	Rutaceae	Fruit peel
Oregano	*Origanum* spp.. *Thymbra spicata* L.. *Coridothymus capitatus* Rechb. fi l.. *Satureja* spp. *Lippia graveolens*	Lamiaceae	Herb
Palmarosa	*Cymbopogon martinii* (Roxb.) H. Wats var. sofi a Burk H. Wats var. *motia* Burk	Poaceae	Leaf
Parsley seed	*Petroselinum crispum* (Mill.) Nym. ex A.W. Hill	Apiaceae	Fruit
Patchouli	*Pogostemon cablin* (Blanco) Benth.	Lamiaceae	Leaf
Pennyroyal	*Mentha pulegium* L.	Lamiaceae	Herb
Pepper	*Piper nigrum* L.	Piperaceae	Fruit
Peppermint	*Mentha x piperita* L.	Lamiaceae	Leaf
Petitgrain	*Citrus aurantium* L. subsp. *aurantium*	Rutaceae	Leaf
Pimento leaf	*Pimenta dioica* (L.) Merr.	Myrtaceae	Fruit
Pine needle	*Pinus silvestris* L.. P. *nigra* Arnold	Pinaceae	Leaf/twig
Pine needle, Dwarf	*Pinus mugo* Turra	Pinaceae	Leaf/twig
Pine silvestris	*Pinus silvestris* L.	Pinaceae	Leaf/twig
Pine white	*Pinus palustris* Mill.	Pinaceae	Leaf/twig
Rose	*Rosa* x *damascena* Miller	Rosaceae	Flower
Rosemary	*Rosmarinus officinalis* L.	Lamiaceae	Feaf
Rosewood	*Aniba rosaeodora* Ducke	Lauraceae	Wood
Rue	*Ruta graveolens* L.	Rutaceae	Herb
Sage, Dalmatian	*Salvia officinalis* L.	Lamiaceae	Herb
Sage, Spanish	*Salvia lavandulifolia* L.	Lamiaceae	Leaf
Sage, three lobed (Greek. Turkish)	*Salvia fruticosa* Mill. (syn. S. *triloba* L.)	Lamiaceae	Herb

Trade Name	Species	Plant Family	Used Plant Part(s)
Sandalwood, East Indian	*Santalum album* L.	Santalaceae	Wood
Sassafras, Brazilian (Ocotea cymbarum oil)	*Ocotea odorifera* (Vell.) Rohwer [*Ocotea pretiosa* (Nees) Mez.]	Lauraceae	Wood
Sassafras, Chinese	*Sassafras albidum* (Nutt.) Nees.	Lauraceae	Root bark
Savory	*Satureja hortensis* L.. *Satureja montana* L.	Lamiaceae	Leaf
Spearmint, Native	*Mentha spicata* L.	Lamiaceae	Leaf
Spearmint, Scotch	*Mentha gracilis* Sole	Lamiaceae	Leaf
Star anise	*Illicium verum* Hook fil.	Illiciaceae	Fruit
Styrax	*Styrax officinalis* L.	Styracaceae	Resin
Tansy	*Tanacetum vulgare* L.	Asteraceae	Flowering herb
Tarragon	*Artemisia dracunculus* L.	Asteraceae	Herb
Tea tree	*Melaleuca* spp.	Myrtaceae	Leaf
Thyme	*Thymus vulgaris* L.. T. *zygis* Loefl. ex L.	Lamiaceae	Herb
Valerian	*Valeriana officinalis* L.	Valerianaceae	Root
Vetiver	*Vetiveria zizanoides* (L.) Nash	Poaceae	Root
Wintergreen	*Gaultheria procumbens* L.	Ericaceae	Leaf
Wormwood	*Artemisia absinthium* L.	Asteraceae	Herb
Ylang Ylang	*Cananga odorata* Hook. f. et Thoms.	Annonaceae	Flower

1.5 Quality of plant derivatives bearing essential oils

While distillation is unquestionably the process of isolating plant EOs in a suitable form to be exploited in the flavour and fragrance field or to study the potential bioactivity of the mixture, it is not an efficient strategy for the high-throughput assessment of the quality of the plant raw material by the characterisation of its volatile and semi-volatile fraction. This is because distillation is a long process and requires a significant amount of matrix. Moreover, it is very difficult or even impossible to be combined with the analytical step in a Total Analysis System, meaning an automatic system in which the sample preparation and analytical steps are merged into a single one to reduce the workload to a minimum [16].

There are alternative strategies to characterise the volatile fractions of raw plant materials and thus assure the quality of the corresponding essential oils. These strategies rely on suitable sample preparation techniques that exploit the ability of the volatile fraction to vaporize spontaneously and/or under appropriate conditions, and that can be online combined with gas chromatography analysis.

1.5.1 Headspace Solid-Phase Microextraction (HS-SPME)

Headspace solid-phase microextraction (HS-SPME) is the most frequently applied sample preparation technique to extract volatiles from liquid and solid matrices, including plant raw materials [16]. It is described as a solvent-free sample preparation technique that integrates sampling, extraction, concentration, and sample introduction into one system. In HS-SPME, a short, thin fused-silica rod coated with a minimal amount of the extracting phase is exposed for a well-defined time directly to the head space above the sample, and analytes are recovered onto the extracting phase [17]. The analyte extraction from headspace by the

fiber may occur by sorption, absorption, or a mixture of both mechanisms according to the polymer coating. The overall amount of analyte recovered on the fiber depends on two closely related but distinct equilibria: the first is the matrix/headspace equilibrium responsible for the headspace composition, and the second is the headspace/polymeric fiber coating equilibrium [16]. When the fiber is introduced into the vial, the analytes are removed from the head space. The drop of the analytes concentration in the head space, disrupt the equilibrium between the matrix and the headspace and this leads to an additional indirect extraction of the analyte from the matrix into the headspace. This process continues till the three phase equilibrium is reached which implies that the amount of analyte extracted on to the fibre remains constant for further increase in sampling time.

1.5.1.1 Multiple Headspace Extraction (MHE) Approach

HS-SPME can be employed to qualitatively characterise the volatile fraction of the sample matrix as well as to extract the whole amount of specific analytes for quantitative analysis. In the latter case, the multiple head space extraction (MHE) approach is applied. When using the MHE approach, consecutive extractions of the same sample are performed. After each sampling, a portion of the head headspace is removed, and consequently, an additional amount of compound migrates from the matrix to the headspace to re-establish the three-phase equilibrium. Under optimal conditions, after the first extraction, the analyte concentrations in the two phases (i.e., matrix and headspace) will be smaller, even though the ratio between the analyte concentration in the two phases will be the same. The amount of analyte extracted with the second extraction will be lower than that isolated with the first extraction (i.e., the corresponding chromatographic peak area will be decreased). Repeating the extraction until complete depletion of the matrix, the sum of the analyte peak areas of each extraction corresponds to the area of the overall amount of analyte present in the matrix. Under optimal conditions, the amount of analyte removed by consecutive extractions decreases exponentially, and, in practice, extractions are not performed to complete depletion of the matrix. Still, from a limited number of consecutive extractions, the peak area corresponding to the total amount of analyte present in the sample can be obtained by extrapolation based on a mathematical relationship which will be better described is section 1.8.1 [18].

1.5.1.2 Limitations of HS-SPME for the characterisation of the semi-volatile fraction of plant raw materials

In the HS-SPME extraction process, for most compounds, the rate-limiting step is the transfer of analytes from the sample into its headspace, making the extraction of volatile analytes faster than that of semivolatiles. The latter usually requires an extremely long extraction time not only to reach equilibrium but also to be recovered in a suitable amount to meet the sensitivity of the downstream analytic platform under non-equilibrium conditions and thus to obtain a reliable profile of the volatile fraction in the plant material.
The extraction of semi-volatile compounds is usually accelerated by agitating the sample, maximizing the sample/headspace interface, and heating the sample. An alternative way of speeding up extraction kinetics of less volatile compounds involves applying vacuum conditions during HS-SPME sampling. The positive effect of low sampling pressure conditions on HS-SPME has been thoroughly described by Psillakis *et al*. [17,19–21], who

proved that vacuum is a powerful experimental parameter to increase the extraction kinetic of semi-volatile compounds during the HS-SPME process. This is because in the case of semivolatiles and under non-equilibrium conditions, a reduced pressure inside the sampler container decreases the resistance to mass transfer in the gas zone at the solid-headspace interface. As a consequence, higher extraction efficiencies for semi-volatile compounds can be achieved in shorter sampling time and potentially at milder extraction temperatures which are to be preferred for the following reasons: 1) to prevent the formation of artefacts, 2) to avoid the discrimination of the more volatile markers of the matrix and thus 3) to provide a more reliable profile of the plant material volatile and semi-volatile fractions.
The characterisation of the semi-volatile fractions of plant raw materials and derivatives is, in some cases, fundamental in defining their origin, trade value, and potential applications. This is true for Frankincense resins, whose semi-volatile fraction compositions discriminate samples of different origins and market prices, and *Cannabis sativa* L. plant inflorescences in which the composition of the semi-volatile fraction determines whether the plant is intended for fiber/seed production, therapeutic purposes, or recreational use.

1.6 Analytical strategies for the qualitative and quantitative composition of plant volatile and semi-volatile fractions and essential oils

In addition to physical tests (i.e., moisture content, specific gravity, optical rotation, refractive index, residue on evaporation, freezing or congealing point, solubility in dilute alcohol), the study of the quality of an essential oil strongly relies upon the qualitative and often quantitative characterisation (i.e., separation, identification, and quantification) of its main components. Being the latter all volatile or semi-volatile compounds, the technique of choice to perform such an investigation is capillary gas chromatography (GC), commonly coupled with a flame ionisation detector (FID) or a mass spectrometer with a single quadruple (MS) as an analyser. GC-MS/FID is also the analytical platform of choice to hyphenate HS-SPME sampling [22].

1.6.1 Qualitative analysis

The core of the chromatographic systems is the column whose efficiency (i.e., dispersion of the analyte band as it travels through the chromatographic system) and selectivity (i.e., the ability of the chromatographic system to chemically distinguish between sample components) depend on its geometry and the chemistry of the stationary phase [22]. Wall-coated open-tubular columns (WCOT) are the most commonly used column type, and they contain a liquid stationary phase as a thin film on the inner wall of fused silica capillary [23]. Typical dimensions of capillary columns are listed below (bold values indicate the most frequently used dimensions):

- Length (L): 5, 10, **20, 25, 30**, 50, 60, 100 m
- Inner diameter (ID or d_c): **0.10**, 0.15, **0. 18**, 0.20, **0.25**, 0.30, **0.32**, **0.53** mm
- Film thickness: **0.10**, **0.20**, **0.25**, **0.5**, **1.0** 1.5, 2.0, 5.0, 8.0 µm

With this type of column, the separation is caused by gas-liquid partition, which is the repeated solvation and vaporisation of the solutes [23]. Methyl polysiloxanes (SE30, OV-1, OV 101, DB-1, HP-1, PS 347.5, etc.) and methyl phenyl-polysiloxanes (SE-52, SE-54, DB-5, HP-5, PS-086, etc.) based columns are the most used apolar stationary phases in EO routine analysis. They possess a good solubility for non-polar and weakly polar analytes forming

primarily dispersion forces, and compounds are separated according to their boiling point. Polar polyethyleneglycol-based columns (PEG-20M, CW-20M, DB-Wax, etc.), which, on the contrary, separate compounds according to their polarity, are often combined to apolar stationary phases to obtain a complete separation of the highest possible number of components [7].

In addition to these conventional columns, in the last 20 years, Ionic liquids (ILs) have aroused great interest as an alternative to conventional polar columns also in the EO analysis field [24]. ILs, also known as fused salts, are a class of non-molecular ionic solvents composed of unsymmetrically substituted nitrogen-containing cations (e.g., imidazole, pyrrolidine, pyridine) with inorganic anions (e.g., Cl^-, $PF6^-$, BF_4^-). ILs have negligible vapor pressures at room temperature, possess a wide range of viscosities, can be custom-synthesized to be miscible or immiscible, often have high stability, and are capable of undergoing multiple solvation interactions with many types of molecules, all characteristics that make them ideal GC stationary phases [25]. In addition, they have proved outstanding and different selectivity compared to conventional polar stationary phases [22].

Irrespective of the chemistry of the stationary phase, identification is generally carried out either by chromatographic data only (Kováts indices, linear retention indices, relative retention time, retention time locking), measurable with a universal detector such as FID, or by their combination with spectral data, when a mass spectrometer GC- MS is employed as an analyser [7].

1.6.2 Quantitative analysis

The quantitative analysis of EOs is undoubtedly a complex task. Various different GC detectors (universal, selective, or specific detectors) can be employed. In general, in the EO field, universal detectors such as flame ionization (FID) and mass spectrometry detectors (MS) are preferred for everyday work because of the matrix's complex chemical nature [26]. A true quantitation of all components in an EO is very uncommon as it would require an unacceptably long analysis time due to the complexity of the matrix. Therefore, it is generally performed for specific markers only. It is determined from the compound chromatographic area normalized vs. an internal (or external) standard and calculated by a calibration curve constructed from amounts of pure marker standard in the operative concentration range (i.e., external/internal multilevel calibration) [26].

There are alternative strategies to describe the composition of EO in terms of constituent abundance, which are all based on the assumption that all the components of the mixture are detected with the chosen methods. These strategies are 1) the relative percentage abundance and 2) the normalised percentage abundance. Relative percentage abundance is measured by relating the absolute area of each constituent to the sum of the areas of all the compounds forming the EO. This approach is helpful in describing the relative components ratio of an EO, but it cannot be employed to compare the composition of a group of EOs. In the latter case, the normalized % abundance can be applied, provided that the samples vary in qualitative and quantitative compositions within a limited range. To measure the normalised percentage abundance, the GC raw data of a selected number of markers of the EOs under investigation, usually common to all investigated samples, are normalized vs. one or more internal standards (or an external standard if an automatic injector is available) and, from them, the normalized % abundance is calculated [26].

Relative percentage abundance and normalised percentage abundance are generally calculated taking into account the analyte response factors and cannot be applied using an MS as a detector because with the latter, the analyte structure conditions not only the formation of ions but also their abundance [26].

1.6.3 Enantioselective GC

The biosynthesis of specialised chiral metabolites in plants is very often stereo-chemically guided, resulting in some cases in enantiomeric excess. The enantiomer characterisation of chiral essential oil components is usually required to define the geographical origin of the sample, 2) to detect adulteration, 3) to relate a chemical structure to its bioactivity (i.e., interaction with specific receptors or enzyme) [27].
Capillary GC is currently the method of choice for enantiomer analysis of EOs, and enantioselective-GC (Es-GC) has become an essential tool for stereochemical analysis mainly after the introduction of cyclodextrin (CD) derivatives as chiral stationary phases (CSPs) which proved high enantioselectivity and a wide range of application. Naturally occurring cyclodextrins are cycle non-reducing oligosaccharides of six to twelve β-(D)-glucopyranose units linked by a-1,4-glycosidic bonds, which form through the degradation of starch by the enzyme glycosyl transferase. The use of derivatised cyclodextrins coated on glass or fused silica capillary started an impressive development of enantioselective GC. Nowadays, the most commonly used cyclodextrins as stationary phases present 6 (α-CD), 7 (β-CD), or 8 (γ-CD) β-(D)-glucopyranose units with bulky substituents on the primary C6-hydroxyl group (i.e., *tert*-butyldimethylsilyl, TBDMS, or *tert*-hexyldimethylsilyl) and smaller substituents (symmetrical; i.e, first-generation or asymmetrical, i.e., second-generation) at the C2 and C3-secondary hydroxyl groups (mainly methyl, ethyl, and acetyl), the latter being responsible for the column enantioselectivity. When employing cyclodextrins, the separation of the enantiomers is due to the differences in the fast and reversible interaction between the distomeric CD selector and the enantiomer. These interactions include, among others inclusion, hydrogen bonding, dispersion forces, dipole-dipole interaction, and electrostatic interactions. Because the separation is based on a fast kinetic and is thermodynamically driven, the best separation is obtained at a temperature as low as possible [22].

1.6.4 High-speed GC

In the last 10-15 years, high-speed GC analysis has been introduced in the EO field (flavour and fragrance field) for routine analysis to minimise the time required for the analysis while preserving good separation and qualitative and quantitative reliable data [22]. The speed of GC analysis can be increased by: a) increasing the carrier gas flow rate, b) increasing temperature program heating rates, c) using faster carrier gas such as hydrogen, d) reducing the column length, e) reducing the column diameter, f) reducing the thickness of the stationary phase [28]. The most commonly used strategies to improve the speed of the analysis are the use of short columns (i.e., 5-10 m) with a conventional inner diameter (Short capillary column GC, SCC-GC) and the use of short columns with reduced inner dimeters and film thickness (Fast GC, F-GC). The former strategy can be exploited in routine qualitative and quantitative analysis of medium complexity samples where there is a margin for a rational reduction of efficiency (i.e., the baseline separation is maintained despite the

reduced column efficiency). An alternative strategy to shorten the analysis time while preserving column efficiency is employing columns with narrow inner diameters [22]. The current widespread use of F-GC is in part due to the work of Klee and Blumberg [28], who developed the method translation approach to scale a GC method optimised on a conventional GC column. If the current method meets all analytical needs except speed, then the translation is the best way to go, especially if the analysis involves many (e.g., > 20) components. According to the concept of GC method translation, the speed of a GC analysis can be influenced by translatable and non-translatable parameters. Column geometry (i.e., column length, inner diameter, film thickness), carrier gas (i.e., type and flow rate), and heating rates are translatable ones while non-translatable parameters include stationary phase, phase ratio and initial and plateau temperature. Two methods are mutually translatable if they have identical non translatable parameters and the same normalised temperature programme [29].

1.7 References

[1] E. Schmidt, Production of Essential Oils, in: K.H.C. Baser, G. Buchbauer (Eds.), Handb. Essent. Oils Sci. Technol. Appl. Second Ed., 2015: pp. 83–118.

[2] Council of Europe, European Pharmacopoeia, 10th ed., Council of Europe, Strasburg, France, 2020.

[3] ISO - ISO 9235:1997 - Aromatic natural raw materials — Vocabulary, (n.d.). https://www.iso.org/standard/16866.html (accessed May 15, 2022).

[4] K.H. Can Başer, G. Buchbauer, Handbook of Essential Oils, CRC Press, 2015. https://doi.org/10.1201/b19393.

[5] P. Burger, H. Plainfossé, X. Brochet, F. Chemat, X. Fernandez, Extraction of Natural Fragrance Ingredients: History Overview and Future Trends, Chem. Biodivers. 16 (2019). https://doi.org/10.1002/cbdv.201900424.

[6] M.C. González-Mas, J.L. Rambla, M.P. López-Gresa, M.A. Blázquez, A. Granell, Volatile Compounds in Citrus Essential Oils: A Comprehensive Review, Front. Plant Sci. 10 (2019). https://doi.org/10.3389/fpls.2019.00012.

[7] P. Rubiolo, B. Sgorbini, E. Liberto, C. Cordero, C. Bicchi, Essential oils and volatiles: sample preparation and analysis. A review., Flavour Fragr. J. 25 (2010) 282–290. https://doi.org/10.1002/ffj.1984.

[8] M.A. Alvarez, Plant Secondary Metabolism Chapter 3, in: Plant Biotechnol. Heal., Springer International Publishing, Cham, 2014: pp. 15–31. https://doi.org/10.1007/978-3-319-05771-2_3.

[9] M.E. Maffei, J. Gertsch, G. Appendino, Plant volatiles: Production, function and pharmacology, Nat. Prod. Rep. 28 (2011) 1359. https://doi.org/10.1039/c1np00021g.

[10] Guidance on Essential Oils in Cosmetic Products - European Directorate for the Quality of Medicines & HealthCare, (n.d.). https://www.edqm.eu/en/guidance-on-essential-oils-in-cosmetic-products (accessed June 4, 2022).

[11] Chlodwig Franz and Johannes Novak, Sources of Essential Oils, in: K.H.C. Baser, G. Buchbauer (Eds.), Handb. Essent. Oils Sci. Technol. Appl. Second Ed., 2015: pp. 39–73.

[12] Z. Zebec, J. Wilkes, A.J. Jervis, N.S. Scrutton, E. Takano, R. Breitling, Towards synthesis of monoterpenes and derivatives using synthetic biology, Curr. Opin. Chem. Biol. 34 (2016) 37–43. https://doi.org/10.1016/j.cbpa.2016.06.002.

[13] C. Sell, Chemistry of Essential Oils, in: K.H.C. Baser, G. Buchbauer (Eds.), Handb. Essent. Oils Sci. Technol. Appl. Second Ed., 2015: pp. 121–149.

[14] P.M. Dewik, Medicinal Natural Products: A Biosynthetic Approach, 3rd ed., 2006.

[15] J. Glas, B. Schimmel, J. Alba, R. Escobar-Bravo, R. Schuurink, M. Kant, Plant Glandular Trichomes as Targets for Breeding or Engineering of Resistance to Herbivores, Int. J. Mol. Sci. 13 (2012) 17077–17103. https://doi.org/10.3390/ijms131217077.

[16] P. Rubiolo, B. Sgorbini, E. Liberto, C. Cordero, C. Bicchi, Analysis of the Plant Volatile Fraction, in: Chem. Biol. Volatiles, John Wiley & Sons, Ltd, Chichester, UK, 2010: pp. 49–93. https://doi.org/10.1002/9780470669532.ch3.

[17] E. Psillakis, Vacuum-assisted headspace solid-phase microextraction: A tutorial review, Anal. Chim. Acta. 986 (2017) 12–24. https://doi.org/10.1016/j.aca.2017.06.033.

[18] L.S.E. Bruno Kolb, The Technique of Head-Space-Gas Chromatography, in: Static Headspace-Gas Chromatogr. Theory Pract., 1st ed., Wiley-VCH Verlag, United States of America, 2006: pp. 45–116.

[19] E. Psillakis, E. Yiantzi, L. Sanchez-Prado, N. Kalogerakis, Vacuum-assisted headspace solid phase microextraction: Improved extraction of semivolatiles by non-equilibrium headspace sampling under reduced pressure conditions, Anal. Chim. Acta. 742 (2012) 30–36. https://doi.org/10.1016/j.aca.2012.01.019.

[20] E. Psillakis, A. Mousouraki, E. Yiantzi, N. Kalogerakis, Effect of Henry's law constant and operating parameters on vacuum-assisted headspace solid phase microextraction, J. Chromatogr. A. 1244 (2012) 55–60. https://doi.org/10.1016/j.chroma.2012.05.006.

[21] E. Psillakis, The effect of vacuum: an emerging experimental parameter to consider during headspace microextraction sampling, Anal. Bioanal. Chem. 412 (2020) 5989–5997. https://doi.org/10.1007/s00216-020-02738-x.

[22] C. Cagliero, C. Bicchi, A. Marengo, P. Rubiolo, B. Sgorbini, Gas chromatography of essential oil: State-of-the-art, recent advances, and perspectives, J. Sep. Sci. 45 (2022) 94–112. https://doi.org/10.1002/jssc.202100681.

[23] W. Engewald, K. Dettmer-Wilde, H. Rotzsche, Columns and Stationary Phases, in: Pract. Gas Chromatogr., Springer Berlin Heidelberg, Berlin, Heidelberg, 2014: pp. 59–116. https://doi.org/10.1007/978-3-642-54640-2_3.

[24] C. Cagliero, C. Bicchi, C. Cordero, E. Liberto, P. Rubiolo, B. Sgorbini, Analysis of essential oils and fragrances with a new generation of highly inert gas chromatographic columns coated with ionic liquids, J. Chromatogr. A. 1495 (2017) 64–75. https://doi.org/10.1016/j.chroma.2017.03.029.

[25] J.L. Anderson, D.W. Armstrong, G.-T. Wei, Ionic Liquids in Analytical Chemistry, Anal. Chem. 78 (2006) 2892–2902. https://doi.org/10.1021/ac0693940.

[26] C. Bicchi, E. Liberto, M. Matteodo, B. Sgorbini, L. Mondello, B. d'Acampora Zellner, R. Costa, P. Rubiolo, Quantitative analysis of essential oils: a complex task, Flavour Fragr. J. 23 (2008) 382–391. https://doi.org/10.1002/ffj.1905.

[27] G.D. Barbara d'Acampora Zellner, Paola Dugo, and L. Mondello, Analysis of Essential Oils, in: K.H.C. Baser, G. Buchbauer (Eds.), Handb. Essent. Oils Sci. Technol. Appl. Second Ed., 2015: pp. 151–177.

[28] M.S. Klee, L.M. Blumberg, Theoretical and Practical Aspects of Fast Gas Chromatography and Method Translation, J. Chromatogr. Sci. 40 (2002) 234–247. https://doi.org/10.1093/chromsci/40.5.234.

[29] P. Rubiolo, C. Cagliero, C. Cordero, E. Liberto, B. Sgorbini, C. Bicchi, Gas Chromatography in the Analysis of Flavours and Fragrances, in: Pract. Gas Chromatogr., Springer Berlin Heidelberg, Berlin, Heidelberg, 2014: pp. 717–743. https://doi.org/10.1007/978-3-642-54640-2_20.

[30] NIST Chemistry WebBook, (n.d.). https://webbook.nist.gov/chemistry/ (accessed January 29, 2022).

[31] EPI Suite™-Estimation Program Interface | US EPA, Downloaded Oct. 2021. (n.d.). https://www.epa.gov/tsca-screening-tools/epi-suitetm-estimation-program-interface (accessed February 2, 2022).

1.8 Research projects

1.8.1 Adulteration of Essential Oils: A Multitask Issue for Quality Control. Three Case Studies: *Lavandula angustifolia* Mill., *Citrus limon* (L.) Osbeck and *Melaleuca alternifolia* (Maiden & Betche) Cheel

Francesca Capetti[1†], Arianna Marengo[1†], Cecilia Cagliero[1], Erica Liberto[1], Carlo Bicchi[1], Patrizia Rubiolo[1] and Barbara Sgorbini[1*]

Affiliation
[1]Dipartimento di Scienza e Tecnologia del Farmaco, Università degli Studi di Torino, Turin, Italy

*Corresponding author
Prof. Dr. Barbara Sgorbini, Dipartimento di Scienza e Tecnologia del Farmaco, Università degli Studi di Torino, Via Pietro Giuria 9, I-10125, Turin, Italy. E-mail: barbara.sgorbini@unito.it. Phone: +39 011 6707135 Fax: +39 011 670

[†]: These authors contributed equally to the work

Received: July 30, 2021
Revised: September 10, 2021
Accepted: September 12 2021

Bibliography
Molecules. 2021 Sep 16;26(18):5610.
DOI: 10.3390/molecules26185610.

1.8.1.1 Abstract

The quality control of essential oils (EO) principally aims at revealing the presence of adulterations and at quantifying compounds that are limited by law by evaluating EO chemical compositions, usually in terms of the normalised relative abundance of selected markers, for comparison to reference values reported in pharmacopoeias and/or international norms. Common adulterations of EO consist of the addition of cheaper EO or synthetic materials. This adulteration can be detected by calculating the percent normalised areas of selected markers or the enantiomeric composition of chiral components. The dilution of the EO with vegetable oils is another type of adulteration. This adulteration is quite devious, as it modifies neither the qualitative composition of the resulting EO nor the marker's normalised percentage abundance, which is no longer diagnostic, and an absolute quantitative analysis is required. This study aims at verifying the application of the two above approaches (i.e., normalised relative abundance and absolute quantitation) to detect EO adulterations, with examples involving selected commercial EO (lavender, bergamot and tea tree) adulterated with synthetic components, EO of different origin and lower economical values and heavy vegetable oils. The results show that absolute quantitation is necessary to highlight adulteration with heavy vegetable oils, providing that a reference quantitative profile is available.

Keywords: *Citrus limon* (ex. *Citrus* × *bergamia*); *Lavandula angustifolia*; *Melaleuca alternifolia*; adulteration of essential oils; chiral analysis.

1.8.1.2 Introduction

Essential oils (EO) are complex mixtures of volatile compounds that are characterised by important biological activities for the plant itself and for humans who have learned to exploit their properties over the centuries. The ISO norm 9235:2013 defines an EO as "… a product obtained from a natural raw material of plant origin, by steam distillation, bymechanical processes from the epicarp of *citrus* fruits, or by dry distillation, after separation of the aqueous phase—if any—by physical processes" [1]. The European Pharmacopoeia terms an EO as "an Odorous product, usually of complex composition, obtained from a botanically defined plant raw material by steam distillation, dry distillation, or a suitable mechanical process without heating. Essential oils are usually separated from the aqueous phase by a physical process that does not significantly affect their composition" [2]. In both definitions, it is clear that only products obtained by steam/hydrodistillation can be named EO, while products obtained by different extraction procedures involving the use of solvents must be defined as extracts. EO are mainly characterised by the presence of terpenes/terpenoids and phenolic compounds (i.e., phenylpropanoids), that derive from the mevalonate/methyl erithrytol and shikimic acid pathways, respectively. The chemical composition of an EO is usually expressed in the literature in terms of the relative percentage abundance (i.e., % area) or normalised percentage abundance (i.e., norm % areas) [3]. Only a few papers have reported the true quantitation of EO, as determining this is considered difficult and time-consuming. The quality control of EO is necessary to guarantee their safe use, as well as to detect adulterations and fraud. Unfortunately, the adulteration of EO is not uncommon along supply chains, thus generating concerns in the EO industry. EO can often be adulterated via the addition of cheaper EO (e.g., sweet orange added to bitter orange, corn mint added to peppermint or lavandin added to lavender) or via the addition of cheap synthetic materials (e.g., synthetic linalool and linalyl acetate added to bergamot EO) [4]. This type of adulteration can be detected quite easily via the determination of the normalised percentage areas of selected markers. Moreover, since biosynthesis in plants is stereochemically guided and terpenes/terpenoids are generally chiral compounds with a specific enantiomeric composition [5,6], chiral marker compounds become diagnostics for detecting the adulteration of essential oils via the addition of synthetic volatile compounds. Enantiomeric recognition is therefore also necessary to improve the quality control and uncover fraud and adulteration via the addition of cheap synthetic materials or volatiles from other sources to EO [4]. Dilution with vegetable oils, resulting in a reduction in scent, is another type of EO adulteration. Vegetable oils are selected, as they are relatively cheap and because they present a density and texture that are similar to those of EO [4]. This type of adulteration is quite devious, as it modifies neither the qualitative composition of the EO nor the relative percentage abundance of the marker compounds. However, the dilution of the final product interferes with the EO sensory and biological properties, in addition to committing commercial fraud. In this case, the normalised percentage area is no longer diagnostic, and a true quantitative analysis is required, provided that acceptable reference quantitative data are available. To the best of the authors' knowledge, several papers describing strategies for revealing EO adulterations that occur via the addition of cheaper EO or synthetic compound shave been reported in the literature and have recently been

reviewed [4,7,8]. Conversely, there are few papers that describe approaches to reveal the addition of vegetable oils to dilute EO [9–11]. The most applied technique is infrared (IR) spectroscopy coupled with a multivariate analysis. However, the precise identification of vegetable oil is often difficult due to the signal overlap of similar molecules [11]. Very recently, Truzzi et al. introduced a new method based on 13C-NMR spectroscopy to recognise adulterant vegetable oils in EO; the method does not require additional data elaboration with a multivariate analysis [12].This study evaluates and compares different approaches to detect adulterations of three representative EO (i.e., bergamot, lavender and tea tree EO)—in particular, the determination of the normalised percentage areas and/or the enantiomeric composition of selected markers and the true absolute quantitative analysis. These three EO were selected due to their global market impact, which includes a constant increase both in terms of production and worldwide market share [13]. Both conventional and chiral GC analyses were performed, and the latter was combined with HS-SPME sampling to avoid damage to the chiral column degradation due to non-eluted residues of vegetable oil.

1.8.1.3 Materials and methods

Essential Oils, Standards and Materials

Genuine EO from botanically authenticated samples of *Citrus limon*(L.) Osbeck (ex *Citrus×bergamia*, Risso et Poit, bergamot), *Lavandula angustifolia* Mill. (lavender) and *Melaleuca alternifolia*, (Maiden & Betche) Cheel (Australian tea tree and Chinese tea tree) were supplied by Erboristeria Magentina (Poirino, Italy). The EO were obtained via steamdistillation for lavender and tea tree EO and via cold expression for bergamot. Twenty different batches were considered for each EO. Some EO samples were also purchased in the local shops (commercial samples). **Table 1** lists the EO used in this work, together with the specialised metabolites chosen as marker compounds and their target ions used for quantitation.

The above genuine EO were spiked on purpose (spiked samples) to build a model of adulterations: (1) bergamot and lavender EO were supplemented with synthetic racemic linalool and linalyl acetate (9% and 11%, respectively, for bergamot EO and 27% of both linalool and linalyl acetate for lavender EO), (2) Australian TTO was mixed with 50% Chinese tea tree and (3) all the investigated EO were mixed with different amounts of sunflower vegetable oil (from 5% to 50%).

Table 1, List of the investigated EO and the selected marker compounds, together with their target ion (m/z), used for the quantitation.

Essential Oil	Botanical Name	Plant Part Used	Selected Marker Compounds	Target Ion
Bergamot	*Citrus limon* (L.) Osbeck	Peel	Linalool, linalyl acetate	71, 93
Lavender	*Lavandula angustifolia* Mill.	Aerial part	Linalool, linalyl acetate	71, 93
Tea tree	*Melaleuca alternifolia* (Maiden & Betche) Cheel	Leaves	4-terpineol, α-terpineol	71, 59

Pure standard commercially available samples (purity > 98%) of linalool, inalylacetate, 4-terpineol, α-terpineol, (R)-(−)-linalool, (S)-(+)-linalool, (R)-(−)-linalyl acetate, (S)-(+)-linalyl acetate, (R)-(−)-4-terpineol, (S)-(+)-4-terpineol, (R)-(+)-α-terpineol and (S)-(−)-α-terpineol were purchased from Merck, Darmstadt, Germany. Tridecane (C13) was used as the internal standard and purchased from Merck. The alkane standard mixture(C9–C25) was prepared

to calculate the retention indices (final concentration: 100µg/mL). Cyclohexane was HPLC grade and supplied by Carlo Erba, Milano, Italy.

GC Analysis Conditions

GC-MS analyses were carried out on an Agilent 6890 GC unit coupled to an Agilent 5975 MSD (Agilent, Little Falls, DE, USA), equipped with a MPS-2 multipurpose sampler (Gerstel, Mülheim a/d Ruhr, Germany), using the following conditions: injector temperature: 230◦C; injection mode: split; ratio: 1/20; carrier gas: helium; flow rate: 1 mL min−1;columns: MEGA 5 (df 0.25µm,dc 0.25 mm and length 30 m) and 2,3-di-O-ethyl-6-O-t-butyldimethylsilyl-β-CD (2,3DE6TBDMS-β-CD) [20] (df 0.25µm,dc 0.25 mm and length 25 m) (Mega, Legnano, Milan, Italy). Temperature programs: for the MEGA 5 column from 50◦C (1 min) to 300◦C (5 min) at 3◦C $min^{-1}$and for the cyclodextrin column from 40◦C (1 min) to 220◦C (5 min) at 2◦C min^{-1}. The marker compounds were identified by comparing their mass spectra and retention indices to those of authentic standards, to those that were commercial (Wiley, Nist and Adams) and/or homemade libraries or from the literature [21,22]. GC-FID analyses were carried out on a Shimadzu 2010 GC unit under the same conditions as reported above. The relative percentage compositions of the analysed EO were determined using GC-FID peak areas and applying response factors [3,23]. For the GC-MS and GC-FID analyses with the MEGA 5 column, the genuine, spiked and commercial essential oils were diluted in cyclohexane (5 mg/mL). Tridecane (C13) was used as the internal standard (final concentration in the dilution: 0.1 mg/mL). For the GC-MS and GC-FID analyses with the 2,3DE6TBDMS-β-CD column, the genuine, spiked and commercial EO were sampled using HS-SPME (for the conditions, see the following sections) to avoid cyclodextrin column degradation due to non-eluted residues of vegetable oil.

HS-SPME Sampling Conditions

For the genuine, spiked and commercial EO samples, 2µL of the dilution in cyclo-hexane (5 mg/mL) were introduced in a 20-mL headspace vial, immediately hermetically closed with a PTFE-silicone septa and sampled for 20 min at room temperature (i.e., 25◦C) by HS-SPME. Stable flex carboxen/divinylbenzene/PDMS (CAR/DVB/PDMS) SPME fibres (2 cm long) from Supelco Co. (Bellafonte, PA, USA) were chosen. After sampling, the fibre was automatically removed from the vapor phase (headspace)and introduced into the GC injector to allow the complete thermal desorption of the sampled analytes to occur in the GC column. Blank runs were carried out to verify the absence of carryover effects. The fibre performance was periodically checked (every ten analyses) by adopting in-fibre external standardisation and by analysing a standard aqueous solution containing some of the selected markers (5 µL of a 2 mg mL^{-1} solution containing 4-terpineol, linalool and linalyl acetate) [24,25].

Quantitative Analysis

For the true quantitation of the selected markers in genuine, spiked and commercial EO, the external calibration method was chosen. Stock standard solutions were prepared via the addition of an aliquot of pure standard to an appropriate volume of cyclohexane (final concentration: 10 $mgmL^{-1}$). Suitable dilutions of each stock standard mixture were then prepared (final concentrations in the range of 5–0.1 $mgmL^{-1}$). The resulting stock and

diluted solutions were supplemented with C13 (final concentration a dilution of 0.1 mg/mL), stored at 0◦C and renewed weekly. A calibration curve was built by analysing the above diluted solutions. For the true quantitation of the selected enantiomers, the MHS-SPME approach was adopted by using the same diluted solutions that were sampled by MHS-SPME and using the total vaporization approach [26]. MHS-SPME is the most appropriate approach for volatile component quantitation in liquid or solid matrices that are sampled by the headspace. MHS-SPME is the SPME extension of the MHE-static HS that was developed by Kolb et al. [27,28], and is based on successive dynamic gas extraction from a single sample; the marker analyte peak area decays exponentially with the number of extractions, and the amount present initially in a given matrix (in this case, the EO) is represented by the sum of the areas from each extraction. The total area of the analyte(s) under investigation for quantitation is determined using the following equation:

$$A_T = \sum_{i=1}^{\infty} A_i = \frac{A_1}{(1-e^{-q})} = \frac{A_1}{(1-Q)} \quad (1)$$

where A1 is the analyte area after the first extraction, AT is the total analyte area (derived from the sum of the areas from each extraction) and Q: e^{-q}, −q is a constant calculated from the following linear regression analysis equation:

$$lnAi = -q(i-1) + lnA1 \quad (2)$$

where Ai is the peak area obtained from the ith extraction. In everyday practice, a few extractions (generally, 3–5) are sufficient to obtain a reliable exponential equation that describes the analyte decay, from which the total area of the analyte in the sample can besuccess fully extrapolated. The analytes are then quantified using an external standard approach that is performed by submitting standard mixtures of selected markers at different concentrations to MHS-SPME. MHS-SPME can also be carried out under non-equilibrium conditions [29,30], provided that the sampling parameters are rigorously standardised and the amount of sample is suitable to give linear analyte decay(s). Figure S1 in the Supplementary Materials shows the GC-MS-extracted ions of linalool (m/z= 71) in a bergamot EO, with three consecutive extractions from a sample (on the left) and its linear decay diagram (on the right).

1.8.1.4 Results and discussion

In the routine quality control of EO, tens of samples are analysed every year, and usually, some borderline samples may be found. These EO demand special attention. EO adulteration can successfully be testified only when a suitable reference profiling of genuineness obtained with the appropriate analytical methods (i.e., % areas through conventional GC analysis, enantiomeric composition through enantioselective GC analysisand true quantitation) is available either from international organisations (e.g., pharmacopoeias or ISO norms) or built in-house by analysing a consistent number of certified genuine samples. This study is fully in line with this strategy and consists of: (1) the creation of the reference profiles of the EO under investigation, including their enantiomeric recognition, via the analysis of different batches of genuine EO (20 samples

of each EO), (2) the analysis of EO adulterated via the addition of synthetic volatile compounds or cheap EO and (3) the analysis of adulterated EO via the addition of vegetable oil requiring a true quantitation to detect the dilution. This study focuses on some commercially available EO samples that were found to beat the limit of acceptance when compared to the pharmacopoeia monograph—namely, two lavender, one bergamot and two tea tree (TTO) EO.

Reference Chemical Profiles of Genuine Essential Oils

Generally, the reference profile should include the minimum, average and maximum percent normalised area values for each selected marker compound, which should be calculated using a sufficient (significantly representative) number of controlled genuine samples. **Figure 1** shows the GC-MS patterns of genuine bergamot, lavender and tea tree EOs. These EO were characterised mostly by monoterpenes/monoterpenoids and sesquiterpenes/sesquiterpenoids; each EO profile presented some predominant compounds (e.g., linalool and linalyl acetate in bergamot and lavender EO and 4-terpineol and γ-terpinene in the tea tree EO), together with other relatively minor compounds.

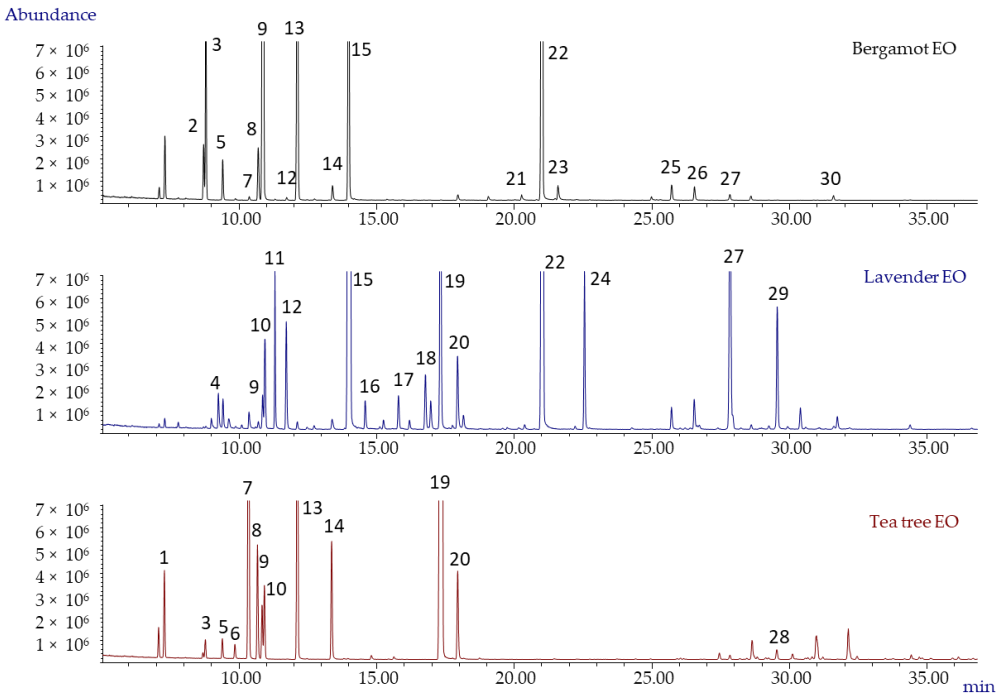

Figure 1 GC-MS patterns of genuine bergamot, lavender and TTO EO. Legend: (1) α-pinene, (2) sabinene, (3) β-pinene, (4) 3-octanone, (5) β-myrcene, (6) α-phellandrene, (7) α-terpinene, (8) p-cymene, (9) limonene, (10) 1,8-cineole, (11) cis-β-ocimene, (12) trans-β-ocimene, (13) γ-terpinene, (14) α-terpinolene, (15) linalool, (16) 1-octen-3-yl acetate, (17) camphor, (18) lavandulol, (19) 4-terpineol, (20) α-terpineol, (21) neral, (22) linalyl acetate, (23) geranial, (24) lavandulyl acetate, (25) neryl acetate, (26) geranyl acetate, (27) trans-β-caryophyllene, (28) aromadendrene, (29) trans-β-farnesene and (30) β-bisabolene. For the analysis conditions, see the main text.

Table 2 reports the composition of the investigated EOs in terms of the normalised relative abundance (minimum, maximum and average % areas, together with the standard deviation values) of the characteristic marker compounds determined by analysing twenty

genuine batches for each EO. **Table 2** also reports the Italian/European Pharmacopoeia % area ranges.

All of the analysed batches were in agreement with the Italian or European Pharmacopoeia, as it is evident from the minimum and maximum normalised % areas, respectively, and the ranges that were narrower than those of the pharmacopoeias for the selected markers, which indicates the high homogeneity of the selected samples. The average reference composition of bergamot EO was also in agreement with Verzera *et al.* [14], who analysed 1082 genuine samples.

Table 2 Normalised relative abundance (minimum, maximum and average normalised % area) of the marker compounds in bergamot, lavender and tea tree essential oils (number of samples: 20)

	***Citrus limon* (L.) Osbeck**							
	Compounds	**I^t_sexp**	**I^t_slit**	**Min**	**Max**	**Average**	**σ**	**Ital. Ph.**
2	sabinene	976	976	0.8	1.0	0.9	0.1	0.5–2.0
3	β-pinene	978	980	5.6	6.9	6.5	0.4	5.0–10.0
5	β-myrcene	992	991	0.7	1.5	1.0	0.2	
7	α-terpinene	1018	1018	0.1	0.2	0.1	0.1	
8	*p*-cymene	1028	1026	0.2	0.7	0.4	0.2	
9	limonene	1031	1031	34.3	40.9	37.8	2.3	30.0–50.0
12	*trans*-β-ocimene	1051	1050	0.1	0.2	0.1	0.1	
13	γ-terpinene	1061	1062	5.3	8.0	6.7	0.9	6.0–18.5
14	α-terpinolene	1089	1088	0.3	0.6	0.3	0.1	
15	linalool	1100	1098	9.6	12.3	10.7	0.8	6.0–15.0
21	neral	1243	1240	0.1	0.3	0.2	0.1	
22	linalyl acetate	1264	1257	30.0	35.8	31.5	1.6	23.0–35.0
23	geranial	1273	1270	0.1	0.5	0.3	0.1	max 0.5
25	neryl acetate	1369	1365	0.3	0.8	0.5	0.1	
26	geranyl acetate	1386	1383	0.3	0.7	0.4	0.1	0.1–0.7
27	*trans*-β-caryophyllene	1419	1418	0.1	0.6	0.3	0.1	0.2–0.5
30	β-bisabolene	1510	1509	0.1	0.4	0.2	0.1	
	***Lavandula angustifolia* Mill.**							
	Compounds	**I^t_sexp**	**I^t_slit**	**Min**	**Max**	**Average**	**σ.**	**Eur. Ph.**
4	3-octanone	989	986	0.4	1.3	0.9	0.3	0.1–5.0
9	limonene	1031	1031	0.4	1.1	0.7	0.2	max 1.0
10	1,8-cineole	1033	1033	1.3	2.6	2.4	1.2	max 2.5
11	*cis*-β-ocimene	1041	1040	0.7	3.2	2.4	0.6	
12	*trans*-β-ocimene	1051	1050	0.2	2.2	1.8	0.5	
15	linalool	1100	1098	23.8	33.0	29.5	2.5	20.0–45.0
16	1-octen-3-yl acetate	1116	1110	0.4	1.1	0.7	0.2	
17	camphor	1147	1143	0.6	1.2	1.0	0.2	max 1.2
18	lavandulol	1171	1166	0.6	1.7	0.9	0.4	min 0.1
19	4-terpineol	1178	1177	2.6	6.0	3.6	1.0	0.1–8.0
20	α-terpineol	1191	1189	0.1	2.0	1.0	0.6	max 2.0
22	linalyl acetate	1264	1257	25.1	40.7	35.4	4.0	25.0–47.0
24	lavandulyl acetate	1293	1289	2.7	5.3	3.5	0.7	min 0.2
27	*trans*-β-caryophyllene	1419	1418	1.8	5.1	3.5	1.0	
29	*trans*-β-farnesene	1460	1458	1.2	5.2	2.5	1.0	
	***Melaleuca alternifolia* (Maiden & Betche) Cheel**							
	Compounds	**I^t_sexp**	**I^t_slit**	**Min**	**Max**	**Average**	**σ.**	**Eur. Ph.**
1	α-pinene	936	939	1.8	6.0	3.8	1.8	1.0–6.0
3	β-pinene	978	980	0.1	1.1	0.6	0.3	
5	β-myrcene	992	991	0.1	1.1	0.5	0.4	
6	α-phellandrene	1004	1005	0.0	0.6	0.3	0.2	
7	α-terpinene	1018	1018	7.7	10.5	9.2	0.7	5.0–13.0
8	*p*-cymene	1028	1026	0.7	3.6	2.1	0.8	0.5–12.0
9	limonene	1031	1031	0.8	3.7	2.5	1.0	0.5–4.0
10	1,8-cineole	1033	1033	1.9	7.1	3.9	1.5	max 15.0
13	γ-terpinene	1061	1062	14.3	22.4	19.2	2.4	10.0–28.0
14	α-terpinolene	1089	1088	2.0	4.7	3.1	0.8	1.5–5.0
19	4-terpineol	1178	1177	32.4	47.1	40.5	3.4	min 30.0
20	α-terpineol	1191	1189	2.6	7.1	5.0	1.4	1.5–8.0
28	aromadendrene	1439	1439	0.1	5.8	1.3	1.4	max 7.0

I^t_sexp: experimental programmed temperature retention index; I^t_slit: tabulated programmed temperature retention index.

Table 3 reports the percentage enantiomeric composition (EC%) of some representative chiral markers in the investigated genuine EO. They were determined using the same number of samples as those used to build up the reference profiles (n= 20). **Tables S1–S3** in the Supplementary Materials report the EC% of all the enantiomeric compounds in the investigated genuine EO. The EC% values were calculated using the following formula:

$$EC\% = \frac{Area\ enantiomer\ R\ or\ S}{Area\ enantiomer\ R + Area\ enantiomer\ S} \times 100$$

Table 3, Percent enantiomeric composition (EC%) of some representative markers in genuine and adulterated bergamot (commercial bergamot EO: CB-1 EO), lavender (commercial lavender EO: CL-1 EO), and TTO (commercial tee tree oil: CT-1 EO) EO compared to the literature data (n = 20).

			Bergamot EO			Lavender EO		
	I^tsexp	**I^tslit**	**Genuine**	**Adulterated CB-1 EO**	**Reference Values [15]**	**Genuine**	**Adulterated CL-1 EO**	**Reference Values [1]**
(*R*)-(−)-linalool	1181	1174	99.6	76.0	99.4–99.7	93.8	66.4	
(*S*)-(+)-linalool	1196	1189	0.4	24.0	0.3–0.6	6.2	33.6	max 12%
(*R*)-(−)-linalyl acetate	1233	1231	99.7	89.1	99.7–99.9	99.4	80.4	
(*S*)-(+)-linalyl acetate	1243	1237	0.3	10.9	0.1–0.3	0.6	19.6	max 1%
			Chinese TTO			**Australian TTO**		
	I^tsexp	**I^tslit**	**Genuine**			**Genuine**	**Adulterated CT-1 EO**	**Reference Values [16,17]**
(*R*)-(−)-4-terpineol	1258	1253	57.8			30.8	45.5	
(*S*)-(+)-4-terpineol	1250	1248	42.2			69.2	54.5	67.4–69.6
(*R*)-(+)-α-terpineol	1317	1309	77.0			75.8	76.7	71.0–78.0
(*S*)-(−)-α-terpineol	1302	1296	23.0			24.2	23.3	

The results obtained for bergamot were compared to those reported by Mondello *et al.* [15], which were obtained via the analysis of about 100 genuine EO samples. The samples here used to build up the reference profile were all found to be genuine, as the EC% was perfectly superimposable with the literature data. Bergamot EO are characterised by a clear predominance of (R)-(−)-linalool and (R)-(−)-linalyl acetate versus (S)-enantiomers by 98.6% and 98.7%, respectively. Furthermore, lavender EO are also characterised by a clear predominance of (R)-(−)-linalool and (R)-(−)-linalyl acetate versus S-enantiomers by 93.8% and 99.4%, respectively, which is confirmed by the literature data [18] and pharmacopoeia [1].Different is the situation of TTO, where the three markers (i.e., limonene,α-terpineol and 4-terpineol) from Australia and China have similar normalised % abundances when analysed with conventional GC, therefore making it almost impossible to distinguish between them. The Australian TTO, however, presents a diagnostic enantiomeric ratio, the abundance of (R)-enantiomers of limonene and α-terpineol being remarkably higher than the (S)-form (i.e., 61.0% and 39.0% for (R)- and (S)-limonene and 75.8% and 24.2% for(R)- and (S)-α-terpineol), while 4-terpineol is mainly present in the (S)-form. Conversely, their EC% in Chinese tea tree EO are significantly different. These data indicate that enantiomeric recognition is therefore a diagnostic to distinguish the different origins, which, incidentally, also significantly characterise their economic value. The informative value of chiral recognition for TTO has also been recognised by ISO that included the enantiomeric ratio of 4-terpineol in the 2017 revision of ISO 4730 Standard [16] that specifies the enantiomeric ratio for 4-terpineol as (S)-(+) 67–71% and (R)-(−) 29–33%. In this case too, the results here reported for the investigated Australian samples are in agreement with both the ISO norm and the data of Wong et al. [17] for about 60 genuine samples.

Adulteration with Cheaper Essential Oils or Synthetic Compounds

To evaluate the genuineness of the investigated commercial EO, the genuine lavender and bergamot EO chosen to build up the reference profiling were first adulterated with synthetic linalool and linalyl acetate (spiked samples) [19] and the genuine samples of Australian TTO with Chinese TTO (mixed origins sample) (see Section 3 for details).**Table 4** shows that the normalised relative abundances of linalool, linalyl acetate and α-terpineol increased in both the commercial and spiked samples and are borderline compared to the reference chemical profile, but this increase was not sufficient to decide a clear adulteration, since they still were within the reference range reported by the pharmacopoeias. Conversely, the TTO sample obtained by mixing the two origins (i.e., Australian and Chinese) did not show a significant variation in terms of the normalised relative abundance of 4-terpineol, probably because of the similar compositions of the two EO.

On the other hand, **Table 3** shows that the enantiomeric composition dramatically changed—in particular, in bergamot samples, (S)-(+)-linalool increased from 0.4% to 24% and (S)-(+)-linalyl acetate from 0.3% to 10.9%. The same was true for lavender EO, where(S)-(+)-linalool was raised from 6.2% to 33.6% and (S)-(+)-linalyl acetate from 0.6% to 19.6% (See **Table 3**).

Table 4 Normalised relative % abundance of linalool, linalyl acetate, 4-terpineol and α-terpineol in genuine, spiked and commercial samples of bergamot, lavender, and TTO EO obtained with conventional GC.

			***Citrus limon* EO**					***Lavandula angustifolia* EO**					
			Genuine		**Spiked Samples**		**Com. Sample CB-1 EO**	**Genuine**		**Spiked Samples**		**Com. Sample CL-1 EO**	
	I^tsexp	I^tslit	%	σ	%	σ	%	%	σ	%	σ	%	σ
linalool	1100	1098	11.4	0.1	15.2	0.1	15.0	30.0	0.2	38.8	0.1	39.2	0.3
linalyl acetate	1260	1259	27.5	0.2	32.6	0.4	33.1	35.0	0.4	42.8	0.1	42.9	0.5
			***Melaleuca alternifolia* EO**										
			Australian		**Mixed Origins**		**Com. Sample CT-1 EO**						
	I^tsexp	I^tslit	%	σ	%	σ	%	σ					
4-terpineol	1178	1177	44.0	0.6	42.6	0.1	41.4	0.6					
α-terpineol	1190	1189	3.0	0.1	4.8	0.04	5.0	0.7					

In both cases, the EC% values exceeded the maximum reference values, clearly showing their adulterations. This is also evident in Figure 2 reporting the chromatogram of linalool and linalyl acetate enantiomers in a genuine and in a spiked bergamot EO, both submitted to enantioselective GC with 2,3 di-O-ethyl-6-t-butyldimethyl silyl-β-cyclodextrin (2,3DE6TBDMS-β-CD) as the chiral selector.

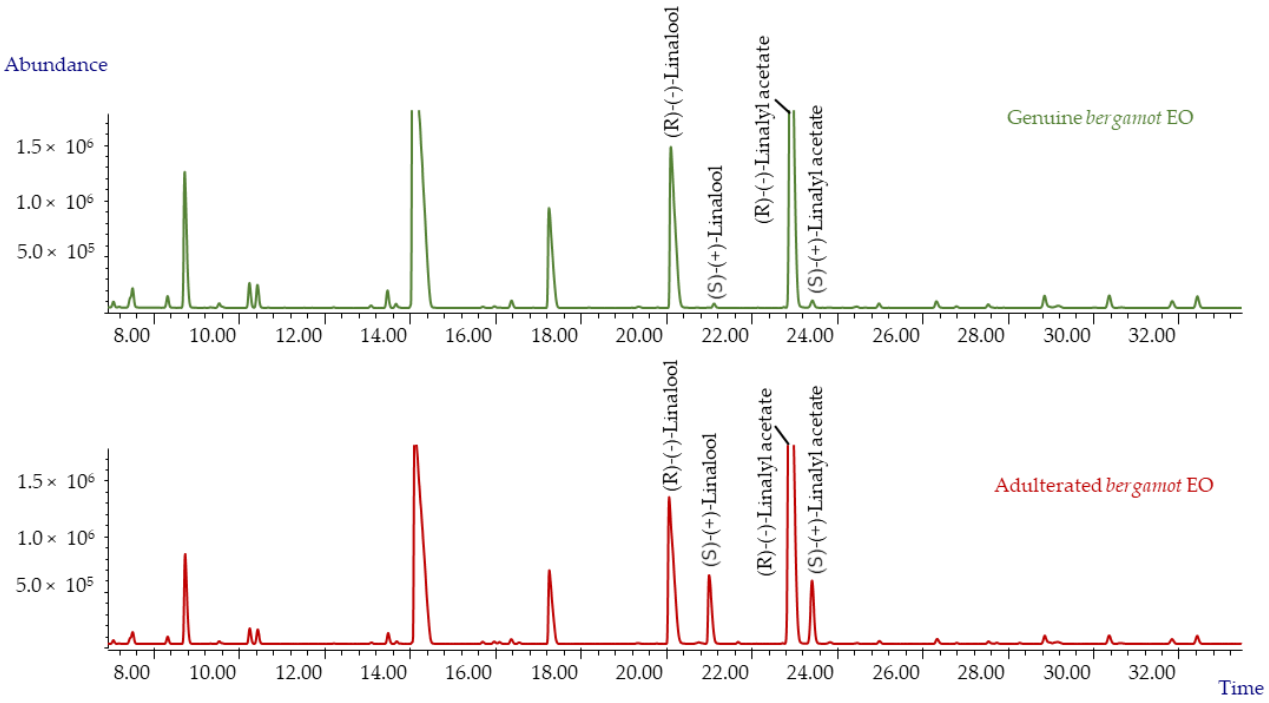

Figure 2 Linalool and linalyl acetate in a genuine and an adulterated bergamot EO analysed with a 2,3DE6TBDMS-β-CD chiral column phase.

A similar behaviour was observed for the mixture of Australian and Chinese TTO that resulted in a significant change in the enantiomeric composition of 4-terpineol, with a drop of EC% from the expected 68% to 69% indicated by ISO to 54.5% (see **Table 3**).

Commercial EO Adulterated with Vegetable Oils

As mentioned previously, the addition of vegetable oil produces a dilution of the EO that does not affect the qualitative GC profile but results in a decrease of the absolute amounts of the markers. **Figure 3** shows the GC-MS patterns of both genuine and spiked on purpose lavender EO (analysed with an oven temperature program up to 300◦C). The GC patterns clearly indicate the absence of peaks due to vegetable oils, and it is perfectly superimposable from a qualitative point of view. However, the profile of the spiked sample presents peaks of lower intensity, maybe indicative of a dilution effect due to the presence of a heavy vegetable oil.

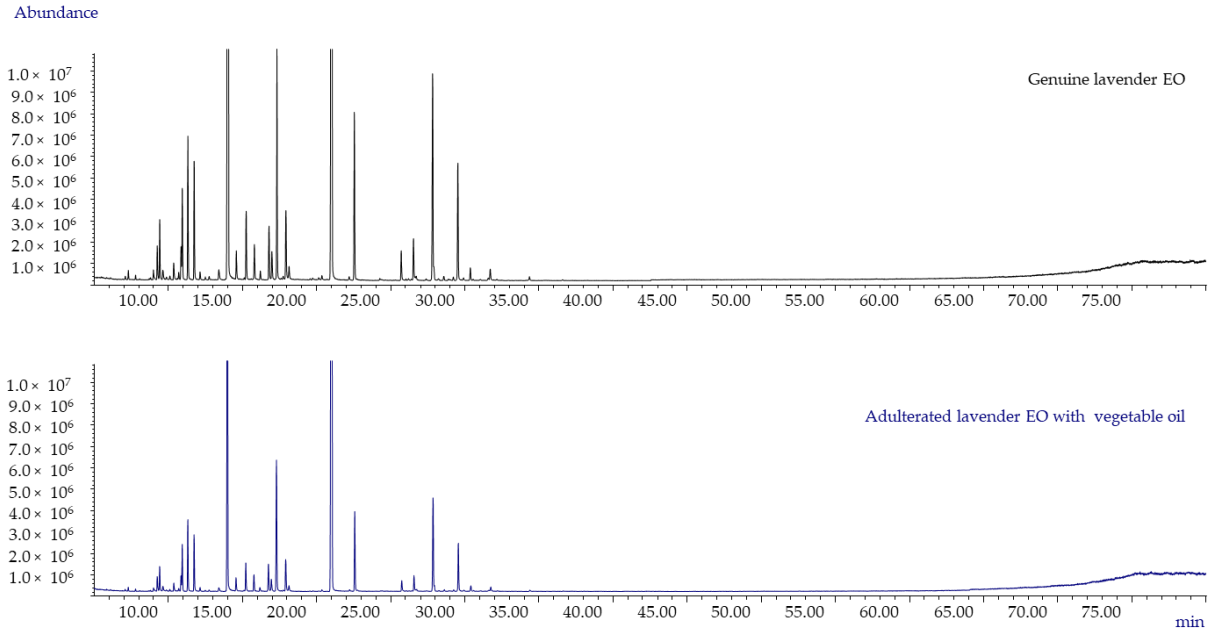

Figure 3 GC-MS patterns of both genuine and spiked on purpose lavender EO (analysed with an oven temperature program up to 300 °C).

One of the commercial lavender EO samples (CL-2 EO) showed normalised peak area intensities of the selected markers significantly lower than those observed in genuine EO. The sample was submitted to the European Pharmacopoeia test to detect fatty oils [1]by putting a drop of the EO onto filter paper and a slight translucent spot after 24 h was evidenced. The conventional GC and enantioselective GC analyses did not provide results suitable to measure the % of adulteration; therefore, a true quantitative analysis was required. A series of experiments were carried out to evaluate the reliability of this approach by adulterating the three oils of this study with different amounts of vegetable oils to confirm the % adulteration experimentally, although only one suspected commercial lavender sample (CL-2 OE) was the object of investigation. The data obtained for the commercial and adulterated EO were the same as those calculated in the genuine samples and already reported in **Table 2** (data not shown, as it is redundant), driving us to perform a true quantitative analysis. **Table S4** reports the equations for the calibration curves that were obtained with an external standard approach and used to quantitate the marker compounds, together with their correlation coefficient and the selected range of concentrations. **Table 5** reports the absolute concentrations of the selected markers in the genuine, the spiked and the commercial lavender oil EO under investigation.

Table 5 Absolute concentrations of the selected marker compounds in the investigated essential oils.

Essential Oil		(Linalool) (g/100 g)	σ	(Linalyl acetate) (g/100 g)	σ	(4-Terpineol) (g/100 g)	σ	(α-Terpineol) (g/100 g)	σ
C. limon	genuine	10.5	0.2	25.9	0.4				
	5% spiked	9.6	0.1	23.8	0.6				
	20% spiked	7.1	0.3	21.8	0.2				
	50% spiked	5.0	0.1	14.4	0.3				
L. angustifolia	genuine	23.4	1.2	27.0	0.9				
	5% spiked	20.1	0.5	23.4	0.2				
	20% spiked	18.4	0.3	21.2	0.6				

Essential Oil		(Linalool) (g/100 g)	σ	(Linalyl acetate) (g/100 g)	σ	(4-Terpineol) (g/100 g)	σ	(α-Terpineol) (g/100 g)	σ
	50% spiked	13.4	0.2	15.3	0.4				
	CL-2 EO	14.5	0.3	16.8	0.2				
M. alternifolia	genuine					44.2	2.7	8.5	1.5
	5% spiked					42.0	2.2	6.9	0.9
	20% spiked					33.5	1.8	3.5	0.2
	50% spiked					26.7	2.1	2.4	0.1

These results showed that the commercial sample was adulterated about 40–50% with vegetable oil. For a further confirmation, the absolute quantification was also carried out on the enantiomers of the markers of the CL-2 EO. The quantitative analysis was carried out with a Multiple Headspace Solid-Phase Microextraction (MHS-SPME) combined with an enantioselective GC-FID-MS to avoid the degradation of the cyclodextrin column performance due to non-eluted residues of heavy vegetable oil. **Table 6** reports the absolute concentrations of the enantiomers of linalool and linalylacetate in the genuine, spiked with vegetable oil and CL-2 EO. The absolute concentrations of the single enantiomers clearly decreased with increasing the degree of adulteration, indicating the reliability of this approach to measure the EO adulteration with vegetable oils.

Table 6 Absolute concentrations of the enantiomers of linalool and linalyl acetate in both genuine and vegetable oil-spiked CL-2 EO.

Essential Oil		EC%	((R)-(−)-Linalool) (g/100 g)	σ	EC%	((S)-(+)-Linalool) (g/100 g)	σ
L. angustifolia	genuine	99.6	22.1	0.2	0.4	1.5	0.1
	5% spiked	99.6	19.2	0.2	0.4	1.3	0.1
	20% spiked	99.6	16.7	0.3	0.4	0.91	0.1
	50% spiked	99.6	12.3	0.2	0.4	0.62	0.08
	CL-2 EO	99.6	14.5	0.2	0.4	0.74	0.09
		EC%	**((R)-(−)-Linalyl acetate) (g/100 g)**	**σ**	**EC%**	**((S)-(+)-Linalyl acetate) (g/100 g)**	**σ**
	genuine	99.7	26.7	0.4	0.3	0.44	0.2
	5% spiked	99.7	23.1	0.2	0.3	0.34	0.2
	20% spiked	99.7	20.8	0.2	0.3	0.29	0.1
	50% spiked	99.7	15.1	0.1	0.3	0.21	0.06
	CL-2 EO	99.7	16.8	0.2	0.3	0.26	0.07

The results on the enantiomeric recognition of the CL-2 EO showed that it was adulterated between 40% and 50% with a heavy vegetable oil. The degree of adulteration of the sample analysed should be considered as indicative, since it was not possible to analyse the sample before the adulteration. This confirms the need for a representative genuine GC pattern.

1.8.1.5 Conclusions

The quality control of EO to highlight the presence of synthetic "naturally identical" substances or of less expensive EO can successfully be carried out by evaluating the chemical composition in terms of the normalised percentage area or true quantitation of the diagnostic markers to be compared with the reference data reported in pharmacopeia or ISO norm monographies. Most of the EO samples analysed in routine quality controls comply with the reference data (i.e., pharmacopoeia, ISO norm and in-house built reference profiling). Conversely, borderline EO samples require a more accurate evaluation to confirm or exclude their adulteration.

This study shows different approaches on how to deal with a successful quality control of borderline EO samples by using enantiomeric recognition and an absolute quantitative analysis of the selected marker compounds as a complement to the normalised relative abundances, thus making possible to highlight a number of EO adulterations with examples from real world samples. The approaches here adopted were based on gas chromatography, which is the technique of choice to characterise an EO. These methods afford to detect simultaneously both the presence of compounds deriving from different (cheaper) EO with a single GC run, to monitor the addition of synthetic racemic compounds by enantioselective and EO dilution with vegetable oil(s). Moreover, these approaches are very useful in routine quality control, because they do not require extra statistical elaboration, and analyses can be carried out using fast methods with the adoption of narrow bore GC columns, thanks to the repeatability of the separations ensured by the method translation software [31,32].

Adulteration with vegetable oils cannot be revealed using the above approach and requires an absolute quantitative analysis. This method of course requires reference concentration values obtained from the analysis of a consistent number of certified genuine EO samples. A quantitative analysis is often considered to be a complex time-consuming procedure; however, as clearly shown in this study, the quantitation of a limited number of selected markers is often sufficient to highlight an adulteration with vegetable oil(s); that is, the number of required analyses is rather low.

Direct methods based on spectroscopic methods have also been developed with success to deal with this problem: they include fluorescence spectroscopy [9], infrared spectroscopy [11] and Raman spectrometry [10]. These methods, however, generally require the use of multivariate statistical elaborations (principal component analysis and independent component analysis) or the building up of artificial neural networks, thus implying a further step of data processing. Very recently, Truzzi et al. reported a method based on NMR spectroscopy without a further statistical step not only able to detect the presence of an adulteration with vegetable oils but, also, to identify the added adulterant through its 13C-NMR fingerprint [12].

The availability of separation and direct methods (in particular, NMR) is an effective step ahead to monitor EO adulterations, since it is now possible to define their quality both in terms of the characteristic qualitative and quantitative marker composition and detection and identification of adulterants of low economic value.

In conclusion, the approaches adopted in this study, in combination with the methods based on NMR spectroscopy, open up a concrete possibility of identifying unambiguously EO adulterations by vegetable oil in quality control laboratories.

1.8.1.6 Supplementary Material

Table S1, Genuine Lavandula angustifolia EO enantiomeric composition

I^tsexp	I^tslit	Compound	Percent Enantiomeric Composition
1139	1133	(S)-(-)-camphor	9.0
1147	1141	(R)-(+)-camphor	91.0
1180	1174	(R)-(-)-linalool	93.8
1197	1189	(S)-(+)-linalool	6.2
1196	1192	(S)-(-)-borneol	17.8
1204	1200	(R)-(+)-borneol	82.2
1233	1231	(R)-(-)-linalyl acetate	99.4
1243	1237	(S)-(+)-linalyl acetate	0.6
1444	1454	(R)-(+)-germacrene D	9.3
1457	1462	(S)-(-)-germacrene D	90.7

Table S2, Genuine Citrus limon EO enantiomeric composition

I^tsexp	I^tslit	Compound	Percent Enantiomeric Composition
952	944	(R)-(+)-β-pinene	6.6
961	955	(S)-(-)-β-pinene	93.4
979	972	(R)-(+)-sabinene	15.5
993	988	(S)-(-)-sabinene	84.5
1060	1056	(S)-(-)-limonene	1.8
1071	1072	(R)-(+)-limonene	98.2
1181	1174	(R)-(-)-linalool	98.6
1198	1189	(S)-(+)-linalool	1.4
1233	1231	(R)-(-)-linalyl acetate	98.7
1243	1237	(S)-(+)-linalyl acetate	1.3
1399	1403	(1R,9S)-(-)-*trans*-β-caryophyllene	1E

Table S3, Melaleuca alternifolia EO enantiomeric composition

I^tsexp	I^tslit	**Compound**	**% enantiomeric composition (Australian)**	**% enantiomeric composition (Chinese)**
929	921	(R)-(+)-α-pinene	n.r.	n.r.
929	923	(S)-(-)-α-pinene	n.r.	n.r.
952	944	(R)-(+)-β-pinene	67.9	5.3
963	955	(S)-(-)-β-pinen	32.1	94.7
1020	1017	(R)-(-)-phellandrene	39.4	47.7
1024	1020	(S)-(+)-phellandrene	60.6	52.3
1060	1056	(S)-(-)-limonene	39.0	2.0
1077	1072	(R)-(+)-limonene	61.0	98.0
1250	1248	(S)-(+)-4-terpineol	67.2	42.2
1258	1253	(R)-(-)-4-terpineol	32.8	57.8
1302	1296	(S)-(-)-α-terpineol	24.2	23.0
1317	1309	(R)-(+)-α-terpineol	75.8	77.0

Table S4 Equations of the calibration curves used to quantitate the marker compounds together with their correlation coefficient and the selected range of concentration.

Compound	Calibration range (mg/mL)	Calibration curve equation	Correlation values
linalool	0.047 – 4.7	y = 65878209x + 12265089	0.9894
linalyl acetate	0.047 – 4.7	y = 71332322x + 13224402	0.9896
4-terpineol	0.5 - 5.0	y = 32642349x + 4197503	0.9989
α-terpineol	0.5 - 5.0	y = 20059684x + 2201700	0.9993
(R)-(-)-linalool	0.047 – 4.7	y = 94371962x + 17161963	0.9989
(S)-(+)-linalool	0.047 – 4.7	y = 94648975x + 17010288	0.9992
(R)-(-)-linalyl acetate	0.5 - 5.0	y = 90768850x + 13321659	0.9994
(S)-(+)-linalyl acetate	0.5 - 5.0	y = 90026414x + 7356410	0.9990

1.8.1.7 References

1. European Directorate for the Quality of Medicines & HealthCare (EDQM), European Pharmacopoeia, 10th ed.; 2021.
2. Aromatic Natural Raw Materials—Vocabulary; ISO NORM 9235:2013, International Organization for Standardization.
3. Bicchi, C.; Liberto, E.; Matteodo, M.; Sgorbini, B.; Mondello, L.; d'Acampora Zellner, B.; Costa, R.; Rubiolo, P. Quantitative analysis of essential oils: A complex task. Flav Fragr. J. **2008**, 23, 382–391.
4. Can Baser, K.H.; Buchbauer, G. (Eds.) Handbook of Essential Oilss—Science, Technology and Applications; CRC Press: Boca Raton, FL, USA, 2020.
5. Cagliero, C.; Sgorbini, B.; Cordero, C.; Liberto, E.; Rubiolo, P.; Bicchi, C. Enantioselective Gas Chromatography with Derivatized Cyclodextrins in the Flavour and Fragrance Field. Israel J. Chem. **2016**, 56, 925–939.
6. Dewick, P.M. Medicinal Natural Products: A Biosynthetic Approach; Wiley: Chirchester, UK, 2009.
7. Do, T.K.T.; Hadji-Minaglou, F.; Antoniotti, S.; Fernandez, X. Authenticity of essential oils. Trends Anal. Chem. **2015**, 66, 146–157.
8. Boren, K.E.; Young, D.G.; Woolley, C.L.; Smith, B.L.; Carlson, R.E. Detecting Essential Oil Adulteration. J. Environ. Anal. Chem. **2015**, 2, 1000132.
9. Feudjio, W.M.; Ghalila, H.; Nsangou, M.; Majdi, Y.; Kongbonga, Y.M.; Jaïdane, N. Fluorescence Spectroscopy Combined with Chemometrics for the Investigation of the Adulteration of Essential Oils. Food Anal. Methods **2017**,10, 2539–2548.
10. Vargas Jentzsch, P.; Gualpa, F.; Ramos, L.A.; Ciobotă, V. Adulteration of clove essential oil: Detection using a handheld Raman spectrometer. Flav. Fragr. J. **2017**, 33, 184–190.
11. Truzzi, E.; Marchetti, L.; Bertelli, D.; Benvenuti, S. Attenuated Total Reflectance–Fourier Transform Infrared (ATR–FTIR) Spectroscopy Coupled with Chemometric Analysis for Detection and Quantification of Adulteration in Lavender and Citronella Essential Oils. Phytochem. Anal. **2021**, No. pca.3034.
12. Truzzi, E.; Marchetti, L.; Benvenuti, S.; Ferroni, A.; Rossi, M.C.; Bertelli, D. Novel Strategy for the Recognition of Adulterant Vegetable Oils in Essential Oils Commonly Used in Food Industries by Applying (13)C NMR Spectroscopy. J. Agric. Food Chem. **2021**, 69, 8276–8286.
13. Essential Oils Market. Available online: https://www.statista.com/study/60656/essential-oils-market/ (accessed on 1st July 2021).
14. Verzera, A.; Lamonica, G.; Mondello, L.; Trozzi, A.; Dugo, G. The composition of bergamot oil. Perf. Flavor. **1996**, 21, 19–35.
15. Mondello, L.; Verzera, A.; Previti, P.; Crispo, F.; Dugo, G. Multidimensional capillary GC-GC for the analysis of complex samples. Enantiomeric distribution of monoterpene hydrocarbons, monoterpene alcohols and linalyl acetate of bergamot (Citrus bergamia Risso et Poiteau) oils. J. Agric. Food Chem. **1998**, 46, 4275–4282.
16. ISO 4730:2017. Essential Oil of Melaleuca, terpinen-4-ol Type (Tea Tree Oil). Available online: www.iso.org (accessed on 1st July 2021).
17. Wong, Y.F.; Davies, N.W.; Chin, S.T.; Larkman, T.; Marriott, P.J. Enantiomeric distribution of selected terpenes for authenticity assessment of Australian Melaleuca alternifolia oil. Ind. Crops Prod. **2015**, 67, 475– 483.
18. Sgorbini, B.; Cagliero, C.; Boggia, L.; Liberto, E.; Reichenbach, S.E.; Rubiolo, P.; Cordero, C.; Bicchi, C. Parallel dual secondary-column-dual detection comprehensive two-dimensional gas chromatography: A flexible and reliable analytical tool for essential oils quantitative profiling. Flav. Fragr. J. **2015**, 30, 366–80.

19. Agnel, R.; Teisseire, P. Essential Oil of French Lavender—Its Composition and Its Adulteration. Perf. Flavor. **1984**, 9, 53–56.
20. Bicchi, C.; D'Amato, A.; Manzin, V.; Galli, A.; Galli, M. Cyclodextrin derivatives in the gas chromatographic separation of racemic mixtures of volatile compounds X. 2,3-Di-O-ethyl-6-O-tert-butyldimethylsilyl-β- and -γ-cyclodextrins. J. Chromatogr. A **1996**, 742, 161–173.
21. Adams, R.P. Identification of Essential Oil Components by Gas Chromatography/Mass Spectrometry, 4th ed.; Allured Publ.: Carol Stream, IL, USA, 2007.
22. Liberto, E.; Cagliero, C.; Sgorbini, B.; Bicchi, C.; Sciarrone, D.; D'Acampora Zellner, B.; Mondello, L.; Rubiolo, P. Enantiomer identification in the flavour and fragrance fields by "interactive" combination of linear retention indices from enantioselective gas chromatography and mass spectrometry. J. Chromatogr. A **2008**, 1195, 117–126.
23. Costa, R.; d'Acampora Zellner, B.; Crupi, M.L.; De Fina, M.R.; Valentino, M.R.; Dugo, P.; Dugo, G.; Mondello, L. GC-MS, GC-O and enantio-GC investigation of the essential oil of Tarchonanthus camphoratus L. Flav. Fragr. J. **2008**, 23, 40–48.
24. Wang, Y.; O'Reilly, J.; Chen, Y.; Pawliszyn, J. Equilibrium in-fibre standardisation technique for solid-phase microextraction. J. Chromatogr. A **2005**, 1072, 13–17.
25. Bicchi, C.; Cordero, C.; Liberto, E.; Sgorbini, B.; Rubiolo, P. Reliability of fibres insolid phase microextraction for routine analysis of the headspace of aromaticand medicinal plants. J. Chromatogr. A **2007**, 1152, 138–149.
26. Markelov, M.; Guzowski, J.P. Matrix independent headspace gas chromatographic analysis. This full evaporation technique. Anal. Chim. Acta **1993**, 276, 235–245.
27. Kolb, B.; Ettre, L.S. Static Headspace-Gas Chromatography, Theory and Practice; Wiley–VCH: New York, NY, USA, 1997.
28. Ezquerro, O.; Ortiz, G.; Pons, B.; Tena, M.T. Determination of benzene, toluene, ethylbenzene and xylenes in soils by multiple headspace solid-phase microextraction. J. Chromatogr. A **2004**, 1035, 17–22.
29. Bicchi, C.; Ruosi, M.R.; Cagliero, C.; Cordero, C.; Liberto, E.; Rubiolo, P.; Sgorbini, B. Quantitative analysis of volatiles from solid matrices of vegetable origin by high concentration capacity headspace techniques: Determination of furan in roasted coffee. J. Chromatogr. A **2011**, 1218, 753–762.
30. Sgorbini, B.; Bicchi, C.; Cagliero, C.; Cordero, C.; Liberto, E.; Rubiolo, P. Herbs and spices: Characterization and quantitation of biologically-active markers for routine quality control by multiple headspace solid-phase microextraction combined with separative or non-separative analysis. J. Chromatogr. A **2015**, 1376, 9–17.
31. Klee, M.S.; Blumberg, L.M. Theoretical and practical aspects of fast gas chromatography and method translation. J. Chromatogr. Sci. **2002**, 40, 234–247.
32. GC Method Translation Software Available online: https://www.agilent.com/en-us/support/gas-chromatography/gcmethodtranslation?searchTermRedirect=gc%20method%20translation (accessed on 1st July 2021).

1.8.2 Exploiting the Versatility of Vacuum Assisted Headspace Solid-Phase Microextraction in Combination with the Selectivity of Ionic Liquids-Based GC Stationary Phases to Discriminate *Boswellia Ssp*. Resins Through Their Volatile and Semi-Volatile Fractions

Francesca Capetti[1], Patrizia Rubiolo[1], Carlo Bicchi[1], Arianna Marengo[1], Barbara Sgorbini[1], Cecilia Cagliero[1*]

Affiliation:
[1]Dipartimento di Scienza e Tecnologia del Farmaco, Università degli Studi di Torino, Turin, Italy

*Corresponding author
Cecilia Cagliero, Via P. Giuria 9, 10125 Turin, Italy, e-mail: cecilia.cagliero@unito.it

Received: January 22, 2020
Revised: February 11, 2020
Accepted: February 18, 2020

Bibliography

Journal of separation science
DOI: 10.1002/jssc.202000084

1.8.2.1 Abstract

The frankincense resins, secreted from *Boswellia* species, are an uncommon example of a natural raw material where every class of terpenoids is present in similar proportions. Diterpenoids (serratol, incensole, and incensole acetate) are used to discriminate samples from different species and origins. Headspace solid-phase microextraction has been used for frankincense analysis, although it requires long sampling time for medium- to low-volatility markers; headspace solid-phase microextraction under vacuum can overcome this limit. Gas chromatography is used for analysis but the separation of incensole and serratol needs polar stationary phases. In this study, we develop a method to discriminate frankincenses based on vacuum-assisted headspace solidphase microextraction combined with fast gas chromatography-mass spectrometry with ionic liquid–based stationary phases. The optimized conditions for solid samples were: air evacuation below 0◦C, 15 min of incubation time, and 15 min of extraction time. Losses of volatiles due to vial air-evacuation in the presence of the sample were minimized by sample amount above 100 mg and low sample temperature. Fast gas chromatography provides the baseline separation of all markers in 20 min. By applying vacuum sampling and fast gas chromatography, the total analysis was reduced to 50 min compared to 120 min (60 min sampling plus 60 min analysis) as previously reported. The method was successfully applied to commercial frankincense samples.

Key words: fast gas chromatography, ionic liquids, resins, stationary phases

1.8.2.2 Introduction

The burning of incense is probably the oldest perfuming method in existence, and frankincense gum oleoresins (also known as olibanum) are a central ingredient in many incense mixtures. Frankincense resins are secreted from trees of the genus *Boswellia*, and typically appear as pea- to thumb sized grains with a translucent, whitish-yellow to dark brown color. About 30 species of *Boswellia* are known and many of them are used to produce frankincense resins. The main commercial sources are: *Boswellia sacra* Flueck. (Arabian Frankincense), which is a top quality product and native to Oman and Somalia; *Boswellia serrata* Roxb. ex Colebr.(Indian Frankincense) from India and widely used in Ayurvedic, Hindu, and Buddhist medicines; *Boswellia papyrifera* (Caill. ex Delile) Hochst., which grows in coastal regions of Sudan, Eritrea, Ethiopia, and northern Somalia; and *Boswellia frereana* Birdw., which is typically found in Somalia, but is of lower commercial interest [1]. Besides the most commercially relevant plants, other rarer species are available, such as the endemic *Boswellia* species from the island of Socotra, *Boswellia ameero* Balf. f., *Boswellia dioscoridis* Thulin, *Boswellia elongata* Balf. f., and *Boswellia socotrana* Balf. f. [2]. Frankincense resin is an uncommon example of a natural raw material in which each terpenic class (mono-, sesqui-, di-, and triterpenoids) is present in rather similar proportions. Boswellic acids, which are pentacyclic triterpenic acids, are nonvolatile markers [3] and have shown to possess anti-inflammatory properties, while the essential oil from frankincense resins is a common raw material in perfumery. The market value of frankincense is strongly influenced by differences in composition, and approximately varies from 5 US$/kg for *B. serrata* to 150 US$ kg−1 for *B. sacra* [4]. The volatile and semivolatile fractions of *Boswellia* species are rather complex and differ notably in composition and odor. In general, the resins mainly contain mono-, sesqui-, and diterpenoids, with *B. papyrifera*, in particular, being characterized by n-octyl acetate, n-octanol, and the significant presence of diterpenoids. These diterpenoids are cembrane derivatives; in particular, serratol (also known as cembrenol), incensole, and incensole acetate (see **Fig. 1**). They are present in most *Boswellia* resins although in different amounts and proportions [2,4–7]. They can therefore be used to discriminate between samples of different species and origins, and act as a complement to the fast screening method, which is based on a quality evaluation of odor and a visual assessment of color that is commonly used. The characterization of the frankincense volatile fractionis generally carried out via the direct use of GC-MS on the essential oils that are obtained from the steam- or hydrodistillation of the resins. This, however, is not a convenient approach to fast screening as it is time-consuming and requires considerable sample amounts. SPME, and in particular when combined with headspace (HS)-SPME, can well fit to this aim. HS-SPME is a solvent-free high concentration capacity sampling technique [8], where target analytes are transferred from the matrix to a polymeric fiber coating via two consecutive steps (matrix/headspace and headspace/fiber), and recovery is maximized when the equilibrium of the full process is reached. The time needed to reach equilibrium depends on several factors, such as the properties of the analytes, matrix, and fiber coating. Although conventional HS-SPME was already applied to characterize frankincense resins [7,9,10], it shows obvious limits to achieve equilibrium with semivolatiles and implies long extraction times and high extraction temperatures. These limits can be overcome by vacuum-assisted HS-SPME (Vac-HS-

SPME), a technique where a low sampling pressure is applied during HS-SPME sampling. Vacuum facilitates the volatilization of semivolatiles by reducing the resistance found in the thin gas film layer adjacent to the sample-headspace interface. Analytes are transferred to the headspace faster and the time needed to reach equilibrium is reduced. Sampling under vacuum greatly improves the extraction kinetics (speed) of lower volatility compounds resulting in high extraction efficiency and sensitivity over time [11,12]. The complexity of the volatile fraction of frankincense resins means that it is mandatory that a GC stationary phase (SP) with the appropriate selectivity to separate all olibanum components, in particular the characterizing markers, is chosen for use. Most studies involve GC analyses carried out with apolar columns because of their efficiency, stability at high temperature, and high amount of available data (i.e. retention indices) for analyte identification. Unfortunately, apolar SPs do not separate two of the discriminating diterpenic markers (incensole and serratol), which often leads to erroneous identification (i.e. the coelution peak has also been hypothesized to be isoincensole) [6]. Polar columns are therefore mandatory for the correct characterization of the resins. In this respect, the introduction of ionic liquids (ILs) for use as SPs has opened up new possibilities in the separation of critical pairs of compounds in natural matrices [13–18]. These SPs show peculiar selectivity and a comparable, or higher polarity than conventional polydimethylsiloxane- and polyethyleneglycolbased columns, and, at the same time, provide similar, or even higher maximum allowable operating temperatures and lower bleeding than most polyethyleneglycol -based SPs. This article describes the development of a simple and fast method to sample volatiles and semivolatiles markers characteristic of *Boswellia* spp. resins. The proposed method uses Vac-HS-SPME combined with fast GC-MS with narrow bore columns coated with IL SPs to discriminate between frankincenses and is applicable to quality control methods [19–23].

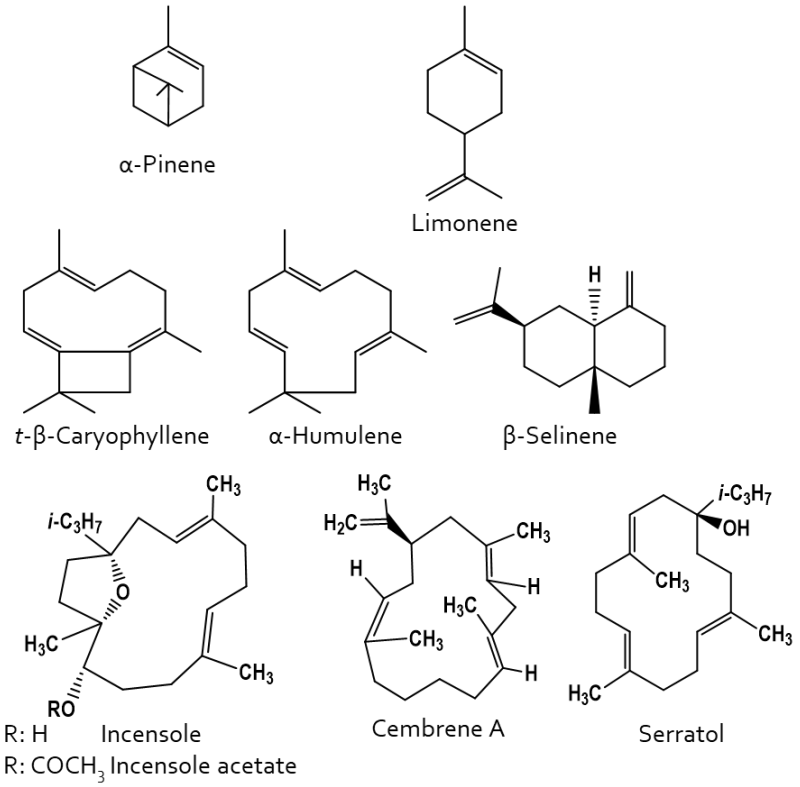

Figure 1 Chemical structures of the main markers of the frankincense resins

1.8.2.3 Materials and Methods

Chemicals and samples:

Incensole, incensole acetate, and serratol (cembrenol)were all provided by Professor G. Appendino (Università del Piemonte Orientale, Novara, Italy). Standard solutions of incensole, incensole acetate, and serratol were prepared in cyclohexane at a concentration of 100 mg/L and stored at 4◦C. Two authentic *Boswellia* spp. resin samples (one *B. socotrana* Balf. f. and one *B. papyrifera* [Caill. ex Delile] Hochst) were provided by Professor G. Appendino (Università del Piemonte Orientale, Novara, Italy), while a further three commercial frankincense samples, labeled as *B. sacra*, were bought from a local herbalist's shop and were called frankincense 1, 2, and 3. Each frankincense sample was first frozen using liquid nitrogen, then pulverized with a mortar and pestle, and finally stored at −18◦C. The essential oils of the *B. socotrana* and *B. papyrifera* samples, obtained via hydrodistillation according to the European Pharmacopoeia procedure [24], were also analyzed to optimize the chromatographic method.

Vacuum-assisted and regular HS-SPME

The experimental setup adopted to perform Vac-HS-SPME experiments consisted of a commercial headspace 20-mL vial hermetically sealed with a joint stainless steel cap containing a hole that could tightly accommodate a Thermogreen® LB-1 septum with half-hole (6 mm diameter × 9 mm length; Sigma–Aldrich Merck). The gastight cap was provided by Professor Eleftheria Psillakis [25]. The air-evacuation step and the HS-SPME sampling were carried out using Thermogreen® LB-1 septa. The solid sample was placed inside the vial, the vial was then stored at −18◦C for 1 h and finally air-evacuated. The air-evacuation step was carried out using a 22-gauge hypodermic needle sealed to a 5-mL syringe that was tightly secured to the tubing of a N 820.3 FT.18 (7 mbar ultimate vacuum) pumping unit manufactured by KNF Lab (Milan, Italy). The needle was then inserted through the septum and the vial was air-evacuated. Two air-evacuation times (45 and 120 s respectively) were tested. GC desorption lasted 10 min to avoid carryover. To remove the cap, atmospheric pressure was restored inside the vial by piercing the septum with a disposable syringe needle. Regular (Reg-)HS-SPME experiments were performed with the previously described experimental setup, while omitting the air-evacuation step. Divinyl benzene/carboxen/polydimethylsiloxane fibers (1:2 cm long, df: 50/30 mm) were used for both Vac-HS-SPME and Reg-HS-SPME. The fibers were purchased from Supelco Co. (Bellafonte, PA, USA) and conditioned before use as recommended by the manufacturer. Three different sample amounts, 5, 40, and 100 mg, and two sampling temperatures, 50 and 80◦C, were tested. Sampling time profiles were obtained by sampling 100 mg of the investigated matrices at 80◦C for 5, 15, 30, and 60 min. All extractions were run in triplicate. The HS-SPME parameters were optimized using the frankincense resin from *B. socotrana*. All other frankincense resins were sampled by adopting the optimized conditions (100 mg of matrix extracted for 15 min at 80◦C).

Instrumental setup

Analyses were carried out using a Shimadzu GC-FID-MS system consisting of a Shimadzu GC 2010, equipped with flame ionization detector (FID), in parallel with a Shimadzu

QP2010-PLUS GC-MS system; data were processed and elaborated using Shimadzu GC-MS Solution 2.51 and GC Solution 2.53SU software (Shimadzu, Milan, Italy).

Columns:
GC analyses were carried out using two 30 m × 0.25 mm dc, 0.25 µm df conventional columns coated with 95% methyl-polysiloxane, 5% phenyl (SE-52), and autobondable nitroterephthalic-acid–modified polyethylene glycol (FFAPEXT) from Mega (Legnano, Mi, Italy). A conventional IL based SLB-IL60i (30 m × 0.25 mm dc, 0.25 µm df) column, and a narrow bore SLB-IL60 (15m× 0.10mmdc, 0.08 µm df) column from Supelco (Bellefonte, PA, USA) were also used.

GC conditions:
Analyses were carried out under the following conditions: temperatures: injector, 250◦C, transfer line, 270◦C, ion source, 200◦C; carrier gas: He; flow control mode: constant linear velocity; flow rate: 1 ml/min; injection mode: split; and split ratio: 1:20. The MS was operated in electron ionization mode at 70 eV, scan rate: 666 u/s, mass range: 35–350 m/z; FID temperature, 250◦C; and sampling rate, 40 ms. Temperature programs are as follows: (i) 50◦C//5◦C/min//250◦C (5 min) for conventional SE-52, FFAP-EXT, SLB-IL60i columns; (ii) 40◦C//10◦Cmin−1//180◦C//15◦Cmin−1//230◦C (2 min) for the narrow bore SLB-IL60 column. The GC system was alternatively operated with MS or FID as detectors. Identification was performed via comparisons of linear retention indices and mass spectra either with those of authentic standards, or with data stored in commercial and in-house libraries and the results were confirmed using those of previous publications [2,5,7].

Data elaboration:
All elaboration was carried out using Excel (Microsoft) with the exception of the heat map, which was created usingMorpheus software (https://software.broadinstitute.org/morpheus).

1.8.2.4 Results and Discussion

The development of a fast semiautomatic method entails the investigation of each analytical step. In this study, two *Boswellia* essential oils (*B. socotrana* and *B. papyrifera*) were analyzed first on different SPs in order to find a column that could separate most frankincense components, and, in particular, the diterpenoid markers. The second step dealt with the careful optimization of sampling conditions (sample amount, sampling time, and temperature) using *B. socotrana* as the model sample. Vac-HS-SPME and Reg-HSSPME were tested in this step. Finally, the chromatographic method was sped-up to fast GC by translating the analytical conditions from conventional to narrow bore columns. The developed method was then validated on a series of commercial frankincense samples.

Choice of the GC SP:
The choice of a SP that separates as many components aspossible is, of course, a crucial step for the effective characterization of a sample. The diterpenoid markers incensole, incensole acetate and serratol, and the essential oils of *B. socotrana* and *B. papyrifera* were

analyzed with a range of commercially available columns to define the most appropriate SP for their analysis. As has already been mentioned, apolar columns are not appropriate for the analyses of frankincense resins because of the coelution of incensole and serratol (**Figure 2a**). Two polar olumns were therefore tested; the first was a polyethylene–glycol based SP (FFAP-EXT) and the second was an IL-based SP (SLB-IL60i). **Figure 2b** and **c** shows that both columns separate diterpenoids with a good resolution but the SLBIL60i was chosen because of its higher resolution (22 with SLB-IL60i versus 14 with the FFAP-EXT column) and low bleeding. This column not only separates the diterpenic markers but also the other characterizing components. **Figure 3** reports the GC-MS profiles, using the SLB-IL60i column, of the *B. socotrana* and *B. papyrifera* frankincense resins, as sampled by Vac-HS-SPME (see Section 3.2). The SLB-IL60i column was therefore used in this study. Supporting Information **Table S1** reports the list of the compounds identified, their retention times in the conventional and narrow-bore IL-based columns, together with their molecular formula, molecular weight, and main physicochemical properties (logP, boiling point, and vapor pressure).

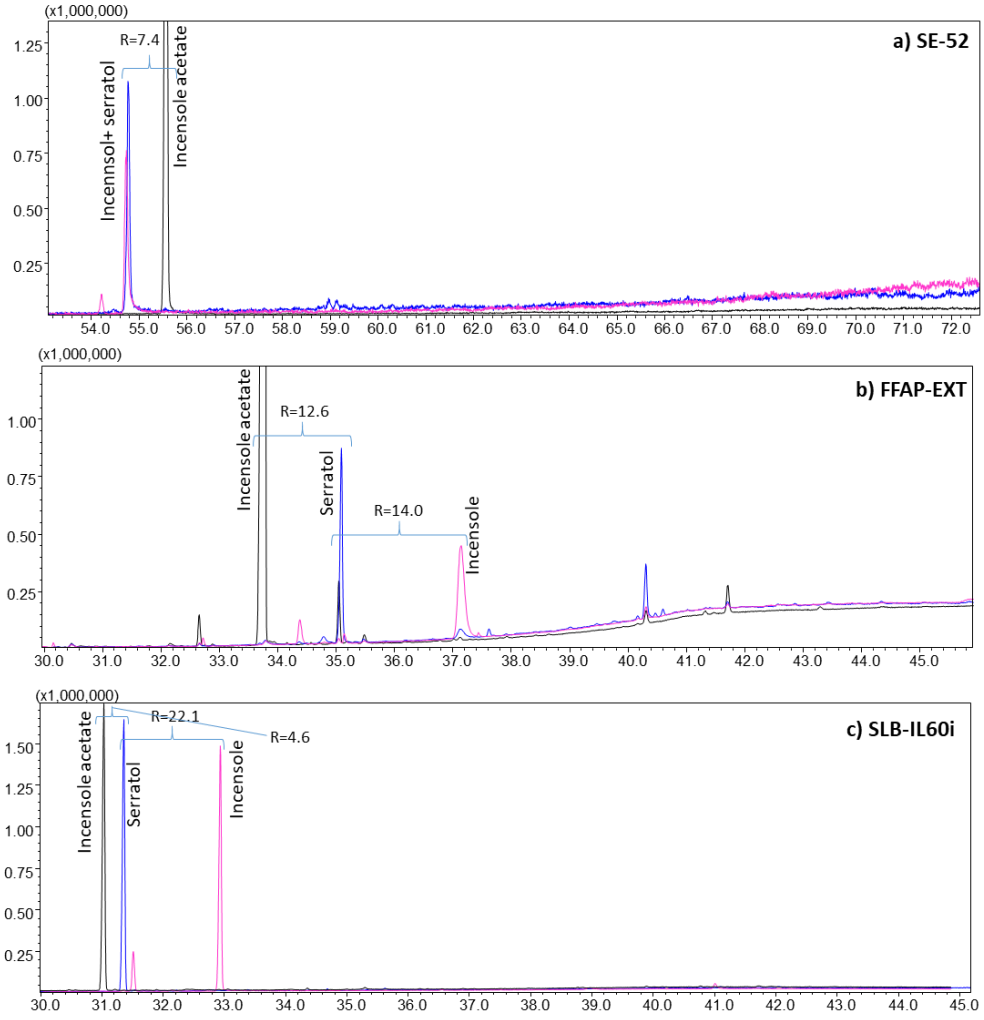

Figure 2, GC-MS profiles of incensole (pink), serratol (blue), and incensole acetate (black) on the conventional SE-52 (a), FFAP-EXT (b), and SLB-IL60i (c) columns. For analysis conditions, see experimental section

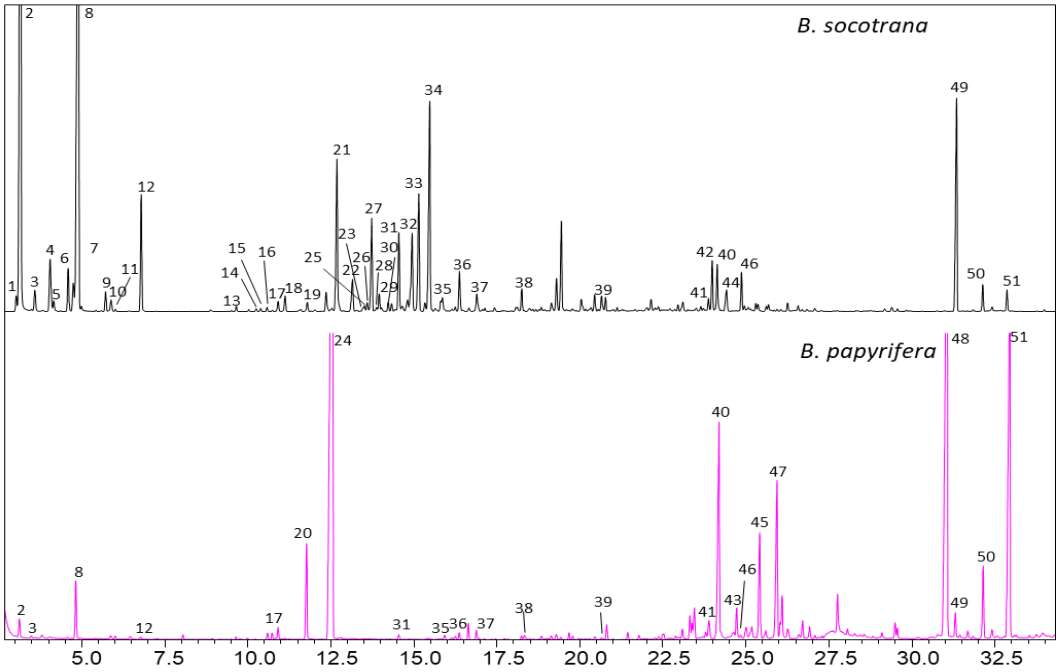

Figure 3, Vac-HS-SPME GC-MS profiles of B. socotrana (black) and B. papyrifera (pink) obtained with the SLB-IL60i column. Analysis conditions: See experimental section. Legend: (1) α-Thujene, 2. α-Pinene, 3. Camphene, 4. β-Pinene, 5. Sabinene, 6. β-Myrcene, 7. α-Phellandrene, 8. Limonene, 9. β-Phellandrene, 10. 1,8-Cineole, 11. trans-β-Ocimene, 12. para-Cymene, 13. o-Methylanisole, 14. α-Cubebene, 15. cis-Sabinene hydrate, 16. p-Cymenene, 17. α-Terpinolene, 18. α-Copaene, 19. β-Bourbonene, 20. Octanol, 21. β-Elemene, 22. trans–Pinocarveol, 23. cis-Verbenol, 24. Octyl acetate, 25. 1,8-Menthadien-4-ol, 26. trans-Verbenol, 27. trans-β-Caryophyllene, 28. Aromadendrene, 29. γ-Selinene, 30. Germacrene D, 31. α-Fenchol, 32. α-Humulene, 33. α-Selinene, 34. β-Selinene, 35. Myrtenol, 36. trans-Carveol, 37. cis-Carveol, 38. Carvone, 39.Verbenone, 40. Cembrene, 41. Limonene-1,2-diol, 42. Caryophyllene oxide, 43. Hydrocarbon diterpene 1, 44. α-Eudesmol, 45. Hydrocarbon diterpene 2, 46. β-Eudesmol, 47. Hydrocarbon diterpene 3, 48. Incensole acetate, 49. Serratol, 50. Cembrene A, 51. Incensole

Sample preparation: Optimization of the Vac-HS-SPME:

The suitable characterization of frankincense resins by HS-SPME entails the optimization of the sampling conditions to ensure that all classes of volatiles and semivolatiles are recovered (mono-, sesqui-, and diterpenoidic compounds) with extraction times that are compatible with those of the chromatographic run. In this section, the performance of the Reg-HS-SPME sampling of a *B. socotrana* resin is compared to that of Vac-HS-SPME. Preliminary experiments showed that the 2 cm long divinyl benzene/carboxen/polydimethylsiloxane fiber provided a complete picture of frankincense composition, and it was therefore chosen for use in the following tests. The next experiments aimed to optimize the conditions for the pre equilibration of the frankincense with the headspace for the subsequent Reg- and Vac-HS-SPME samplings. This step is critical because it influences the repeatability of the results, in particular with Vac-HS-SPME. An equilibration time of 15 min was chosen as it was the minimum time for which repeatability gave an RSD% of below 15% (except for compounds in traces) over five experiments under any applied conditions (data not reported). The sample amount was first optimized by sampling 5, 40, and 100 mg of frankincense for 15 min with both Reg- and Vac-HS-SPME at a sampling temperature of 80◦C [7,9]. With Reg-HS-SPME, the abundance of the high volatility analytes (mono- and sesquiterpenoids) increased with sample amount, while that of the diterpenoids was always very low and did not seem to be significantly affected. The results with 5 mg of sample show that: (i) for monoterpenoids, the

performance of regular sampling is about 50% higher than that of Vac; (ii) for sesquiterpenoids, the difference is lower, but Reg sampling is still more effective than Vac; while (iii) for diterpenoids, the peak areas with Vac sampling are double than those of Reg. **Table 1** reports the relative analyte abundances obtained by sampling with Vac-HS-SPME versus Reg-HS-SPME. The poorer performance of Vac-HS-SPME compared to Reg-HSSPME with the most volatile components is due to the airevacuation step in which they are significantly aspired with air. This loss is not observed for the less volatile compounds for which the reduced pressure of Vac-HS-SPME promoted vaporization to the headspace, although with longer extraction times (i.e., closer to the equilibrium) the two techniques provide similar results (data not reported). As suitable enrichment, in particular for the monoterpenoids, cannot be achieved with 5 mg of resin, the sample amount was increased to 40 mg. The results show that some monoterpenoids are still lost during the air-evacuation step with Vac-HS-SPME, but that the medium volatility compounds show a good improvement (**Table 1**). Finally, 100 mg of sample was evaluated and the results show: (i) Reg-HS-SPME and Vac-HS-SPME have comparable responses for the high volatility components; (ii) slightly improved recovery of medium volatility components (about 1.5 higher); and (iii) drastic improvements in diterpenoids, with peak areas being almost four times higher than Reg-HS-SPME. Further experiments were carried out to exclude any discriminative loss from the headspace over time; air-evacuation times of 45 and 120 s were applied, resulting in perfectly overlapping patterns even for the most volatile compounds. The results show that the slight peak-area differences between Reg-HS-SPME and Vac-HS-SPME are probably related to competition with the adsorbent [12]. The sample amount was then fixed at 100 mg. The sampling time was then optimized by checking the behavior of the frankincense markers when processed with the two investigated techniques with 5, 15, 30, and 60 min of sampling. The results are summarized in Fig. 4. α-Pinene and limonene (monoterpene hydrocarbons) were taken as a reference for the most volatile frankincense components; these compounds reached equilibrium with both Reg-HS-SPME and Vac-HS-SPME, but the longer extraction times necessary with Reg sampling produce a decrease in the extraction efficiency, which is probably related to adsorption competition. Similar behaviour can also be observed for intermediate volatile compounds (trans-β-caryophillene, α-humulene, and β-selinene), although the extraction performance of Vac-HS-SPME was slightly better than that of Reg-HS-SPME. Finally, the extraction time profiles of the diterpenoid markers (serratol, incensole, and cembrene A) show that sampling under reduced pressure permits recovery to be sped-up even with short extraction times (15 min), although equilibrium could not be reached, even over 60 min, by either technique. There were extreme differences in the extraction times needed to reach equilibrium in the different classes of terpenoids with Reg-HS-SPME, and these are in agreement with literature data [26]. The use of Vac-HS-SPME for 15 min was then chosen for the following experiments as it provides the suitable recovery of all compound groups in a short sampling time. The possibility of decreasing the extraction temperature to 50◦Cwas also explored, but a significant decrease in the abundance of diterpenoids was observed (see Supporting Information Fig. S1), meaning that higher extraction temperatures were mandatory.

Table 1 Relative analyte abundance (RAA) obtained by sampling 5, 40, 100mg of B. socotrana with Vac-HS-SPME vs. Reg-HS-SPME for 15 min at 80°C. Legend: red triangle RAA < 0.75, yellow line 0.75 < RAA < 1.25, green triangle RAA > 1.25

Compound Name	5 mg	40 mg	100 mg
alpha-Tujene	0.66	0.60	0.76
alpha-Pinene	0.68	0.69	0.79
Camphene	0.70	0.54	0.76
beta-Pinene	0.50	0.53	0.82
Sabinene	0.41	0.50	0.81
beta-Myrcene	0.60	0.59	0.84
alpha-Phellandrene	0.59	0.67	0.91
Limonene	0.50	0.60	0.84
beta-Phellandrene	0.49	0.55	0.90
1,8-Cineole	0.39	0.53	1.02
p-Cymene	0.49	0.56	0.84
o-Methyl-anisole	0.47	0.56	0.77
p-Cymenene	0.54	0.67	0.99
alpha-Terpinolene	0.37	0.67	1.02
alpha-Copaene	0.33	0.96	1.47
beta-Elemene	0.36	1.01	1.43
trans-Pinocarveol	0.30	0.65	1.00
trans-Caryophyllene	0.35	1.00	1.37
Germacrene D	0.42	1.01	1.40
alfa-Fenchol	0.37	0.83	1.04
alpha-Humulene	0.36	1.12	1.34
alpha-Selinene	0.42	1.25	1.42
beta-Selinene	0.43	1.21	1.41
trans-Carveol	0.43	0.94	1.12
cis-Carveol	0.43	0.98	1.16
Carvone	0.43	0.83	1.11
Limonene-1,2-diol	0.64	1.28	1.10
Caryophyllene oxide	0.33	1.51	1.48
Cembrene	1.19	3.31	2.92
beta-Eudesmol	0.83	2.19	1.85
Serratol	2.32	3.07	3.66
Cembrene A	2.50	2.99	3.71
Benzylbenzoate	1.53	2.32	2.29
Incensole	2.06	2.70	3.93

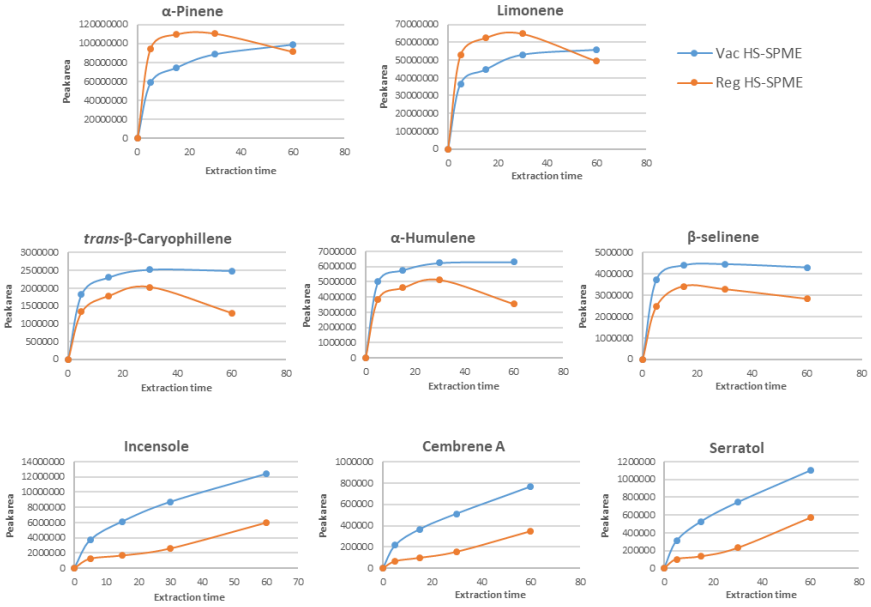

Figure 4 Extraction time profiles of α-pinene, limonene (monoterpenoids), trans-β-caryophyllene, α-humulene, and β-selinene (sesquiterpenoids), serratol, incensole, and cembrene A (diterpenoids) obtained with Vac-HS-SPME (blue) and Reg-HS-SPME (orange).Sampling amount: 100 mg, sampling temperature: 80°C

Speed-up of the analysis step:

The third part of the study was focused on speeding-up the GC analysis to make it compatible with the sampling time. The above chromatographic method was translated to a 15 m × 0.10 mm dc, 0.08 µm df column using the method translation approach [19,20,22]. The analysis time was thus reduced to 19 min, while the separation of all the markers was maintained. Figure 5 reports the translated GC-FID patterns, with the narrow-bore SLB-IL60 column, of the diterpenic markers and the *B. socotrana* and *B. papyrifera* resins.

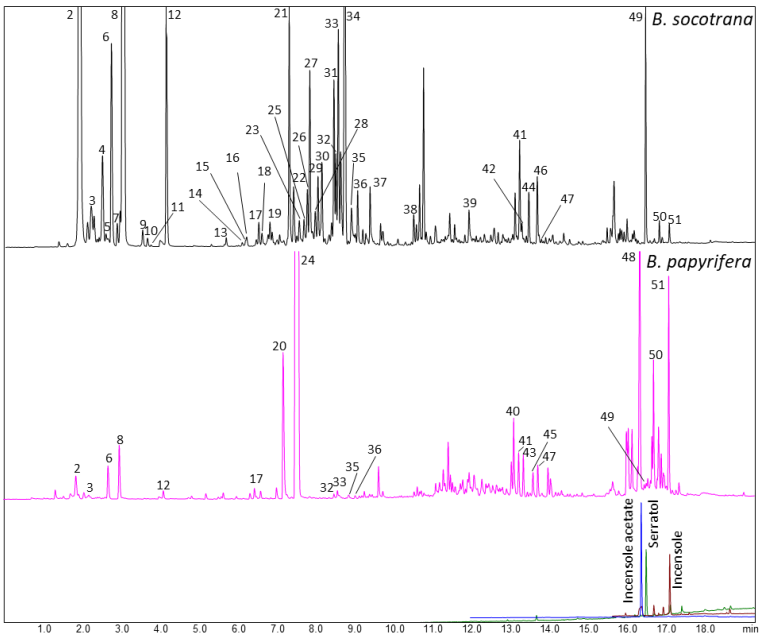

Figure 5 Vac-HS-SPME Fast-GC-MS profiles of B. socotrana (black), B. papyrifera (pink), incensole (brown), serratol (green), and incensole acetate (blue) obtained with the SLB-IL60i column. Analysis conditions: see experimental section. Legend: See caption of Fig 2

Application of the optimized method to real-world frankincense samples:

The two authentic and the three commercial frankincense samples were analyzed with the optimized Vac-HS-SPME–fast-GC-FID-MS method, and the resulting patterns were compared to those obtained with Reg-HS-SPME. The optimal conditions adopted with Vac-HS-SPME were 100 mg of frankincense resin, sampled at 80◦C for 15 min combined with 15 min of pre-equilibrium (total sampling time 30 min). Supporting Information **Tables S2** and **S3** report the mean peak area of each analyte in each sample together with the repeatability (%RSD). The results show thatVac-HS-SPME is more repeatable than Reg-HS-SPME reaching %RSD in general below 10% with the exception of traces. Due to the high number of analytes, the results were summarized in a heat map (**Figure 6**) where the areas of each analyte (row) is scaled in function of their abundance in each sample from minimum (blue) to maximum (red). The samples were also hierarchically clustered by applying the one minus Pearson correlation. The results of the heat map show that: (i) the commercial frankincense 3 sample labeled as *B. sacra*, was actually *B. papyrifera* as proved not only by the high abundance of markers such as octyl acetate, octanol, incensole, and incensole acetate, but also by its clustering with the authentic *B. papyrifera*; (ii) Vac-HS-SPME when compared to Reg-HS-SPME provides a drastic increase of recovery of both hydrocarbons and oxygenated diterpenoids and most oxygenated sesquiterpenoids as it is clear, for instance, from the difference in intensity of (a) incensole, incensole acetate, cembrene, cembrene A, and the other diterpene hydrocarbons in *B. papyrifera* samples or (b) caryophillene oxide, α and β-eudesmol, and serratol in *B. socotrana* and in the commercial sample 2.

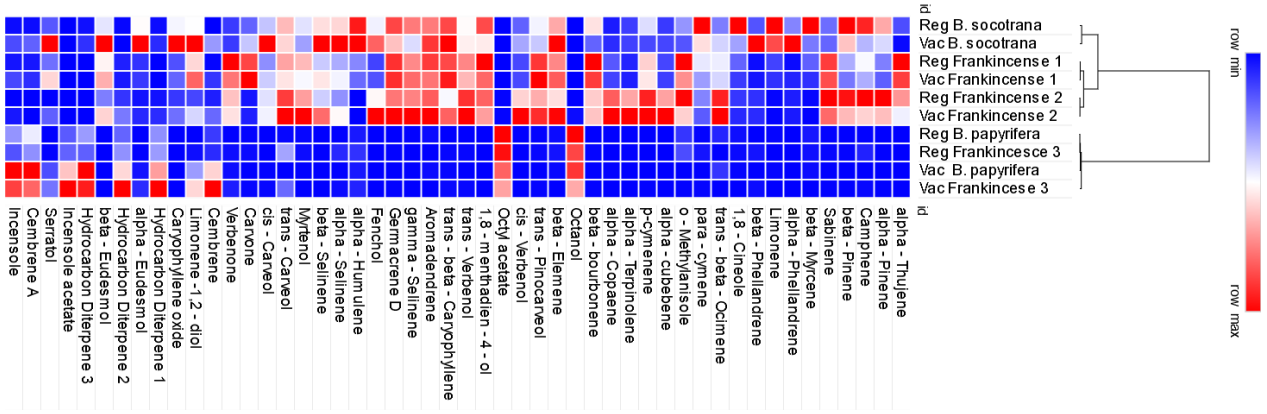

Figure 6 Heat map on the investigated samples sampled by Reg-HS-SPME (Reg) and Vac-HS-SPME (Vac). Samples are hierarchically clustered by applying the one minus Pearson correlation

Conclusion:

A fast and versatile method has been optimized to discriminate *Boswellia spp.* resins using their volatile and semivolatile fractions. The method is based on HS-SPME under reduced pressure (Vac-HS-SPME), which increases the release of semivolatile compounds (i.e. diterpenoidic compounds) in the headspace and enables their sampling in 30 min. Vac-HS-SPME was successfully combined with fast GC, with columns coated with an IL-based SP, providing the baseline separation of all markers in 20 min. After a preliminary air-evacuation, it is possible to overlap sampling and analysis steps enabling to analyze up to five samples of *Boswellia* resins in 2 h that is the analysis time commonly required for a

single sample with conventional methods (60 min sampling and 60 min analysis). The reported method is simple, fast, automated, and compatible with the processing of a large number of samples, as is required in a routine quality control laboratory. This study shows, for the first time, that Vac-HS-SPME can successfully be applied to the analysis of semivolatiles in solid samples in the plant and natural products fields and that losses of volatiles due to vial air-evacuation in the presence of the sample can be effectively minimized by using low sample temperature (below 0◦C) and a sample amount above 100 mg. Further studies are under way to optimize the method for quantitation.

1.8.2.5 References

1. Al-Harrasi, A., Csuk, R., Khan, A., Hussain, J., Distribution of theanti-inflammatory and anti-depressant compounds: Incensole and incensole acetate in genus Boswellia. Phytochemistry 2019, 161, 28–40.

2. Mothana, R.A.A., Hasson, S. S., Schultze, W.,Mowitz,A., Lindequist, U., Phytochemical composition and in vitro antimicrobial and antioxidant activities of essential oils of three endemic Soqotraen *Boswellia* species. Food Chem. 2011, 126, 1149–1154.

3. Zhang, C., Sun, L., Tian, R.-t., Jin, H.-y., Ma, S.-c., Gu, B.-r., Combination of quantitative analysis and chemometric analysis for the quality evaluation of three different frankincenses by ultra high performance liquid chromatography and quadrupole time of flight mass spectrometry. J. Sep. Sci. 2015, 38, 3324–3330.

4. Niebler, J., Incense materials, in: Buettner, A. (Ed.), Springer Handbook of Odor, Springer International Publishing, Cham 2017, pp. 63–86.

5. Mertens, M., Buettner, A., Kirchhoff, E., The volatile constituents of frankincense —a review. Flavour Frag. J. 2009, 24, 279–300.

6. Niebler, J., Buettner, A., Identification of odorants in frankincense (*Boswellia sacra* Flueck.) by aroma extract dilution analysis and two-dimensional gas chromatography-mass spectrometry/ olfactometry. Phytochemistry 2015, 109, 66–75.

7. Niebler, J., Buettner, A., Frankincense revisited, Part I: Comparative analysis of volatiles in commercially relevant *Boswellia* species. Chem. Biodivers. 2016, 13, 613–629.

8. Sgorbini, B., Cagliero, C., Cordero, C., Liberto, E., Rubiolo, P., Bicchi, C., in: Hostettmann, K., Stuppner, H., Marston, A., Chen, S.(Eds.), Encyclopedia of Analytical Chemistry,Wiley, Hoboken, NJ 2014, pp. 1–10.

9. Hamm, S., Bleton, J., Connan, J., Tchapla, A., A chemical investigation by headspace SPME and GC–MS of volatile and semi-volatile terpenes in various olibanum samples. Phytochemistry 2005, 66, 1499–1514.

10. Hamm, S., Bleton, J., Tchapla, A., Headspace solid phase microextraction for screening for the presence of resins in Egyptian archaeological samples. J. Sep. Sci. 2004, 27, 235–243.

11. Psillakis, E., Vacuum-assisted headspace solid-phase microextraction: A tutorial review. Anal. Chim. Acta 2017, 986, 12–24.

12. Trujillo-Rodriguez, M. J., Pino, V., Psillakis, E., Anderson, J. L., Ayala, J. H., Yiantzi, E., Afonso, A. M., Vacuum-assisted headspace-solid phase microextraction for determining volatile free fatty acids and phenols. Investigations on the effect of pressure on competitive adsorption phenomena in a multicomponent system. Anal. Chim. Acta 2017, 962, 41–51.

13. Cagliero, C., Bicchi, C., Ionic liquids as gas chromatographic stationary phases: How can they change food and natural-product analyses? Anal. Bioanal. Chem. 2020, 412, 17–25.

14. Mazzucotelli, M., Bicchi, C., Marengo, A., Rubiolo, P., Galli, S., Anderson, J. L., Sgorbini, B., Cagliero, C., Ionic liquids as stationary phases for gas chromatography — Unusual selectivity of ionic

liquids with a phosphonium cation and different anions in the flavor, fragrance and essential oil analyses. J. Chromatogr. A 2019, 1583, 124–135.
15. Cagliero, C., Bicchi, C., Cordero, C., Liberto, E., Rubiolo, P., Sgorbini, B., Ionic liquids as water-compatible GC stationary phases for the analysis of fragrances and essential oils. Anal. Bioanal. Chem. 2018, 410, 4657–4668.
16. Cagliero, C., Bicchi, C., Cordero, C., Liberto, E., Rubiolo, P., Sgorbini, B., Analysis of essential oils and fragrances with a new generation of highly inert gas chromatographic columns coated with ionic liquids. J. Chromatogr. A 2017, 1495, 64–75.
17. Cagliero, C., Bicchi, C., Cordero, C., Liberto, E., Sgorbini, B., Rubiolo, P., Room temperature ionic liquids: New GC stationary phases with a novel selectivity for flavor and fragrance analyses. J. Chromatogr. A 2012, 1268, 130–138.
18. Ragonese, C., Sciarrone, D., Grasso, E., Dugo, P., Mondello, L., Enhanced resolution of *Mentha piperita* volatile fraction using a novel medium-polarity ionic liquid gas chromatography stationary phase. J. Sep. Sci. 2016, 39, 537–544.
19. Mazzucotelli, M., Minteguiaga, M. A., Sgorbini, B., Sidisky, L., Marengo, A., Rubiolo, P., Bicchi, C., Cagliero, C., Ionic liquids as water-compatible GC stationary phases for the analysis of fragrances and essential oils: Quantitative GC–MS analysis of officially-regulated allergens in perfumes. J. Chromatogr. A 2020, 1610, 460567.
20. Cagliero, C., Guglielmetti, A., Cordero, C., Liberto, E., Marengo, A., Sgorbini, B., Rubiolo, P., Bicchi, C., "Truly natural": Fully automated stir-bar sorptive extraction with enantioselectiveGC-MS quantitation of chiral markers of peach aroma. LC GC N. Am. 2019, 37, 35–42.
21. Cagliero, C., Bicchi, C., Cordero, C., Rubiolo, P., Sgorbini, B., Liberto, E., Fast headspace-enantioselective GC-mass spectrometricmultivariate statistical method for routine authentication of flavoured fruit foods. Food Chem. 2012, 132, 1071–1079.
22. Bicchi, C., Blumberg, L., Cagliero, C., Cordero, C., Rubiolo, P., Liberto, E., Development of fast enantioselective gas-chromatographic analysis using gas-chromatographic method-translation software in routine essential oil analysis (lavender essential oil). J. Chromatogr. A 2010, 1217, 1530–1536.
23. Rubiolo, P., Liberto, E., Sgorbini, B., Russo, R., Veuthey, J.-L., Bicchi, C., Fast-GC–conventional quadrupole mass spectrometry in essential oil analysis. J. Sep. Sci. 2008, 31, 1074–1084.
24. European Pharmacopoeia Ph. Eur. 10th Edition. https://www.edqm.eu/en/european_pharmacopoeia_10th_edition.
25. Psillakis, E., Methods and vial closures for headspace extraction under vacuum. US patent 62/939,359. 2019.
26. Deibler, K. D., Acree, T. E., Lavin, E. H., Solid phase microextraction application in gas chromatography/olfactometry dilution analysis.J. Agric. Food Chem. 1999, 47, 1616–1618.

1.8.2.6 Supplementary Material

Table S1, Identified compounds, retention times (RT) on the conventional and narrow bore ionic liquid-based columns, molecular formula, molecular weight and main physicochemical properties (LogP, boiling point and vapour pressure).

#	Compound	RT (min) SBL-IL60i	RT (min) SBL-IL60 NB	Molecular Formula	Molecular Weight	LogP[a]	Boiling Point °C (760 mmHg)[a]	Vapour pressure mmHg (25°C)[a]
1	**α-Tujene**	3.04	1.77	$C_{10}H_{16}$	136	4.022 (est)	150-152	4.8
2	**α-Pinene**	3.18	1.90	$C_{10}H_{16}$	136	4.830	156	4.8
3	**Camphene**	3.60	2.20	$C_{10}H_{16}$	136	4.220	159	3.4
4	**β-Pinene**	4.06	2.49	$C_{10}H_{16}$	136	4.160	163-166	2.9
5	**Sabinene**	4.17	2.58	$C_{10}H_{16}$	136	3.940	163-165	2.6
6	**β-Myrcene**	4.60	2.73	$C_{10}H_{16}$	136	4.170	166-167	2.3
7	**α-Phellandrene**	4.76	2.87	$C_{10}H_{16}$	136	4.408	175-176	1.9
8	**Limonene**	4.92	3.05	$C_{10}H_{16}$	136	4.570	175-177	0.2
9	**β-Phellandrene**	5.74	3.53	$C_{10}H_{16}$	136	4.354	174-176	1.6
10	**1,8-Cineole**	5.89	3.65	$C_{10}H_{18}O$	154	2.740	176-177	1.9
11	***trans*-β-Ocimene**	6.03	3.74	$C_{10}H_{16}$	136	4.418 (est)	174-175	1.6
12	***p*-Cymene**	6.81	4.13	$C_{10}H_{14}$	134	4.100	176-178	1.5
13	***o*-Methylanisole**	9.68	5.67	$C_8H_{10}O$	122	2.740	170-172	1.9
14	**α-Cubebene**	10.28	6.09	$C_{15}H_{20}$	204	6.263 (est)	245-246	0.014
15	***cis* Sabinene hydrate**	10.42	6.17	$C_{10}H_{18}O$	154	2.351	200-201	0.075
16	***p*-Cymenene**	10.61	6.20	$C_{10}H_{12}$	104	2.351 (est)	-	-
17	**α-Terpinolene**	10.95	6.52	$C_{10}H_{16}$	136	4.470	183-185	1.1
18	**α-Copaene**	11.15	6.60	$C_{15}H_{24}$	204	5.710	246-251	0.038
19	**β-Bourbonene**	11.82	6.80	$C_{15}H_{24}$	204	6.128 (est)	121	0.025
20	**Octanol**	11.81	7.23	$C_8H_{18}O$	130	3.00 (est)	-	-
21	**β-Elemene**	12.72	7.30	$C_{15}H_{24}$	204	5.772 (est)	251-253	0.028
22	***trans*-Pinocarveol**	13.19	7.42	$C_{10}H_{16}O$	152	2.379 (est)	217-218	0.028
23	***cis*-Verbenol**	13.50	7.56	$C_{10}H_{16}O$	152	2.554 (est)	214-215	0.033
24	**Octyl acetate**	12.58	7.60	$C_{10}H_{20}O_2$	172	3.842 (est)	206-211	0.19

#	Compound	RT (min) SBL-IL6oi	RT (min) SBL-IL6o NB	Molecular Formula	Molecular Weight	LogP[a]	Boiling Point °C (760 mmHg)[a]	Vapour pressure mmHg (25°C)[a]
25	**1,8-menthadien-4-ol**	13.54	7.68	$C_{10}H_{16}O$	152	2.740 (est)	224	-
26	***trans*-Verbenol**	13.63	7.77	$C_{10}H_{16}O$	152	2.554 (est)	214-215	0.033
27	***trans*-β-Caryophyllene**	13.77	7.83	$C_{15}H_{24}$	204	6.300	256-259	0.013
28	**Aromadendrene**	13.91	7.97	$C_{15}H_{24}$	204	6.427 (est)	258-259	0.023
29	**γ-Selinene**	13.99	8.04	$C_{15}H_{24}$	204	6.729 (est)	269-270	0.012
30	**Germacrene-D**	14.27	8.15	$C_{15}H_{24}$	204	6.566 (est)	279-280	0.007
31	**α-Fenchol**	14.59	8.46	$C_{10}H_{18}O$	154	2.550 (est)	202-203	0.069
32	**α-Humulene**	14.98	8.51	$C_{15}H_{24}$	204	6.592 (est)	166-168	0.0080
33	**α-Selinene**	15.19	8.57	$C_{15}H_{24}$	204	6.409 (est)	270	0.012
34	**β-Selinene**	15.52	8.73	$C_{15}H_{24}$	204	6.327 (est)	260-263	0.017
35	**Myrtenol**	15.90	8.89	$C_{10}H_{16}O$	152	3.220	221-222	0.018
36	***trans*-Carveol**	16.41	9.05	$C_{10}H_{16}O$	152	2.819 (est)	231-232	0.012
37	***cis*-Carveol**	16.94	9.37	$C_{10}H_{16}O$	152	2.819	232	0.012
38	**Carvone**	18.29	10.50	$C_{10}H_{14}O$	150	3.070	137-138	0.16
39	**Verbenone**	20.70	11.92	$C_{10}H_{14}O$	150	2.139 (est)	-	0.077
40	**Cembrene**	24.20	13.15	$C_{20}H_{32}$	272		-	-
41	**Limonene-1,2-diol**	23.93	13.27	$C_{10}H_{18}O_2$	170	1.299 (est)	241-242	0.0060
42	**β-Caryophyllene oxide**	24.04	13.28	$C_{15}H_{24}O$	220	4.429 (est)	280	0.0070
43	**Hydrocarbon Diterpene 1**	24.78	13.39	$C_{20}H_{32}$	272	-	-	-
44	**α-Eudesmol**	24.48	13.46	$C_{15}H_{26}O$	222	4.650	299-302	0.00010
45	**Hydrocarbon Diterpene 2**	25.48	13.64	$C_{20}H_{32}$	272	-	-	-
46	**β-Eudesmol**	24.93	13.68	$C_{15}H_{26}O$	222	4.568 (est)	301-302	0.00010
47	**Hydrocarbon Diterpene 3**	26.00	13.77	$C_{20}H_{32}$	272	-	-	-
48	**Incesole acetate**	31.12	16.39	$C_{21}H_{34}O_3$	318	-	-	-
49	**Serratol**	31.45	16.47	$C_{20}H_{34}O$	290	-	-	-
50	**Cembrene A**	32.22	16.83	$C_{20}H_{32}$	272	-	-	-
51	**Incensole**	32.95	17.08	$C_{19}H_{32}O_2$	292	-	-	-

a: The Good Scents Company - Flavor, Fragrance, Food and Cosmetics Ingredients information [website]. Available at: http://www.thegoodscentscompany.com/. Est = estimated

Table S2, Mean peak area and %RSD on three replicates of the analytes on the investigated samples sampled by Reg-HS-SPME

	B. socotrana		***B. papyrifera***		**Frankincense 1**		**Frankincense 2**		**Frankincesce 3**	
	Mean	**% RSD**	**Mean**	**% RSD**	**Mean**	**% RSD**	**Mean**	**% RSD**	**Mean**	**% RSD**
α-Thujene	1913	8.10	-	-	12695	7.98	8995	13.52	-	-
α-Pinene	3087386	2.09	12558	10.25	1161907	7.90	4610099	0.15	29609	0.98
Camphene	81807	0.63	565	10.51	43095	6.30	87885	4.30	5916	6.72
β-Pinene	95879	3.25	761	10.51	33002	12.11	92646	1.29	1491	1.19
Sabinene	3734	9.39	338	1.05	14683	11.00	16617	1.17	422	5.36
β-Myrcene	399139	5.47	22740	12.67	80077	8.87	11820	10.80	17344	5.17
α-Phellandrene	3024	22.34	-	-	229	8.29	659	2.15	-	-
Limonene	1859518	5.60	32086	14.16	251940	5.79	32186	2.72	12840	5.45
β-Phellandrene	1544	5.68	-	-	232	3.36	900	7.39	348	6.31
1,8-Cineole	10983	3.37	594	7.98	2375	7.42	1434	6.21	483	2.93
***trans*-β-Ocimene**	403	19.30	117	6.04	764	1.67	1538	2.39	-	-
***para*-cymene**	205116	3.55	4079	7.45	95129	6.54	55418	6.66	10848	6.16
***o*-Methylanisole**	6281	1.20	3498	4.25	16654	3.07	16538	4.98	4177	0.73
α-Cubebene	1191	0.83	-	-	1439	11.89	7243	4.08	-	-
***p*-cymenene**	10670	14.09	413	10.96	14450	0.85	22563	4.06	418	7.28
α-Terpinolene	8010	2.66	819	15.81	4913	16.80	41174	4.97	1034	1.23
α-Copaene	3830	6.39	172	0.82	12304	4.80	59047	1.05	-	-
β-Bourbonene	21271	6.58	105	4.04	38077	6.76	22924	6.80	475	0.75
Octanol	-	-	81975	1.47	-	-	-	-	70957	4.35
β-Elemene	66082	3.87	2830	1.55	72580	11.19	55911	7.72	4182	9.86
***trans*-Pinocarveol**	28690	2.09	859	5.43	53297	6.59	39506	10.03	1463	4.21
***cis*-Verbenol**	5585	1.39	-	-	4080	0.94	17285	5.31	-	-
Octyl acetate	-	-	1641536	2.35	-	-	13353	6.36	1598056	2.26
1,8-menthadien-4-ol	15919	4.37	-	-	18630	1.07	15056	1.42	0	-
***trans*-Verbenol**	21479	3.73	-	-	31157	1.44	38200	0.16	498	12.37
trans-β-Caryophyllene	56542	3.14	-	-	56515	1.10	31984	5.40	783	2.98
Aromadendrene	9789	0.36	253	3.35	11422	11.77	10536	17.83	-	-

	B. socotrana		*B. papyrifera*		Frankincense 1		Frankincense 2		Frankincesce 3	
γ-Selinene	36242	6.95	165	3.87	34870	1.37	35521	2.38	-	-
Germacrene D	40558	8.73	323	1.31	42482	0.65	36146	4.65	560	7.83
α-Fenchol	37757	3.31	-	-	10395	10.57	40929	3.53	-	-
α-Humulene	31363	9.94	1552	0.27	8695	16.37	-	-	3167	8.35
α-Selinene	49388	11.84	86	30.60	28808	8.74	24287	2.39	6683	26.24
β-Selinene	86298	6.16	272	7.55	60772	7.17	61912	6.06	692	17.89
Myrtenol	27077	5.40	2611	7.39	37939	2.43	41075	1.22	3312	6.32
***trans*-Carveol**	20623	2.62	1706	7.84	22022	0.87	28109	4.39	11126	5.02
***cis*-Carveol**	9714	0.82	168	32.83	7077	5.22	11134	0.74	163	5.66
Carvone	6077	3.64	429	5.91	26262	2.72	1422	2.98	836	5.50
Verbenone	16129	3.63	2870	9.54	118748	0.89	74643	2.82	5612	2.76
Cembrene	2748	4.84	7800	8.13	3183	15.84	5380	6.05	6411	17.03
Limonene-1,2-diol	20886	5.76	5967	8.54	23322	4.96	10092	9.29	6744	8.20
Caryophyllene oxide	3442	14.09	-	-	1130	4.38	774	23.49	-	-
Hydrocarbon Diterpene 1	436	1.14	5915	7.81	-	-	694	2.96	6363	5.51
α-Eudesmol	9862	6.38	920	7.69	2687	14.05	1520	0.42	963	5.95
Hydrocarbon Diterpene 2	743	10.19	3192	7.04	1391	7.27	1939	22.00	4364	7.36
β-Eudesmol	10690	7.43	-	-	12459	12.80	5864	5.66	-	-
Hydrocarbon Diterpene 3	335	15.43	3407	1.29	-	-	-	-	2089	1.83
Incensole acetate	-	-	37018	2.06	-	-	-	-	40604	7.87
Serratol	13589	11.16	519	8.45	17368	6.79	310	23.96	721	0.29
Cembrene A	860	7.49	16451	15.91	1609	10.51	70	4.04	10068	30.88
Incensole	1618	15.69	18205	20.63	2768	1.30	345	15.99	10208	31.51

Table s3, Mean peak area and %RSD on three replicates of the analytes on the investigated samples sampled by Vac-HS-SPME

	B. socotrana		***B. papyrifera***		**Frankincense 1**		**Frankincense 2**		**Frankincesce 3**	
	Mean	**% RSD**	**Mean**	**% RSD**	**Mean**	**% RSD**	**Mean**	**% RSD**	**Mean**	**% RSD**
α-Thujene	228	7.71	-	-	11142	6.15	5962	21.43	-	-
α-Pinene	1964510	5.76	13243	5.49	862636	7.01	2899533	0.60	21066	11.28
Camphene	31517	7.08	279	8.38	30246	7.60	51816	3.06	1495	5.86
β-Pinene	59432	3.39	681	14.12	22859	14.00	61260	0.11	943	8.18
Sabinene	3488	5.34	244	15.39	14137	9.30	13250	7.32	319	10.72
β-Myrcene	99634	0.00	14606	5.07	42027	4.45	6718	6.65	6128	11.38
α-Phellandrene	11655	18.16	-	-	803	20.00	569	24.85	-	-
Limonene	1588754	7.27	26001	19.19	185996	7.84	23969	2.65	13227	3.20
β-Phellandrene	9485	25.16	-	-	372	4.54	774	10.88	223	5.07
1,8-Cineole	3690	0.36	399	6.73	1500	6.51	1122	3.15	294	4.81
***trans*-β-Ocimene**	682	15.14	171	5.64	690	9.01	1645	16.04	-	-
***para*-cymene**	116975	4.47	3073	4.97	65342	2.03	39119	0.69	5035	3.06
***o*-Methylanisole**	4404	6.15	1985	0.18	12553	5.45	10671	3.59	2034	0.59
α-Cubebene	1427	2.28	-	-	1260	10.50	10606	1.40	0	-
***p*-cymenene**	3751	17.80	403	14.23	13357	1.50	24100	1.72	557	0.89
α-Terpinolene	8364	2.18	696	15.04	4153	13.00	60721	2.32	678	3.65
α-Copaene	6028	8.99	356	1.51	9510	3.90	72294	1.73	-	-
β-Bourbonene	7488	8.28	200	15.24	33659	5.78	23456	9.92	240	13.29
Octanol	-	-	73410	6.36	-	-	1822	-	54730	4.65
β-Elemene	98526	10.74	2123	7.26	80874	9.00	97780	7.27	698	6.48
***trans*-Pinocarveol**	23668	9.27	625	4.07	59480	5.30	54420	8.82	1023	15.97
***cis*-Verbenol**	9612	1.41	-	-	4141	2.10	29354	5.58	-	-
Octyl acetate	-	-	1322387	7.88	-	-	14379	1.35	1121090	0.68
1,8-menthadien-4-ol	10028	0.75	-	-	14883	2.30	12841	1.34	-	-
***trans*-Verbenol**	22457	8.40	-	-	27028	2.56	42272	0.24	534	1.99
trans-β-Caryophyllene	65743	7.36	841	10.05	62435	0.89	53246	9.55	1206	12.96
Aromadendrene	11509	1.82	247	14.06	9921	15.08	12885	12.27	-	-

	B. socotrana		*B. papyrifera*		Frankincense 1		Frankincense 2		Frankincesce 3	
	Mean	% RSD	Mean	% RSD	Mean	% RSD	Mean	% RSD	Mean	% RSD
γ-Selinene	20588	5.16	115	7.80	37698	1.33	47620	0.99	-	-
Germacrene D	29290	8.78	310	14.85	42856	1.75	46882	5.31	520	6.23
α-Fenchol	64421	4.49	-	-	12621	8.98	79812	9.15	-	-
α-Humulene	32957	10.56	1492	7.54	6818	14.98	-	-	2201	8.00
α-Selinene	85101	3.12	90	13.97	40638	9.76	43614	5.59	1824	14.65
β-Selinene	152678	2.86	268	17.71	84044	6.92	120692	6.17	322	16.94
Myrtenol	19692	1.74	2066	3.66	29532	3.54	58639	6.64	1941	4.70
trans-Carveol	19019	10.23	1364	8.97	18166	5.56	31704	1.68	7699	0.83
cis-Carveol	25038	3.40	345	18.70	10093	6.77	11984	0.22	453	10.30
Carvone	11961	4.19	254	4.71	30353	8.30	2092	12.75	576	12.03
Verbenone	15909	3.45	5543	5.84	91930	1.80	67701	0.31	9187	4.79
Cembrene	16027	5.44	28776	7.36	7237	13.67	11817	0.52	47084	0.62
Limonene-1,2-diol	35977	7.00	15160	2.54	30091	6.87	18571	0.95	23333	9.34
Caryophyllene oxide	7176	7.69	-	-	1402	3.65	1564	7.46	-	-
Hydrocarbon Diterpene 1	1742	20.30	14464	3.48	-	-	1759	3.94	20943	8.04
α-Eudesmol	18605	5.79	1546	3.48	2877	12.76	2283	2.94	2381	1.51
Hydrocarbon Diterpene 2	596	18.17	8255	6.89	1205	8.90	3748	0.49	13864	6.83
β-Eudesmol	23810	2.64	-	-	15653	5.98	13967	1.37	-	-
Hydrocarbon Diterpene 3	1047	1.96	11223	3.50	-	-	-	-	10604	3.20
Incensole acetate	-	-	129906	5.90	-	-	-	-	210843	14.90
Serratol	78347	9.72	12043	2.42	45640	7.98	14987	12.01	18101	14.10
Cembrene A	6783	6.60	35420	14.44	3118	6.98	122	3.18	28406	15.79
Incensole	9423	5.64	61859	4.76	8931	4.05	3142	0.80	54180	13.77

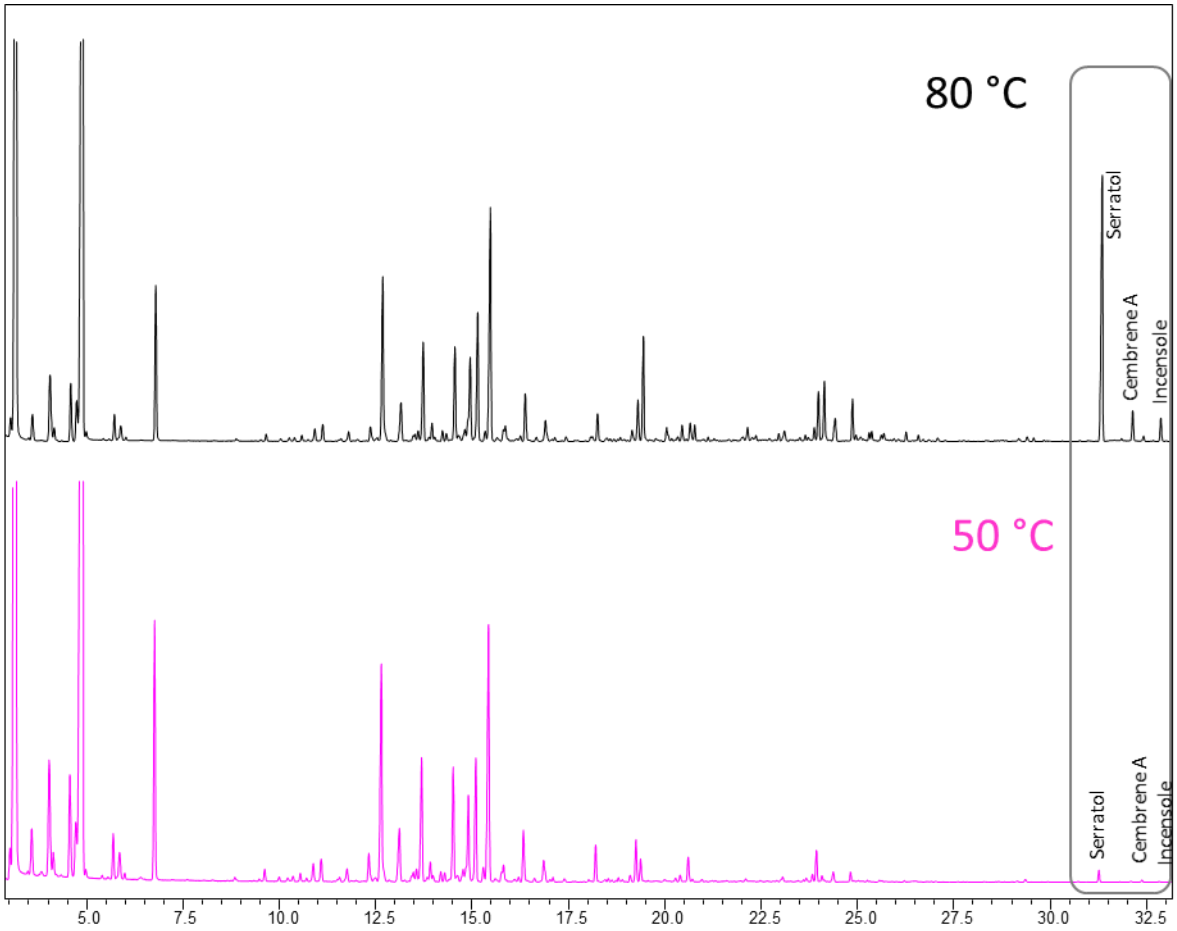

Figure S1, Vac-HS-SPME GC-MS profile of 100mg of B. socotrana obtained by sampling for 15 min with a sampling temperature of 80°C (black) and 50°C (pink). Column: conventional SLB-IL60i. Analysis conditions: see experimental section.

1.8.3 A Sustainable Approach for the Reliable and Simultaneous Determination of Terpenoids and Cannabinoids in Hemp Inflorescences by Vacuum Assisted Headspace Solid-Phase Microextraction

Francesca Capetti[1], Patrizia Rubiolo[1], Giulia Mastellone[1], Arianna Marengo[1], Barbara Sgorbini[1], Cecilia Cagliero[1*]

Affiliation:
[1] Dipartimento di Scienza e Tecnologia del Farmaco, Università di Torino, Via P. Giuria 9, 10125 Turin, Italy

*Corresponding author:
Cecilia Cagliero, Via P. Giuria 9, 10125 Turin, Italy, e-mail: cecilia.cagliero@unito.it

Received: February 8, 2022
Revised: April 9, 2022
Accepted: April 10, 2022

Bibliography
Advances in Sample Preparation
DOI: 10.1016/j.sampre.2022.100014

1.8.3.1 Abstract

Cannabis sativa L. is an intriguing plant that has been exploited since ancient times for recreational, medical, textile and food purposes. The plant's most promising bioactive constituents discovered so far belong to the terpenoid and cannabinoid classes. These specialised metabolites are highly concentrated in the plant aerial parts and their chemical characterisation is crucial to guarantee the safe and efficient use of the plant material irrespective of which use it is. Thanks to their volatile nature, the profiling of *Cannabis* terpenes, and in particular of mono and sesquiterpenes, can be performed by headspace solid-phase microextraction (HS-SPME) online combined to GC-MS analysis. The recovery of cannabinoids from solid matrices by HS-SPME prior to GC-MS analysis is also feasible but requires long sampling times and high sampling temperatures that can eventually discriminate the extraction of the most volatile markers as well as determine the formation of artefacts.

The reduction of the total pressure in the headspace can be exploited to increase the extraction kinetic of semi-volatile compounds such as cannabinoids during the HS-SPME process. This study investigates for the first time the advantages and disadvantages of using vacuum assisted HS-SPME over regular HS-SPME as a sample preparation process in an analytical protocol based on HS-SPME combined to fast GC-MS analysis that aims at comprehensively characterising both the terpenoid and cannabinoid profiles of *Cannabis* inflorescences in a single step. The results proved that vacuum conditions in the HS should be preferred over atmospheric pressure conditions as they ensure the fast recovery of cannabinoid markers at relatively lower sampling temperatures (i.e., 90°C) that do not discriminate the most volatile fraction nor cause the formation of artefacts when the sampling time is minimised.

Key words: *Cannabis sativa* inflorescences; vacuum assisted headspace solid-phase microextraction; volatilome; terpenoids; cannabinoids

1.8.3.2 Introduction

Cannabis sativa L. can be considered as one of the most studied plants in reason of its relevance in the illicit drug market and in the textile and food industry [1] as well as of its potential medical usage. Whether the plant is intended for recreational purposes, fiber production (hemp) or medical use, it depends on the content of two major cannabinoids in the aerial parts of the plant: the psychoactive (-)-trans-Δ9-tetrahydrocannabinol (Δ^9-THC) and cannabidiol (CBD), the latter displaying several biological activities but not the psychotropic one [2,3]. Illicit drug chemotype, also known as Type 1, contains an excess of Δ^9-THC and a limited amount of CBD. Contrary, in the Cannabis chemotype used in manufacturing (industrial hemp or type III) the ratio is reversed and Δ^9-THC content cannot exceed 0.2%. Finally, type II chemotype, which is used for medical purposes, is defined as having high mean contents of both CBD and Δ^9-THC (i.e., Bedrocan®: 22% THC, <1% CBD; Bediol® 6.5% THC, 8% CBD) [3], [4], [5].
Other than Δ^9-THC and CBD, the plant may synthesise several specialised metabolites, including additional phytocannabinoids and terpenes, amongst others [6], which are both produced by stalked glandular trichomes that are highly concentrated on female inflorescences [7]. Phytocannabinoids are C21 compounds known as terpenophenolic compounds. They are produced by the plant in their acidic form which under heating or during storage is decarboxylated into the active neutral form [6]. At least 104 cannabinoids have been isolated so far [8]: the predominant ones are Δ^9-tetrahydrocannabinolic acid (Δ^9-THCA), cannabidiolic acid (CBDA), cannabichromenic acid (CBCA) and cannabigerolic acid (CBGA), which is the precursor of the former compounds. Other minor cannabinoids include cannabinolic acid (CBNA) and Δ^8-THCA, which are artefacts of Δ^9-THCA, and cannabielsoin acid (CBEA) and cannabinodiolic acid (CBNDA) which derive from CBDA [9]. Terpenes are *Cannabis* most abundant specialised metabolites including at least 120 identified terpenoids [8]. Literature data suggest that varying pharmaceutical properties between different *Cannabis* varieties can be attributed to synergistic interactions, known as the 'entourage effect', between cannabinoids and terpenes [9]. A comprehensive qualitative characterisation of both the cannabinoid and terpene profiles of the plant raw material is therefore of utmost importance not only to define its rational use (i.e., whether the plant under investigation was cultivated for fiber production, medical or drug purposes) but also to guarantee the efficacy and safety of its potential pharmaceutical application.

The most employed method of extraction of cannabinoids from plant raw material is solid-liquid extraction (SLE) using ethanol or acetone as extracting solvents due to their affinity and consequent high extracting efficiency for cannabinoids [10,11]. High performance liquid chromatography (HPLC) and gas chromatography (GC) coupled to mass spectrometry are the analytical techniques of choice for the following qualitative and quantitative analysis [11]. HPLC is usually employed when the acid and the neutral form of the investigated cannabinoids must be measured separately, while GC analyses enable the characterisation of the "total-cannabinoid content" (e.g. the combined amount of THC and THCA) as GC systems, by definition, work with high temperatures that lead unavoidably to the decarboxylation of the cannabinoid acids [11]. The "total-cannabinoid content" is usually

measured as it best represents the pharmacological activity of the material, unless differently stated by legislation [12].
Thanks to their volatile nature, the isolation of terpenes, and in particular of mono and sesquiterpenes, from plant raw material is straightforward and their profiling can be performed by headspace solid-phase microextraction (HS-SPME) online combined to GC-MS analysis [5].
The recovery of cannabinoids from solid matrices by HS-SPME is also feasible but requires long sampling times in combination to high sampling temperatures due to their low volatility and low tendency to escape to the headspace. In 2004 Lachenmeier *et al.* optimised a successful HS-SPME method followed by on-coating derivatisation of the cannabinoids with N-methyl-N-trimethylsilyltrifluoroacetamide (MSTFA) for the extraction of cannabinoids from hemp food products using 90°C as sampling temperature and 30 min of extraction time [13] while in 2005 Ilias *et al.* showed that cannabinoids extraction should be performed at 150°C to maximise their recovery in short sampling times (i.e., 5 min) [14]. However, in a very recent work, Czégény *et al.* investigated the effect of temperature on the composition of pyrolysis products of CBD in e-cigarettes. They tested different operating temperatures (250–400°C) and they proved that, depending on the temperature and atmosphere (i.e., inert of oxidative condition), 25–52% of CBD can be converted into other cannabinoids amongst which Δ^9-THC, Δ^8-THC, cannabinol and cannabichromene (CBC) are the predominant pyrolysates [15]. Even though when performing HS-SPME it is usually unlikely to reach such extreme temperatures, the results of Czégény et al. suggest that (1) reduced sampling temperature should be preferred to obtain a truthful cannabinoid fingerprint profile in the plant raw material, (2) CBD potential degradation should be investigated during the optimisation of the sampling temperature.

As thoroughly described by Psillakis *et al*. [16-19] vacuum is a powerful experimental parameter to consider to increase the extraction kinetic of semi-volatile compounds during the HS-SPME process. This is because in the case of semivolatiles and under non-equilibrium conditions, a reduced pressure inside the sample container decreases the resistance to mass transfer in the gas zone at the solid-headspace interface. As a consequence, higher extraction efficiencies for semi-volatile compounds can be achieved in shorter sampling time and potentially at milder extraction temperatures [20,21].
This study investigates the advantages and disadvantages of using vacuum assisted HS-SPME (Vac-HS-SPME) over regular HS-SPME (Reg-HS-SPME) as sample preparation process to be exploited in analytical protocols aiming at comprehensively characterising both the terpene and cannabinoid profiles of Cannabis inflorescences in a single step employing a total analysis system.

1.8.3.3 Materials and Methods

Chemicals and samples

Cannabidiol (CBD) and cannabichromene (CBC) standard solutions 1.0 mg mL^{-1} in methanol were purchased from Merck KGaA, Darmstadt, Germany. Dried Cannabis inflorescences from type III chemotype were purchased from an authorised local hemp shop. The dried plant material was pulverised by an electric blender and stored at -18°C.

HS-SPME procedures under reduced (Vac-HS-SPME) and atmospheric pressure conditions (Reg-HS-SPME)

Divinylbenzene/carboxen/polydimethylsiloxane (DVB/CAR/PDMS) 50/30 µm (2 cm length) and over coated PDMS/DVB 75 µm (coating thickness includes 65 µm coating + 10 µm OC (overcoating)) fibers were employed for the experiments. The fibers were purchased from Merck KGaA, Darmstadt, Germany and conditioned following the manufacturer's instructions. Reg-HS-SPME experiments were performed using conventional headspace 20 mL crimp vials provided by Restek, Bellefonte, USA and 20 mm magnetic ring crimp cap, fitted with 20.6 mm septa (Butyl red/PTFE grey, 55 shore A, 1.3 mm). Vac-HS-SPME experiments were performed in the same commercial headspace 20 mL crimp vials hermetically sealed with a stainless-steel closure (provided by Prof. Elefteria Psillakis) having a hole that could tightly accommodate a Thermogreen® LB-1 septum with half-hole (Supelco, Bellefonte, USA) through which the air evacuation step and the SPME sampling were performed. For the inflorescences, 10 mg of the pulverised sample were placed inside the vial which was again stored at –18°C for one hour and then air-evacuated [20]. The air-evacuation step was performed with a 22-gauge hypodermic needle sealed to a 5 mL syringe tightly secured to the tubing of a N 820.3 FT.18 (7 mbar ultimate vacuum) pumping unit manufactured by KNF Lab (Milan, Italy). The needle was inserted through the septum and the vial was air-evacuated for one minute. For Reg-HS-SPME the procedure was the same, while omitting the air evacuation step. For CBD standard sampling, 10 µL of the 1.0 mg mL^{-1} solution were introduced through the closure septum after the air evacuation step. For Reg-HS-SPME experiments, the liquid sample was introduced in the vial by the open vial-technique [22]. After the sampling the fiber was withdrawn and the SPME device moved to the GC-MS system for analysis. GC desorption lasted 10 min to minimise carry-over. 10 mg of pulverised plant material were sampled at three different extraction temperatures (i.e., 80, 90 and 150°C) under both Vac- and Reg-HS-SPME experiments. Sampling-time profiles were obtained for all the above mentioned conditions by sampling for 5, 15, and 30 min. 10 µL of CBD standard solution 1.0 mg mL^{-1} were sampled at 90 and 150°C for 5 min, under both pressure conditions. All extractions were run in triplicate.

Instrumental set-up

GC-MS systems and columns: Analyses were carried out on two different instruments: (1) a MPS-2 multipurpose sampler (Gerstel, Mülheim a/d Ruhr, Germany) installed on a Shimadzu GC-FID-MS system consisting of a Shimadzu GC 2010 system, equipped with FID, in parallel with a Shimadzu QP2010-PLUS GC–MS mass spectrometer (Shimadzu, Milan, Italy); (2) a MPS-2 multipurpose sampler (Gerstel, Mülheim a/d Ruhr, Germany) installed on an Agilent 6890 N GC system coupled to a 5975 MSD mass spectrometer (Agilent

Technologies, Santa Clara, CA). GC analyses were carried out using two MEGA-5 95% methyl-polysiloxane 5%-phenyl (MEGA, Legnano, MI, Italy) columns: a conventional 30 m × 0.25 mm dc, 0.25 µm df column installed on the Agilent 6890 N GC - 5975 MSD and a narrow bore 15 m × 0.18 mm dc, 0.18 µm df column installed on the Shimadzu GCMS-QP2010. Data was processed with the ChemStation Version E.02.02.1431 data processing system (Agilent Technologies, Santa Clara, CA).

GC-MS conditions: Analyses were carried out under the following conditions. Temperatures: injector: 250 °C, transfer line: 270 °C, ion source: 200 °C; carrier gas: He; flow control mode: constant linear velocity; flow rate: 1.00 mL min^{-1} (conventional column), 0.72 mL min^{-1} (narrow bore column); injection mode: split; split ratio: 1:20. The MS was operated in electron ionisation mode (EI) at 70 eV, scan rate: 666 u/s, mass range: 35–350 m/z. Temperature programs: (i) 50°C (one minute)// 3°C/min//250°C (5 min) for conventional MEGA-%; (ii) 50°C (30 s) //7.2°C/min// 250°C (two minutes) for the narrow bore column. The chromatographic conditions for the narrow bore columns were obtained by translating the method parameters through the Agilent method translator software [23]. Identification was performed via comparisons of linear retention indices and mass spectra either with those of authentic standards, or with data stored in commercial [24] and in-house libraries.

1.8.3.4 Results and Discussion

Table S1 in the supplementary materials provides the list of the target compounds together with their physicochemical properties (i.e., $LogK_{ow}$, boiling point and vapour pressure). The mono and sesquiterpene markers to be investigated were chosen according to the results of Jin *et al.* who comprehensively profiled reference specialised metabolites, in *Cannabis* inflorescences, leaves, stem barks and roots for the three *Cannabis* chemotypes (i.e., Type I, II and III) [8].

Preliminary optimisation of the fiber coating and chromatographic conditions:

The first set of experiments aimed at selecting (1) the optimum fiber coating that could extract all the investigated analytes with acceptable sensitivity and (2) the best chromatographic conditions providing an acceptable resolution of all the investigated markers in a reasonable time for high throughput analyses. In our study, two fiber coatings were tested: the PDMS/DVB and the DVB/CAR/PDMS fibers. **Figure 1A** and **B** shows the profiles obtained with the two investigated coatings when sampling 10 mg of matrix with Reg-HS-SPME at 90°C for 30 min of extraction. The chromatographic analyses were performed employing a conventional 30 m × 0.25 mm dc, 0.25 µm df MEGA-5 column. Irrespective of the fiber coating, the most abundant compounds amongst the recovered mono and sesquiterpenes were β-myrcene (3), trans-β-caryophyllene (11) and selina-3,7(11)-diene (20) while only one cannabinoid (i.e., CBD (29)) was recovered. In agreement with the results of *Ilias et al*. [14], the PDMS/DVB fiber proved to be more efficient for the recovery of CBD compared to the triphasic fiber which, however, extracted a quantitative richer mono and sesquiterpene profile. The PDMS/DVB fiber was chosen for the following experiments because of its higher recovery of CBD while still providing an acceptable sensitivity for the investigated mono and sesquiterpene metabolites.

The employed conventional MEGA-5 column proved to separate the main selected markers with an acceptable resolution. The possibility to improve the analysis speed and to decrease the use of gas with a greener analytical protocol was then investigated. The chromatographic analysis was speeded up by translating the method to a 15 m × 0.18 mm dc, 0.18 µm df column using the method translation approach [23,25,26]. Figure 1C reports the translated GC-MS profile of the investigated hemp inflorescences with the narrow-bore MEGA-5 column. The analysis time was reduced from 72.67 to 30.28 min, while maintaining the separation and the elution pattern of the investigated markers.

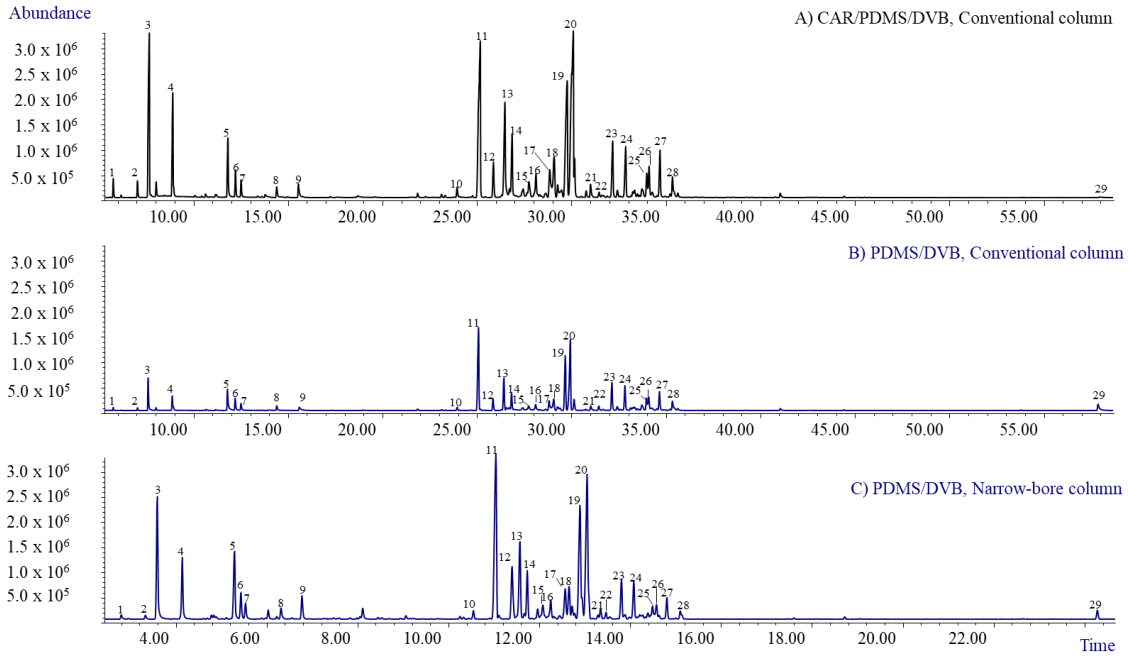

Figure 1, Reg-HS-SPME GC-MS profiles of the investigate hemp inflorescences obtained with different polymer coatings and chromatographic conditions. A) Polymer coating: CAR/PDMS/DVB; Column: conventional MEGA-5; GC-MS instrument: Agilent 6890 N GC coupled to a 5975 MSD. B) Polymer coating: PDMS/DVB; Column: conventional MEGA-5; GC-MS instrument: Agilent 6890 N GC coupled to a 5975 MSD. C) Polymer coating: PDMS/DVB; Column: narrow-bore MEGA-5; GC-MS instrument: Shimadzu QP2010-PLUS GC–MS system. GC-MS Analysis conditions: see experimental section. Reg-HS-SPME parameters: sampling temperature 90°C, extraction time 30 minutes. Legend: 1) α-Pinene, 2) β-Pinene, 3) β-Myrcene, 4) Limonene, 5) Linalool, 6) Fenchol, 7) cis-Pinene hydrate, 8) Borneol, 9) α-Terpineol, 10) α-Patchoulene, 11) trans-β-Caryophyllene, 12) trans-α-Bergamotene, 13) α-Humulene, 14) trans-β-Farnesene, 15) β-Selinene, 16) α-Selinene, 17) α-Farnesene, 18-19) Sesquiterpenes (MW 204), 20) Selina-3,7(11)-diene, 21) trans-Nerolidol, 22) Caryophyllene oxide, 23) Guaiol, 24) 10-epi-γ-Eudesmol, 25) β-Eudesmol, 26) α-Eudesmol, 27) Bulnesol, 28) α-Bisabolol, 29) Cannabidiol

<u>Vacuum HS-SPME and regular HS-SPME:</u>

Due to their relative high molecular weights and boiling points (e.g. CBD 428.52°C, 760 mmHg, [27]) cannabinoids have a low tendency to escape to headspace and require high sampling temperatures to be recovered by HS-SPME [14]. However, in view of a reliable and comprehensive HS-SPME method suitable for the simultaneous qualitative characterisation of both the terpenoid and the cannabinoid fractions of *Cannabis* inflorescences, high sampling temperatures are not advisable for two reasons. First, they may decrease the distribution coefficient between the fiber and the headspace (i.e., K_{fs}) of the most volatile components reducing their recovery [28]. In addition, high sampling temperature, especially when combined with relatively long extraction times, may induce decomposition of some compounds and/or creation of other components or artefacts [29]. According to the theory, a reduced pressure inside the HS sample container increases the

compounds' molecular diffusion coefficient in air and favours their vapour flux at the solid surface. As a result, reducing the total headspace pressure is an alternative and complementary strategy, compared to the adoption of high sampling temperatures, to speed up the extraction kinetic of semi-volatile compounds [30].

In this study we compared the performances of Vac-HS-SPME to those of Reg-HS-SPME under different sampling temperatures (i.e., 150°C, 90°C and 80°C) and extraction times (i.e., 5, 15, 30 min) and we explored whether Vac-HS-SPME could be a more suitable sample preparation technique for the simultaneous characterisation of both the terpenoid and cannabinoid profiles of Cannabis inflorescences. For the following discussion CBD will be considered as representative of the plant cannabinoids, while β-myrcene and trans-β-caryophyllene of the mono and sesquiterpene markers, respectively.

Tables 1, 2 and 3 report (1) the average peak area and % RSD (n = 3) of all the investigated compounds when testing 10 mg of matrix under the different experimental conditions and (2) the relative analyte abundance (RAA) defined as the ratio between the average peak area obtained under vacuum to that measured at atmospheric pressure conditions at 150°C, 90°C and 80°C, respectively. **Figure 2** shows the extraction temperature profiles of β-myrcene, *trans*-β-caryophyllene and CBD acquired when sampling 10 mg of the matrix for 5 min at the different investigated temperatures. Finally, **Figure 3** provides the extraction times profiles for CBD for each sampling temperature (i.e., 150, 90 and 80°C). In all the cases, the results of both reduced and atmospheric pressure conditions are reported.

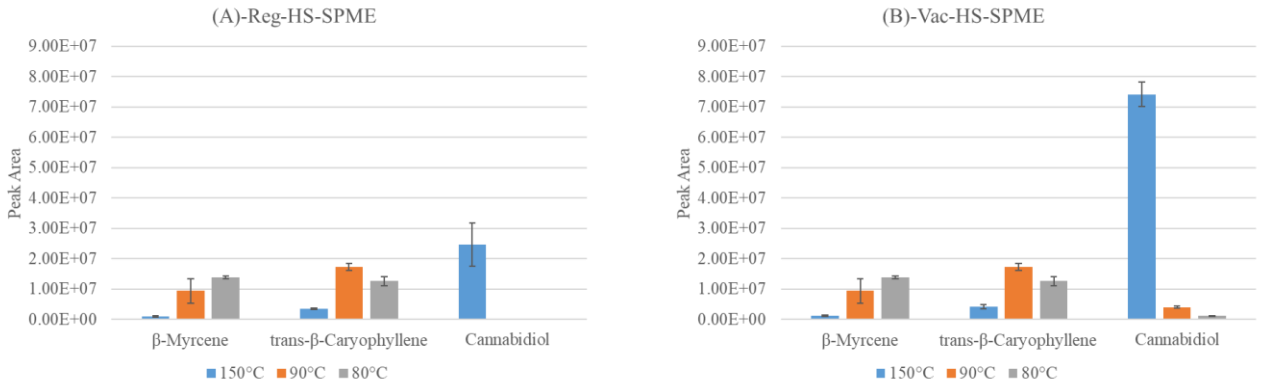

Figure 2, Extraction temperature profiles of CBD, β-myrcene and trans-β-caryophyllene obtained under A) regular (Reg-HS-SPME) and (B) reduced (Vac-HS-SPME) pressure conditions. Experimental parameters: PDMS/DVB fiber; 10 mg of sample; 5 minutes of extraction time.

Table 1, Mean peak area, %RSD (n=3) and Relative Analyte Abundance (RAA) of investigated markers sampled by Reg and Vac-HS-SPME at 150 °C. RAA defines the ration between Vac-HS-SPME and Reg-HS-SPME area. Legend: red triangle RAA < 0.8, yellow line 0.8 < RAA < 1.2, green triangle RAA > 1.2

Compound	5 minutes					15 minutes					30 minutes				
	Reg-HS-SPME		Vac-HS-SPME		RAA	Reg-HS-SPME		Vac-HS-SPME		RAA	Reg-HS-SPME		Vac-HS-SPME		RAA
	Average Area	% RSD	Average Area	% RSD		Average Area	% RSD	Average Area	% RSD		Average Area	% RSD	Average Area	% RSD	
α-Pinene	4.7E+04	18.9	8.1E+04	9.4	▲ 1.7	4.2E+04	44.4	4.8E+04	4.0	▬ 1.2	4.1E+04	44.7	4.7E+04	7.3	▬ 1.1
β-Pinene	4.1E+04	18.6	7.6E+04	16.2	▲ 1.8	4.9E+04	35.5	4.1E+04	5.7	▬ 0.8	6.1E+04	21.4	3.5E+04	6.6	▼ 0.6
β-Myrcene	1.0E+06	15.7	1.3E+06	20.4	▲ 1.3	9.0E+05	49.5	6.7E+05	7.5	▼ 0.7	7.8E+05	43.3	5.4E+05	4.8	▼ 0.7
Limonene	5.5E+05	10.7	8.0E+05	12.7	▲ 1.5	4.8E+05	39.0	4.7E+05	19.1	▬ 1.0	4.6E+05	32.8	4.3E+05	9.4	▬ 0.9
Linalool	6.2E+05	8.6	9.4E+05	6.4	▲ 1.5	7.0E+05	8.4	5.8E+05	10.5	▬ 0.8	6.4E+05	6.7	4.7E+05	11.2	▼ 0.7
Fenchol	2.8E+05	6.7	4.1E+05	6.3	▲ 1.5	3.2E+05	8.7	2.8E+05	9.2	▬ 0.9	3.2E+05	10.0	2.2E+05	5.3	▼ 0.7
cis-Pinene hydrate	2.3E+05	6.6	3.6E+05	7.7	▲ 1.6	2.6E+05	9.1	2.5E+05	6.8	▬ 1.0	2.6E+05	2.4	2.1E+05	5.0	▬ 0.8
Borneol	1.7E+05	4.8	2.4E+05	5.6	▲ 1.4	2.0E+05	5.9	1.7E+05	11.0	▬ 0.8	2.0E+05	6.4	1.3E+05	2.1	▼ 0.6
α-Terpineol	3.3E+05	7.3	3.8E+05	6.6	▬ 1.1	3.8E+05	8.7	2.8E+05	11.4	▼ 0.7	4.0E+05	15.5	2.1E+05	2.3	▼ 0.5
α-Patchoulene	1.1E+05	5.5	1.3E+05	10.8	▬ 1.2	1.4E+05	14.7	1.1E+05	12.4	▬ 0.8	1.8E+05	5.0	6.6E+04	16.7	▼ 0.4
trans-β-Caryophyllene	3.5E+06	5.9	4.2E+06	17.9	▬ 1.2	4.3E+06	3.9	2.7E+06	13.0	▼ 0.6	5.1E+06	8.1	1.5E+06	8.0	▼ 0.3
trans-α-Bergamotene	2.0E+06	7.3	2.0E+06	11.0	▬ 1.0	2.3E+06	7.9	1.2E+06	10.8	▼ 0.5	2.6E+06	15.6	7.2E+05	4.8	▼ 0.3
α-Humulene	1.5E+06	5.3	1.6E+06	16.2	▬ 1.1	1.8E+06	2.8	1.1E+06	11.4	▼ 0.6	2.1E+06	9.8	6.3E+05	15.4	▼ 0.3
trans-β-Farnesene	5.8E+05	5.4	6.3E+05	17.1	▬ 1.1	6.8E+05	12.4	3.5E+05	11.0	▼ 0.5	7.6E+05	9.1	1.8E+05	20.2	▼ 0.2
β-Selinene	4.1E+05	6.0	3.0E+05	16.9	▼ 0.7	4.4E+05	21.2	2.2E+05	13.6	▼ 0.5	5.4E+05	34.8	1.3E+05	10.5	▼ 0.2
α-Selinene	3.7E+05	5.6	3.8E+05	12.0	▬ 1.0	4.2E+05	4.4	3.3E+05	6.9	▬ 0.8	4.5E+05	7.5	3.1E+05	2.7	▼ 0.7
α-Farnesene	7.7E+05	6.8	7.5E+05	19.0	▬ 1.0	8.5E+05	3.7	4.1E+05	15.8	▼ 0.5	1.0E+06	13.0	2.0E+05	6.2	▼ 0.2
Sesquiterpene (MW 204)	4.1E+06	6.4	4.2E+06	16.9	▬ 1.0	4.9E+06	2.2	2.7E+06	11.6	▼ 0.5	5.5E+06	13.2	1.4E+06	17.0	▼ 0.3
Selina-3,7(11)-diene	5.0E+06	12.7	4.9E+06	29.9	▬ 1.0	5.9E+06	9.6	2.8E+06	12.3	▼ 0.5	6.9E+06	20.8	1.6E+06	7.4	▼ 0.2
Caryophyllene oxide	4.6E+05	13.8	5.0E+05	9.2	▬ 1.1	6.0E+05	9.1	3.3E+05	10.1	▼ 0.6	6.8E+05	14.3	2.1E+05	5.5	▼ 0.3
Guaiol	3.7E+06	11.1	5.0E+06	13.3	▲ 1.3	4.7E+06	14.5	2.9E+06	11.0	▼ 0.6	5.3E+06	21.7	1.8E+06	5.7	▼ 0.3
10-epi-γ-Eudesmol	3.6E+06	10.6	4.4E+06	12.1	▬ 1.2	4.5E+06	13.3	2.8E+06	11.1	▼ 0.6	5.2E+06	21.7	1.7E+06	3.6	▼ 0.3
β-Eudesmol	1.9E+06	10.3	3.2E+06	10.9	▲ 1.7	2.7E+06	37.0	1.3E+06	9.8	▼ 0.5	3.6E+06	17.9	7.4E+05	4.0	▼ 0.2
α-Eudesmol	1.5E+06	11.8	3.5E+06	6.7	▲ 2.3	2.6E+06	57.1	1.1E+06	11.9	▼ 0.4	4.0E+06	23.5	7.1E+05	5.7	▼ 0.2
Bulnesol	3.5E+06	13.3	5.0E+06	10.3	▲ 1.4	4.6E+06	19.2	3.0E+06	9.7	▼ 0.6	5.1E+06	23.2	1.8E+06	6.4	▼ 0.3
α-Bisabolol	2.6E+06	14.1	3.9E+06	12.1	▲ 1.5	3.1E+06	21.6	1.9E+06	8.5	▼ 0.6	3.5E+06	23.0	1.1E+06	4.1	▼ 0.3

Compound	5 minutes					15 minutes					30 minutes				
	Reg-HS-SPME		Vac-HS-SPME		RAA	Reg-HS-SPME		Vac-HS-SPME		RAA	Reg-HS-SPME		Vac-HS-SPME		RAA
	Average Area	% RSD	Average Area	% RSD		Average Area	% RSD	Average Area	% RSD		Average Area	% RSD	Average Area	% RSD	
CBD	2.5E+07	28.9	7.4E+07	5.5	▲ **3.0**	6.7E+07	7.7	1.1E+08	2.3	▲ **1.6**	7.8E+07	22.6	1.2E+08	0.9	▲ **1.6**
CBC	1.2E+06	19.8	4.3E+06	3.2	▲ 3.5	4.0E+06	8.5	5.8E+06	2.2	▲ 1.5	4.7E+06	24.0	5.9E+06	17.4	▲ 1.3
Supposed Δ^9-THC	9.5E+05	39.2	4.0E+06	9.6	▲ 4.2	2.9E+06	16.8	7.4E+06	2.4	▲ 2.5	3.5E+06	52.2	9.0E+06	2.7	▲ 2.6

Table 2, Mean peak area, %RSD (n=3) and Relative Analyte Abundance (RAA) of investigated markers sampled by Reg and Vac-HS-SPME at 90 °C. RAA defines the ration between Vac-HS-SPME and Reg-HS-SPME area. Legend: red triangle RAA < 0.8, yellow line 0.8 < RAA < 1.2, green triangle RAA > 1.2

Compound	5 minutes					15 minutes					30 minutes				
	Reg-HS-SPME		Vac-HS-SPME		RAA	Reg-HS-SPME		Vac-HS-SPME		RAA	Reg-HS-SPME		Vac-HS-SPME		RAA
	Average Area	% RSD	Average Area	% RSD		Average Area	% RSD	Average Area	% RSD		Average Area	% RSD	Average Area	% RSD	
α-Pinene	4.9E+05	58.9	4.7E+05	12.6	▬ 1.0	4.2E+05	9.0	3.2E+05	1.0	▬ 0.8	5.1E+05	2.3	2.4E+05	0.4	▼ 0.5
β-Pinene	4.6E+05	43.1	4.4E+05	11.1	▬ 0.9	4.4E+05	6.2	2.2E+05	4.8	▼ 0.5	4.8E+05	12.8	1.7E+05	1.1	▼ 0.4
β-Myrcene	9.4E+06	43.1	6.6E+06	17.0	▼ 0.7	9.9E+06	4.2	4.7E+06	3.6	▼ 0.5	1.1E+07	1.0	3.5E+06	2.3	▼ 0.3
Limonene	5.2E+06	36.8	3.8E+06	14.0	▼ 0.7	5.5E+06	3.5	2.8E+06	6.1	▼ 0.5	6.0E+06	0.2	2.1E+06	2.1	▼ 0.3
Linalool	6.8E+06	7.3	7.0E+06	8.0	▬ 1.0	6.3E+06	2.7	4.4E+06	5.2	▼ 0.7	6.7E+06	4.8	2.9E+06	4.8	▼ 0.4
Fenchol	2.7E+06	8.8	3.1E+06	9.9	▬ 1.2	2.7E+06	3.7	2.0E+06	4.5	▼ 0.7	3.0E+06	0.5	1.3E+06	4.8	▼ 0.4
cis-Pinene hydrate	1.7E+06	6.0	2.4E+06	6.8	▲ 1.4	1.8E+06	3.9	1.5E+06	6.0	▬ 0.9	2.0E+06	2.2	1.0E+06	5.0	▼ 0.5
Borneol	1.2E+06	5.3	1.7E+06	7.0	▲ 1.4	1.3E+06	4.0	1.2E+06	6.6	▬ 0.9	1.4E+06	3.7	7.6E+05	1.5	▼ 0.5
α-Terpineol	2.3E+06	4.9	3.1E+06	11.6	▲ 1.3	2.5E+06	3.7	2.0E+06	4.7	▬ 0.8	2.7E+06	4.7	1.4E+06	2.4	▼ 0.5
β-Patchoulene	8.4E+05	8.3	9.2E+05	10.6	▬ 1.1	1.0E+06	3.0	5.0E+05	5.5	▼ 0.5	1.1E+06	5.0	3.3E+05	27.5	▼ 0.3
trans-β-Caryophyllene	1.7E+07	6.7	2.0E+07	13.1	▬ 1.1	2.0E+07	3.4	1.2E+07	4.4	▼ 0.6	2.2E+07	3.5	7.3E+06	2.0	▼ 0.3
trans-α-Bergamotene	5.6E+06	7.2	1.1E+07	4.6	▲ 1.9	9.0E+06	5.1	1.0E+07	0.8	▬ 1.1	1.1E+07	7.4	7.3E+06	1.0	▼ 0.6
α-Humulene	7.5E+06	6.8	9.5E+06	9.2	▲ 1.3	9.5E+06	3.4	6.3E+06	2.0	▼ 0.7	1.0E+07	4.8	4.0E+06	2.1	▼ 0.4
trans-β-Farnesene	3.9E+06	6.5	4.7E+06	15.8	▬ 1.2	5.3E+06	2.1	2.9E+06	5.1	▼ 0.6	5.6E+06	5.5	1.6E+06	2.5	▼ 0.3
β-Selinene	2.0E+06	6.6	2.1E+06	13.9	▬ 1.1	2.8E+06	3.5	1.2E+06	4.5	▼ 0.5	3.1E+06	7.4	6.9E+05	2.0	▼ 0.2
α-Selinene	1.8E+06	7.0	2.7E+06	7.8	▲ 1.5	2.4E+06	3.7	2.0E+06	1.5	▬ 0.8	2.8E+06	6.7	1.9E+06	4.7	▼ 0.7
α-Farnesene	3.2E+06	9.7	5.3E+06	15.0	▲ 1.7	5.0E+06	2.5	3.6E+06	6.2	▼ 0.7	5.7E+06	8.0	1.8E+06	0.5	▼ 0.3
Sesquiterpene (MW 204)	1.2E+07	11.7	2.0E+07	8.6	▲ 1.7	1.7E+07	9.6	1.3E+07	6.1	▬ 0.8	2.0E+07	3.5	7.5E+06	0.3	▼ 0.4

Compound	5 minutes					15 minutes					30 minutes				
	Reg-HS-SPME		Vac-HS-SPME		RAA	Reg-HS-SPME		Vac-HS-SPME		RAA	Reg-HS-SPME		Vac-HS-SPME		RAA
	Average Area	% RSD	Average Area	% RSD		Average Area	% RSD	Average Area	% RSD		Average Area	% RSD	Average Area	% RSD	
Selina-3,7(11)-diene	1.5E+07	6.3	2.4E+07	8.0	▲ 1.6	2.1E+07	3.4	1.5E+07	1.7	▼ 0.7	2.4E+07	4.2	8.7E+06	1.7	▼ 0.4
Caryophyllene oxide	6.3E+05	18.7	1.5E+06	5.4	▲ 2.3	1.2E+06	8.5	1.5E+06	2.3	▲ 1.3	1.7E+06	22.3	1.4E+06	3.4	▬ 0.8
Guaiol	3.3E+06	5.9	1.0E+07	10.3	▲ 3.1	6.6E+06	7.7	1.3E+07	1.2	▲ 1.9	1.0E+07	6.0	1.2E+07	1.3	▬ 1.2
10-epi-γ-Eudesmol	2.9E+06	4.1	8.5E+06	7.5	▲ 2.9	5.5E+06	6.8	9.8E+06	1.6	▲ 1.8	8.0E+06	8.0	9.3E+06	1.7	▬ 1.2
β-Eudesmol	1.5E+06	18.8	4.1E+06	7.9	▲ 2.8	2.9E+06	6.1	6.4E+06	13.1	▲ 2.2	4.6E+06	7.4	5.2E+06	0.6	▬ 1.1
α-Eudesmol	1.2E+06	20.4	3.2E+06	5.9	▲ 2.6	2.2E+06	7.8	5.9E+06	32.4	▲ 2.6	3.3E+06	7.8	3.9E+06	1.9	▬ 1.2
Bulnesol	1.8E+06	9.2	7.2E+06	9.4	▲ 4.0	4.4E+06	8.3	9.9E+06	2.0	▲ 2.2	7.2E+06	7.0	1.0E+07	3.3	▲ 1.4
α-Bisabolol	1.1E+06	10.6	5.0E+06	9.5	▲ 4.7	3.1E+06	8.3	8.3E+06	2.0	▲ 2.7	5.4E+06	11.0	9.1E+06	1.2	▲ 1.7
CBD	4.5E+04	13.9	4.1E+06	9.3	▲ **91.1**	7.5E+04	13.1	9.8E+06	8.7	▲ **131.0**	2.0E+05	15.0	1.6E+07	5.5	▲ **80.5**
CBC	n.d.	n.c.	1.7E+05	15.0	n.c.	n.d.	n.c.	3.8E+05	20.9	n.c.	n.d.	n.c.	9.6E+05	14.2	n.c.
Supposed Δ^9-THC	n.d.	n.c.	2.3E+05	21.9	n.c.	n.d.	n.c.	4.7E+05	14.9	n.c.	n.d.	n.c.	8.3E+05	28.8	n.c.

Table 3, Mean peak area, %RSD (n=3) and Relative Analyte Abundance (RAA) of investigated markers sampled by Reg and Vac-HS-SPME at 80 °C. RAA defines the ration between Vac-HS-SPME and Reg-HS-SPME area. Legend: red triangle RAA < 0.8, yellow line 0.8 < RAA < 1.2, green triangle RAA > 1.2

Compound	5 minutes					15 minutes					30 minutes				
	Reg-HS-SPME		Vac-HS-SPME		RAA	Reg-HS-SPME		Vac-HS-SPME		RAA	Reg-HS-SPME		Vac-HS-SPME		RAA
	Average Area	% RSD	Average Area	% RSD		Average Area	% RSD	Average Area	% RSD		Average Area	% RSD	Average Area	% RSD	
α-Pinene	6.7E+05	13.1	3.9E+05	8.2	▼ 0.6	5.9E+05	13.8	2.8E+05	10.9	▼ 0.5	6.3E+05	8.0	2.3E+05	15.0	▼ 0.4
β-Pinene	6.6E+05	6.0	3.4E+05	8.6	▼ 0.5	5.8E+05	12.9	3.2E+05	9.4	▼ 0.6	5.8E+05	8.2	1.8E+05	12.6	▼ 0.3
β-Myrcene	1.4E+07	3.9	5.5E+06	5.6	▼ 0.4	1.2E+07	14.5	4.0E+06	9.6	▼ 0.3	1.3E+07	6.8	3.4E+06	13.0	▼ 0.3
Limonene	7.2E+06	3.9	3.5E+06	5.1	▼ 0.5	6.5E+06	13.5	2.3E+06	8.3	▼ 0.4	7.0E+06	7.0	2.1E+06	9.9	▼ 0.3
Linalool	6.1E+06	5.6	7.5E+06	5.9	▲ 1.2	6.6E+06	4.2	5.4E+06	6.0	▬ 0.8	7.2E+06	3.0	3.8E+06	10.2	▼ 0.5
Fenchol	2.4E+06	5.1	3.1E+06	5.1	▲ 1.3	2.7E+06	5.4	2.3E+06	5.9	▬ 0.8	3.1E+06	5.1	1.5E+06	11.5	▼ 0.5
cis-Pinene hydrate	1.4E+06	6.2	2.4E+06	5.6	▲ 1.7	1.7E+06	3.9	1.8E+06	4.5	▬ 1.0	1.9E+06	5.0	1.2E+06	8.0	▼ 0.6
Borneol	8.4E+05	7.4	1.7E+06	5.5	▲ 2.0	1.2E+06	3.0	1.2E+06	3.5	▬ 1.1	1.3E+06	6.5	9.1E+05	5.3	▼ 0.7
α-Terpineol	1.4E+06	8.1	3.1E+06	4.9	▲ 2.2	2.2E+06	0.9	2.3E+06	2.1	▬ 1.1	2.5E+06	6.4	1.7E+06	4.0	▼ 0.7
α-Patchoulene	6.1E+05	14.9	9.3E+05	7.3	▲ 1.5	1.0E+06	3.0	5.1E+05	4.8	▼ 0.5	1.1E+06	5.6	3.5E+05	10.1	▼ 0.3

Compound	5 minutes					15 minutes					30 minutes				
	Reg-HS-SPME		Vac-HS-SPME		RAA	Reg-HS-SPME		Vac-HS-SPME		RAA	Reg-HS-SPME		Vac-HS-SPME		RAA
	Average Area	% RSD	Average Area	% RSD		Average Area	% RSD	Average Area	% RSD		Average Area	% RSD	Average Area	% RSD	
trans-β-Caryophyllene	1.3E+07	12.0	1.9E+07	6.2	▲ 1.5	2.1E+07	1.0	1.2E+07	4.2	▼ 0.6	2.2E+07	4.2	8.8E+06	8.0	▼ 0.4
trans-α-Bergamotene	2.9E+06	14.2	8.7E+06	3.0	▲ 3.0	6.8E+06	2.9	9.8E+06	2.7	▲ 1.5	9.0E+06	5.5	9.1E+06	3.9	- 1.0
α-Humulene	4.5E+06	6.3	8.9E+06	4.9	▲ 2.0	8.5E+06	2.5	6.1E+06	3.9	▼ 0.7	1.0E+07	5.7	4.7E+06	6.1	▼ 0.5
trans-β-Farnesene	2.0E+06	8.4	4.3E+06	8.4	▲ 2.1	4.7E+06	0.4	2.8E+06	10.0	▼ 0.6	5.7E+06	6.2	2.2E+06	14.6	▼ 0.4
β-Selinene	8.8E+05	9.8	1.9E+06	7.9	▲ 2.1	2.0E+06	15.8	1.2E+06	8.3	▼ 0.6	2.9E+06	5.4	8.8E+05	11.2	▼ 0.3
α-Selinene	9.4E+05	9.7	2.5E+06	4.9	▲ 2.7	2.0E+06	1.8	1.9E+06	5.5	- 0.9	2.5E+06	5.9	1.6E+06	9.0	▼ 0.6
α-Farnesene	1.5E+06	11.7	4.7E+06	2.2	▲ 3.2	3.6E+06	10.9	3.3E+06	11.5	- 0.9	5.2E+06	7.0	2.7E+06	14.2	▼ 0.5
Sesquiterpene (MW 204)	6.7E+06	7.1	1.7E+07	4.5	▲ 2.6	1.5E+07	3.5	1.3E+07	6.3	- 0.9	1.9E+07	5.3	1.0E+07	9.0	▼ 0.6
Selina-3,7(11)-diene	7.9E+06	10.4	2.2E+07	2.6	▲ 2.8	1.7E+07	3.9	1.8E+07	5.5	- 1.0	2.3E+07	5.5	1.3E+07	25.3	▼ 0.6
Caryophyllene oxide	1.8E+05	10.6	1.1E+06	3.3	▲ 6.1	6.4E+05	8.8	1.4E+06	2.0	▲ 2.1	1.0E+06	9.1	1.4E+06	2.1	▲ 1.3
Guaiol	1.2E+06	9.5	7.0E+06	4.9	▲ 5.9	3.9E+06	3.1	1.1E+07	8.5	▲ 2.7	6.2E+06	7.8	1.1E+07	9.1	▲ 1.8
10-epi-γ-Eudesmol	1.1E+06	9.8	6.1E+06	4.3	▲ 5.5	3.4E+06	2.9	8.3E+06	3.8	▲ 2.4	5.3E+06	7.3	8.7E+06	3.9	▲ 1.6
β-Eudesmol	4.6E+05	11.1	2.7E+06	5.3	▲ 5.9	1.4E+06	26.8	4.4E+06	9.1	▲ 3.2	2.8E+06	10.8	5.3E+06	20.4	▲ 1.9
α-Eudesmol	3.9E+05	10.7	2.2E+06	4.7	▲ 5.7	1.3E+06	10.9	3.3E+06	6.4	▲ 2.6	2.2E+06	13.8	4.9E+06	47.6	▲ 2.3
Bulnesol	6.3E+05	8.9	4.8E+06	4.6	▲ 7.6	2.5E+06	4.9	7.8E+06	7.2	▲ 3.2	4.2E+06	8.7	8.9E+06	7.1	▲ 2.1
α-Bisabolol	3.1E+05	8.1	3.0E+06	5.2	▲ 9.5	1.5E+06	8.0	6.1E+06	10.6	▲ 4.1	2.7E+06	12.1	7.8E+06	10.7	▲ 2.8
CBD	n.d.	n.c.	1.1E+06	6.7	n.c.	7.0E+04	46.4	6.2E+06	6.6	▲ **88.8**	2.4E+05	2.1	1.3E+07	12.5	▲ **53.8**
CBC	n.d.	n.c.	n.d.	n.c.	n.c.	n.d.	n.c.	2.2E+05	64.3	n.c.	n.d.	n.c.	4.2E+05	49.4	n.c.
Supposed Δ^9-THC	n.d.	n.c.	3.7E+04	51.9	n.c.	n.d.	n.c.	3.2E+05	64.2	n.c.	n.d.	n.c.	5.1E+05	43.4	n.c.

In good agreement with the outcomes of Ilias *et al.* [14], sampling under extremely high temperatures (i.e., 150°C) maximised the recovery of CBD even within a short sampling time (i.e., 5 min) and under both pressure conditions as stands out in **Figure 2**. In addition to CBD, two other less abundant cannabinoids were recovered. One of them is cannabichromene (CBC), whose identity was confirmed by comparing its retention time and mass spectrum to those of a certified standard, while the other one is supposed to be Δ^9-THC, as its mass spectrum matches NIST and WILEY MS data as well as its linear retention index [24]. **Figures. S1, S2 and S4** in the supplementary materials report the mass spectra of the detected cannabinoids.

The positive effect of vacuum on the recovery of CBD was more important after 5 min of sampling (i.e., CBD RAA equal to 3) compared to 15 and 30 min (i.e., CBD RAA equal to 1.6) suggesting that equilibrium was being approached after 15 min of extraction. In contrast, irrespective of the pressure conditions, sampling at 150°C significantly discriminated against the recovery of the more volatile markers (i.e., mono and sesquiterpenes). This trend was probably due to the combination of two phenomena: (1) a decrease of the distribution coefficient between the fiber and the headspace (i.e., K_{fs}) [28], (2) an intensification of competitive adsorption and displacement of low molecular weight analytes given the extremely high amount of extracted CBD [31]. Therefore, 150°C as sampling temperature proved to be inappropriate for the simultaneous characterisation of the terpene and cannabinoid profiles.

The recovery of CBD was significantly reduced when sampling at relatively lower temperature (i.e., 80 and 90°C) compared to 150°C. Despite this, very promising results were obtained at 90°C especially when sampling under reduced pressure conditions. What is striking in **Figure 3** is the steep rise in the extraction kinetic of CBD obtained when sampling at reduced pressure conditions. At 90°C, irrespective of the sampling time, the amount of CBD extracted with vacuum was at least sixty times greater than that recovered under regular conditions and in just 5 min, vacuum ensured the extraction of a sufficient amount of CBD to meet the instrument sensitivity and to provide a good picture of CBD abundance in the inflorescences. As regards the more volatile markers (i.e., β-myrcene, *trans*-β-caryophyllene), at 90°C their recovery was on average 10 times higher than that obtained at 150°C irrespective of the pressure conditions. As evidenced by the RAA values reported in **Table 2** and in **Figure 4**, with 5 min of sampling, lowering the total pressure in the headspace did not improve the extraction of the monoterpene markers (RAA close to one) while, on average, it doubled the recovery of sesquiterpenes, as was expected by their lower volatilities. With longer sampling times (i.e., 15 and 30 min) the RAA significantly dropped for both mono and sesquiterpenes indicating decreased mass loadings under vacuum conditions.

The results obtained when sampling at 80°C were very similar to those observed at 90°C. Under regular conditions, the amount of CBD extracted after 5 min was below the instrument limit of detection (signal to noise ratio below three) while when sampling with vacuum the amount of CBD recovered was far above the instrument limit of quantification (signal to noise ratio close to 1000). When sampling at 80°C the amount of CBD extracted after 5 min of sampling was four times lower than that recovered at 90°C and the repeatability of the extraction of the minor cannabinoids drops down to RSD values higher than 40% while there were no significant differences in the recovery of the most volatile markers, irrespective of the extraction times. These results suggest that under vacuum conditions, 90°C is a more suitable extraction temperature compared to 80°C for the simultaneous optimal recovery of both the volatile (i.e., mono and sesquiterpenes) and semi-volatile markers (i.e., cannabinoids) of *Cannabis* inflorescences.

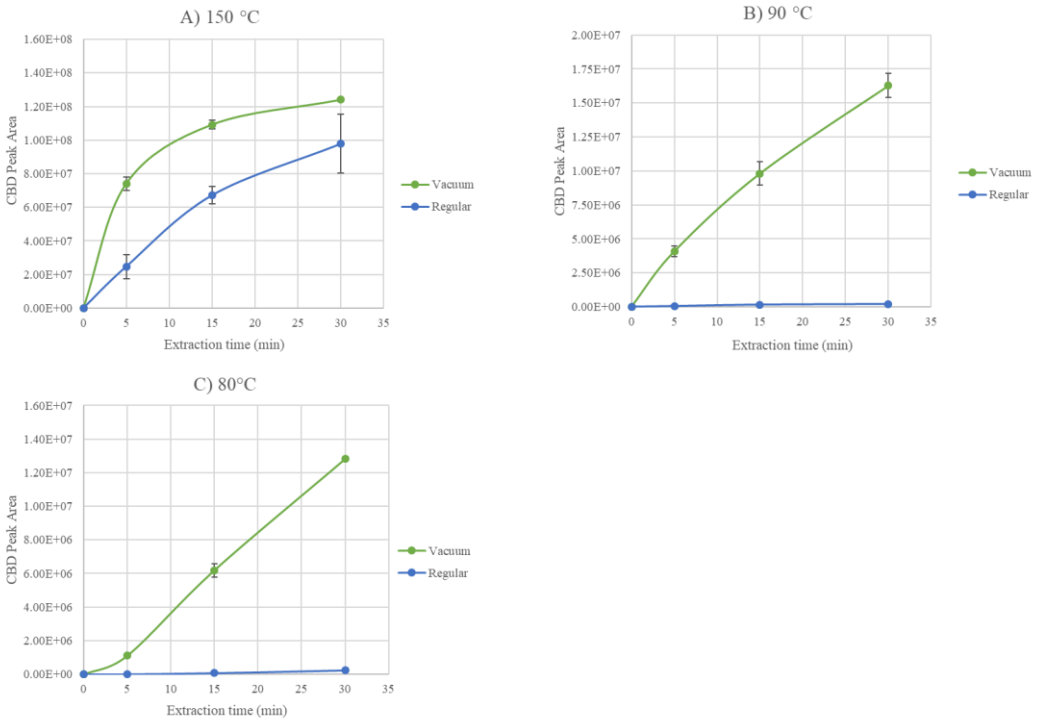

Figure 3, Extraction time profiles for CBD obtained under reduced (Vac-HS-SPME, green profile) and regular (Reg-HS-SPME, blue profile) conditions. Experimental parameters: PDMS/DVB fiber; 10 mg of sample; extraction times 5, 15, 30 minutes; Sampling temperature: A) 150°C; B) 90°C; C) 80°C.

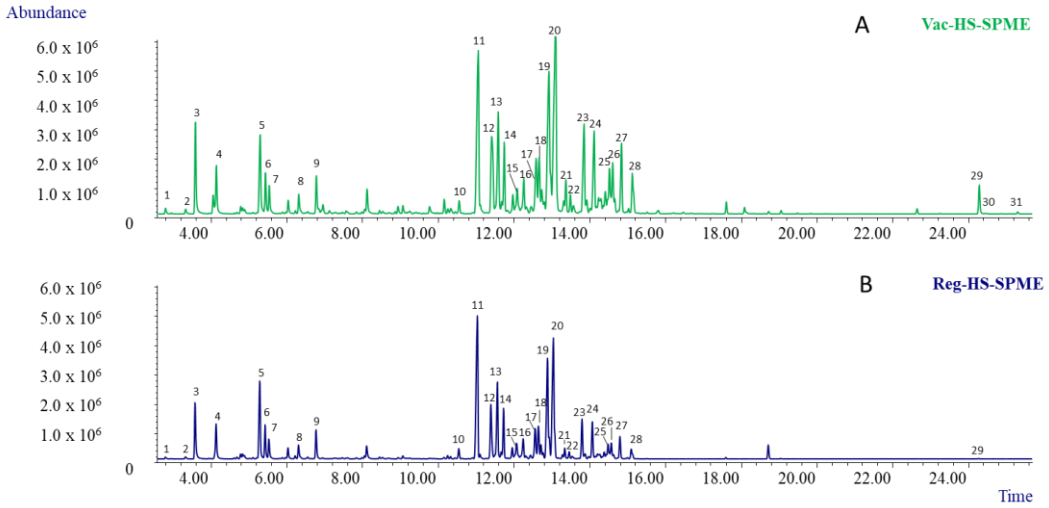

Figure 4, HS-SPME GC-MS profiles obtained when sampling 10 mg of matrix at 90°C for 5 minutes under reduced pressure (A) and atmospheric pressure (B) conditions. Legend: 1) α-Pinene, 2) β-Pinene, 3) β-Myrcene, 4) Limonene, 5) Linalool, 6) Fenchol, 7) cis-Pinene hydrate, 8) Borneol, 9) α-Terpineol, 10) β-Patchoulene, 11) trans-β-Caryophyllene, 12) trans-α-Bergamotene, 13) α-Humulene, 14) trans-β-Farnesene 15) β-Selinene, 16) α-Selinene17) α-Farnesene, 18-19) Sesquiterpenes (MW 204), 20) Selina-3,7(11)-diene, 21) trans-Nerolidol, 22) Caryophyllene oxide23) Guaiol, 24) 10-epi-γ-Eudesmol, 25) β-Eudesmol, 26) α-Eudesmol, 27) Bulnesol, 28) α-Bisabolol, 29) Cannabidiol, 30) Cannabichromene, 31) Cannabinoid 2 (Supposed Δ^9-THC)

<u>Thermal stability of CBD under the investigated sampling conditions</u>

In light of the results obtained by Czégény *et al.* [15], the thermal stability of CBD at 150°C and 90°C was studied. First, to ensure that no CDB degradation occurs within the analytical instrument, one µL of a CBD standard solution 1 mg mL^{-1} was directly injected and analysed by GC-MS. **Figure 5A** reports the obtained chromatogram which proved a standard purity in-line with that declared by the manufacturer and excluded the possibility of CBD degradation within the gas chromatograph.

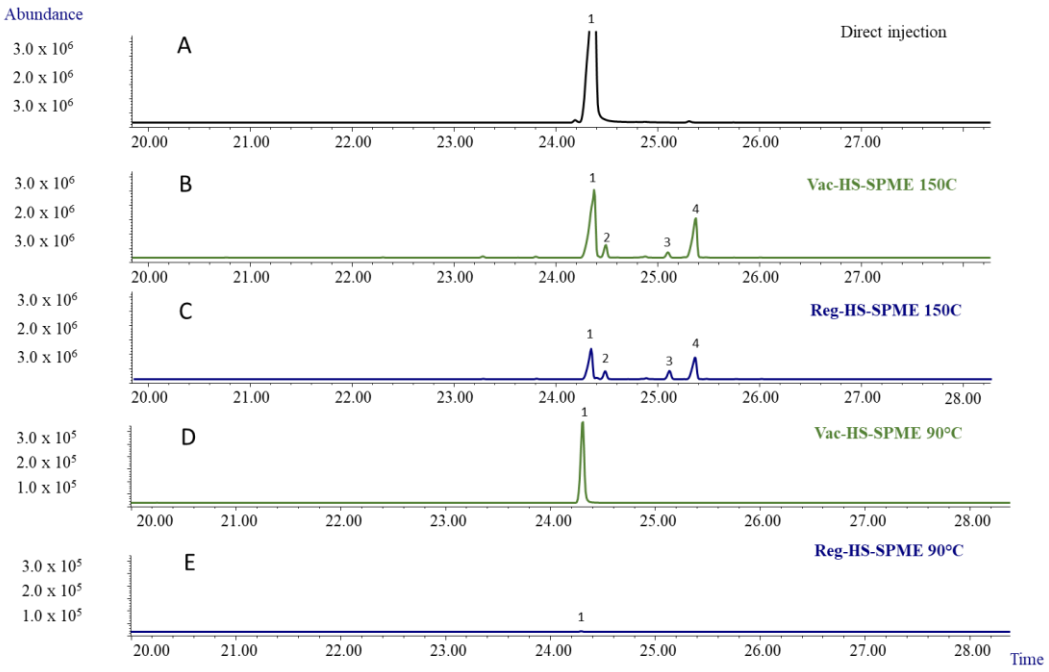

Figure 5, GC-MS profiles of CBD standard solution obtained with MEGA-5 narrow-bore column under the following conditions: A) injection of 1 µL of CBD standard solution 1 mg mL^{-1}; B) 10 µL of CBD standard solution 1 mg mL^{-1} recovered by Vac-HS-SPME after 5 minutes at 150°C; C) 10 µL of CBD standard solution 1 mg mL^{-1} recovered by Reg-HS-SPME after 5 minutes at 150°C; D) 10 µL of CBD standard solution 1 mg mL^{-1} recovered after 5 minutes by Vac-HS-SPME at 90°C; E) 10 µL of CBD standard solution 1 mg mL^{-1} recovered by Reg-HS-SPME after 5 minutes at 90°C. GC-MS Analysis conditions: see experimental section. Legend: 1) Cannabidiol, 2) Cannabichromene, 3) Cannabinoid 1 (supposed Δ^{8}-tetrahydrocannabinol), 4) Cannabinoid 2 (supposed Δ^{9}-tetrahydrocannabinol).

10 µL of the same 1.0 mg mL^{-1} CBD standard solution were then sampled by HS-SPME, under both pressure conditions for 5 min at 150 and 90°C. Three replicates for each sampling temperature were performed. The chromatograms reported in **Figure 4B** and **C** demonstrate that after 5 min of extraction at 150°C, under both pressure conditions, CBD undergoes degradation forming three cannabinoids. The first one is CBC whose identity was again confirmed by comparing its retention time and mass spectrum to those of a certified standard. The other two cannabinoids are supposed to be Δ^{9}-THC, Δ^{8}-THC as their mass spectra matched NIST and WILEY MS data as well as their linear retention index [24]. The relative amount of CBD undergoing to degradation was measured according to the following formula

$$\%\ of\ degraded\ CBD = \left(\frac{Total\ area - Area\ CBD}{Total\ area}\right) \times 100$$

where the total area is the sum of the areas of all the detected cannabinoids. The results proved that the percentage of the degraded CBD was not constant amongst the replicates and accounted for 19.5 ± 17.1% and 38.7 ± 17.4% under vacuum and regular conditions respectively. Cannabinoid 2 (i.e., supposed Δ^{9}-THC) was the most abundant degradation products with a relative abundance of 14.6 ± 12.6% and 20.9 ± 15%, under vacuum and regular conditions, respectively. The same degradation trend is not observed by direct injection into the gas chromatograph, even though the CBD is exposed to even higher temperature (i.e., injection port temperature 250°C), probably because the exposure time is too short to cause the degradation.

Figure 5 D and **E** report the chromatograms obtained when sampling10 µL of the same 1.0 mg mL^{-1} CBD standard solution at 90°C. The results show that, at the investigated temperature, no degradation products were generally detected irrespective of the pressure conditions. Cannabinoid 2 (i.e., supposed Δ^{9}-THC) was detected only in one replicate under vacuum condition, but its relative

abundance was in any case below 0.6%. These results provide further evidence that relative low sampling temperatures (i.e., 90°C) should be preferred for a more reliable characterisation of *Cannabis* inflorescences volatile and semi-volatile fractions.

1.8.3.5 Conclusions

The primary aim of this study was to investigate whether Vac-HS-SPME could be a suitable sample preparation technique to be combined to fast GC-MS analysis for the simultaneous characterisation of both the volatile (i.e., mono and sesquiterpenes) and semi-volatile (i.e., cannabinoids) fractions of *Cannabis sativa inflorescences*. The results proved that compared to Reg-HS-SPME, vacuum conditions in the HS ensure the fast recovery of cannabinoid markers at considerably lower sampling temperature (i.e., 90°C) that do not discriminate the most volatile fraction nor cause the formation of artefacts when the sampling time is minimised. The possibility of accelerating the following GC-MS analysis, by the use of a short narrow bore column, was also assessed and a satisfactory resolution of all the investigated markers was obtained in less than 30 min. Overall, since it is fast, totally automatable and solvent-free, the combination of Vac-HS-SPME and fast GC-MS should be considered as a green alternative analytical approach for the characterisation of *Cannabis sativa* inflorescences. Despite these very promising results, further experiments are still required to concretize the use of Vac-HS-SPME and fast GC-MS analysis for the reliable qualitative and quantitative characterisation of *Cannabis* samples. These experiments should aim at (1) validating a protocol, based on vac-HS-SPME and fast GC-MS analysis, to quantify specific cannabinoid markers (i.e., CBD and Δ^9-THC) and (2) at proving that the quantification results, obtained at relatively low temperatures, describe the absolute total amount of the investigated cannabinoids (i.e., the sum of the acidic and neutral form in the inflorescence) rather than the only neutral form.

1.8.3.6 References

[1] F. Pellati, V. Brighenti, J. Sperlea, L. Marchetti, D. Bertelli, S. Benvenuti, New Methods for the Comprehensive Analysis of Bioactive Compounds in Cannabis sativa L. (hemp), Molecules. 23 (2018) 2639. https://doi.org/10.3390/molecules23102639.

[2] G. Appendino, G. Chianese, O. Taglialatela-Scafati, Cannabinoids: Occurrence and Medicinal Chemistry, Curr. Med. Chem. 18 (2011) 1085–1099. https://doi.org/10.2174/092986711794940888.

[3] D. Jin, P. Henry, J. Shan, J. Chen, Identification of Chemotypic Markers in Three Chemotype Categories of Cannabis Using Secondary Metabolites Profiled in Inflorescences, Leaves, Stem Bark, and Roots, Front. Plant Sci. 12 (2021). https://doi.org/10.3389/fpls.2021.699530.

[4] European Monitoring Centre for Drugs and Drug Addiction (EMCDDA), Cannabis legislation in Europe, Publ. Off. Eur. Union, Luxemb. (2018) 1–30. https://doi.org/https://data.europa.eu/doi/10.2810/930744.

[5] L. Calvi, D. Pentimalli, S. Panseri, L. Giupponi, F. Gelmini, G. Beretta, D. Vitali, M. Bruno, E. Zilio, R. Pavlovic, A. Giorgi, Comprehensive quality evaluation of medical Cannabis sativa L. inflorescence and macerated oils based on HS-SPME coupled to GC–MS and LC-HRMS (q-exactive orbitrap®) approach, J. Pharm. Biomed. Anal. 150 (2018) 208–219. https://doi.org/10.1016/j.jpba.2017.11.073.

[6] E. Benvenuto, B.B. Misra, F. Stehle, C.M. Andre, J.-F. Hausman, G. Guerriero, Cannabis sativa: The Plant of the Thousand and One Molecules, (2016). https://doi.org/10.3389/fpls.2016.00019.

[7] E.B. Russo, Taming THC: potential cannabis synergy and phytocannabinoid-terpenoid entourage effects, Br. J. Pharmacol. 163 (2011) 1344–1364. https://doi.org/10.1111/j.1476-5381.2011.01238.x.

[8] D. Jin, K. Dai, Z. Xie, J. Chen, Secondary Metabolites Profiled in Cannabis Inflorescences, Leaves, Stem Barks, and Roots for Medicinal Purposes, Sci. Rep. 10 (2020) 3309. https://doi.org/10.1038/s41598-020-60172-6.

[9] R. Pavlovic, S. Panseri, L. Giupponi, V. Leoni, C. Citti, C. Cattaneo, M. Cavaletto, A. Giorgi, Phytochemical and Ecological Analysis of Two Varieties of Hemp (Cannabis sativa L.) Grown in a Mountain Environment of Italian Alps, Front. Plant Sci. 10 (2019). https://doi.org/10.3389/fpls.2019.01265.
[10] G. Mastellone, A. Marengo, B. Sgorbini, F. Scaglia, F. Capetti, F. Gai, P.G. Peiretti, P. Rubiolo, C. Cagliero, Characterization and Biological Activity of Fiber-Type Cannabis sativa L. Aerial Parts at Different Growth Stages, Plants. 11 (2022) 419. https://doi.org/10.3390/plants11030419.
[11] C. Citti, D. Braghiroli, M.A. Vandelli, G. Cannazza, Pharmaceutical and biomedical analysis of cannabinoids: A critical review, J. Pharm. Biomed. Anal. 147 (2018) 565–579. https://doi.org/10.1016/j.jpba.2017.06.003.
[12] Recommended Methods for the Identification and Analysis of Cannabis and Cannabis Products, 2013. https://doi.org/10.18356/1e8e4f16-en.
[13] D.W. Lachenmeier, L. Kroener, F. Musshoff, B. Madea, Determination of cannabinoids in hemp food products by use of headspace solid-phase microextraction and gas chromatography mass spectrometry, Anal. Bioanal. Chem. 378 (2004) 183–189. https://doi.org/10.1007/s00216-003-2268-4.
[14] Y. Ilias, S. Rudaz, P. Mathieu, P. Christen, J.-L. Veuthey, Extraction and analysis of differentCannabis samples by headspace solid-phase microextraction combined with gas chromatography-mass spectrometry, J. Sep. Sci. 28 (2005) 2293–2300. https://doi.org/10.1002/jssc.200500130.
[15] Z. Czégény, G. Nagy, B. Babinszki, Á. Bajtel, Z. Sebestyén, T. Kiss, B. Csupor-Löffler, B. Tóth, D. Csupor, CBD, a precursor of THC in e-cigarettes, Sci. Rep. 11 (2021) 8951. https://doi.org/10.1038/s41598-021-88389-z.
[16] E. Psillakis, Vacuum-assisted headspace solid-phase microextraction: A tutorial review, Anal. Chim. Acta. 986 (2017) 12–24. https://doi.org/10.1016/j.aca.2017.06.033.
[17] E. Psillakis, The effect of vacuum: an emerging experimental parameter to consider during headspace microextraction sampling, Anal. Bioanal. Chem. 412 (2020) 5989–5997. https://doi.org/10.1007/s00216-020-02738-x.
[18] E. Psillakis, A. Mousouraki, E. Yiantzi, N. Kalogerakis, Effect of Henry's law constant and operating parameters on vacuum-assisted headspace solid phase microextraction, J. Chromatogr. A. 1244 (2012) 55–60. https://doi.org/10.1016/j.chroma.2012.05.006.
[19] E. Psillakis, E. Yiantzi, L. Sanchez-Prado, N. Kalogerakis, Vacuum-assisted headspace solid phase microextraction: Improved extraction of semivolatiles by non-equilibrium headspace sampling under reduced pressure conditions, Anal. Chim. Acta. 742 (2012) 30–36. https://doi.org/10.1016/j.aca.2012.01.019.
[20] F. Capetti, P. Rubiolo, C. Bicchi, A. Marengo, B. Sgorbini, C. Cagliero, Exploiting the versatility of vacuum-assisted headspace solid-phase microextraction in combination with the selectivity of ionic liquid-based GC stationary phases to discriminate Boswellia spp. resins through their volatile and semivolatile fractions, J. Sep. Sci. 43 (2020) 1879–1889. https://doi.org/10.1002/jssc.202000084.
[21] B.J. Pollo, K.L. Romero-Orejón, A.J. Marsaioli, P.T.V. Rosa, F. Augusto, Vacuum-assisted headspace solid-phase microextraction and gas chromatography coupled to mass spectrometry applied to source rock analysis, Adv. Sample Prep. 1 (2021) 100001. https://doi.org/10.1016/j.sampre.2021.100001.
[22] L.S.E. Bruno Kolb, The Technique of Head-Space-Gas Chromatography, in: Static Headspace-Gas Chromatogr. Theory Pract., 1st ed., Wiley-VCH Verlag, United States of America, 2006: pp. 45–116.
[23] GC Calculators and Method Translation Software | Agilent, (n.d.). https://www.agilent.com/en/support/gas-chromatography/gccalculators (accessed January 29, 2022).
[24] NIST Chemistry WebBook, (n.d.). https://webbook.nist.gov/chemistry/ (accessed January 29, 2022).
[25] C. Bicchi, L. Blumberg, C. Cagliero, C. Cordero, P. Rubiolo, E. Liberto, Development of fast enantioselective gas-chromatographic analysis using gas-chromatographic method-translation software in routine essential oil analysis (lavender essential oil), J. Chromatogr. A. 1217 (2010) 1530–1536. https://doi.org/10.1016/j.chroma.2010.01.003.
[26] M. Mazzucotelli, M.A. Minteguiaga, B. Sgorbini, L. Sidisky, A. Marengo, P. Rubiolo, C. Bicchi, C. Cagliero, Ionic liquids as water-compatible GC stationary phases for the analysis of fragrances and essential oils: Quantitative GC–MS analysis of officially-regulated allergens in perfumes, J. Chromatogr. A. 1610 (2020) 460567. https://doi.org/10.1016/j.chroma.2019.460567.

[27] EPI SuiteTM-Estimation Program Interface | US EPA, Downloaded Oct. 2021. (n.d.). https://www.epa.gov/tsca-screening-tools/epi-suitetm-estimation-program-interface (accessed February 2, 2022).
[28] H. Lord, J. Pawliszyn, Evolution of solid-phase microextraction technology, J. Chromatogr. A. 885 (2000) 153–193. https://doi.org/10.1016/S0021-9673(00)00535-5.
[29] S. Risticevic, H. Lord, T. Górecki, C.L. Arthur, J. Pawliszyn, Protocol for solid-phase microextraction method development, Nat. Protoc. 5 (2010) 122–139. https://doi.org/10.1038/nprot.2009.179.
[30] E. Yiantzi, N. Kalogerakis, E. Psillakis, Vacuum-assisted headspace solid phase microextraction of polycyclic aromatic hydrocarbons in solid samples, Anal. Chim. Acta. 890 (2015) 108–116. https://doi.org/10.1016/j.aca.2015.05.047.
[31] M.J. Trujillo-Rodríguez, V. Pino, E. Psillakis, J.L. Anderson, J.H. Ayala, E. Yiantzi, A.M. Afonso, Vacuum-assisted headspace-solid phase microextraction for determining volatile free fatty acids and phenols. Investigations on the effect of pressure on competitive adsorption phenomena in a multicomponent system, Anal. Chim. Acta. 962 (2017) 41–51. https://doi.org/10.1016/j.aca.2017.01.056.

1.8.3.7 Supplementary Material

Table S1, identified compounds, linear retention indexes (I^t_s Lit) on the conventional and narrow bore MEGA-5 columns, molecular formula, molecular weight and main physicochemical properties ($LogK_{ow}$, boiling point and vapour pressure)

Compound	**I^t_s Lit.**[30]	**I^t_s Exp. (MEGA-5)**	**I^t_s Exp. (MEGA-5 NB)**	**Molecular Formula**	**Molecular Weight**	**$LogK_{ow}$** [31]	**Boiling Point (°C) 760mmHg** [31]	**Vapour pressure (mmHg) 25°C** [31]
α-Pinene	939	934	927	$C_{10}H_{16}$	136	4.83	155.50	4.75E+00
β-Pinene	980	976	966	$C_{10}H_{16}$	136	4.16	166.00	2.93E+00
β-Myrcene	991	993	983	$C_{10}H_{16}$	136	4.17	167.00	2.01E+00
Limonene	1031	1029	1018	$C_{10}H_{16}$	136	4.57	178.00	1.44E+00
Linalool	1098	1100	1086	$C_{10}H_{18}O$	154	2.97	198.00	1.60E-01
Fenchol	1112	1112	1093	$C_{10}H_{18}O$	154	3.17	209.98	1.13E-01
cis-Pinene hydrate	1121	1120	1098	$C_{10}H_{18}O$	154	2.85	200.80	7.03E-02
Borneol	1165	1165	1144	$C_{10}H_{18}O$	154	2.85	210.00	5.02E-02
α-Terpineol	1189	1190	1169	$C_{10}H_{18}O$	154	3.33	217.50	4.23E-02
α-Patchoulene	1388	1387	1377	$C_{15}H_{24}$	204	5.87	248.65	2.44E-02
trans-β-Caryophyllene	1418	1415	1404	$C_{15}H_{24}$	204	6.30	256.80	3.12E-02
trans-α-Bergamotene	1437	1434	1427	$C_{15}H_{24}$	204	6.57	255.38	2.77E-02
α-Humulene	1454	1449	1437	$C_{15}H_{24}$	204	6.95	270.56	1.53E-02
trans-β-Farnesene	1458	1458	1447	$C_{15}H_{24}$	204	7.17	254.57	3.49E-02
β-Selinene	1485	1481	1467	$C_{15}H_{24}$	204	6.38	248.39	4.37E-02
α-Selinene	1494	1490	1477	$C_{15}H_{24}$	204	6.30	253.52	3.31E-02
α-Farnesene	1509	1507	1495	$C_{15}H_{24}$	204	7.10	261.11	2.50E-02
Selina-3,7(11)-diene	1542	1539	1526	$C_{15}H_{24}$	204	6.35	262.04	1.74E-02
trans-Nerolidol	1564	1565	1545	$C_{15}H_{26}O$	222	5.68	291.92	5.92E-04
Caryophyllene oxide	1577	1581	1552	$C_{15}H_{24}O$	220	4.91	263.48	1.00E-02
Guaiol	1595	1594	1573	$C_{15}H_{26}O$	222	5.24	297.63	3.63E-05
10-epi-γ-eudesmol	1596	1613	1590	$C_{15}H_{26}O$	222	4.94	294.08	6.06E-005

Compound	**I^t_s Lit.**[30]	**I^t_s Exp. (MEGA-5)**	**I^t_s Exp. (MEGA-5 NB)**	**Molecular Formula**	**Molecular Weight**	**LogK$_{ow}$** [31]	**Boiling Point (°C) 760mmHg** [31]	**Vapour pressure (mmHg) 25°C** [31]
β-Eudesmol	1649	1645	1616	$C_{15}H_{26}O$	222	4.88	286.47	1.19E-04
α-Eudesmol	1652	1648	1622	$C_{15}H_{26}O$	222	4.81	290.99	8.63E-05
Bulnesol	1663	1666	1651	$C_{15}H_{26}O$	222	4.90	297.63	5.13E-05
α-Bisabolol	1683	1682	1657	$C_{15}H_{26}O$	222	5.63	299.83	1.36E-04
Cannabidiol (CBD)	2375*	2420	2366	$C_{21}H_{30}O_2$	314	8.01	428.51	2.75E-08
Cannabichromene (CBC)		-	2383	$C_{21}H_{30}O_2$	314	7.98	408.96	5.07E-08
Supposed Δ^8- Tetrahydrocannabinol (Δ^8-THC)		-	2445	$C_{21}H_{30}O_2$	314	7.41	407.23	4.63E-08
Supposed Δ^9- Tetrahydrocannabinol (Δ^9-THC)	2470*	-	2460	$C_{21}H_{30}O_2$	314	7.60	407.23	4.63E-08

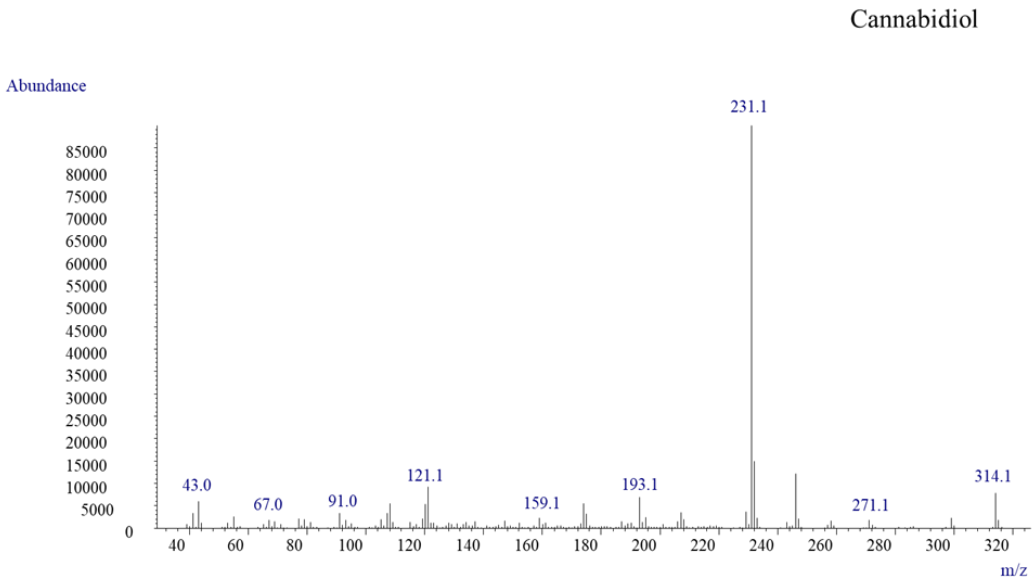

Figure S1, Cannabidiol mass spectrum. The MS was operated in electron ionisation mode (EI) at 70 eV, scan rate: 666 u/s, mass range: 35–350 m/z.

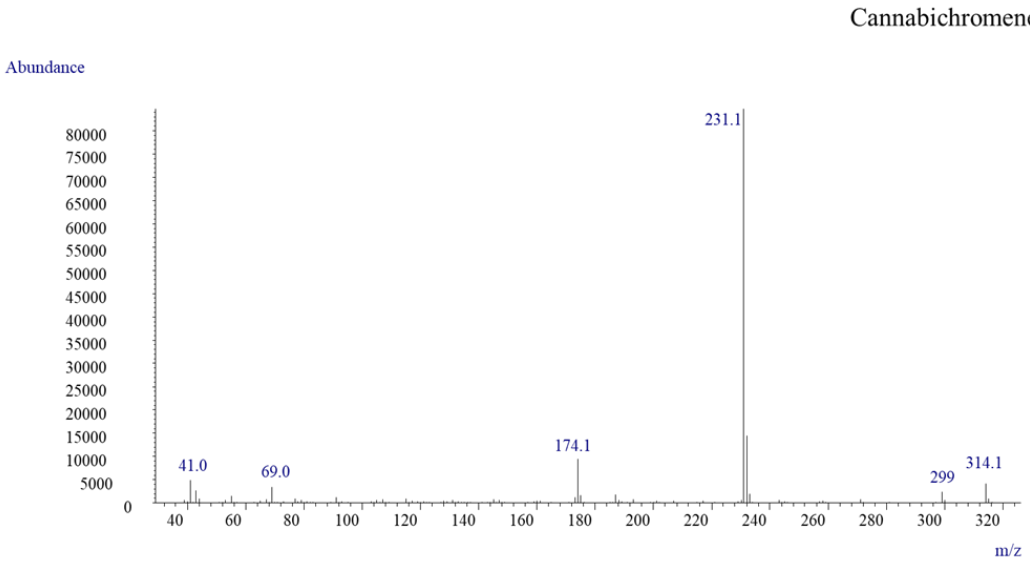

Figure S2, Cannabichromene mass spectrum. The MS was operated in electron ionisation mode (EI) at 70 eV, scan rate: 666 u/s, mass range: 35–350 m/z.

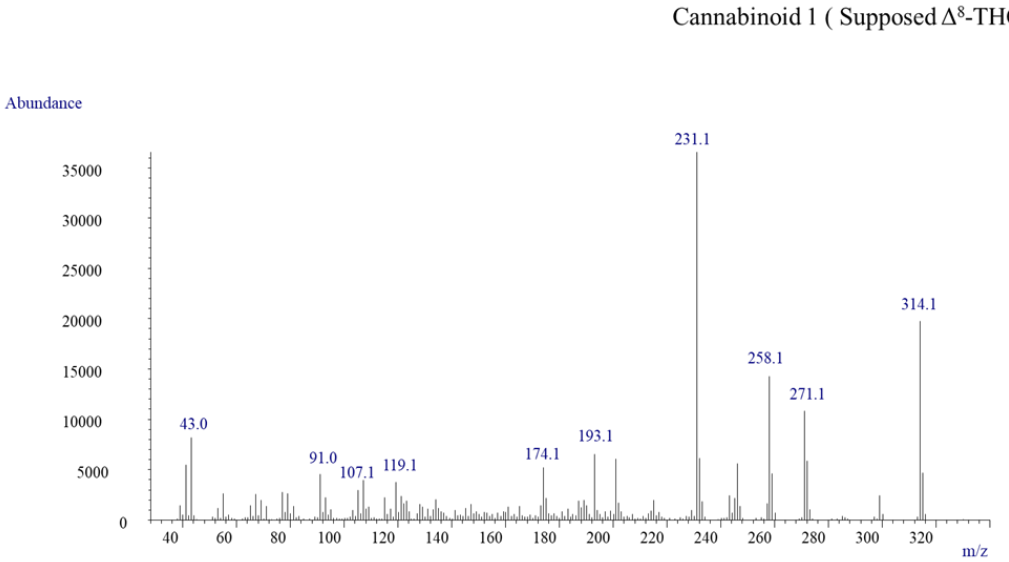

Figure s3, Cannabinoid 1 mass spectrum. The MS was operated in electron ionisation mode (EI) at 70 eV, scan rate: 666 u/s, mass range: 35–350 m/z.

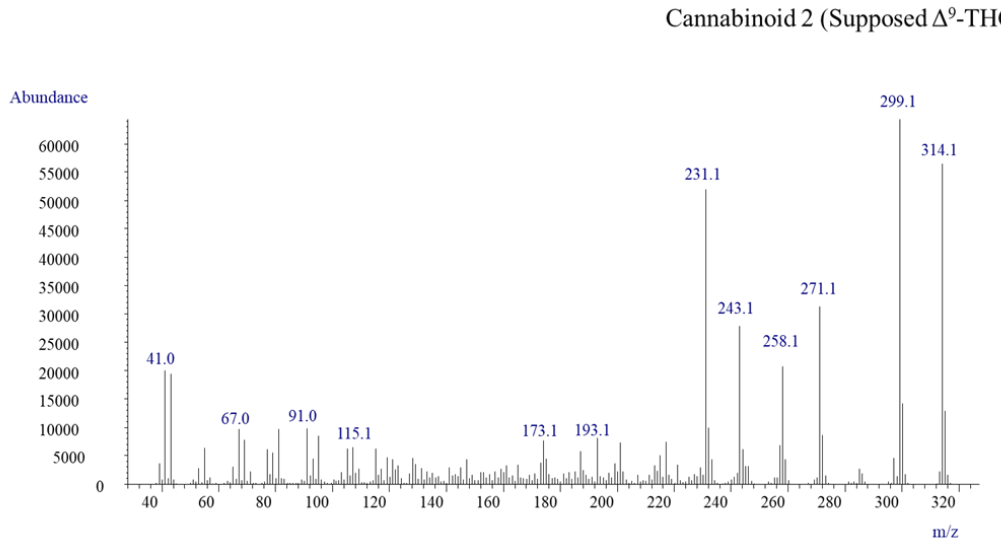

Figure S4, Cannabinoid 2 mass spectrum. The MS was operated in electron ionisation mode (EI) at 70 eV, scan rate: 666 u/s, mass range: 35–350 m/z.

2 Chapter 2:

Essential Oils as Tyrosinase Inhibitors

2.1 Introduction

Tyrosinase is a copper-containing enzyme characteristic of several bacteria, fungi, animals, and plants. In plants, tyrosinase catalyses the oxidation of polyphenol compounds to quinones which then polymerize into dark melanin giving the undesirable browning, which leads to food degradation and loss in nutritional quality during postharvest and handling processes. In insects, tyrosinase is one of the key enzymes in the molting process, and tyrosinase inhibitors are considered attractive agents to control insect pests [1]. Finally, in humans, tyrosinase is the crucial enzyme in the biosynthetic pathway of melanin, the biological pigment found in hair, skin, and in the iris, where it plays a pivotal role in the absorption of free radicals and the protection of the cell DNA from ionizing radiations including UV light.

This chapter describes the role of tyrosinase in the formation of melanin pigments in humans. It provides two research projects aiming at identifying new tyrosinase inhibitors suitable to treat hyperpigmentation disorders among essential oil components.

2.2 Tyrosinase role in melanin biosynthesis in human skin

Melanin is produced inside melanocytes, dendritic cells that reside in the epidermis basal layer and that form together with 30-40 associated keratinocytes, the melanin units. Melanocytes produce melanin inside specific organelles called melanosomes which are then transferred to the associated keratinocytes, where they accumulate around the cell nucleus providing photoprotection. It is interesting to highlight that the number of melanocytes is the same irrespective of the skin colour (which is determined by the number and distribution of melanosomes) and that albinism is an inherited disorder characterised by total or partial loss of melanin due to the complete absence or partial dysfunction of tyrosinase enzyme [2].

Melanogenesis is a complex biosynthetic pathway characterised by several enzymatic and chemical reactions leading to melanin formation from the amino acid L-tyrosine. Tyrosinase enzyme activity is fundamental during melanogenesis as it regulates its rate-limiting reactions meaning the oxidation of L-tyrosine to *o*-dopaquinone. Tyrosinase catalyses the hydroxylation of L-tyrosine to L-dopa thanks to its monophenolase activity and subsequently the oxidation of L-DOPA to *o*-dopaquinone by its diphenolase activity. The resulting *o*-dopaquinone molecule spontaneously undergoes intramolecular cyclisation forming leukodopachrome which is then oxidised by another *o*-dopaquinone molecule to dopachrome. The dopachrome tautomerase enzyme then gradually decomposes dopachrome to dihydroxyindole (DHI) and dihydroxyindole-2-carboxylicacid (DHICA), and the letters are then oxidised to eumelanin. In parallel, in the presence of cysteine or glutathione, *o*-dopaquinone is converted to 5-S-cysteinyl-dopa or glutothionyldopa, which are then oxidised to benzothiazine intermediates to produce pheomelanin.

Although three enzymes are involved in the biosynthetic pathway, only L-tyrosine oxidation to *o*-dopaquinone cannot occur without the enzyme activity. The remaining reaction can occur spontaneously at physiological pH [3].

Melanogenesis is regulated by several factors, including microphtalmia transcription factor (MITF), which controls the tyrosinase transcription, and the alpha- melanocyte-stimulating hormone (α-MSH), which binds the melanocortin -1 receptor (MC1R), increasing the melanin formation. However, the most potent way to induce melanin synthesis is by exposure to sun lights which causes the formation of reactive oxygen species (ROS) that act as signals for the proliferation of melanocytes and melanogenesis [2].

Genetic conditions, exogenous causes such as exposure to UV light or certain drugs, chemicals and physiological conditions, such as aging, can significantly increase the melanin production leading to minor aesthetic problems, such as freckles and solar lentigo, as well as to severe dermatological conditions including cancer and post-inflammatory melanoderma [3]. The downregulation of tyrosinase is a very general approach to reducing excessive melanin production, and tyrosinase inhibitors as skin whitening agents are gaining significant prominence clinically and cosmetically [2].

2.3 Skin depigmentation agents interfering with tyrosinase activity

On the EU market, tyrosinase inhibitors employed as skin-whitening agents can be grouped into two main categories according to their field of use: tyrosinase inhibitors banned by the EU cosmetic regulation 1223/2009 (i.e., hydroquinone and monobenzyl ether hydroquinone) due to their severe side effects but still used to treat hyperpigmentation disorders under medical supervision and tyrosinase inhibitors still allowed in cosmetics products (i.e., β-arbutin, aloesin, kojic acid) [2].

Hydroquinone is a naturally occurring hydroxyphenol in plants and foods such as coffee, cranberries, and blueberries. It inhibits tyrosinase by acting as an alternative substrate to L-tyrosine, leading to the formation of reactive oxygen species (ROS), which damage tyrosinase. It has proven to be a successful bleaching agent determining reversible skin depigmentation by several clinical trials, and

it is nowadays considered the gold standard for the treatment of hyperpigmentation disorders [2]. In Europe, hydroquinone is used in topical formulation at concentrations between 1 % and 5% under medical prescription only. In contrast, its usage in cosmetics formulation was banned in 2010 due to the severe side effects associated with its long-term application. The reported side effects include allergic contact dermatitis, discoloration of the nail, impaired wound healing, neuropathy, and exogenous ochronosis, a rare cosmetically disfiguring condition characterized by a localized dark blue hyperpigmentation. The hydroquinone derivative, monobenzone (also knowns as monobenzyl ether of hydroquinone), is another powerful inhibitor of melanogenesis. It is metabolised by tyrosinase-producing ROS and quinone-haptens. The first damage tyrosinase and block melanogenesis, while the latter trigger an immunological response that destroys melanocytes even at non-exposed sites. Monobenzone usage is strictly restricted to the treatment of quite severe hyperpigmentation disorders, and it cannot be used safely in cosmetics as it is responsible for permanent generalized depigmentation.

As regards the cosmetically legal tyrosinase inhibitors, the most prevalent ones include, in descending order of detection frequency: kojic acid, β- arbutin, and aloesin.

Kojic acid is a naturally produced secondary metabolite in several *Aspergillus strains* [4]. It inhibits tyrosinase by chelation of its copper atom in its active site. Its efficacy as a skin-whitening agent has been proven in clinical studies, which also highlighted concerning side effects, including erythema, stinging sensation, and contact eczema. However, using kojic acid 1% in cosmetic leave-on products such as face and hand cream is still considered safe by the European Scientific Committee on Consumers Safety [4].

β-Arbutin is a β-D-glucopyranoside of hydroquinone found in bearberry *(*i.e., *Arctostaphylos uva-ursi* (L.) Spreng). Several β-arbutin derivatives such as α-arbutin and deoxy-arbutin have been synthesised to improve its penetration through the skin. However, although β-arbutin is still legally available in Europe as a cosmetic ingredient in concentrations up to 7%, the SCCS has raised safety concerns regarding its use as a cosmetic ingredient. The concern is related to the possible hydrolysation of the glyosidic bond during storage or by the bacterial flora when applied to the skin leading to the release of hydroquinone [2].

Aloesin is another plant-derivative phenolic compound (cumarin-type) isolated from *Aloe vera* (L.) Burm.f. with promising tyrosinase inhibitory activity. Aloesin modulated melanogenesis via competitive inhibition of tyrosinase, and studies on human volunteers have proven its inhibitory effect on UV-induced hyperpigmentation [5].

2.4 Tyrosinase inhibitors from natural products

Plants have been essential sources of tyrosinase inhibitors as three out of five of the most employed tyrosinase inhibitors medically and cosmetically are plant specialised metabolites (i.e., hydroquinone, β-arbutin, and aloesin).

Up to date, several phenolic compounds have been investigated as tyrosinase inhibitors, and promising candidates have been identified among flavonoids (i.e., neorauflavane [3], kaempferol and quercetin [6], and resveratrol [3]) phenylpropanoids *(p*-cumaric acid [7], chlorogenic acid [8], cinnamaldehyde [9], eugenol and isoeugenol [10]–[12]) and simple phenols and phenolic acids (hydroquinone, β-arbutine, resorcinol, guaiacol, cuminic acid, benzoic acid, anisic acid, anisaldehyde, benzaldehyde, *p*-hydroxybenzaldehyde [1]).

Terpenoid derivatives with promising skin whitening potentials identified so far include thymol [12]–[14], carvacrol [12], and citral [15, 16], for which a more in-depth description is provided in section 2.15.

2.5 The research of new bioactive compounds from plant matrices

Assigning bioactive constituents among several components of a natural product is not trivial due to the often highly complex chemical composition of the matrix under investigation and the potential interaction among the different mixture bioactive constituents (i.e., additive, synergistic, and antagonist interactions).

In 2019 Kellogg *et al.* [17] thoroughly described the main pitfalls and questions that very often arise during the research of new bioactive constituents from natural products and proposed a common research scheme. The approach will be briefly described in the following paragraph.

The potential biological activity of a natural product is usually first established with an *in vitro* assay. *In vitro* assays are generally preferred over non-clinical (i.e., animal model) or clinical studies because they provide the speed and scale that is necessary to characterise the matrix constituents responsible for its bioactivity comprehensively and to identify new lead compounds. It follows, therefore, that the assay must be relevant and robust in order to provide informative data and to prevent waste of time, fund and efforts. Other than determining the activity of the matrix, the *in vitro* assay is fundamental to comprehensively characterise the bioactivity of the matrix, meaning the compounds responsible for its action. The gold standard approach for identifying bioactive mixture components is bioassay-guided fractionation and purification, in which the extract is subjected to successive rounds of fractionation, with each fraction prioritised for the next stage based on the biological assay data. The process theoretically can proceed until the isolation and purification of the single compound/s responsible for the activity. However, thanks to the availability of countless purified standards of individual botanical compounds, this rarely happens, and fractionation is carried on until enriched fractions with a limited and more manageable number of potential bioactive constituents are isolated. Then, the research generally proceeds to exclusion testing of the bioactivity of individual compounds belonging to the isolated active fraction/s.

2.5.1 *In vitro* assay

Enzymes are undoubtedly essential drug targets, and many drugs today function through the inhibition of enzymes mediating disorders phenotypes [18]. This is the case for skin whitening agents used to treat hyperpigmentation disorders which reduce melanin formation by inhibiting the tyrosinase enzyme. Tyrosinase activity is relatively easy to monitor *in vitro*. A homogenous (i.e., also referred to as "mix and measure") colorimetric readout-based assay [19] is employed as the reaction product (i.e., Dopachrome) is a coloured chemical whose formation can be followed by monitoring the increase in absorbance at 475 nm by the use of a spectrophotometer. Nonetheless, there are specific assay parameters that should be optimise to develop an *in vitro* assay that is relatively representative of the *in vivo* enzymatic activity and, therefore that is effective at identifying promising inhibitors. These parameters include the choice of the correct enzyme form, the enzyme and substrate concentration, and the composition of the buffer solution in which the reaction is carried out. For the latter point, the nature of the inhibitors that are meant to be tested should be taken into account [19].

The best enzyme form to be employed in the enzymatic assay is the human native form of the enzyme. However, the latter is often not easy to isolate, and even when isolation is possible, the cost may be unaffordable. This is the case for human tyrosinase (*hs*TYR), which is not commercially available. Therefore it has very often been replaced by a readily available and low-cost mushroom tyrosinase from *Agaricus bisporus* (*ab*TYR) [20]. Among the scientific community, there are divergent opinions regarding the use of *ab*TYR in high throughput screening devoted to the research o new lead compounds as tyrosinase inhibitors. While Roulier *et al* [20] firmly believe that *ab*TYR may be a deceptive model due to differences in the interaction pattern and inhibition value between

*hs*TYR and *ab*TYR, Mukherjee *et al* [21] argue that the use of *ab*TYR is justified as both *hs*TYR and *ab*TYR share the same catalytic site and epidermal growth factor (EGF)-like domain. In light of these facts, the author believes that, while it is true that the sole *ab*TYR inhibition should not lead to a direct assumption regarding *hs*TYR inhibition, it is implausible to replace *ab*TYR with *hs*TYR in high throughput screening where significant amounts of the enzyme are required.

Irrespective of the enzyme form, the substrate and enzyme concentration should be optimised to have a substrate concentration low enough to detect both competitive and non-competitive inhibitors. Still, it must be sufficiently high to design a robust assay with low variability [18], [19], [22]. A general rule for developing an assay sensitive to competitive and non-competitive inhibitors is to set the substrate concentration in the assay equal to the substrate $K_{m,}$ which is the substrate concentration permitting the enzyme to achieve half V_{max}. In turn, V_{max} describes the highest number of substrate molecules that can be transformed into products over a given time when all the enzyme active sites are occupied. The latter parameters can be determined experimentally through kinetic studies by plotting initial reaction velocities (v_o) against substrate concentration and fitting the data point by non-linear regression to the classical *Michealis Menten* steady-state model, which is described by the following equation

$$v_0 = \frac{V_{max} \times S}{S + K_M}$$

Where v_o is the initial reaction velocity (nmols min^{-1}) S is the concentration of substrate (μM), V_{max} is the maximal reaction velocity (nmols min^{-1}), and K_M is the Michaelis constant μM). Initial reaction velocities (v_o) are obtained from the initial velocity region of the reaction progress curve, which is built by mixing the enzyme and the substrate and measuring the subsequent product that is generated over a period of time [19].

Once the substrate concentration has been optimised, the incubation time should be set to provide reliable data in the shortest possible time (especially in high-throughput screening of several matrices and when miniaturised technologies are not available) while ensuring that the conversion of substrate to product is still linear to time [18].

Enzymatically catalysed reactions, as in the case of tyrosinase, are performed in an aqueous solution and near physiological pH to mimic the intracellular environment of the native enzyme. When testing natural compounds as potential enzyme inhibitors, the latter are generally first dissolved in dimethyl sulfoxide (DMSO), which is the solvent of choice in light of its great solvating power for many compounds, its miscibility with water, and its compatibility with several enzymes when kept at a concentration below 5%. In order to improve the solubility of poorly water-soluble chemicals such as essential oils constituents during the investigation of their bioactivity, solubilising agents such as bovine serum albumin (BSA), casein, tween-80, and triton X-100 (26) could be used. However, divergent views exist on this topic as, for example, some legitimate inhibitors bind to BSA, lowering the free compound for enzyme inhibition and causing false negative (i.e., missing some hits) [23].

2.5.2 Fractionation

Fractionation of complex matrices into purified fractions and eventually isolation of bioactive compounds (i.e., when the corresponding standard is not commercially available) relay on preparative pressure liquid chromatography methods. Contrary to analytical chromatography, in which separation aims at comprehensively identifying and eventually quantifying the mixture components, preparative chromatography is a purification process that aims at the isolation of a consistent amount of simplified fractions or ultimately pure substances from a mixture [24]. Preparative pressure liquid chromatography methods include flash chromatography, medium pressure liquid chromatography, and high-pressure preparative liquid chromatography, which differ

in the actual backpressure they can stand, the achievable resolution, and the preparative scale required [24]. The most common strategy for isolating constituents from natural products is to employ flash chromatography to obtain simplified fractions from which pure compounds can eventually be isolated by preparative high-pressure liquid chromatography [17].

Flash chromatography is a variant of conventional column chromatography in which pressure is applied to increase the flow rate of the eluent, which results in a faster separation and reduced operation times [24]. During the last decade, several automated flash chromatography systems using pre-packed flash columns have been developed, significantly simplifying the fractionation process compared to using glass columns filled with suitable packing material.

2.6 References

[1] I. Kubo and I. Kinst-Hori, "Tyrosinase Inhibitors from Anise Oil," *J. Agric. Food Chem.*, vol. 46, no. 4, pp. 1268–1271, 1998, doi: 10.1021/jf9708958.

[2] B. Desmedt *et al.*, "Overview of skin whitening agents with an insight into the illegal cosmetic market in Europe," *J. Eur. Acad. Dermatology Venereol.*, vol. 30, no. 6, pp. 943–950, 2016, doi: 10.1111/jdv.13595.

[3] T. Pillaiyar, M. Manickam, and V. Namasivayam, "Skin whitening agents: medicinal chemistry perspective of tyrosinase inhibitors," *J. Enzyme Inhib. Med. Chem.*, vol. 32, no. 1, pp. 403–425, Jan. 2017, doi: 10.1080/14756366.2016.1256882.

[4] C. L. Burnett *et al.*, "Final report of the safety assessment of kojic acid as used in cosmetics," *Int. J. Toxicol.*, vol. 29, no. 6, 2010, doi: 10.1177/1091581810385956.

[5] J. W. Lin, H. M. Chiang, Y. C. Lin, and K. C. Wen, "Natural products with skin - Whitening effects," *J. Food Drug Anal.*, vol. 16, no. 2, pp. 1–10, 2008.

[6] I. Kubo and I. Kinst-Hori, "Tyrosinase inhibitory activity of the olive oil flavor compounds," *J. Agric. Food Chem.*, vol. 47, no. 11, pp. 4574–4578, Nov. 1999, doi: 10.1021/jf990165v.

[7] J. Y. Lim, K. Ishiguro, and I. Kubo, "Tyrosinase inhibitory p-coumaric acid from ginseng leaves," *Phyther. Res.*, vol. 13, no. 5, pp. 371–375, 1999, doi: 10.1002/(SICI)1099-1573(199908/09)13:5<371::AID-PTR453>3.0.CO;2-L.

[8] E. Ersoy, E. Eroglu Ozkan, M. Boga, M. A. Yilmaz, and A. Mat, "Anti-aging potential and anti-tyrosinase activity of three Hypericum species with focus on phytochemical composition by LC–MS/MS," *Ind. Crops Prod.*, vol. 141, no. September, 2019, doi: 10.1016/j.indcrop.2019.111735.

[9] C.-T. T. Chang, W.-L. L. Chang, J.-C. C. Hsu, Y. Shih, and S.-T. T. Chou, "Chemical composition and tyrosinase inhibitory activity of Cinnamomum cassia essential oil," *Bot. Stud.*, vol. 54, no. 1, pp. 2–8, Aug. 2013, doi: 10.1186/1999-3110-54-10.

[10] B. Marongiu *et al.*, "Supercritical CO2 extract of Cinnamomum zeylanicum: Chemical characterization and antityrosinase activity," *J. Agric. Food Chem.*, vol. 55, no. 24, pp. 10022–10027, 2007, doi: 10.1021/jf071938f.

[11] E. Tangke Arung, E. Matsubara, I. Wijaya Kusuma, E. Sukaton, K. Shimizu, and R. Kondo, "Inhibitory components from the buds of clove (Syzygium aromaticum) on melanin formation in B16 melanoma cells," *Fitoterapia*, vol. 82, no. 2. pp. 198–202, 2011, doi: 10.1016/j.fitote.2010.09.008.

[12] M. D. M. Garcia-Molina, J. L. Muñoz-Muñoz, F. Garcia-Molina, P. A. García-Ruiz, and F. Garcia-Canovas, "Action of tyrosinase on ortho-substituted phenols: Possible influence on browning and melanogenesis," *J. Agric. Food Chem.*, vol. 60, no. 25, pp. 6447–6453, 2012, doi: 10.1021/jf301238q.

[13] H. Satooka and I. Kubo, "Effects of thymol on B16-F10 melanoma cells," *J. Agric. Food Chem.*, vol. 60, no. 10, pp. 2746–2752, Mar. 2012, doi: 10.1021/jf204525b.

[14] H. Satooka and I. Kubo, "Effects of thymol on mushroom tyrosinase-catalyzed melanin formation," *J. Agric. Food Chem.*, vol. 59, no. 16, pp. 8908–8914, Aug. 2011, doi: 10.1021/jf2014149.

[15] X.-W. Huang, Y.-C. Feng, Y. Huang, and H.-L. Li, "Potential cosmetic application of essential oil extracted from *Litsea cubeba* fruits from China," *J. Essent. Oil Res.*, vol. 25, no. 2, pp. 112–119, Apr. 2013, doi: 10.1080/10412905.2012.755479.

[16] R. Matsuura, H. Ukeda, and M. Sawamura, "Tyrosinase inhibitory activity of citrus essential oils," *J. Agric. Food Chem.*, vol. 54, no. 6, pp. 2309–2313, 2006, doi: 10.1021/jf051682i.

[17] J. J. Kellogg, M. F. Paine, J. S. McCune, N. H. Oberlies, and N. B. Cech, "Selection and characterization of botanical natural products for research studies: a NaPDI center recommended approach," *Nat. Prod. Rep.*, vol. 36, no. 8, pp. 1196–1221, 2019, doi: 10.1039/C8NP00065D.

[18] K. P. Williams and J. E. Scott, "Enzyme Assay Design for High-Throughput Screening," in *High Throughput Screening. Methods in Molecular Biology (Methods and Protocols)*, 2nd ed., vol. 565, W. P. Janzen and Bernasconi Paul, Eds. Clifton, N.J.: Humana Press, 2009, pp. 107–126.

[19] H. B. Brooks *et al.*, *Basics of Enzymatic Assays for HTS*, no. Md. Bethesda (MD), 2004.

[20] B. Roulier, B. Pérès, and R. Haudecoeur, "Advances in the Design of Genuine Human Tyrosinase Inhibitors for Targeting Melanogenesis and Related Pigmentations," *J. Med. Chem.*, vol. 63, no. 22, pp. 13428–13443, Nov. 2020, doi: 10.1021/acs.jmedchem.0c00994.

[21] P. K. Mukherjee, R. Biswas, A. Sharma, S. Banerjee, S. Biswas, and C. K. Katiyar, "Validation of medicinal herbs for anti-tyrosinase potential," *J. Herb. Med.*, vol. 14, pp. 1–16, Dec. 2018, doi: 10.1016/j.hermed.2018.09.002.
[22] M. G. Acker and D. S. Auld, "Considerations for the design and reporting of enzyme assays in high-throughput screening applications," *Perspect. Sci.*, vol. 1, no. 1–6, pp. 56–73, 2014, doi: 10.1016/j.pisc.2013.12.001.
[23] W. P. Janzen and P. Bernasconi, Eds., *High Throughput Screening*, vol. 565. Totowa, NJ: Humana Press, 2009.
[24] K. Hostettmann, A. Marston, and M. Hostettmann, *Preparative Chromatography Techniques*. Berlin, Heidelberg: Springer Berlin Heidelberg, 1998.
[25] Council of Europe, *European Pharmacopoeia*, 10th ed. Strasburg, France: Council of Eutope, 2020.
[26] F. Capetti *et al.*, "Citral-Containing Essential Oils as Potential Tyrosinase Inhibitors: A Bio-Guided Fractionation Approach," *Plants 2021, Vol. 10, Page 969*, vol. 10, no. 5, p. 969, May 2021, doi: 10.3390/PLANTS10050969.
[27] D. Fiocco *et al.*, "Lavender and peppermint essential oils as effective mushroom tyrosinase inhibitors: A basic study," *Flavour Fragr. J.*, vol. 26, no. 6, pp. 441–446, Nov. 2011, doi: 10.1002/ffj.2072.
[28] D. Fiocco, M. Arciuli, M. P. Arena, S. Benvenuti, and A. Gallone, "Chemical composition and the anti-melanogenic potential of different essential oils," *Flavour Fragr. J.*, vol. 31, no. 3, pp. 255–261, May 2016, doi: 10.1002/ffj.3315.
[29] Z. Aumeeruddy-Elalfi, A. Gurib-Fakim, and M. F. Mahomoodally, "Kinetic studies of tyrosinase inhibitory activity of 19 essential oils extracted from endemic and exotic medicinal plants," *South African J. Bot.*, vol. 103, pp. 89–94, 2016, doi: 10.1016/j.sajb.2015.09.010.
[30] A. Moghrovyan, N. Sahakyan, A. Babayan, N. Chichoyan, M. Petrosyan, and A. Trchounian, "Essential Oil and Ethanol Extract of Oregano (Origanum vulgare L.) from Armenian Flora as a Natural Source of Terpenes, Flavonoids and other Phytochemicals with Antiradical, Antioxidant, Metal Chelating, Tyrosinase Inhibitory and Antibacterial Activity," *Curr. Pharm. Des.*, vol. 25, no. 16, pp. 1809–1816, 2019, doi: 10.2174/1381612825666190702095612.

2.7 Research projects

2.7.1 Citral-Containing Essential Oils as Potential Tyrosinase Inhibitors: A Bio-Guided Fractionation Approach

Francesca Capetti [1,†], Massimo Tacchini [2,†], Arianna Marengo [1], Cecilia Cagliero [1], Carlo Bicchi [1], Patrizia Rubiolo [1] and Barbara Sgorbini [1,*]

Affiliation:
[1]Dipartimento di Scienza e Tecnologia del Farmaco, Università degli Studi di Torino, Turin, Italy

*Corresponding author
Prof. Dr. Barbara Sgorbini, Dipartimento di Scienza e Tecnologia del Farmaco, Università degli Studi di Torino, Via Pietro Giuria 9, I-10125, Turin, Italy. E-mail: barbara.sgorbini@unito.it. Phone: +39 011 6707135 Fax: +39 011 670

[†]: These authors contributed equally to the work

Received: April 15, 2021
Revised: May 2, 2021
Accepted: May 9, 2021

Bibliography
Plants (Basel, Switzerland)
DOI: 10.3390/plants10050969

2.7.1.1 Abstract

Excessive melanin production causes serious dermatological conditions as well as minor aesthetic problems (i.e. freckles and solar lentigo). The downregulation of tyrosinase is a widespread approach for the treatment of such disorders, and plant extracts have often proven to be valuable sources of tyrosinase inhibitors. Citral (a mixture of neral and geranial) is an important fragrance ingredient that has shown anti-tyrosinase potential. It is highly concentrated in the essential oils (EOs) of *Cymbopogon schoenanthus* (L.) Spreng., *Litsea cubeba* (Lour.) Pers., *Melissa officinalis* L. and *Verbena officinalis* L. However, only *L. cubeba* EO has been investigated for use as a potential skin-whitening agent. This work evaluates the *in vitro* tyrosinase inhibitory activity of these EOs and studies, using bio-assay oriented fractionation, whether their differing chemical compositions influence the overall EO inhibitory activities via possible synergistic, additive and/or competitive interactions between EOs components. The inhibitory activity of *C. schoenanthus* EO and that of *M. officinalis* EOs, with negligible (+)-citronellal amounts, were in-line with their citral content. On the other hand, *L. cubeba* and *V. officinalis* EOs inhibited tyrosinase to considerably greater extents as they contained β-myrcene, which contributed to the overall EO activities. Similar observations were made for *M. officinalis* EO, which bears high (+)-citronellal content which increased citral activity.

Key words: tyrosinase inhibition; essential oils; citral

2.7.1.2 Introduction

Tyrosinase is the key enzyme in the biosynthesis of melanin pigments in several bacteria, fungi, plants, animals and humans. In humans, tyrosinase catalyses the rate limiting steps in the melanin biosynthetic pathway. This biosynthesis is characterized by several enzymatic and chemical reactions that lead to melanin formation from the amino acid L-tyrosine, with tyrosinase catalysing its hydroxylation to *o*-dopaquinone via its monophenolase and diphenolase activities. Although there are other enzymes involved in melanogenesis, only the tyrosinase-catalysed reactions cannot occur spontaneously, whereas the remaining steps can proceed without enzyme activity at physiological pH [1]. For this reason, tyrosinase downregulation is a very widespread approach to the reduction of excessive melanin production, and the use of tyrosinase inhibitors as skin-whitening agents has demonstrated significant clinical and cosmetic prominence [2].

On the EU market, the tyrosinase inhibitors that are employed as skin-whitening agents can be grouped into two main categories: those banned under EU cosmetic regulation 1223/2009 (i.e. hydroquinone and monobenzyl ether hydroquinone) due to their severe side effects, but that are still used to treat hyperpigmentation under medical supervision; and tyrosinase inhibitors that are permitted for use in cosmetics products (i.e. arbutin, aloesin, kojic acid) [2], [3]. This second group, however, is still characterized by potentially significant side-effects; clinical studies on kojic acid have indeed highlighted cases of erythema, stinging sensations and contact eczema after application. Similarly, the European Scientific Committee on Consumer Safety has raised concerns regarding the use of arbutin as a cosmetic ingredient [2], due to the potential hydrolysis of its glyosidic bond that releases hydroquinone. There is therefore a need for novel molecule templates and/or mixtures of bioactive compounds to treat hyper-pigmentation.

Plants have been valuable sources of skin-whitening agents, and three out of five of the most employed agents, both medically and cosmetically, are plant specialized metabolites (i.e. hydroquinone, β-arbutin, aloesin). To date, phenolic compounds have principally been investigated as potential tyrosinase inhibitors, and these include flavonoids (e.g. quercetin [4]) stilbenes (e.g. resveratrol [1]), phenylpropanoids (e.g. cinnamaldehyde [5] and eugenol [6]) and phenolic acids (e.g. anisic acid and benzoic acid [7]). The interest for terpenoids has been considerably lower and they have relatively been under-investigated as anti-tyrosinase agents.

Citral is among the limited number of terpenoid derivatives with anti-tyrosinase properties that have been studied. It is a mixture of two isomers, *cis*- and *trans*-3,7-dimethyl-2,6-octadienal (i.e., neral and geranial), which have been proven to block the *in vitro* enzymatic activity of mushroom tyrosinase [8]. In addition to its importance as odorous ingredient in beverages, foods and cosmetics, citral has shown promising *in vitro* biological activities including anti-fungal, anti-bacterial, antioxidant and anti-inflammatory effects [9–11]. Moreover, recent studies have highlighted that citral has potential therapeutic significance as smooth muscle relaxer and local anesthetic, as it promotes relaxation in tracheal, uterine and aortic smooth muscles and to inhibit nerve excitability in animal models [12–15].

Citral is obtained from the essential oils (EOs) of several botanical species, including *Cymbopogon schoenanthus* (L.) Spreng., *Litsea cubeba* (Lour.) Pers., *Melissa officinalis* L. and *Verbena officinalis* L. To the best of authors' knowledge, only *L. cubeba* EO has been investigated for its tyrosinase inhibitory activity [16]. Therefore, this study aims to evaluate the tyrosinase inhibitory activities of *C. schoenanthus*, *L. cubeba*, *M. officinalis* and *V. officinalis* EOs, using an *in vitro* colorimetric assay, to assess whether the different chemical compositions influence the overall EO inhibitory activities via any possible synergistic, additive and/or competitive interactions between their components. This study uses a bioassay-guided fractionation approach to evaluate comprehensively the EOs constituents and their enantiomers, when chiral, that contribute to the EO inhibitory activity against

a mushroom source of tyrosinase, which is a good model system for the preliminary screening of tyrosinase inhibitors [17].

2.7.1.3 Materials and Methods

Reagents

Dimethyl sulfoxide (DMSO), mushroom tyrosinase from *Agaricus bisporus* (J.E. Lange) Imbach, L-tyrosine, kojic acid, citral, citronellal, β-myrcene, (+)-limonene, (-)-limonene, (±)-limonene, (±)-α and β pinene were purchased from Merck Life Science S.r.l.. *Litsea cubeba*, *Verbena officinalis* and *Cymbopogon schoenanthus* EOs were supplied by Erboristeria Magentina S.r.l. and three batches of different years (i.e., 2020, 2019, 2018) were tested for each EO. Three samples of *Melissa officinalis EOs* were investigated; one was provided by Agronatura (Spigno Monferrato, Alessandria), one by Erboristeria Magentina S.r.l., while the last was purchased from a local shop and was from Specchiasol S.r.l. In the text, the authors refer to the different EOs of *Melissa officinalis* as *M. officinalis* EOs 1, 2 and 3 respectively. The provided EOs were obtained following the procedures described in the European Pharmacopoeia [24]. *Melissa officinalis* and *Verbena officinalis* EOs were produced by hydrodistillation from the leaves and plants aerial parts respectively; similarly, *Litsea cubeba* and *Cymbopogon schoenanthus* EOs were obtained by steam distillation of the fresh fruits and fresh aerial parts respectively. Each EO was individually analysed by GC-MS as soon as it was purchased/provided by the corresponding manufacturer, every storage year and just before the study of its mushroom tyrosinase inhibitory activity.

In Vitro Tyrosinase Inhibitory Assay

The tyrosinase inhibitory activities of the EOs, as well as of their respective hydrocarbon and oxygenated fractions and pure compounds were investigated *in vitro* using a colorimetric readout-based enzyme assay that was optimized by Zengh et al. [25], with slight modifications: the assay was carried out at room temperature and tyrosinase inhibition was measured considering control and sample absorbance after 6 minutes of incubation, rather than after 20 minutes, so as to operate under the linear portion of the enzymatic reaction, which provides more accurate inhibition results [26],[27]. Mushroom tyrosinase from *Agaricus bisporus* (J.E. Lange) Imbach was selected for this study. L-Tyrosine was used as the substrate, meaning that the overall tyrosinase inhibitory activity was investigated without distinguishing between tyrosinase monophenolase and diphenolase activity. Photometric measurements at 475 nm were performed on a Thermo spectronic Genesys 6 and kojic acid was used as the positive control inhibitor. The solutions of the investigated potential inhibitors (EOs, EO isolated fractions, EO individual compounds and kojic acid) were prepared in DMSO. **Table 1** reports the tested concentrations for each investigated potential inhibitor. The mushroom tyrosinase solution 200 U/mL (27.9 µg/mL) was prepared in sodium phosphate buffer (pH 6.8) and aliquots of 9 mL were stored at -18 °C and thawed just before the experiments. Tyrosine solution 0.1 mg/mL was prepared in sodium phosphate buffer (pH 6.8) and renewed daily. The reaction mixture components were placed in the vial in the following order: 1 mL of mushroom tyrosinase solution 200 U/mL; 1 mL of sodium phosphate buffer solution; 10 µl of EO/single compound/kojic acid solution; and, finally, 1 mL of tyrosine solution 0.1 mg/mL. The final DMSO percentage in the reaction mixture was 0.3 %. The assay was performed in a sealed 4 mL vial to avoid the loss of any EO components into the surrounding environment and to minimize their release into the headspace above the reaction mixture. The reaction mixture was incubated in a thermostatic water bath at 25 °C for 6 minutes. Subsequently, the absorbance at 475 nm was registered, as this wavelength allows the identification of dopachrome. The absorbance corresponding to 100% of tyrosinase activity was measured by replacing the EOs/individual compound/kojic acid solution with 10 µL of pure DMSO. Blank solutions were prepared as follows: 2 mL of sodium phosphate buffer

solution, 10 µL of EO/ individual compound/kojic acid/DMSO solution and 1 mL of tyrosine solution 0.1 mg/mL. The percentage of tyrosinase inhibition was measured according to the equation below:

$$\% \text{ Inhibition} = \Delta A \text{ (Control)} - \Delta A \text{ (Sample)} / \Delta A \text{ (Control)} \times 100$$

$$\Delta A \text{ (Control) or (Sample)} = A_{475} \text{ (Control) or (Sample)} - A_{475} \text{ (Control Blank) or (Sample Blank)}$$

Table 1 Tested concentrations for the investigated essential oils and for both the relative isolated fractions (hydrocarbon and oxygenated) and individual compounds

Tested sample	**[Stock solution] (mg/mL)**	**[Sample] reaction mixture (µg/mL)**
L. cubeba EO	5.0 - 50.0	16.7 - 166.7
L. cubeba EO oxygenated fraction	40.0	133.3
L. cubeba EO hydrocarbon fraction	10.0	33.3
V. officinalis EO	5.0 - 50.0	16.7 - 166.7
V. officinalis EO oxygenated fraction	40.0	133.3
V. officinalis EO hydrocarbon fraction	10.0	33.3
C. schoenanthus EO	5.0 - 50.0	16.7 - 166.7
M. officinalis EO 1	5.0 - 50.0	166.7
M. officinalis EO 1 oxygenated fraction	48.0	160.0
M. officinalis EO 1 hydrocarbon fraction	2.0	6.7
M. officinalis EO 2	5.0 - 50.0	16.7 - 166.7
M. officinalis EO 3	5.0 - 50.0	16.7 - 166.7
Citral	3.0 - 50.0	10 - 166.7
(+)-Citronellal	10.0, 50.0	33.3, 166.7
Citral + (+)-Citronellal	20.0 + 10.0	66.7 + 33.3
β-Myrcene	0.1 - 10.0	0.3 - 33.3
(-)-*trans*-β-caryophyllene	20.0	66.7
(+)-Limonene	10.0	33.3
(-)-Limonene	10.0	33.3
(±)-Limonene	10.0	33.3
(±)-α-Pinene	2.0	6.7
(±)-β-Pinene	2.0	6.7
kojic acid	0.02 - 0.2	0.067 - 0.67

Determination of Concentration-Response Curve and IC50 for inhibitors

The concentration-response curve for each inhibitor was determined by plotting the inhibitory activity as a function of inhibitor concentration in the reaction mixture. IC50 values for the inhibitors were obtained by interpolation from the concentration-response curve.

Flash Column Chromatography

EO fractionation was carried out on a flash column chromatography system Puri-Flash 450 by Sepachrom, equipped with both UV and ELSD detectors. Amount of EO fractionated: 900.0 mg. Stationary phase: Spherical silica gel particles, 50 µm, 25 mg (Purezza®-Sphera Cartridge Stationary); mobile phase: petrolether (A) and ethyl acetate (B); flow-rate 25 mL/min. Linear gradient elution was adopted from 100% of A to 80% of A and 20% of B over 20 minutes.

Analysis Conditions

The EOs solutions and those of their respective fractions were prepared in cyclohexane at a concentration of 5.0 mg/mL and analysed by GC-MS. Citral, citronellal, β-myrcene and limonene were quantified in each EO and the corresponding isolated fractions using the external standard calibration method. Suitable calibration levels were prepared in cyclohexane and analysed by GC-MS. Tridecane (C13) 1.0 mg/mL was used as the internal standard to normalize the analyte signals. **Table 2** summarizes the considered concentration range for each quantified compound.

GC-MS analyses were carried out using a Gerstel MPS-2 multipurpose sampler installed on an Agilent 6890 N GC coupled to a 5975 MSD and equipped with a ChemStation Version E.02.02.1431 data processing system (Agilent Technologies, Santa Clara, CA). GC conditions: injector temperature: 250°C; injection mode: split; ratio: 1/20; carrier gas: helium; constant flow rate: 1 mL/min; columns: Mega 5 (95 % polydi-methylsiloxane, 5 % phenyl) df 0.25 µm, dc 0.25 mm, length 25 m, from MEGA. Temperature program: 50°C//3°C/min//180°C//10°C/min//250°C (5 min). MSD conditions: MS operated in EI mode (70 eV); scan range: 35 to 350 amu; dwell time 40 ms; ion source temperature: 230°C; quadrupole temperature: 150°C; transfer-line temperature: 280°C. EO markers were identified by comparing both their linear retention indices (I^T_s), calculated versus a C9-C25 hydrocarbon mixture, and their mass spectra either against those of authentic samples, or from commercially available mass spectral libraries (Adams, 2007). EO chiral analyses were performed by adopting the same analysis conditions on a 2,3-di-O-methyl-6-O-t-butyldimethylsilyl-β-CD (2,3DM6TBDMS-β-CD) df 0.25 µm, dc 0.25 mm, length 25 m from MEGA. Temperature programs: 40°C (1 min)//2°C/min//220°C (5 min).

GC-FID analyses were carried out on the same instrument. GC conditions: injector temperature: 250°C; injection mode: split; ratio: 1/20; carrier gas: hydrogen; flow rate: 1 mL/ min. Temperature programs: 40°C (1 min)//2°C/min //220°C (5 min).

Table 2 Diagnostic ions (m/z) used for SIM-MS quantitation of selected marker compounds that characterise the investigated essential oils together with the calibration range, the calibration curve equation, correlation values, and regression standard error.

Compound	Diagnostic Ion	Calibration Range (mg/mL)	Calibration Curve Equation	Correlation Values	Regression Standard Error
Neral	69	0.39–1.95	y = 0.4548x + 0.0412	0.9983	0.01543
Geranial	69	0.61–3.05	y = 0.7701x + 0.1207	0.9964	0.05848
Citral		1.00–5.00	y = 0.7067x + 0.1034	0.9956	0.09788
Limonene	68	0.10–2.50	y = 0.6003x + 0.0828	0.9910	0.07348
β-Myrcene	93	0.01–0.08	y = 1.3304x – 0.0023	0.9994	0.001033
Citronellal	69	0.08–4.08	y = 0.5325x – 0.020	0.9999	0.01427
Citronellal	69	0.01–0.08	y = 0.4685x – 0.0083	1.0000	0.0004276

2.7.1.4 Results and Discussion

Chemical Composition and Citral Content of the Investigated Essential Oils

In our attempt to comprehensively characterize all of the potential EO components that contribute to the considered biological activity, the investigated EOs were analysed by GC, with both FID and MS detection. The normalized relative percentage abundances (calculated from the absolute areas normalized to the internal standard C13 by using response factors [18,19]) of all the detected compounds were determined and used to compare EO compositions. **Figure 1** reports the GC-MS profile of the investigated EOs analysed with a conventional column. **Table 3** lists, for each investigated EO, the compounds that displayed a normalized percentage abundance above 0.1, while the complete EO chemical compositions are reported in the Supplementary Materials (**Tables S1–S5**).

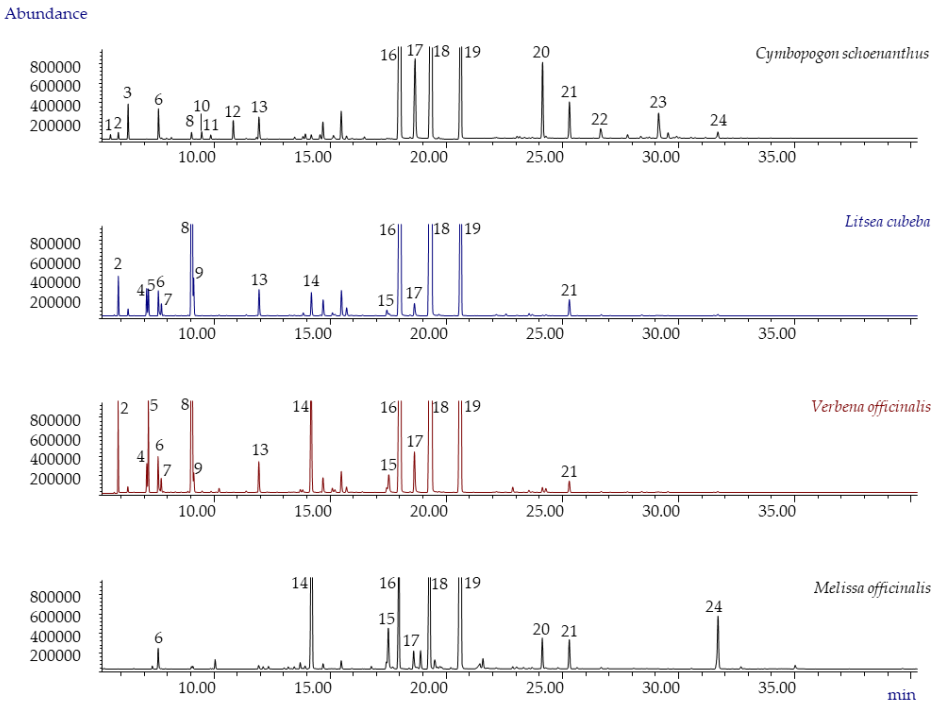

Figure 1 GC-MS profiles of Cymbopogon schoenanthus (batch 2020), Litsea cubeba (batch 2020), Verbena officinalis (batch 2020), and Melissa officinalis 1 essential oils. Legend: (1) tricyclene, (2) α-pinene, (3) camphene, (4) sabinene, (5) β-pinene, (6) 6-methyl-5-hepten-2-one, (7) β-myrcene, (8) limonene, (9) 1,8-cineole, (10) cis-β-ocimene, (11) trans-β-ocimene, (12) 4-nonanone, (13) linalool, (14) citronellal, (15) nerol, (16) neral, (17) geraniol, (18) geranial, (19) ISTD (C13), (20) geranyl acetate, (21) trans-β-caryophyllene, (22) trans-isoeugenol, (23) γ-cadinene, (24) caryophyllene oxide. For analysis conditions, see Section Materials and Methods

Table 3 Normalized percentage abundance of the compounds identified in the essential oils under investigation. For complete compositions see Supplementary Materials Table S1-S5.

Compound			*C. schoenanthus*		*L. cubeba*		*V. officinalis*		*M. officinalis* ₁		*M. officinalis* ₂		*M. officinalis* ₃	
	$I^t s_{exp}$	$I^t s_{lit}$	Norm. Rel. % Abundance*	CV	Norm. Rel. % Abundance*	CV	Norm. Rel. % Abundance*	CV	Norm. Rel. % Abundance	CV	Norm. Rel. % Abundance	CV	Norm. Rel. % Abundance	CV
Tricyclene	926	930											0.11	2.5
α-Thujene	930	931	0.15	11.7										
α-Pinene	941	939	0.22	8.4	1.3	0.6	3.7	1.2			0.43	1.2	0.40	3.9
Camphene	954	953	1.2	4.2	0.26	0.4	0.22	1.9			0.31	0.7	0.95	2.6
Sabinene	976	976			0.97	2.6	1.1	0.2			0.17	8.4	0.13	4.8
β-Pinene	978	980			1.0	3.1	4.0	0.2			0.55	12.5	1.0	3.0
1-Octen-3-ol	982	978							0.21	4.4				
6-Methyl-5-hepten-1-one	989	989	1.2	3.2	1.0	5.2	1.5	1.0	1.4	0.5	0.51	5.8	0.87	2.6
β-Myrcene	992	991			0.47	5.5	0.57	0.8			0.14	4.3		
p-Cymene	1026	1024									0.11	0.2		
Limonene	1029	1031	0.29	5.9	15.0	0.1	10.9	5.4			4.2	0.2	3.7	2.0
1,8-Cineole	1030	1033			1.5	0.1	0.78	6.0			0.91	0.1	0.34	2.5
cis-β-Ocimene	1040	1040	0.31	5.0										
trans-β-Ocimene	1050	1050	0.19	0.6										
γ-Terpinene	1059	1062					0.20	1.4			0.29	2.0		
α-Terpinolene	1086	1088												
Linalool	1098	1098	1.1	0.7	1.1	9.7	1.5	7.8	0.32	1.6	1.2	2.6	0.95	4.8
Nonal	1098	1103							0.17	1.7				
*cis- R*ose oxide	1109	1111							0.20	0.3				
trans-Rose oxide	1126	1127							0.10	0.8				
Isopulegol	1144	1146					0.14	3.1	0.52	2.8				
Citronellal	1155	1153	0.22	9.7	1.1	10.4	5.2	1.3	19.6	0.4	0.26	5.8	0.31	1.6
Borneol	1163	1165	0.24	2.3										
4-Terpineol	1175	1177			0.17	7.9	0.25	0.2					0.20	5.5
α-terpineol	1188	1189	0.18	1.0	0.40	9.5	0.32	8.7			0.22	1.5		
Nerol	1229	1228			0.32	10.6	0.25	4.5	0.45	3.9				
trans-β-Citronellol	1231	1228			0.13	3.6	1.2	0.5	4.1	0.7			0.11	1.8
Neral	1243	1240	32.0	0.2	30.8	0.3	27.5	0.1	19.7	0.1	21.4	0.8	16.5	0.7
Piperitone	1252	1252							0.10	2.8			0.17	1.4
Geraniol	1257	1255	5.16	6.3	0.78	0.8	2.4	0.2	1.7	2.7	1.6	0.5	3.3	1.4
Methyl citronellate	1263	1261							1.6	1.8				
Geranial	1274	1270	41.8	1.1	39.4	1.8	33.2	0.6	29.6	0.2	28.8	0.2	26.5	0.2
Citronellyl formate	1275	1277							1.0	0.2			0.66	0.6
α-Terpinyl acetate	1348	1350			0.11	1.8								

Compound			*C. schoenanthus*		*L. cubeba*		*V. officinalis*		*M. officinalis* ₁		*M. officinalis* ₂		*M. officinalis* ₃	
	I^tS_{exp}	I^tS_{lit}	Norm. Rel. % Abundance*	CV	Norm. Rel. % Abundance*	CV	Norm. Rel. % Abundance*	CV	Norm. Rel. % Abundance	CV	Norm. Rel. % Abundance	CV	Norm. Rel. % Abundance	CV
α-Cubebene	1351	1347									0.33	0.5	0.34	0.2
Methyl geranate	1323	1324							0.86	1.6				
Citronellyl acetate	1355	1354					0.30	0.5	0.18	4.0				
Neryl acetate	1365	1366							0.13	0.53			0.26	2.3
α-Copaene	1371	1372			0.13	9.8	0.13	4.1			0.79	0.4	0.81	0.3
Geranyl acetate	1384	1383	4.2	0.6			0.29	1.0	2.5	0.2	0.92	0.4	1.6	0.2
β-Elemene	1388	1391	0.13	3.9			0.25	0.3			0.09	3.6	0.12	0.1
trans-β-Caryophyllene	1414	1418	2.1	1.3	0.93	0.1	0.69	2.8	2.6	1.4	27.8	1.0	20.0	0.5
trans-Isoeugenol	1447	1450	0.71	4.4										
α-Humulene	1454	1447							0.13	7.0	3.0	0.3	2.6	0.7
Germacrene D	1475	1480	0.21	3.2										
γ-Cadinene	1508	1513	1.8	2.4							0.59	0.2	0.99	0.9
δ-Cadinene	1519	1524	0.32	1.2							0.52	2.0	0.81	2.3
Caryophyllene oxide	1575	1580	0.43	3.9	0.11	0.7			5.7	1.7	1.6	1.7	8.5	1.2

* Average values were derived from the analyses of three EOs obtained from the same botanical species but of different years of production.

CV: Coefficient of Variation = (Standard Deviation /Mean) * 100

All of the investigated EOs are rich in neral (*cis*-3,7-dimethyl-2,6-octadienal) and geranial (*trans*-3,7-dimethyl-2,6-octadienal), which are the most abundant compounds. The neral/ geranial ratio was very similar in all the investigated EOs and corresponded to 0.74 ± 0.05. The *C. schoenanthus* and *L. cubeba* EOs display the highest neral and geranial content, which accounts for, on average, 60 % of their entire EO compositions, and which is 1.5-times greater than in *V. officinalis* EO and in the three *M. officinalis* EOs (i.e. Sample 1,2 and 3). The additional oxygenated compounds that are common to all the EOs are 6-methyl-5-hepten-1-one, linalool and citronellal. The latter is significantly more abundant in the *M. officinalis* EO 1 than in the other investigated EOs, including the *M. officinalis* EO 2 and 3.
The abundance of the hydrocarbon fraction varies significantly in the different EOs. *M. officinalis* EO 1 contains only *trans*-β-caryophyllene and α-humulene as sesquiterpene hydrocarbons, which account for 2.7 % and 0.13 % of the total EO, respectively. The *C. schoenanthus* EO presents a slightly richer hydrocarbon fraction than *M. officinalis* EO 1 (i.e., 7.0%), containing both monoterpenes (i.e., camphene, *cis*-β-ocimene, limonene, α-pinene, trans-β-ocimene, α-thujene) and sesquiterpenes (i.e., *trans*-β-caryophyllene, γ-cadinene, δ-cadinene, germacrene D, β-elemene) in moderate amounts. In the *L. cubeba* and *V. officinalis* EOs, the hydrocarbon fraction accounts for 20% of the total EO and limonene is the most abundant (i.e., 15.0 and 10.9%, respectively), followed by α-pinene, β-pinene, sabinene, *trans*-β-caryophyllene, β-myrcene, camphene and α-copaene. Finally, *M. officinalis* EO 2 and 3 are characterised by the highest hydrocarbon fraction content (38.8% and 31.8% of the total EO, respectively). In both samples, the hydrocarbon fraction mainly contains sesquiterpenes, namely *trans*-β-caryophyllene (27.8% and 20.0% respectively), and α-humulene (3.0% and 2.6%), and a reduced monoterpene fraction that is mainly characterized by limonene (4.2% and 3.2%, respectively).
Three samples of *L. cubeba*, *V. officinalis* and *C. schoenanthus* EOs produced in different years as well as three samples of *M. officinalis* EOs from distinct manufactures were investigated. GC-MS analyses of *C. schoenanthus*, *L. cubeba*, *M. officinalis* and *V. officinalis* did not reveal significant qualitative and quantitative differences in the chemical composition of the three samples of different years of production. This may be ascribed to optimal storage conditions, i.e. in an amber-glass container at 4°C in the dark with a negligible head space. On the other hand, GC-MS analyses showed significant differences in the abundances of citronellal and *trans*-β-caryophyllene in the three investigated *M. officinalis* EOs. Citronellal amounted to 19.6%, 0.26% and 0.31% in the *M. officinalis* EO 1,2 and 3 respectively. On the contrary, as previously described, *trans*-β-caryophyllene is considerably more abundant in the *M. officinalis* EOs 2 and 3 than in *M. officinalis* EO 1. These results are in agreement with the findings reported by Seidler-Lozykawska *et al.*, who highlighted significant differences in citral, citronellal and *trans*-β-caryophyllene abundances in the EOs obtained from 22 selected *M. officinalis* genotypes originating from European botanical gardens [20].
A true quantitation was performed by the external standard calibration to accurately evaluate the abundance of potential bioactive specialized compounds (i.e., neral, geranial, limonene, β-myrcene and citronellal. **Table 2** and **4** report the diagnostic ions (m/z) used for SIM-MS quantitation of the marker compounds under investigation together with the calibration range, the calibration curve equation, correlation values and regression standard error of each analyte and the quantitation results, respectively.

Table 4 Absolute concentrations of potentially bioactive components in the investigated essential oils

Essential Oil	Batch	[β-Myrcene] (g/100 g)	CV	[Limonene] (g/100 g)	CV	[Citronellal] (g/100 g)	CV	[Neral] (g/100 g)	CV	[Geranial] (g/100 g)	CV	[Citral] (g/100 g)	CV
L. cubeba	2020	0.4	5.9	14.7	1.1	1.2	0.1	24.5	2.9	34.3	3.8	59.4	3.5
	2019	0.4	7.2	11.3	1.1	0.9	0.2	25.7	2.0	37.9	2.6	64.6	2.4
	2018	0.3	4.8	8.8	13.4	1.7	1.0	27.7	3.5	37.5	3.6	65.6	3.5
C. schoenanthus	2020	0.1	8.8	2.1	3.6	0.4	0.3	25.9	1.0	37.1	1.4	63.8	1.3
	2019	0.1	3.8	2.2	3.2	0.5	1.0	23.9	2.3	34.1	1.4	58.7	1.7
	2018	0.1	7.5	2.4	1.5	0.4	0.7	26.7	2.7	37.8	0.9	64.8	1.4
V. officinalis	2020	0.4	5.0	10.3	2.6	5.3	0.9	21.6	3.5	28.8	3.0	50.6	3.2
	2019	0.5	1.2	16.7	4.9	4.7	2.0	16.5	3.2	24.1	2.4	41.2	2.3
	2018	0.5	3.8	15.5	4.4	5.1	1.7	16.8	4.9	24.9	3.6	42.4	4.0
M. officinalis	1	0.0	8.9	0.0	-	0.4	4.5	15.5	0.3	22.4	0.0	36.0	0.1
	2	0.1	5.2	4.3	3.1	0.4	7.7	18.4	1.2	27.7	0.4	46.9	0.5
	3	0.1	9.0	3.3	2.6		3.5	18.0	0.4	28.2	0.4	44.0	0.2

In Vitro Inhibitory Activity of the Investigated Essential Oils against Mushroom Tyrosinase

As previously described, the EOs of *C. schoenanthus*, *M. officinalis*, *L. cubeba* and *V. officinalis* present high levels of citral, that is characterized by non-competitive inhibitory activity against a fungal source of tyrosinase [21],[8],[16]. This study aimed at examining the *in vitro* tyrosinase inhibitory activities of these EOs to explore whether their inhibitory activity can be ascribed to their citral content only, or whether there are other bioactive compounds that influence the inhibitory effects of the EOs.

Mushroom tyrosinase was here adopted because of its high homology to human tyrosinase, its relatively low cost and ready availability, which make it a good model system for the preliminary screening of tyrosinase inhibitors [17]. The precision of the *in vitro* tyrosinase inhibition test was evaluated in terms of repeatability (by performing the enzymatic inhibition assay five times in the same day) and intermediate precision (by repeating the enzymatic inhibition assay five times every four weeks over a period of six months). **Table 5** reports the coefficient of variation (CV) for inhibition tests carried out with kojic acid, which was used as positive control, and with *L. cubeba* EO. Results were satisfactory as the CV never exceeded 7 % for repeatability and 10 % for intermediate precision. Similar precision values were obtained for all the tested EOs.

*Table 5 Data precision expressed as CV for both repeatability (n=5) and intermediate precision (n=6). *Values represent the average of three assays.*

	Repeatability (n=3)		**Intermediate precision**	
	% inhibition	CV	% inhibition*	CV
***Kojic acid* (1.7 µg/mL)**	64 58 61 66 64	6	59 69 67 58 70 66	8
***Litsea cubeba* EO (166.7 µg/mL)**	57 58 55 62 65	7	51 59 60 56 67 57	11

Citral concentration-response curve was studied by plotting the observed inhibitory activity as a function of its concentration in the reaction mixture. All of the EOs were tested at a concentration of 166.7 µg/mL, which provided, irrespective of the EO, a resulting citral concentration within its concentration-response curve linearity range ($y = 0.3956x + 1.8094$, $R^2 = 0.9951$, regression error: 2.08448, linearity range: 6.7-166.7 µg/mL) and did not generate solubility issues in the reaction mixture.

The box plot reported in **Figure 2** presents the percentage of tyrosinase inhibition for each EO. For *L. cubeba*, *V. officinalis* and *C. schoenanthus* EOs, the results reported in **Figure 2** correspond to the mushroom tyrosinase inhibitory activity of the EOs of 2020 because the analysis of variance revealed no statistically significant differences among EOs of different years of production ($p > 0.05$). As regard *L. cubeba* and C. *schoenanthus* EOs, these outcomes are in good agreement with the results obtained from the quantitative GC-MS analyses that revealed almost identical citral amount in the EOs of different years of production. The batch 2020 of *V. officinalis* EO contains a slightly higher citral amount than the batches 2019 and 2018. However, according to citral concentration-response curve, the citral excess in batch 2020 is not sufficient to determine a statistically significant higher percentage of enzymatic inhibition considering the random error associated with the measurements. For additional details see **Figure 1** in the Supplementary material. On the other hand, the analysis of variance (ANOVA) followed by Tukey-Kramer post-hoc test revealed that the three tested *M. officinalis* EOs, provided by distinct manufacturers, inhibited mushroom tyrosinase to different extents, which will be further described in the following paragraphs. The greatest inhibitory activities were observed for the EOs of *L. cubeba*, *M. officinalis* 1 and *V. officinalis*, which inhibited 59 ± 6 %, 55 ± 7 % and 52 ± 6 % of tyrosinase activity, respectively, when tested at a concentration of 166.7 µg/mL.

Statistically significant (P< 0.05) lower activities were observed for the EOs of *C. schoenanthus* and *M. officinalis* 2 and 3 whose enzyme inhibitory activity was 42 ± 5%, 40 ± 5% and 38 ± 6%, respectively. **Table 6** provides the inhibitor concentration that halved the enzyme activity in the given experimental conditions (IC50) for each investigated inhibitor (i.e. EOs, single compounds and kojic acid). All of the EOs effectively inhibited mushroom tyrosinase and displayed an inhibitory activity that was, on average, 100-times lower than that of kojic acid, which was used as the positive control.

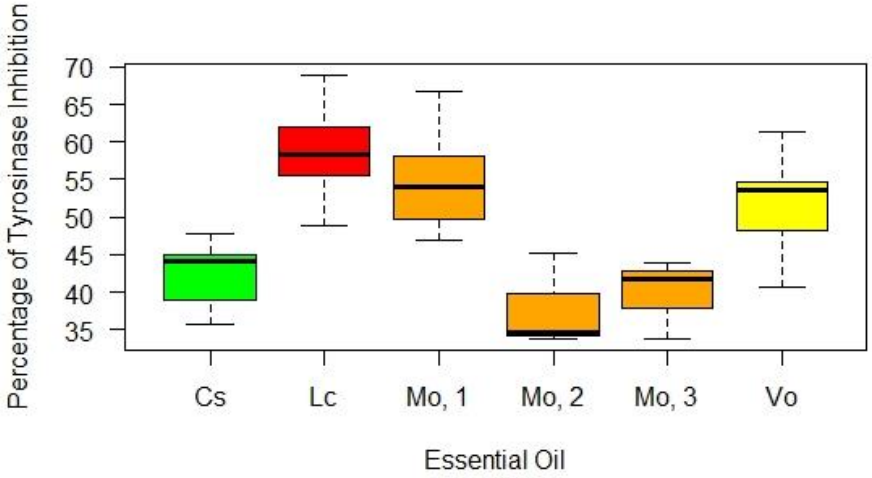

Figure 2 Percentage of tyrosinase inhibition for each investigated EO tested at a concentration of 166.7 µg/mL. Legend: Cs: Cymbopogon schoenanthus (batch 2020); Lc: Litsea cubeba (batch 2020); Mo,1: Melissa officinalis 1; Mo,2: Melissa officinalis 2; Mo,3: Melissa officinalis 3; Vo: Verbena officinalis (bacth 2020).

Table 6 IC_{50} values of each investigated essential oil and of some bioactive components together with their relative standard deviation value.

Inhibitor	IC_{50} (µg/mL)
Kojic acid	1.0 ± 0.4
Citral	121.8 ± 13.7
β-Myrcene	13.3 ± 3.1
C. schoenanthus EO	216.7 ± 18.3
L. cubeba EO	125.0 ± 16.5
M. officinalis EO 1	152.2 ± 21.1
M. officinalis EO 2	220.1 ± 27.7
M. officinalis EO 3	209.2 ± 22.5
V. officinalis EO	167.0 ± 19.1

Identification of Additional Bioactive Components, Besides Citral, by Bioassay-Guided Fractionation

The histogram reported in **Figure 3** compares the percentage of experimentally measured enzymatic inhibitions to the values that would be expected if neral and geranial (considered as sum, i.e. citral) were the only active compounds in the investigated EOs. These values were measured via interpolation from citral concentration-response curve. As can be noted, *C. schoenanthus*, *M. officinalis* 2 and *M. officinalis* 3 displayed inhibitory activities that were in line with their citral content, while *L. cubeba*, *M. officinalis* 1 and *V. officinalis* EOs inhibited mushroom tyrosinase to a greater extent than expected.

A bio-guided approach was adopted to identify the additional compounds that contribute to citral activity. The oxygenated and hydrocarbon fractions of *L. cubeba*, *M. officinalis 1* and *V. officinalis* EOs were isolated by flash chromatography and individually tested for their mushroom tyrosinase inhibitory activities. The fractions phytohemical compositions are reported in the Supplementary Materials (Tables S1-S5). The isolated fractions were tested at the same concentration as their resulting concentration when testing 166.7 µg/mL of the respective EO (see Materials and Methods section, **Table 1**). **Table 7** reports the concentration of neral, geranial, citronellal, limonene and β-myrcene in the oxygenated and hydrocarbon fractions of the fractionated EOs.

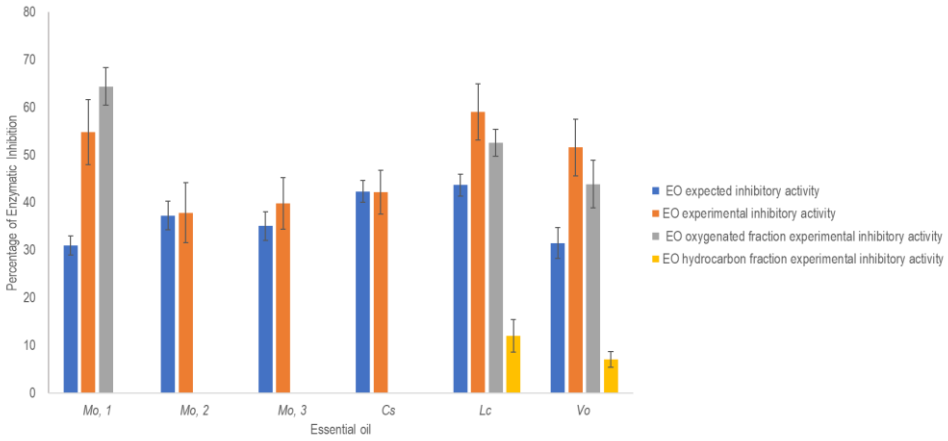

Figure 37 Comparison of the percentage of experimentally measured enzymatic inhibition and the enzymatic inhibition expected with citral as the only bioactive compound in the essential oils. Legend: Cs: Cymbopogon schoenanthus (batch 2020); Lc: Litsea cubeba (batch 2020); Mo,1: Melissa officinalis 1; Mo,2: Melissa officinalis 2; Mo3: Melissa officinalis 3; Vo: Verbena officinalis (batch 2020).

Table 7 Concentration of selected bioactive compounds in the oxygenated and hydrocarbon fractions of the fractionated essential oils.

	[β-Mycene] (g/100g)	CV	[Limonene] (g/100g)	CV	[Citronellal] (g/100g)	CV	[Neral] (g/100g)	CV	[Geranial] (g/100g)	CV	[Citral] (g/100g)	CV
L. cubeba hydrocarbon fraction	1.4	0.3	59.4	6.0								
L. cubeba oxygenated fraction					1.0	1.5	42.2	0.1	53.2	0.5	94.8	0.3
V. officinalis hydrocarbon fraction	1.8	0.2	47.2	0.8								
V. officinalis oxygenated fraction					2.0	2.8	35.1	0.6	42.3	0.2	76.9	0.3
M. officinalis, 1 hydrocarbon fraction												
M. officinalis, 1 oxygenated fraction					14.1	0.4	18.6	0.3	26.7	0.4	44.8	0.4

As for *L. cubeba* and *V. officinalis* EOs, both the oxygenated and hydrocarbon fractions inhibited mushroom tyrosinase, although to different extents. The activities of the oxygenated fractions (53 ± 3% and 44 ± 5, respectively) account for most of the EOs anti-tyrosinase potential and were in line with the respective citral content, suggesting that the compounds that contribute to citral activity belong to the hydrocarbon fractions. The hydrocarbon fractions of *L. cubeba* and *V. officinalis* EOs present quite similar chemical compositions. Limonene (68.4 and 50.3% respectively), *trans*-β-caryophyllene (12.0 and 7.8% respectively), α-pinene (1.7 and 7.5% respective-ly), β-pinene (2.5 and 12.9 % respectively), sabinene (2.7 and 3.8 respectively) and β-myrcene (2.0 and 2.4% respectively) are the most abundant compounds in both fractions and are present in rather similar amounts, except for α-pinene and β-pinene, which prevail in the *V. officinalis* EO hydrocarbon fraction.

The chiral recognition revealed high enantiomeric purities in favour of the (-)-configured enantiomers for *trans*-β-caryophyllene (> 99 % in both EOs), limonene (97 and 94% in *L. cubeba* and *V. officinalis* EO, respectively) and sabinene (87% in both EOs), while different enantiomeric excesses were observed for α- pinene ((-)-enantiomer: 38% in *L. cubeba* EO and 73% in *V. officinalis* EO) and β-pinene ((-)-enantiomer: 67% in *L. cubeba* EO and 88% in *V. officinalis* EO). In both EOs, (-)-limonene accounts for more than 50% of the entire fraction. However, although previous studies have reported an inhibitory activity against mushroom tyrosinase because of its high abundance [22], [23], (-)-limonene here did not show a tyrosinase inhibitory activity. Similar results were obtained for (+)-limonene, the racemic mixture, and the compounds (-)-*trans*-β-caryophyllene, (±)-α-pinene and (±)-β-pinene. Sabinene was not tested as it had already been proven to have negligible mushroom tyrosinase inhibitory effects [8]. In agreement with previous findings [8], β-myrcene reduced mushroom tyrosinase activity. When tested at the concentration observed in 166.7 µg/mL *of L. cubeba* and *V. officinalis* EOs, β-myrcene activity bridged the gap between the EOs' expected inhibitory effects if citral was the only active compound. Contrary to the observations by Matsuura *et al.* [8], β- myrcene proved to be a more potent mushroom tyrosinase inhibitor than citral, as its IC50 was almost ten times lower (13.3 µg/mL vs 121.8 µg/mL). This difference may be ascribed to the different substrates used; Matsuura *et al.*, investigated mushroom tyrosinase diphenolase activity only, as they used L-DOPA as the substrate, whereas, in this study L-tyrosine was used. The current findings suggest that β-myrcene may be more effective at inhibiting mushroom tyrosinase monophenolase activity than the diphenolase one.

The *M. officinalis* EO 1 displays a small hydrocarbon fraction that accounts for less than 3 % of the total, and has no tyrosinase inhibitory activity. However, the *M. officinalis* EO 1 oxygenated fraction inhibited mushroom tyrosinase to a greater extent than would be expected from its citral content (**Figure 3**). This fraction contains significant amounts of citronellal in addition to neral and geranial and the chiral analysis revealed a high enantiomeric purity of citronellal in favour of the (+) enantiomer (98.3%). When tested independently, at a concentration of 166.7 µg/mL, (+)-citronellal inhibited mushroom tyrosinase to a negligible extent, although its activity was significantly enhanced when tested in combination with citral. These results may explain the differences observed in the percentages of mushroom tyrosinase inhibition in the various *M. officinalis* EOs. *M.*

officinalis EO 2 and 3 present very low citronellal contents, which may be the reason why their inhibitory activities are significantly lower than that of *M. officinalis* EO 1.

2.7.1.5 Conclusions

The purposes of this investigation were 1) to examine comprehensively the *in vitro* mushroom tyrosinase inhibitory activities of the *Cymbopogon schoenanthus*, *Litsea cubeba*, *Melissa officinalis* and *Verbena officinalis* EOs and 2) to determine whether their biological activity is ascribed to their citral content only or if there are additional bioactive monoterpenes that contribute to the investigated biological activity by using a bioassay-guided fractionation approach. This study has identified that in *L. cubeba* and *V. officinalis* EOs, β-myrcene contributes to the EOs inhibitory activities despite its little amount and it has been shown to have a greater inhibitory power to citral. The second major finding was that (+)-citronellal enhanced citral mushroom tyrosinase inhibitory power, potentially via synergistic interaction as it displayed no activity on its own. The latter finding explained why in *M. officinalis* EOs that bear negligible (+)-citronellal amounts, the inhibitory activities were in-line with their citral content while the contrary was true for the *M. officinalis* EO with relatively high (+)-citronellal abundance.

Even though further studies are still required to accurately define the type of interactions that occur in between β-myrcene and citral and in between citronellal and citral, and to assess the inhibitory activities of these EOs and individual compounds on human tyrosinase, the results of this study may help to rationally design mixtures of EOs or enriched EOs that improve their biological efficacy and increase their potential as adjuvants in the treatment of hyperpigmentation.

2.7.1.6 Supplementary Materials

Table 1 Normalized relative percentage abundance of the compounds identified in the essential oil of Cymbopogon schoenanthus

	C. schoenanthus			
Compound	I^tS_{exp}	I^tS_{lit}	Norm. Rel. % Abundance	RSD%
α-Thujene	930	931	0.15	11.7
α-Pinene	941	939	0.22	8.4
Camphene	954	953	1.2	4.2
6-methyl-5-hepten-1-one	989	989	1.2	3.2
β-Myrcene	989	991	0.06	2.8
Limonene	1029	1031	0.29	5.9
cis-β-Ocimene	1040	1040	0.31	5.0
trans-β-Ocimene	1050	1050	0.19	0.6
α-terpinolene	1086	1088	0.06	1.3
Linalool	1098	1098	1.1	0.7
Citronellal	1155	1153	0.22	9.7
Borneol	1163	1165	0.24	2.1
α-terpineol	1188	1189	0.18	1.0
Nerol	1229	1228	0.05	20.1
β-Citronellol	1231	1228	0.05	22.0
Neral	1243	1240	32.0	0.2
Piperitone	1252	1254	0.07	7.9
Geraniol	1257	1255	5.2	6.3
Geranial	1274	1270	41.8	1.1
Geranyl acetate	1384	1383	4.2	0.6
β-Elemene	1388	1391	0.13	3.9
trans-β-Caryophyllene	1414	1418	2.1	1.3
trans-Isoeugenol	1447	1450	0.71	4.4
Germacrene D	1475	1480	0.21	3.2
γ-Cadinene	1508	1513	1.8	2.4
δ-Cadinene	1519	1524	0.32	1.2
Caryophyllene oxide	1575	1580	0.43	3.9

Table 2 Normalized relative percentage abundance of the compounds identified in the essential oils of Melissa officinalis EO 2 and 3 (- : not detected)

			M. officinalis $_2$		*M. officinalis* $_3$	
Compound	I^tS_{exp}	I^tS_{lit}	Norm. Rel. % Abundance	RSD%	Norm. Rel. % Abundance	RSD%
Tricyclene	930	926	0.03	2.1	0.11	2.5
α-Thujene	936	931	0.02	6.7	-	
α-Pinene	941	939	0.43	1.2	0.40	3.9
Camphene	954	953	0.31	0.7	0.95	2.6
Sabinene	976	976	0.17	8.4	0.13	4.8
β-Pinene	978	980	0.55	12.5	1.0	3.0
6-methyl-5-hepten2-one	989	985	0.51	5.8	0.87	2.6

			M. officinalis ₂		*M. officinalis* ₃	
Compound	$I^t s_{exp}$	$I^t s_{lit}$	Norm. Rel. % Abundance	RSD%	Norm. Rel. % Abundance	RSD%
β-Myrcene	992	991	0.14	4.3	0.06	13.9
p-Cymene	1024	1026	0.11	0.2	0.09	1.6
Limonene	1028	1031	4.2	0.2	3.7	2.1
1,8-Cineole	1030	1033	0.91	0.1	0.34	2.5
cis-β-Ocimene	1040	1040	0.04	0.6	-	
trans-β-Ocimene	1050	1050	0.05	4.2	-	
γ-Terpinene	1059	1062	0.29	2.1	-	
α-Terpinolene	1086	1088	0.05	12.3	-	
Linalool	1098	1098	1.2	2.6	0.95	4.8
Citronellal	1155	1153	0.26	5.8	0.31	1.6
Borneol	1163	1165	0.06	9.5	-	
4-Terpineol	1175	1177	0.03	29.3	0.20	5.5
α-Terpineol	1188	1189	0.22	1.5	-	
Nerol	1229	1229	0.08	5.2	0.06	0.5
β-Citronellol	1230	1228	0.08	1.8	0.11	1.8
Neral	1242	1240	21.4	0.8	16.5	0.7
Piperitone	1252	1252	0.06	1.0	0.17	1.4
Geraniol	1257	1255	1.64	0.5	3.3	1.4
Geranial	1273	1270	28.8	0.2	26.5	0.2
Citronellyl formate	1277	1275			0.66	0.6
α-Cubebene	1347	1351	0.33	0.5	0.34	0.2
Neryl acetate	1366	1365			0.26	2.3
α-Copaene	1371	1371	0.79	0.4	0.81	0.3
Geranyl acetate	1385	1383	0.92	0.4	1.63	0.2
β- Elemene	1388	1391	0.09	3.6	0.12	0.2
trans-β-Caryophyllene	1413	1418	27.8	1.0	20.09	0.5
α-Humulene	1447	1454	3.0	0.3	2.6	0.7
Germacrene D	1475	1480	0.06	5.5	-	
trans-γ-Cadinene	1507	1511	0.59	0.2	0.99	0.9
δ-Cadinene	1518	1524	0.52	2.0	0.81	2.3
Caryophyllene Oxide	1575	1580	1.6	1.7	8.5	1.2

Table 3, Normalized relative percentage abundance of the compounds identified in the EO of Litsea cubeba and in its hydrocarbon and oxygenated fractions (tr: trace; - : not detected)

			L. cubeba		*Hydrocarbon fraction*		*Oxygenated fraction*	
Compound	$I^t s_{exp}$	$I^t s_{lit}$	Norm. Rel. % Abundance	RSD%	Norm. Rel. % Abundance	RSD%	Norm. Rel. % Abundance	RSD%
α-Thujene	936	931	0.03	11.7	0.04	6.2	-	-
α-Pinene	941	939	1.3	0.7	1.7	5.8	-	-
Camphene	954	953	0.26	0.4	0.41	2.4	-	-
Sabinene	976	976	0.97	2.6	2.7	0.4	-	-
β-Pinene	978	980	1.0	3.1	2. 5	4.2	-	-
6-methyl-5-hepten-2-one	989	985	1.0	5.2	-	-	0.90	1.0

			L. cubeba		*Hydrocarbon fraction*		*Oxygenated fraction*	
Compound	$I^t s_{exp}$	$I^t s_{lit}$	Norm. Rel. % Abundance	RSD%	Norm. Rel. % Abundance	RSD%	Norm. Rel. % Abundance	RSD%
β-Myrcene	992	991	0.47	5.5	2.0	3.1	-	-
α-Phellandrene	1002	1005	tr	-	0.05	1.5	-	-
δ-3-Carene	1008	1011	tr	-	0.14	2.5	-	-
α-Terpinene	1015	1018	tr	-	0.08	4.8	-	-
p-Cymene	1024	1026	tr	-	0.20	2.2	-	-
Limonene	1028	1031	15.0	0.1	68.4	2.1	-	-
cis-β-Ocimene	1040	1040	tr	-	0.10	3.3	-	-
trans-β-Ocimene	1050	1050	tr	-	0.15	0.7	-	-
1,8-Cineole	1030	1033	1.5	0.1	-	-	0.04	10.3
γ-Terpinene	1059	1062	0.05	19.5	0.34	0.9	-	-
α-Terpinolene	1086	1089	0.06	8.3	0.52	5.6	-	-
Linalool	1098	1098	1.1	9.7	-	-	1.5	0.5
Perillene	1099	1099	Tr	-	0.08	2.4	-	-
Citronellal	1154	1153	1.08	10.4	-	-	1.06	3.3
Borneol	1163	1165	0.04	16.6	-	-	0.06	10.0
4-Terpineol	1175	1177	0.17	7.9	-	-	0.20	4.1
α-Terpineol	1188	1189	0.40	9.5	-	-	0.54	6.5
Nerol	1229	1228	0.32	10.6	-	-	0.43	2.1
trans-β-Citronellol	1231	1228	0.13	3.6	-	-	0.16	
Neral	1243	1240	30.81	0.3	-	-	37.5	6.7
Piperitone	1252	1252	0.06	21.2	-	-	0.06	13.0
Geraniol	1257	1255	0.78	0.8	-	-	0.98	3.0
Geranial	1273	1270	39.36	1.8	-	-	48.4	6.4
α-Terpinyl acetate	1348	1350	0.11	1.8	-	-	0.07	
α-Copaene	1371	1372	0.13	9.8	1.63	3.9	-	-
Geranyl acetate	1384	1383	0.04	4.4			2.0	13.0
β-Elemene	1388	1391	0.06	13.3	0.78	4.1	-	-
trans-β-Caryophyllene	1412	1418	0.93	0.1	12.0	4.0	-	-
α-*trans*-bergamotene	1433	1436	tr	-	0.12	9.5	-	-
α-Humulene	1447	1454	0.07	0.4	1.2	8.4	-	-
allo-Aromadendrene	1454	1461	tr	-	0.09	4.7	-	-
trans-β-Farnesene	1457	1458	tr	-	0.35	3.2	-	-
Bicyclogermacrene	1490	1495	0.07	9.3	1.1	2.5	-	-
Germacrene A	1497	1503	tr	-	0.17	5.4	-	-
β-Bisabolene	1505	1509	tr	-	0.52	2.5	-	-
δ-Cadinene	1519	1524	tr	-	0.33	4.0	-	-
Caryophyllene oxide	1575	1580	0.11	0.7	-	-	0.64	6.4

Table 4, Normalized percentage abundance of the compounds identified in the EO of Verbena officinalis and in its hydrocarbon and oxygenated fractions (tr : trace; - : not detected)

			V. officinalis		*Hydrocarbon fraction*		*Oxygenated fraction*	
Compound	$I^t s_{exp}$	$I^t s_{lit}$	Norm. Rel. % Abundance	RSD%	Norm. Rel. % Abundance	RSD%	Norm. Rel. % Abundance	RSD%
α-Thujene	936	931	0.05	1.3	0.13	8.5	-	-
α-Pinene	941	939	3.7	1.2	7.5	6.9	-	-
Camphene	954	953	0.22	1.9	0.57	2.9	-	-

			V. officinalis		*Hydrocarbon fraction*		*Oxygenated fraction*	
Compound	$I^t s_{exp}$	$I^t s_{lit}$	Norm. Rel. % Abundance	RSD%	Norm. Rel. % Abundance	RSD%	Norm. Rel. % Abundance	RSD%
Sabinene	976	976	1.1	0.2	3.82	9.8	-	-
β-Pinene	978	980	4.0	0.2	12.9	11.0	-	-
6-methyl-5-hepten-2-one	989	985	1.5	1.0	-	-	0.62	6.3
β-Myrcene	992	991	0.57	0.8	2.4	0.6	-	-
δ-3-Carene	1008	1011	0.04	0.5	0.17	1.4	-	-
α-Terpinene	1015	1018	tr	-	0.13	1.5	-	-
o-Cymene	1022	1022	tr	-	0.06	2.8	-	-
p-Cymene	1024	1026	0.06	1.5	0.38	5.1	-	-
Limonene	1028	1031	10.9	5.4	50.3	4.2	-	-
1,8-Cineole	1030	1033	0.78	6.0	-	-	0.26	5.9
cis-β-Ocimene	1040	1040	0.07	6.0	0.41	11.2	-	-
trans-β-Ocimene	1050	1050	0.06	5.5	0.43	13.1	-	-
γ-Terpinene	1059	1062	0.20	1.4	1.1	9.4	-	-
α-Terpinolene	1086	1088	0.07	8.4	0.54	13.6	-	-
Linalool	1098	1098	1.5	7.8	-	-	1.9	2.2
Perillene	1099	1099	tr	-	0.15	9.7	-	-
Isopulegol	1144	1146	0.14	3.1	-	-	0.17	5.4
Citronellal	1155	1153	5.2	1.3	-	-	3.4	16.4
Borneol	1163	1165	0.04	1.3	-	-	0.05	2.8
4-Terpineol	1175	1177	0.25	0.2	-	-	0.31	3.4
α-Terpineol	1188	1189	0.32	8.7	-	-	0.48	1.4
Nerol	1229	1229	0.25	4.5	-	-	0.32	4.7
β-Citronellol	1231	1229	1.2	0.5	-	-	1.7	4.8
Neral	1243	1240	27.5	0.1	-	-	37.4	0.1
Piperitone	1252	1252	0.05	7.9	-	-	0.09	1.6
Geraniol	1257	1255	2.4	0.2	-	-	3.47	1.9
Geraniale	1273	1270	33.2	0.6	-	-	46.1	1.8
Citronellyl acetate	1355	1354	0.30	0.5	-	-	0.37	8.2
α-Cubebene	1347	1351	tr	-	0.12	9.5	-	-
α-Copaene	1371	1371	0.13	4.1	1.2	5.8	-	-
β-Bourbonene	1379	1384	tr	-	0.11	5.6	-	-
Geranyl acetate	1384	1383	0.29	1.0	-	-	0.39	3.3
β-Elemene	1388	1391	0.25	0.3	2.2	5.8	-	-
trans-β-caryophyllene	1412	1418	0.69	2.8	7.8	2.5	-	-
trans-α-Bergamotene	1433	1436	tr	-	0.17	8.8	-	-
α-Humulene	1447	1454	0.07	1.9	0.83	0.1	-	-
Aromadendrene	1454	1461	tr	-	0.07	4.7	-	-
trans-β-farnesene	1457	1458	tr	-	0.22	1.0	-	-
Germacrene D	1475	1480	0.05	0.2	0.51	6.8	-	-
Bicyclogermacrene	1489	1494	0.07	0.7	0.74	6.5	-	-
α-Muurolene	1495	1499	tr	-	0.29	9.3	-	-
β-bisabolene	1505	1509	tr	-	0.30	5.2	-	-
trans-γ-Cadinene	1507	1511	tr	-	0.24	10.8	-	-
cis-δ-Cadinene	1518	1519	0.06	0.8	0.68	1.6	-	-
Caryophyllene oxide	1575	1580	0.07	6.7	-	-	0.10	8.8

Table 5, Normalized percentage abundance of the compounds identified in the EO of Melissa officinalis EO 1 and in its hydrocarbon and oxygenated fractions (tr: trace; - : not detected)

			M. officinalis 1		*Hydrocarbon fraction*		*Oxygenated fraction*	
Compound	$I^t s_{exp}$	$I^t s_{lit}$	Norm. Rel. % Abundance	RSD%	Norm. Rel. % Abundance	RSD%	Norm. Rel. % Abundance	RSD%
1-Octen-3-ol	982	978	0.21	4.4	-	-	0.14	10.0
6-Methyl-5-hepten2-one	989	985	1.4	0.50	-	-	0.71	3.1
Linalool	1098	1098	0.32	1.6	-	-	0.28	7.5
Nonal	1103	1098	0.17	1.7	-	-	0.11	3.1
cis-Rose oxide	1109	1111	0.20	0.34	-	-	0.16	8.7
trans-Rose oxide	1126	1127	0.10	0.79	-	-	0.07	10.6
Isopulegol	1143	1146	0.52	2.8	-	-	0.49	4.7
Citronellal	1155	1153	19.6	0.40	-	-	18.3	1.5
Nerol	1229	1229	0.45	3.9	-	-	0.47	7.9
β-Citronellol	1230	1228	4.1	0.72	-	-	4.5	11.0
Neral	1242	1240	19.7	0.08	-	-	22.1	0.9
Piperitone	1252	1252	0.10	2.8	-	-	0.11	6.3
Geraniol	1257	1255	1.7	2.7	-	-	1.83	4.6
Citronellyl acetate	1277		1.6	1.9	-	-	1.6	1.1
Geranial	1273	1270	29.6	0.19	-	-	32.8	1.6
Citronellyl formate	1277	1275	1.0	0.19	-	-	0.14	5.8
Methyl geranate	1324	1323	0.86	1.6	-	-	0.89	5.8
Citronellyl acetate	1355	1354	0.18	4.0	-	-	-	-
Neryl acetate	1366	1365	0.13	35.8	-	-	0.14	1.9
α-Copaene	1371	1371	0.06	0.19	1.84	0.2	-	-
Geranyl acetate	1385	1383	2.5	0.23	-	-	2.8	0.4
β-Elemene	1388	1391	Tr	-	0.96	0.7	-	-
cis-β-Caryophyllene	1399	1404	Tr	-	1.13	0.6	-	-
trans-β-Caryophyllene	1413	1418	2.6	1.4	75.36	0.2	-	-
α-Humulene	1447	1454	0.13	7.0	5.71	0.4	-	-
Aromadendrene	1454	1461	0.07	8.0	2.84	0.6	-	-
α-Muurolene	1494	1499	Tr	-	1.26	1.3	-	-
δ-Cadinene	1518	1524	Tr	-	2.31	1.0	-	-
Caryophyllene oxide	1575	1580	5.7	1.7	-	-	6.3	1.2

2.7.1.7 References

1. Pillaiyar, T.; Manickam, M.; Namasivayam, V. Skin whitening agents: medicinal chemistry perspective of tyrosinase inhibitors. J. Enzyme Inhib. Med. Chem. 2017, 32, 403–425, doi:10.1080/14756366.2016.1256882.
2. Desmedt, B.; Courselle, P.; De Beer, J.O.; Rogiers, V.; Grosber, M.; Deconinck, E.; De Paepe, K. Overview of skin whitening agents with an insight into the illegal cosmetic market in Europe. J. Eur. Acad. Dermatology Venereol. 2016, 30, 943–950, doi:10.1111/jdv.13595.
3. Desmedt, B.; Van Hoeck, E.; Rogiers, V.; Courselle, P.; De Beer, J.O.; De Paepe, K.; Deconinck, E. Characterization of suspected illegal skin whitening cosmetics. J. Pharm. Biomed. Anal. 2014, 90, 85–91, doi:10.1016/j.jpba.2013.11.024.
4. Kubo, I.; Ikuyo, K.H. Flavonols from saffron flower: Tyrosinase inhibitory activity and inhibition mechanism. J. Agric. Food Chem. 1999, 47, 4121–4125, doi:10.1021/jf990201q.
5. Chang, C.-T.T.; Chang, W.-L.L.; Hsu, J.-C.C.; Shih, Y.; Chou, S.-T.T. Chemical composition and tyrosinase inhibitory activity of Cinnamomum cassia essential oil. Bot. Stud. 2013, 54, 2–8, doi:10.1186/1999-3110-54-10.
6. Garcia-Molina, M.D.M.; Muñoz-Muñoz, J.L.; Garcia-Molina, F.; García-Ruiz, P.A.; Garcia-Canovas, F. Action of tyrosinase on ortho-substituted phenols: Possible influence on browning and melanogenesis. J. Agric. Food Chem. 2012, 60, 6447–6453, doi:10.1021/jf301238q.
7. Kubo, I.; Kinst-Hori, I. Tyrosinase Inhibitors from Cumin. J. Agric. Food Chem. 1998, 46, 5338–5341, doi:10.1021/jf980226+.
8. Matsuura, R.; Ukeda, H.; Sawamura, M. Tyrosinase inhibitory activity of citrus essential oils. J. Agric. Food Chem. 2006, 54, 2309–2313, doi:10.1021/jf051682i.
9. Lertsatitthanakorn, P.; Taweechaisupapong, S.; Aromdee, C.; Khunkitti, W. In vitro bioactivities of essential oils used for acne control. Int. J. Aromather. 2006, 16, 43–49, doi:10.1016/j.ijat.2006.01.006.
10. Bouzenna, H.; Hfaiedh, N.; Giroux-Metges, M.-A.; Elfeki, A.; Talarmin, H. Biological properties of citral and its potential protective effects against cytotoxicity caused by aspirin in the IEC-6 cells. Biomed. Pharmacother. 2017, 87, 653–660, doi:10.1016/j.biopha.2016.12.104.
11. Lee, H.J.; Jeong, H.S.; Kim, D.J.; Noh, Y.H.; Yuk, D.Y.; Hong, J.T. Inhibitory effect of citral on NO production by suppression of iNOS expression and NF-κB activation in RAW264.7 cells. Arch. Pharm. Res. 2008, 31, 342–349.
12. Carvalho, P.M.M.; Macêdo, C.A.F.; Ribeiro, T.F.; Silva, A.A.; Da Silva, R.E.R.; de Morais, L.P.; Kerntopf, M.R.; Menezes, I.R.A.; Barbosa, R. Effect of the Lippia alba (Mill.) N.E. Brown essential oil and its main constituents, citral and limonene, on the tracheal smooth muscle of rats. Biotechnol. Reports 2018, 17, 31–34, doi:10.1016/j.btre.2017.12.002.
13. Pereira-de-Morais, L.; Silva, A. de A.; da Silva, R.E.R.; Costa, R.H.S. da; Monteiro, Á.B.; Barbosa, C.R. dos S.; Amorim, T. de S.; de Menezes, I.R.A.; Kerntopf, M.R.; Barbosa, R. Tocolytic activity of the Lippia alba essential oil and its major constituents, citral and limonene, on the isolated uterus of rats. Chem. Biol. Interact. 2019, 297, 155–159, doi:10.1016/j.cbi.2018.11.006.
14. da Silva, R.E.R.; de Morais, L.P.; Silva, A.A.; Bastos, C.M.S.; Pereira-Gonçalves, Á.; Kerntopf, M.R.; Menezes, I.R.A.; Leal-Cardoso, J.H.; Barbosa, R. Vasorelaxant effect of the Lippia alba essential oil and its major constituent, citral, on the contractility of isolated rat aorta. Biomed. Pharmacother. 2018, 108, 792–798, doi:10.1016/j.biopha.2018.09.073.
15. Sousa, D.G.; Sousa, S.D.G.; Silva, R.E.R.; Silva-Alves, K.S.; Ferreira-da-Silva, F.W.; Kerntopf, M.R.; Menezes, I.R.A.; Leal-Cardoso, J.H.; Barbosa, R. Essential oil of Lippia alba and its main constituent citral block the excitability of rat sciatic nerves. Brazilian J. Med. Biol. Res. 2015, 48, 697–702, doi:10.1590/1414-431x20154710.

16. Huang, X.-W.; Feng, Y.-C.; Huang, Y.; Li, H.-L. Potential cosmetic application of essential oil extracted from Litsea cubeba fruits from China. J. Essent. Oil Res. 2013, 25, 112–119, doi:10.1080/10412905.2012.755479.
17. Zolghadri, S.; Bahrami, A.; Hassan Khan, M.T.; Munoz-Munoz, J.; Garcia-Molina, F.; Garcia-Canovas, F.; Saboury, A.A. A comprehensive review on tyrosinase inhibitors. J. Enzyme Inhib. Med. Chem. 2019, 34, 279–309.
18. Bicchi, C.; Liberto, E.; Matteodo, M.; Sgorbini, B.; Mondello, L.; Zellner, B. d'Acampora; Costa, R.; Rubiolo, P. Quantitative analysis of essential oils: a complex task. Flavour Fragr. J. 2008, 23, 382–391, doi:10.1002/ffj.1905.
19. Rubiolo, P.; Sgorbini, B.; Liberto, E.; Cordero, C.; Bicchi, C. Essential oils and volatiles: sample preparation and analysis. A review. Flavour Fragr. J. 2010, 25, 282–290, doi:10.1002/ffj.1984.
20. Seidler-Łozykowska, K.; Bocianowski, J.; Król, D. The evaluation of the variability of morphological and chemical traits of the selected lemon balm (Melissa officinalis L.) genotypes. Ind. Crops Prod. 2013, 49, 515–520, doi:10.1016/j.indcrop.2013.05.027.
21. Kubo, I.; Kinst-Hori, I. Tyrosinase inhibitory activity of the olive oil flavor compounds. J. Agric. Food Chem. 1999, 47, 4574–4578, doi:10.1021/jf990165v.
22. Fiocco, D.; Arciuli, M.; Arena, M.P.; Benvenuti, S.; Gallone, A. Chemical composition and the anti-melanogenic potential of different essential oils. Flavour Fragr. J. 2016, 31, 255–261, doi:10.1002/ffj.3315.
23. Hu, J.J.; Li, X.; Liu, X.H.; Zhang, W.P. Inhibitory effect of lemon essential oil on mushroom tyrosinase activity in vitro. Mod. Food Sci. Technol. 2015, 31, 97–105, doi:10.13982/j.mfst.1673-9078.2015.6.016.
24. Council of Europe European Pharmacopoeia; 10th ed.; Strasburg, France, 2020; ISBN 978-92-871-8921-9.
25. Zheng, Z.P.; Tan, H.Y.; Chen, J.; Wang, M. Characterization of tyrosinase inhibitors in the twigs of Cudrania tricuspidata and their structure-activity relationship study. Fitoterapia 2013, 84, 242–247, doi:10.1016/j.fitote.2012.12.006.
26. Williams, K.P.; Scott, J.E. Enzyme Assay Design for High-Throughput Screening. In High Throughput Screening. Methods in Molecular Biology (Methods and Protocols); Janzen, W.P., Bernasconi Paul, Eds.; Humana Press: Clifton, N.J., 2009; Vol. 565, pp. 107–126.
27. Brooks, H.B.; Geeganage, S.; Kahl, S.D.; Montrose, C.; Sittampalam, S.; Smith, M.C.; Weidner, J.R. Basics of Enzymatic Assays for HTS. In Assay Guidance Manual; Markossian, S., Sittampalam, S., Grossman, A., Eds.; Eli Lilly & Company and the National Center for Advancing Translational Sciences, 2004.

2.7.2 Screening of 47 Essential Oils as Potential Sources of Tyrosinase Inhibitors

2.7.2.1 Introduction

Plant specialised metabolites have often raised interest among the scientific community as potential sources of tyrosinase inhibitors. This trend is not surprising in light of the following considerations. Tyrosinase is a ubiquitous enzyme in both the animal and vegetable kingdom, while plant specialised metabolites play a fundamental role in the plant interaction with the external environment; therefore, the chance of discovering tyrosinase inhibitors among plant specialised metabolites is pretty high. This assumption has been proven by the fact that three out of five of the most employed tyrosinase inhibitors are plant derivatives (i.e., hydroquinone, β-arbutin, and aloesin). As previously discussed in the current thesis, up to date, several phenolic compounds have been investigated as tyrosinase inhibitors, including flavonoids (i.e, Kaempferol [1], quercetin [1], and resveratrol [2], phenylpropanoids (cinnamaldehyde [3], eugenol and isoeugenol [4]) and simple phenols and phenolic acids (hydroquinone, β-arbutine, resorcinol [5])

Among terpenoid derivatives, which are the major constituents of EOs, a limited number of compounds interfering with melanin pigments has been identified so far. These include thymol, carvacrol [6], and citral [7] [8]. While citral is recognised as a tyrosinase inhibitor, in particular a non-competitive one [8], Satooka *et al* [6] proved that thymol and carvacrol are not tyrosinase inhibitors, but their inhibitory mechanism on melanogenesis is due to the inhibition of the redox reaction between dopaquinone and leukodopachrome without any interaction with tyrosinase. Limonene and β-myrcene are terpenoid derivatives for which there are conflicting opinions regarding their tyrosinase inhibitory activity. In fact, while Huang *et al*. [7] ascribed no inhibitory activity to these compounds, β-myrcene was described as a poor tyrosinase inhibitor by Matsura *et al* [8]. Similarly, limonene is considered by Fiocco et al. [9] a potential inhibitor in light of the observed inhibitory activity of a *Citrus x aurantium* L. essential oils (EOs) extremely rich in this terpenoid.

The aim of this study was to evaluate the tyrosinase inhibitory activity of a consistent group of EOs with differing chemical compositions in order to provide new insights into potential tyrosinase inhibitors among terpenoid derivatives.

2.7.2.2 Materials and methods:

Reagents

Dimethyl sulfoxide (DMSO), mushroom tyrosinase from *Agaricus bisporus* (J.E. Lange) Imbach, L-tyrosine, and kojic acid were purchased from Merck Life Science S.r.l.. 47 EOs were enrolled in the study and tested for their inhibitory activities against mushroom tyrosinase. They were all supplied by Erboristeria Magentina S.r.l and obtained following the procedures described in the European Pharmacopoeia [25]. **Table 1** reports the botanical name of the plant used to obtain each EO, as well as the part of the plant used.

In Vitro Tyrosinase Inhibitory Assay

The same colorimetric readout-based enzyme assay as that reported in the previous research project (See section 8.1.3) was employed. The EOs inhibitory activity was tested at a concentration of 166.7 μg/mL, and each measurement was performed in triplicates.

Analysis Conditions

EOs solutions were prepared in cyclohexane at a concentration of 5.0 mg/mL and analysed by GC-MS. GC-MS analyses were carried out using a Gerstel MPS-2 multipurpose sampler installed on an Agilent 6890 N GC coupled to a 5975 MSD and equipped with a ChemStation Version E.02.02.1431 data processing system (Agilent Technologies, Santa Clara, CA). GC conditions: injector temperature: 250°C; injection mode: split; ratio: 1/20; carrier gas: helium; constant flow rate: 1 mL/min; columns: Mega 5 (95 % polydi-methylsiloxane, 5 % phenyl) df 0.25 µm, dc 0.25 mm, length 25 m, from MEGA. Temperature program: 50°C//3°C/min//180°C//10°C/min//250°C (5 min). MSD conditions: MS operated in EI mode (70 eV); scan range: 35 to 350 amu; dwell time 40 ms; ion source temperature: 230°C; quadrupole temperature: 150°C; transfer-line temperature: 280°C. EO markers were identified by comparing both their linear retention indices (ITs), calculated versus a C9-C25 hydrocarbon mixture, and their mass spectra either against those of authentic samples or from commercially available mass spectral libraries (Adams, 2007).

2.7.2.3 Results and discussion:

Table 1 reports the list of the investigated EOs together with their experimentally measured tyrosinase inhibitory activities and the abundance of the main constituents of each sample expressed as normalised percentage abundance. The samples are listed in descending order from the most active ones to those displaying no activity. The EOs selected for the study belong to 18 different botanical families, with the Lamiaceae, Myrtaceae, and Lauraceae being the most represented ones. **Figure 1** displays the distribution of the enrolled samples among the different botanical families. All the EOs were tested at a concentration of 166.7 µg/mL. The percentage of DMSO amounted to 0.3% in the reaction mixture, which experimentally proved not to interfere with the enzymatic activity. The EO concentration to be tested was chosen to be sufficiently high to increase the chance of detecting even those inhibitory activities ascribable to minor compounds.

With the *in vitro* assay adopted for this study, inhibitors of both the monophenolasic and diphenolasic activity could be detected indiscriminately. Therefore, the aim was to collect as much information as possible on the tyrosinase inhibitory activity of many EOs with differing chemical compositions rather than describing the mechanism of inhibition of potential inhibitors.

Confirming literature data [1], [12], the EOs displaying the highest inhibitory activities were those presenting significant amounts of 1) the phenylpropanoids cinnamaldehyde, eugenol, and *trans*-anethole (i.e., *Cinnamomum cassia*, *Cinnamomum verum*, *Syzygium aromaticum*, *Pimpinella anisum*., *Foeniculum vulgare*) and of 2) the aromatic terpenoid derivatives thymol and carvacrol (i.e., *Thymus vulgaris* L. and *Origanum vulgare* L. EOs).

Promising inhibitory activities (i.e., 46 ±4 and 40 ± 4, respectively) were also observed for *Juniperus communis* and *Pinus mugo* EOs. The latter samples both contain the monoterpene β-myrcene, which proved to be a fairly potent tyrosinase inhibitor in our previous work [26]. Despite β-Myrcene accounts for only 10.7% and 12.8% in *Juniperus communis* and *Pinus mugo* EOs, respectively, it is highly likely to be the major responsible for the observed inhibitory activity in light of the results obtained from its dose-response curve [26].

Other EOs that inhibited tyrosinase, even though to a lesser extent, were those EOs displaying significant amounts of both linalool and linalyl acetate, namely: neroli and

petitgrain EOs (both obtained from *Citrus aurantium* samples, but from the flowers and the leaves respectively), clary sage (i.e., *Salvia sclarea)* and lavender *(i.e., Lavandula angustifolia).* Fiocco *et al* [27], [28] explored the inhibitory activity against mushroom tyrosinase of lavender (*Lavandula angustifolia* Mill), clary sage (*Salvia sclarea),* and peppermint (*Mentha x piperita* L.) EOs, among others. They observed inhibitory activities for all EOs, with lavender being a more potent inhibitor than other EOs. Even if these data are not fully comparable to ours due to differences in the experimental conditions employed, our results agree with those of Fiocco *et al.* regarding lavender and clary sage EOs, while discrepancies were observed in the case of peppermint for which in our study no activity was recorded. These discrepancies may be ascribed to the different amounts of β-myrcene in the two considered samples. In our case, β-myrcene could not be detected, while its abundance reached 4.1% in the case of Fiocco *et al.*

Table 1 List of the investigated essential oils and the part of the plant used to obtain them, their botanical and common names, and their % tyrosinase inhibitory activity.

Common Name	**Botanical Species**	**Family**	**Part of the plant used**	**% of Tyrosinase inhibition**	**σ**	**Major constituents of the plant (Normalised Percentage Abundance)**	
Thyme	*Thymus vulgaris* L.	Lamiaceae	Leaf	102	11	**Thymol (50.7%)**, *p*-Cymene(21%), γ-Terpinene (9.3**%),** Linalool (4%), **Carvacrol (2.75%**)	[28], [12]
Anice	*Pimpinella anisum* L.	Apiaceae	Fruit	84	6	***trans*-Anethole (90%)**, Limonene (2.5 %), Estragole (2.2 %), Foeniculin (0.94%), Linalool (0.55 %)	[1]
Fennel	*Foeniculum vulgare* Mill.	Apiaceae	Fruit	82	8	***trans*-Anethole (77%)**, α-Phellandrene (5.6%), Fenchone (5.1 %), Limonene (4.5 %), **β-Myrcene*** (1.9 %)	[1]
Cinnamon bark, Chinese	*Cinnamomum cassia* (L.) J.Presl	Lauraceae	Bark	75	5	***trans*-Cinnamaldehyde (78.5 %),** *trans-o*-metoxy- Cinnamaldehyde (11.5 %), *trans*-Cinnamyl acetate (2.4 %), Cumarine (1.9 %), α-Copaene (0.5%)	[9]
Cinnamon bark, Ceylon	*Cinnamomum verum* J.Presl	Lauraceae	Bark	75	8	***trans*-Cinnamaldehyde (49%)**, **Eugenol (24 %),** Linalool (4.5 %), *trans*-β-Caryophyllene (3,6 %), *trans*-Cinnamyl acetate (2.5 %)	[29]
Cinnamon leaf, Ceylon	*Cinnamomum verum* J.Presl	Lauraceae	Leaf	70	10	**Eugenol (79%)**, *trans*-β-Caryophyllene (3.2 %), Benzil benzoate (2.6%) Eugenyl acetate (2.4%), Linalool (2.1%)	[28], [12], [29]
Clove	*Syzygium aromaticum* (L.) Merr. & L.M.Perry	Myrtaceae	Leaf/Buds	53	4	**Eugenol (86.7 %)** *trans*-β-Caryophyllene (9.9 %), α-Humulene (2 %), δ-Cadinene, Caryophyllene oxide (0.3%)	[28], [12]
Oregano	*Origanum vulgare* L.	Lamiaceae	Leaf	52	7	**Carvacrol (61 %)**, *p*-Cymene (11.8 %), *trans*-β-Caryophyllene (6.5 %) γ-Terpinene (5.9 %), Linalool (3.2%)	[28], [12], [30]
Juniper berry	*Juniperus communis* L.	Cupressaceae	Fruit	46	4	α-Pinene (45.5 %), **Myrcene (10.7%),** β-Pinene (9.1%), Sabinene (7.2 %), Limonene (5.3 %)	

Common Name	Botanical Species	Family	Part of the plant used	% of Tyrosinase inhibition	σ	Major constituents of the plant (Normalised Percentage Abundance)	
Neroli	*Citrus×aurantium* L.	Rutaceae	Flower	42	10	**Linalyl acetate (41.4 %), Linalool (28.5 %),** Limonene (11.4 %), β-Pinene (7.6 %), *trans*-β-Ocimene (2.6 %)	
Pine needle,Dwarf	*Pinus mugo* Turra	Pinaceae	Leaf/twig	40	3	α-Pinene (16.1 %), δ-3-Carene (15.7 %), **Myrcene (12.8 %),** β-Pinene (12.2 %), β-Phellandrene (11%)	
Petitgrain	*Citrus×aurantium* L.	Rutaceae	Leaf	39	11	**Linalyl acetate (60%), Linalool (22 %),** α-Terpineol (4.1 %), Geranyl acetate (3.1 %), Myrcene* (1.8 %)	
Clary sage	*Salvia sclarea* L.	Lamiaceae	Leaf/Flower	24	4	**Linalyl acetate (56.8 %), Linalool (18.9 %),** trans-β-Caryophyllene (5.5 %), α-Terpineol (3.8 %), Neryl acetate (2.8 %)	[28]
Rosa	*Rosa × damascena* Herrm.	Rosaceae	Flower	22	6	Phenyl ethyl alcohol (75 %), Citronellol (11 %), Geraniolo (6 %), **Eugenol (1.4 %),** Methyl eugenol (0.68 %)	
Marjoram	*Origanum majorana* L.	Lamiaceae	Leaf	20	3	4-Terpineol (25.2 %), γ-Terpinene (15.6 %), α-Terpinene (10.4 %), Linalool (10.3 %), Sabinene (6.2 %), **β-Myrcene (1.60%**)	
Lavender	*Lavandula angustifolia* Mill.	Lamiaceae	Leaf	17	3	**Linalyl acetate (37 %), Linalool (29 %),** *trans*-β-caryophyllene (5.1 %), 4-terpineol (5 %), *cis*-β-ocimene (3.2 %)	[27]
Ylang ylang	*Cananga odorata* Hook.f. & Thomson	Annonaceae	Flower	n.a.		δ-Germacrene (14.4 %), *trans*-β-Caryophyllene (14.3 %), Benzyl benzoate (7.8 %), α-Farnesene (7.6 %) Geranyl acetate (6.6%)	
Caraway	*Carum Carvi* L.	Apiaceae	Seed	n.a.		Carvone (56.5 %), Limonene (40.4 %), **β-Myrcene** * (0.6%), *cis*-dihydro-carvone (0.4 %), α-Pinene (0.2 %)	
Camphor	*Cinnamomum camphora* (L.) J.Presl	Lauraceae	Wood	n.a.		1,8-Cineole (35.2 %) Limonene (22.6 %) *p*-Cymene (11.2 %), α-Terpinene (6.8 %)	
Finger citron	*Citrus medica* L.	Rutaceae	Wood	n.a.		α-Cedrene (59 %),Cedrol (38.7%)	

Common Name	Botanical Species	Family	Part of the plant used	% of Tyrosinase inhibition	σ	Major constituents of the plant (Normalised Percentage Abundance)	
Frankincense	*Boswellia sacra* Flueck	Burseraceae	Tree resin	n.a.		Thujopsene (25.4%), β-Cedrene (2 %) α-Pinene (27.8%), Incensole + Serratol (9.1%), Limonene (8.6 %), α-Thujene (6.1 %), *p*-Cymene (4.6 %)	
Myrrh	*Commiphora myrrha* (Nees) Engl.	Burseraceae	Tree resin	n.a.		Ethyl citrate (75.5 %), Furanoeudesma 1,3-diene (7 %), Curzerene (3.7 %), Isofuranodiene (2 %), *cis*-β-ocimene (0.1 %)	
Wintergreen	*Gaultheria procumbens* L.	Ericaceae	Leaf	n.a.		Methyl salicylate (99.8%)	
Mugwort	*Artemisia vulgaris* L.	Compositae	Leaf/Flower	n.a.		α-Thujone (47.7%), Camphor (28.7 %), β-Thujone (8.5%), Camphene (3.2 %), 1,8-cineole (1.40%)	
Cedar leaf	*Thuja occidentalis* L.	Cupressaceae	Leaf/Twig	n.a.		α-Thujone (52.9 %), Fenchone (12.2 %), β-Thujone (9.9 %), Sabinene (3.5 %), Bornyl acetate (2.8%)	
Geranium	*Pelargonium graveolens* L'Hér.	Geraniaceae	Leaf	n.a.		Citronellol (31.1%), Geraniol (13.7%), 10-epi-γ-eudesmol (7.8 %), Citronellyl formate (7.4%), Isomenthone (5.5%)	
Hyssop	*Hyssopus officinalis* L.	Lamiaceae	Leaf	n.a.		Isopinocamphone (43.5 %), β-Pinene (12.6 %), Pinocamphone (12.1 %), Limonene (6.3 %), Biciclogermacrene (2.6 %)	
Mint	*Mentha arvensis* L.	Lamiaceae	Leaf	n.a.		Menthol (35.9%), Menthone (18.7 %), Isomenthone (8.7%), Menthyl acetate (7.5%), Neomenthol (5.9%)	
Peppermint	*Mentha* × *piperita* L.	Lamiaceae	Leaf	n.a.		Menthol (43.3 %), Menthone (25.4 %), Isomenthone (10%), Menthyl acetate (5.6%), Neomenthol (4.7%)	[27]
Rosemary	*Rosmarinus officinalis* L.	Lamiaceae	Leaf	n.a.		1,8-Cineole (57.3%), Camphor (15.1%), α-Pinene (11.5%), β-Pinene (8.4%) , *trans*-β-Caryophyllene (4.3%)	[28][29] [30]

Common Name	Botanical Species	Family	Part of the plant used	% of Tyrosinase inhibition	σ	Major constituents of the plant (Normalised Percentage Abundance)	
Sage, Dalmatian	*Salvia officinalis* L.	Lamiaceae	Leaf	n.a.		α-Thujone (22.5 %), Camphor (18.5 %), 1,8-cineole (11.4%), α-Humulene (7.2 %) β-Thujone (6.2 %)	[28] [29] [30]
Laurel	*Laurus nobilis* L.	Lauraceae	Leaf	n.a.		1,8-Cineole (58.3 %), β-Terpinyl acetate (8.6 %), α-Pinene (7%), Sabinene (5.5%), β-Pinene (4 %)	[29] [30]
Cajeput	*Melaleuca cajuputi* Powell	Myrtaceae	Leaf	n.a.		1,8-Cineole (37.3 %), α-Terpineol (10 %), *trans*-β-Caryophyllene (7.5 %), γ-Terpinene (4.1 %), α-Pinene (3.2 %)	
Eucalyptus lemon-scented	*Corymbia citriodora (*Hook.) K.D.Hill & L.A.S.Johnson	Myrtaceae	Leaf	n.a.		Citronellal (73.2 %), Citronellol (8.9 %), Isopulegol (8.8 %), Citronellyl acetate (2.3 %), *trans*-β-caryophyllene (1.3 %)	
Myrtle	*Myrtus communis* L.	Myrtaceae	Leaf	n.a.		α-Pinene (52 %), 1,8-Cineole (25 %), Limonene (8.2 %), Linalool (2.6 %), Geranyl acetate (2.0 %)	
Niaouly	*Melaleuca quinquenervia (Cav.)* S.T.Blake	Myrtaceae	Leaf	n.a.		1,8-Cineole (52.2 %), Limonene (9.8 %), Viridiflorol (7.6 %), α-Pinene (7.2%) ,α-Terpineol (6.4)	[29]
Tea tree	*Melaleuca alternifolia* (Maiden & Betche) Cheel	Myrtaceae	Leaf	n.a.		4-Terpineol (40.2 %), γ-Terpinene (18.5%), α-Terpinene (9.3 %), α-Terpinolene (3.4 %), *p*-Cymene (3.0 %)	
Jasmine	*Jasminum officinale* L.	Oleaceae	Flower	n.a.		Benzyl acetate (33 %), Benzyl benzoate (14 %), *trans*-Jasmone (9 %), Linalool (6.8 %), Indole (6.8 %)	
Cedar	*Cedrus atlantica* (Endl.) Manetti ex Carrière	Pinaceae	Wood	n.a.		α-Cedrene (59 %),Cedrol (38.7%) Thujopsene (25.4%), β-Cedrene (2 %)	
Pine silvestris	*Pinus sylvestris* L.	Pinaceae	Leaf/twig	n.a.		α-Pinene (38.1 %), β-Pinene (19.2 %), δ-3-carene (15.7 %), Limonene (10 %), *trans*-β-Caryophyllene (3.7 %)	

Common Name	Botanical Species	Family	Part of the plant used	% of Tyrosinase inhibition	σ	Major constituents of the plant (Normalised Percentage Abundance)
Black pepper	*Piper nigrum* L.	Piperaceae	Fruit	n.a.		*trans*-β-Caryophyllene (23.3 %), Limonene (15.2 %), β-Pinene (12.4 %), δ-3-Carene (9.2%), Sabinene (7.0 %)
Citronella	*Cymbopogon winterianus* Jowitt ex Bor	Poaceae	Leaf	n.a.		Citronellal (42.8 %), Geraniolo (21 %), Citronellol (11.5 %), Limonene (6.6 %), Geranyl acetate (3.1 %)
Palmarosa	*Cymbopogon martini (Roxb.)* W.Watson	Poaceae	Leaf	n.a.		Geraniol (79.3%), Geranyl acetate (13.1%), Linalool (2.8%), *trans*-β-Caryophyllene (1.7 %), *trans*-β-ocimene (1.1%)
Vetiver	*Chrysopogon zizanioides* (L.) Roberty	Poaceae	Root	n.a.		Khusinol (4.5 %), β-Vetivene (3.7 %), Khusimene (3%),γ-Vetivene (2.9 %), β-Vetivone (1.4 %)
Sandalwood, East Indian	*Santalum album* L.	Santalaceae	Wood	n.a.		*trans*-β-Caryophyllene (18.1 %), *cis*-α-Santalol (15.0 %), *cis*-β-Santalol (6.8 %), α-Cedrene (5.2 %), *cis*-Thujopsene (4.4 %)
Cardamom	*Elettaria cardamomum (L.)* Maton	Zingiberaceae	Seed	n.a.		1,8-Cineole (39.2%), α-Terpinyl acetate (37.4 %), Linalyl acetate (5.5 %), Sabinene (3.2 %), Linalool (2.7 %)
Ginger	*Zingiber officinale* Roscoe	Zingiberaceae	Rhyzome	n.a.		α-Zingiberene (37.9 %), β-Sesquifellandrene (14.1%), β-Bisabolene (11.5%), Ar-curcumene (9 %), Camphene (3.9 %)

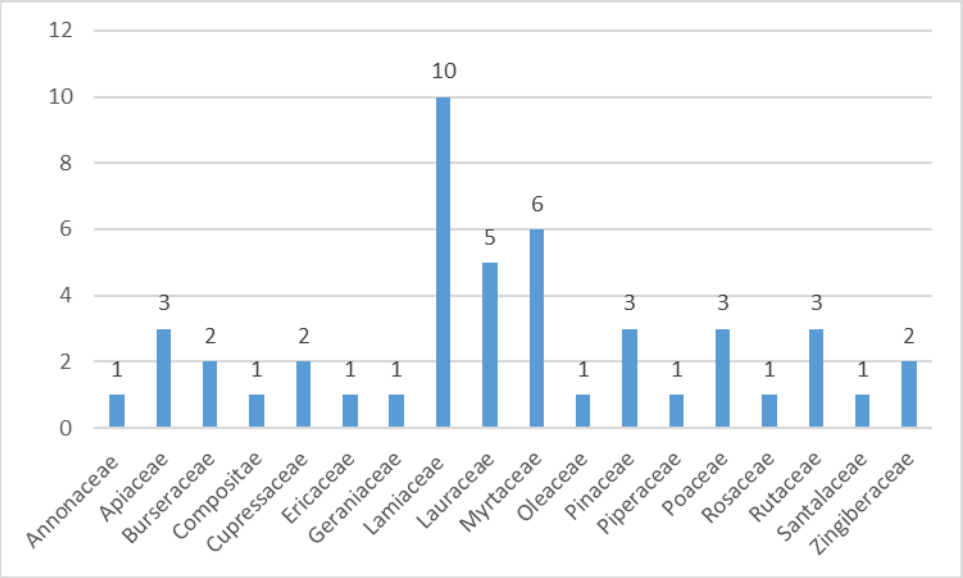

Figure 1 Distribution of the investigated essential oils across different botanical families

2.7.2.4 Conclusions

The aim of this study was to evaluate the tyrosinase inhibitory activity of 47 EOs with differing chemical compositions in order to provide new insights into the potential tyrosinase inhibitors among terpenoid derivatives. 17 EOs out of 47 investigated samples displayed an inhibitory activity whose intensity spanned from 17 ±3 % (i.e., *Lavandula angustifolia*) to complete inhibition in the case of Thyme EO, proving again that plant specialised metabolites are very promising sources of tyrosinase inhibitors. In addition to those EOs containing well-known tyrosinase inhibitors (i.e., cinnamaldehyde, eugenol, and isoeugenol), those displaying the second-highest inhibitory activities were those containing the terpenoid derivative β-myrcene (i.e., *Juniper berry* and *Pine needle* dwarf EOs) confirming the great potential of this compound as tyrosinase inhibitor and erasing any doubts regarding its activity on mushroom tyrosinase.

2.7.2.5 References

[1] I. Kubo and I. Kinst-Hori, "Tyrosinase Inhibitors from Anise Oil," *J. Agric. Food Chem.*, vol. 46, no. 4, pp. 1268–1271, 1998, doi: 10.1021/jf9708958.

[2] B. Desmedt *et al.*, "Overview of skin whitening agents with an insight into the illegal cosmetic market in Europe," *J. Eur. Acad. Dermatology Venereol.*, vol. 30, no. 6, pp. 943–950, 2016, doi: 10.1111/jdv.13595.

[3] T. Pillaiyar, M. Manickam, and V. Namasivayam, "Skin whitening agents: medicinal chemistry perspective of tyrosinase inhibitors," *J. Enzyme Inhib. Med. Chem.*, vol. 32, no. 1, pp. 403–425, Jan. 2017, doi: 10.1080/14756366.2016.1256882.

[4] C. L. Burnett *et al.*, "Final report of the safety assessment of kojic acid as used in cosmetics," *Int. J. Toxicol.*, vol. 29, no. 6, 2010, doi: 10.1177/1091581810385956.

[5] J. W. Lin, H. M. Chiang, Y. C. Lin, and K. C. Wen, "Natural products with skin - Whitening effects," *J. Food Drug Anal.*, vol. 16, no. 2, pp. 1–10, 2008.

[6] I. Kubo and I. Kinst-Hori, "Tyrosinase inhibitory activity of the olive oil flavor compounds," *J. Agric. Food Chem.*, vol. 47, no. 11, pp. 4574–4578, Nov. 1999, doi: 10.1021/jf990165v.

[7] J. Y. Lim, K. Ishiguro, and I. Kubo, "Tyrosinase inhibitory p-coumaric acid from ginseng leaves," *Phyther. Res.*, vol. 13, no. 5, pp. 371–375, 1999, doi: 10.1002/(SICI)1099-1573(199908/09)13:5<371::AID-PTR453>3.0.CO;2-L.

[8] E. Ersoy, E. Eroglu Ozkan, M. Boga, M. A. Yilmaz, and A. Mat, "Anti-aging potential and anti-tyrosinase activity of three Hypericum species with focus on phytochemical composition by LC–MS/MS," *Ind. Crops Prod.*, vol. 141, no. September, 2019, doi: 10.1016/j.indcrop.2019.111735.

[9] C.-T. T. Chang, W.-L. L. Chang, J.-C. C. Hsu, Y. Shih, and S.-T. T. Chou, "Chemical composition and tyrosinase inhibitory activity of Cinnamomum cassia essential oil," *Bot. Stud.*, vol. 54, no. 1, pp. 2–8, Aug. 2013, doi: 10.1186/1999-3110-54-10.

[10] B. Marongiu *et al.*, "Supercritical CO2 extract of Cinnamomum zeylanicum: Chemical characterization and antityrosinase activity," *J. Agric. Food Chem.*, vol. 55, no. 24, pp. 10022–10027, 2007, doi: 10.1021/jf071938f.

[11] E. Tangke Arung, E. Matsubara, I. Wijaya Kusuma, E. Sukaton, K. Shimizu, and R. Kondo, "Inhibitory components from the buds of clove (Syzygium aromaticum) on melanin formation in B16 melanoma cells," *Fitoterapia*, vol. 82, no. 2. pp. 198–202, 2011, doi: 10.1016/j.fitote.2010.09.008.

[12] M. D. M. Garcia-Molina, J. L. Muñoz-Muñoz, F. Garcia-Molina, P. A. García-Ruiz, and F. Garcia-Canovas, "Action of tyrosinase on ortho-substituted phenols: Possible influence on browning and melanogenesis," *J. Agric. Food Chem.*, vol. 60, no. 25, pp. 6447–6453, 2012, doi: 10.1021/jf301238q.

[13] H. Satooka and I. Kubo, "Effects of thymol on B16-F10 melanoma cells," *J. Agric. Food Chem.*, vol. 60, no. 10, pp. 2746–2752, Mar. 2012, doi: 10.1021/jf204525b.

[14] H. Satooka and I. Kubo, "Effects of thymol on mushroom tyrosinase-catalyzed melanin formation," *J. Agric. Food Chem.*, vol. 59, no. 16, pp. 8908–8914, Aug. 2011, doi: 10.1021/jf2014149.

[15] X.-W. Huang, Y.-C. Feng, Y. Huang, and H.-L. Li, "Potential cosmetic application of essential oil extracted from *Litsea cubeba* fruits from China," *J. Essent. Oil Res.*, vol. 25, no. 2, pp. 112–119, Apr. 2013, doi: 10.1080/10412905.2012.755479.

[16] R. Matsuura, H. Ukeda, and M. Sawamura, "Tyrosinase inhibitory activity of citrus essential oils," *J. Agric. Food Chem.*, vol. 54, no. 6, pp. 2309–2313, 2006, doi: 10.1021/jf051682i.

[17] J. J. Kellogg, M. F. Paine, J. S. McCune, N. H. Oberlies, and N. B. Cech, "Selection and characterization of botanical natural products for research studies: a NaPDI center recommended approach," *Nat. Prod. Rep.*, vol. 36, no. 8, pp. 1196–1221, 2019, doi: 10.1039/C8NP00065D.

[18] K. P. Williams and J. E. Scott, "Enzyme Assay Design for High-Throughput Screening," in *High Throughput Screening. Methods in Molecular Biology (Methods and Protocols)*, 2nd ed., vol. 565, W. P. Janzen and Bernasconi Paul, Eds. Clifton, N.J.: Humana Press, 2009, pp. 107–126.

[19] H. B. Brooks *et al.*, *Basics of Enzymatic Assays for HTS*, no. Md. Bethesda (MD), 2004.

[20] B. Roulier, B. Pérès, and R. Haudecoeur, "Advances in the Design of Genuine Human Tyrosinase Inhibitors for Targeting Melanogenesis and Related Pigmentations," *J. Med. Chem.*, vol. 63, no. 22, pp. 13428–13443, Nov. 2020, doi: 10.1021/acs.jmedchem.0c00994.

[21] P. K. Mukherjee, R. Biswas, A. Sharma, S. Banerjee, S. Biswas, and C. K. Katiyar, "Validation of medicinal herbs for anti-tyrosinase potential," *J. Herb. Med.*, vol. 14, pp. 1–16, Dec. 2018, doi: 10.1016/j.hermed.2018.09.002.

[22] M. G. Acker and D. S. Auld, "Considerations for the design and reporting of enzyme assays in high-throughput screening applications," *Perspect. Sci.*, vol. 1, no. 1–6, pp. 56–73, 2014, doi: 10.1016/j.pisc.2013.12.001.

[23] W. P. Janzen and P. Bernasconi, Eds., *High Throughput Screening*, vol. 565. Totowa, NJ: Humana Press, 2009.

[24] K. Hostettmann, A. Marston, and M. Hostettmann, *Preparative Chromatography Techniques*. Berlin, Heidelberg: Springer Berlin Heidelberg, 1998.

[25] Council of Europe, *European Pharmacopoeia*, 10th ed. Strasburg, France: Council of Europe, 2020.

[26] F. Capetti *et al.*, "Citral-Containing Essential Oils as Potential Tyrosinase Inhibitors: A Bio-Guided Fractionation Approach," *Plants 2021, Vol. 10, Page 969*, vol. 10, no. 5, p. 969, May 2021, doi: 10.3390/PLANTS10050969.

[27] D. Fiocco *et al.*, "Lavender and peppermint essential oils as effective mushroom tyrosinase inhibitors: A basic study," *Flavour Fragr. J.*, vol. 26, no. 6, pp. 441–446, Nov. 2011, doi: 10.1002/ffj.2072.

[28] D. Fiocco, M. Arciuli, M. P. Arena, S. Benvenuti, and A. Gallone, "Chemical composition and the anti-melanogenic potential of different essential oils," *Flavour Fragr. J.*, vol. 31, no. 3, pp. 255–261, May 2016, doi: 10.1002/ffj.3315.

[29] Z. Aumeeruddy-Elalfi, A. Gurib-Fakim, and M. F. Mahomoodally, "Kinetic studies of tyrosinase inhibitory activity of 19 essential oils extracted from endemic and exotic medicinal plants," *South African J. Bot.*, vol. 103, pp. 89–94, 2016, doi: 10.1016/j.sajb.2015.09.010.

[30] A. Moghrovyan, N. Sahakyan, A. Babayan, N. Chichoyan, M. Petrosyan, and A. Trchounian, "Essential Oil and Ethanol Extract of Oregano (Origanum vulgare L.) from Armenian Flora as a Natural Source of Terpenes, Flavonoids and other Phytochemicals with Antiradical, Antioxidant, Metal Chelating, Tyrosinase Inhibitory and Antibacterial Activity," *Curr. Pharm. Des.*, vol. 25, no. 16, pp. 1809–1816, 2019, doi: 10.2174/1381612825666190702095612.

3 Chapter 3:

In vitro Dermal Absorption Studies of Essential Oil Components

3.1 Introduction

Part of this doctoral project was devoted to studying the dermal absorption profile of topically applied essential oil (EO) components.

This chapter describes the theoretical aspects required to understand the dermal absorption process of exogenous compounds and the *in vitro* strategies that can be exploited to investigate the process. Two research projects are then presented. The first one deals with the optimization of a solvent-free analytical strategy based on Headspace Solid-Phase Micro-Extraction (HS-SPME) and GC-MS analysis to monitor the permeation kinetic rate, the skin layers' distribution and the emission in the surrounding atmosphere of volatile components released from topic formulations. *Melaleuca alternifolia* (Maiden & Betche) Cheel EO (Tea tree oil) was chosen as a case study for the method optimisation due to the relevant lack of information concerning the percutaneous (dermal) absorption profile of its constituents as described in the opinion of the European Scientific Committee on Consumer Safety [1]. The second study presented in the chapter deals with the application of the optimised analytical strategy for the investigation of the dermal absorption behaviour of those essential oils and their respective bioactive constituents, displaying promising *in vitro* tyrosinase inhibitory activities. For a more in-depth description of the analytical strategy employed for the studies, the readers are referred to Chapter 1 of the current manuscript.

3.2 The skin anatomy and physiology

With a surface area of more than 2 m^2 and an average weight of 4 kg for a typical adult of 70 kg [2], the skin is the most expansive organ by mass and by size in healthy grownups [3]. It is a complex organ whose primary function is to prevent the absorption of exogenous particles [4]. In addition, the skin preserves the body from drying, reduces harmful effects of UV radiation, acts as a sensory organ (touch, temperature), helps regulate temperature, detects infections, and finally, produces vitamin D (i.e., cholecalciferol), which is then transferred to the liver and the kidney where it is transformed into its active form [5].

The skin consists of a series of layers that can be grouped into three major divisions: the epidermis, the dermis, and the hypodermis, all contributing to the overall functionality of the organ with specific properties [6]. The skin structure, and in particular the dermis, also includes hair follicles, sweat glands, and sebaceous glands, which are generally referred to as skin appendages [7]. The skin's different divisions will be briefly described in the following paragraphs.

The epidermis

The epidermis is the outermost layer of the skin. It is an avascular stratified epithelium of around 0.2 mm thickness. It is mainly composed of cells known as keratinocytes but also encloses two types of dendritic cells: melanocytes and Langerhans cells. As keratinocytes structurally form the epidermis, melanocytes impart protection against ultraviolet radiation (UV), while Langerhans cells act as immune sentinels [4].

From the outside in, the epidermis presents the *stratum corneum,* which consists of dead keratinocytes known as corneocytes with no metabolic activity, and the viable epidermis where keratinocytes undergo a process of maturation (i.e., keratinocytes differentiation) to corneocytes as they move upwards towards the skin surface.

The *stratum corneum* presents around 10 to 20 layers of corneocytes that are connected by corneodesmosomes and are surrounded by intercellular lipids forming the so-called "brick and mortar model" with brick-like corneocytes embedded in the cement-like lipid matrix. Each corneocyte is enclosed within a protein-rich cornified cell envelope that provides covalent linkage sites for the intercellular lipids and is filled with keratin which is a complex, fibrous, and water-insoluble protein that imparts strength to the skin. As new keratinocytes differentiate into corneocytes, desquamation occurs, and the outermost cells are sloughed from the surface. Due to its low water content (i.e., 10– 20% in healthy skin [8]), the *stratum corneum* is considered a lipophilic phase in contrast to the hydrophilic viable epidermis and dermis [9].

In the viable epidermis, keratinocytes differentiate and form different strata according to their maturation stage. In almost every part of the body, three strata can be observed, namely the *stratum germinativum*, the *stratum spinosum*, and the *stratum granulosum*. Only in the palms and soles (i.e., thick skin), an additional layer known as *stratum lucidum* is placed in between the *stratum granulosum* and the *stratum corneum*.

The *stratum germinativum* is the epidermis basal cell layer. It is a single layer of stem cells located on the dermal-epidermal junction, which separates the epidermis from the dermis. These cells are responsible for epidermis regeneration; they divide daily into two cells, the progenitor and the maturing cells. The progenitor cell remains in the *stratum germinativum* as a stem cell while the maturing cell undergoes the process of maturation. Along with the stem cells, the *stratum germinativum* also contains melanocytes. The latter are specialised dendritic cells that synthesize melanin pigments which play a crucial role in the absorption of free radicals and the protection of the cell DNA from ionizing radiations, including UV light. Together with 30-40 associated keratinocytes, melanocytes form the melanin units: they produce melanin inside a specific organelle

called melanosomes which are then transferred via dendrites to the associated keratinocytes where they accumulate around the cell nucleus providing photoprotection [10].
The second innermost layer of the epidermis is the *stratum spinosum*. This section is usually 5 to 10 layers thick, and keratinocytes are tethered to one another by strong intercellular junctions known as desmosomes that connect keratin intermediate filaments of adjacent cells, maintaining the structural integrity of the skin. Keratinocytes in the *stratum spinosum* interact with the melanocytes located in the *stratum germinativum* forming the melanin unit.
Above the *stratum spinosum*, there is the *stratum granulosum* which is the first viable layer below the *stratum corneum*. In addition to keratinocytes, it includes Langerhans cells that provide the first line of defense against pathogens. Other than keratin, keratinocytes produce additional proteins that will take part in the formation of the cornified envelope as well as lamellar granules known as Odland bodies which are rich in polar lipids, glycosphingolipids, free sterols, and phospholipids. As keratinocytes turn into corneocytes, the lipids contained in the Odland bodies are reversed into the intercellular space, where they mix with the products of sebaceous secretion (i.e., triglycerides, fatty acids, wax esters, and squalene), forming the lipid matrix embedding the corneocytes in the *stratum corneum*. [11].

<u>The dermis</u>
The dermis is vascular connective tissue 10 to 40 times thicker than the epidermis that provides structural and nutritional support to the skin [11]. It is anchored to the epidermis by the dermal-epidermal junction, which is a semipermeable membrane that allows the diffusion of nutrients from the dermis blood vessel to the viable epidermis.
The dermis contains four major resident cell types that are embedded in a fibrous extracellular matrix. These cells include 1) fibroblasts which synthesise the extracellular matrix components, 2) dermal dendritic cells, 3) macrophages, 4) and mast cells [11].
The extracellular matrix contains mainly collagen (i.e., type I and III collagen), elastic fibers, and ground material. Collagen makes up 90 % of the weight of the dermis, and it provides strength and resilience to the skin. Elastic fibers impart flexibility to the skin, and they are made up of 15% microfibrils and 85% matrix elastin [11]. The ground material is trapped within collagen fibers. The ground material is mainly composed of glycosaminoglycans (e.g., hyaluronic acid) and proteoglycans (i.e., glycosaminoglycans covalently attached to proteins). Glycosaminoglycan are unbranched polysaccharide chains of repeating disaccharide units that can resist compressive forces due to their tendency to adopt highly extended conformations and attract water into the extracellular matrix, which in addition imparts turgor to the skin [11]
The dermis extracellular matrix supports blood vessels, lymphatic channels, sensory nerves (pressure, temperature, and pain), and the inner segments of the sweat glands and pilosebaceous units.
The dermal vasculature is articulated in a superficial and deep vascular plexus. The superficial vascular plexus provides nutrition and waste removal to the overlying epidermis, while the deep vascular plexus is located at the border between the dermis and the hypodermis. It is articulated in larger-caliber vessels connected to the superficial plexus by vertically oriented dermal vessels and to vascular branches within the hypodermis.

The hypodermis

The hypodermis, also known as the subcutaneous adipose tissue, is located in between the dermis and the myofascial. It consists of connective tissue, adipose tissue, and blood vessels. It serves as a store for energy, and it provides mechanical support, insulation, and thermoregulation [11].

Skin appendages

Skin appendages include eccrine sweat glands, apocrine sweat glands, sebaceous glands, and hair follicles, with their associated erector muscles. They are distributed almost throughout the body and what varies depending on the anatomical site is their relative abundance. They all originate in the dermis, cross the different epidermis layers and present their orifice on the skin surface.

Eccrine sweat glands are found in almost every region of the skin. Under temperature controlling determinants and emotional stress, they produce an acidic (pH 5.0) saline solution that reaches the surface of the skin by way of coiled ducts (tubes), where it finally evaporates, cooling down the body temperature. On the contrary, apocrine glands are located in specific body regions only (e.g., the armpit, the breast areola, and the perianal area) and release sweat under hormonal stimulation; their secretions usually have an odor. Sebaceous glands, together with the hair follicle, from the pilosebaceous unit. Sebaceous glands are mainly concentrated on the forehead, in the ear, on the midline of the back, and on anogenital surfaces. They secrete sebum, a mixture of glycerides, free fatty acids, cholesterol, cholesterol esters, wax esters, and squalene. It acts as a skin lubricant and a source of *stratum corneum* plasticizing lipid. In addition, it has antimicrobial effects through squalene and by maintaining acidic conditions (pH 5) on the skin's outer surface.

3.3 The barrier function of the skin and its permeability

The skin's major function is to protect the body from its environment by creating an effective barrier against the absorption of exogenous particles [3,6]. The skin was initially described as an impermeable membrane; however, it is now well established that while it does act as a barrier to exogenous chemicals, it is not a complete one [6]. For this reason, it is now often used as a non-invasive route for administering drugs for systemic, regional, and local delivery.

It is widely recognized that for most chemicals, the layer playing a critical part in the skin's barrier function is the stratum corneum, which serves as a rate-limiting lipophilic barrier against the uptake of chemical and biological toxins as against the trans-epidermal water loss [12]. On the other hand, substances that manage to reach the viable skin layers are destined to be systemically absorbed [2].

3.4 Process of skin permeation and percutaneous absorption

Before going into much detail on how chemicals can be up-taken by the skin, it is essential to clarify a few terms that will be helpful to describe the process adequately. The words "percutaneous absorption" or "dermal absorption" defines the permeation of a topically applied compound through the skin layers and its absorption by the dermis blood vessels and consequent local clearance. "Skin permeation" describes the migration of the compound from the surface of the skin to the bottom of the dermis, including its penetration into and its consequent diffusion across the different layers of the skin [13]

When a chemical dispersed in a vehicle is applied to the skin, it first undergoes a distribution/partitioning process to equilibrium between the vehicle and the skin tissue surface precisely as it would occur between two immiscible solvents and the concentration of chemical on the skin surface at equilibrium is defined by the *stratum corneum* vehicle partition coefficient ($K_{sc\text{-}v}$ [14]). The chemical then passively diffuses through the skin layers driven by its concentration gradient, which is maintained by the constant clearance provided by the dermis blood system.

The *stratum corneum* is the skin layer that displays the most significant resistance to penetration and permeation of exogenous chemicals. However, it is not a complete barrier, and some substances can diffuse through it by two main routes: the *stratum corneum* and the trans-appendage pathway. These pathways are not mutually exclusive, and compounds may permeate the skin through a combination of both according to their physicochemical properties [7]. The trans-appendage path involves the chemical uptake through the sweat pores and the follicular orifices covering the skin surface. This route is of particular importance in the development of drugs to treat acne and cultivate air [15].

The *stratum corneum* pathway includes 1) the tortuous movements of the permeant through the intercellular lipid domain (i.e., lipophilic pathway) and 2) the crossing through the cornified cells (i.e., hydrophilic pathway). The intercellular lipid layer is the only one granting a continuous path through the *stratum corneum,* and it is generally considered the leading route for most chemicals. It is accessible to both lipid and polar molecules, but the amount and rate of diffusion are highly dependent upon their physicochemical properties [7].

3.5 Molecular properties influencing dermal absorption

As discussed before, the skin, and more precisely the *stratum corneum*, is not a complete barrier but rather it is a membrane that is selectively permeable to chemicals with specific physicochemical properties [13,16]

It has been proved that low molecular weight and moderate lipophilic compounds with a decent solubility in aqueous media (i.e., $LogK_{o/w}$ 1-2 according to Guy [17] and $LogK_{o/w}$ 2-3 according to Selzer *et al.* [9]) penetrate and permeate more easily than large molecules with either a very low or a very high octanol-water partition coefficient. The permeant must be sufficiently lipophilic to be soluble in the *stratum corneum* lipid matrix, thus generating a significant concentration gradient across the membrane that favours the compound diffusion

The permeant molecular weight (MW) influences its diffusivity within the *stratum corneum*: the diffusion of the molecule across the *stratum corneum* intercellular lipid domain requires the formation of temporary cavities that enclose the permeant. The higher the permeant molecular weight, the lower the probability of forming such cavities [9]. Several authors agree that 500Dalton is the start of a rapid decline in skin absorption due to molecular size [9,17,18].

The skin permeability coefficient (k_p) is a measure of the skin's conductance to a specific chemical from a particular vehicle. It describes the rate of chemical permeation per unit concentration, and it is expressed as distance/time (cm/min or cm/hr) [17]. It depends on both the compound partition coefficient between the vehicle and the *stratum corneum* (i.e., the relative solubility of the compound in the composite *stratum corneum* compared to the vehicle) and the permeant diffusivity, which is a measure of its mobility within the skin [14]. In particular, the permeability coefficient of a solute across the *stratum corneum* is directly proportional to the *stratum corneum*/vehicle partition coefficient. At the same time, it decreases as the MW of the compound increases [19]. In 1992, Potts and Guy [20] developed an empirical algorithm from an extensive database of permeability coefficients suitable for estimating k_p. According to the algorithm, knowing the compound MW and its $K_{o/w}$, the skin permeability coefficient from an aqueous vehicle is measured as reported in Equation 1.

Equation 1

$$log\ k_p = -2.7 + 0.71 \times logK_{o/w} - 0.0061 \times MW$$

The algorithm employs the $K_{o/w}$ instead of $K_{sc\text{-}w}$ (*stratum corneum*-water partition coefficient) as $K_{o/w}$ as the two proved to be well correlated according to the following Equation 2:

Equation 2

$$K_{sc-w} = K_{o/w}{}^{f}$$

Where the coefficient *"f"* accounts for the partitioning domain presented by octanol and that presented by the lipid SC [19,20]. Potts and Guy [20] found that this value is less than 1 (i.e., 0.71), proving that the partitioning domain of the lipid *stratum corneum* is more polar than octanol.

3.6 How to study the percutaneous absorption of topically exposed compounds?

Dermal absorption can occur from skin exposure to occupational, environmental, cosmetics, and pharmaceutical products. The local and systemic bioavailability of topically exposed compounds is predicted via percutaneous absorption studies that provide fundamental information to assess the safety and efficacy of pharmaceutical products and cosmetics, as well as to establish the risk associated with the exposure to the compound under investigation.

These studies can be carried out *in vivo* using animal models or healthy volunteers and *in vitro* adopting excised human or animal skin [15]. *In vitro* studies offer a series of advantages over *in vivo* experiments as they are cheaper and easier to perform; they provide better reproducibility of the results and less restricted parameters variation [2] while correctly predicting *in vivo* absorption data if the correct methodology is used [2]. In addition, other than evaluating the dermal absorption of specific permeant under expected in-use conditions, *in vitro* permeation studies are helpful in product development (i.e., pharmaceutical and cosmetic sectors) to study the permeation behaviour of the investigated compound.

3.6.1 *In vitro* permeation studies

The systems that model *in vitro* the penetration and permeation process of chemicals through human skin are designed to estimate the amount of permeant that crosses a skin membrane or specific surrogates and reaches a fluid reservoir whose fluid is collected and replaced constantly or periodically, according to the system, to mimic the clearance provided by the dermis blood system. The collected fluid is then analysed by suitable analytical platforms, and the amount of compound recovered in the receptor fluid corresponds to the fraction of the initial dosage that has crossed the membrane.

To study the permeation behaviour of compounds released from a specific vehicle, infinite dose experiments are performed, meaning that the vehicle containing the compound is applied to the skin or the corresponding surrogates in significant excess to keep constant the concentration of the substance on the outside layer of the skin. Typically, the steady-state flux (J_{ss}) (i.e., consistent, constant flux across the membrane) and the experimental permeability coefficient (k_p) are the parameters assessed to describe the permeation behaviour of a permeant. When operating in infinite dose conditions, the cumulative uptake of a substance through a unit of skin surface area (i.e., cumulative amount of substance per cm^2 of skin surface that reaches the receptor fluid) initially increases as a function of time then assumes a linear trend with a constant slope without experiencing a plateau phase as a consistent unchanging movement of the permeant through the membrane is reached (i.e., steady state conditions). The steady-state flux is calculated from the slope of this linear trend, while the experimental k_p is described by the ratio between the steady state flux and the compound concentration in the vehicle.

On the contrary, for risk assessment of topical products and to establish the efficacy of a pharmaceutical formulation, finite dose *in vitro* permeation experiments are performed, meaning that a limited amount of vehicle is applied to the skin to best resemble the expected use conditions (1-5 mg/cm^2 of skin for a solid and up to 10 µl/cm^2 for liquids [21]). Because depletion of the donor

occurs, the cumulative uptake of the investigated substance through a unit of skin surface area tends to a limit [17]. Therefore, when performing finite dose experiments, at the end of the exposure time, the test substance remaining in the *stratum corneum*, the viable skin layers of the skin, and in the vehicle washed off the skin should be assessed as well to measure the total substance disposition and the percentage of recovery [21]. Dermal absorption should be expressed as an absolute amount [µg/cm² of skin surface] and as a percentage of the amount of test substance contained in the intended dose applied per square centimeter of skin surface [22]. The epidermis (except for the *stratum corneum*) and dermis are considered a sink; therefore, the amounts found in these tissues are regarded as absorbed and are added to those found in the receptor fluid. The amounts that are retained by the *stratum corneum* are not considered to be dermally absorbed, and thus they are not expected to contribute to the systemic dose.

A comprehensive picture of the available documents on dermal absorption studies from Europe and the United States was provided by Zsikó *et al*. [3]. These documents promote a harmonized road to conducting dermal and transdermal studies. The Organization for Economic Cooperation and Development (OECD) published several issues on this topic, including the Guidance Notes on Dermal Absorption (No. 156) [23], Test Guidelines 427 (*in vivo* methods) [24], and 428 (*in vitro* methods) [25], and the Guidance Document for the Conduct of Skin Absorption Studies [26]. In addition, there are some other documents such as the World Health Organization International Programme on Chemical Safety (WHO/IPCS) Environmental Health Criteria 235 [27], the opinion of the European Scientific Committee on Consumer Products (SCCP) on basic criteria for the *in vitro* assessment of dermal absorption of cosmetic ingredients [28], the European Centre for Ecotoxicology and Toxicology of Chemicals (ECETOC) Monograph 20 [29], and the United States Environmental Protection Agency (USEPA) report on dermal exposure assessment [30].

3.6.2 Experimental equipment

The tools used to perform *in vitro* permeation studies are called diffusion cells. These cells are usually made of glass and hold three major features 1) a chamber to accommodate the vehicle with the investigated substance (i.e., donor chamber), 2) a membrane through which the substance permeates, and 3) a receptor chamber containing a receptor fluid (also known as receiving phase) in which the compound that has crossed the membrane accumulates [3]. Static and flow-through diffusion cells are available. In a static diffusion cell, the receptor fluid is collected and replaced with a fresh new solution at specific sampling intervals. The donor, the membrane, and the acceptor can be arranged either vertically as in the Franz diffusion [31] cell or horizontally as in the Bronaugh cell [32]. In a flow-through cell, the donor, the membrane, and the acceptor are laid vertically, and the receptor fluid is continuously replaced through the aid of a pump.

In static Franz diffusion cell (FDC), which is the equipment that has been employed for this project, the receptor chamber presents 1) a replacing port trough which fresh new receiving fluid flows, generally from a reservoir contained in a burette; 2) a sampling port from which the old solution flow through pushed by the new phase and finally 3) a circulating water jacket used to thermostat the receiving phase at 37°C and the skin surface at 32 °C

The vehicle containing the compound under investigation can be applied in either infinite dose or finite dose conditions as previously described.

The membrane corresponds to excised human or animal skin, as several studied have proven that the barrier function of the *stratum corneum* is preserved after excision [2]. Excised human tissue (i.e., from reductive mastoplasty, other reductive surgery, or from a cadaver [33]) is considered the gold standard for *in vitro* permeation studies. However, its use is often subject to national and international ethical considerations [21]. Moreover, healthy human tissue is very seldom available in sufficient amounts to perform a consistent number of replicates to obtain data that are informative

and statistically relevant [14]. Numerous animal models have been developed as an alternative to human skin (i.e., primates, porcine, mice, rats, guinea pigs, and snakes [34]). Pig skin, of all models, is usually preferred as it seems to be the closest to human skin according to morphological and functional data. Moreover, it is readably obtained as waste from animal slaughter for food [14], and no approval from the ethics committee is required as the pigs are not slaughtered specifically for the study [35].

The correct composition of the receptor fluid is fundamental to obtaining reliable results from *in vitro* permeation studies. The most preferred receptor fluid is phosphate buffer solution at pH 7.4. A key requirement when performing *in vitro* permeation is that the drug permeation through the skin is not reduced by solubility issues in the receptor fluid, and the highest concentration of the permeant in the receptor fluid should never exceed 10% of its saturation solubility (i.e., sink conditions). Solubilising agents such as bovine serum albumin 5%, ethanol 50%, polyethylene glycol 20 oleyl ether 6% should be employed to increase the compound solubility in the case of lipophilic compounds [9]

A period of sampling of 24 hours is typically required to allow for adequate characterisation of the absorption profile. The frequency of sampling should be chosen adequately to determine the extent/rate of absorption and the absorption profile. Kinetic measurements have to be obtained for at least six post-application time points to be able to estimate the absorption kinetics [22]

3.6.3 *In vitro* release testing

According to the type of membrane placed in between the donor and receptor chambers, FDC is used for either *in vitro* release test (IVRT) or *in vitro* permeation test (IVPT) [3]. IVRT is employed to measure the rate and extent of release of drugs from semisolid dosage form (i.e., creams, gels, and ointments) and liquid suspension [36,37]. As highlighted by both the European Medicine Agency [37] and the United States Food and Drug Administration [38], IVRT is not a measure of bioavailability. It does not reflect *in vivo* performances, but the release rate is a critical quality attribute (CQA) to be specified in the finished product release and shelf-life specification. In addition, the FDA describes IVRT as a valuable test to assess product "sameness" under certain scale-up and post-approval changes for semisolid products. In IVRT, an appropriate inert and synthetic membrane (i.e., polysulfone, cellulose acetate/nitrate mixed ester or polytetrafluoroethylene 70 µm membrane [38] is placed in between the donor and receiving chambers. The membrane must properly separate the product and the receptor medium to avoid dissolution or dispersion of the semisolid into the receptor, it should not bind the active substance, and it should not be rate-limiting to active substance release [37].

3.7 Dermal absorption of essential oil constituents

According to theory, essential oils (EOs) constituents can easily penetrate and permeate through the skin and be dermally absorbed. The distillation process (i.e., hydro or steam distillation) through which EOs are obtained implies that the chemicals forming the EO can only present low molecular weights (i.e., below 300 Daltons) as their boiling points has to be low enough to enable distillation. In addition, all EOs components have good lipophilicity, which, together with the low molecular weight, favours their penetration and permeation through the skin *stratum corneum* and the subsequent dermal absorption. EOs and their components have proved to be promising penetration enhancers which are agents that increase the drug diffusivity through the skin by reducing the barrier resistance of the *stratum corneum* without damaging viable cells [34,39,40]. However, while there are many studies investigating the enhancing effect of monoterpenes and phenylpropanoids on the permeation behaviour of different skin-delivered pharmaceuticals, relatively few publications studied the quantitative dermal absorption and cutaneous accumulation of EO components.

Moreover, several studies that perform such an investigation limit the assessment to infinite dose and occlusive conditions that are not realistic to the real-life scenario [33,41–44]. One of the biggest challenges in using EOs constituents as potential active ingredients in dermal or transdermal formulations is related to their tendency to evaporate, as described by their pretty high vapour pressure values. Especially under in-use conditions with non-occluded systems, their evaporation rate from the vehicle through which they are delivered may significantly compete with the dermal absorption rate, and their skin and systemic bioavailability are likely to be compromised. In 2019 Rafael *et al.* [35] tried to develop models that attempt to predict both the absorption rate through the skin and the evaporative loss under non-occlusive conditions. They experimentally tested, *in vitro*, the evaporation and permeation profile of three fragrance systems (i.e., α-pinene, limonene, and linalool diluted in ethanol) under finite dose conditions and proved that the model describes well the behaviour of the tested fragrance systems. However, the model can only be used as a complementary tool to *in vitro* permeation studies as often the experimental criteria (i.e., vehicle in which the EOs components are diluted) are not in line with those employed to derive the model.

3.8 Analytical approaches to study the dermal absorption profile of essential oils components

The most widely used analytical approaches to determine the quantities of the investigated EO components in the different components of the system at the end of the *in vitro* permeation study (i.e., in the residual vehicle, in the different skin layers if analysed, and the amount present in the receptor fluid) include a conventional solvent extraction technique to isolate the investigated markers from the matrix followed by qualitative and quantitative gas chromatography (GC) analysis or liquid scintillation counting (LSC) when radio labeled markers are available. In the studies of Cal *et al.* [41–43], where the dermal absorption profile of different monoterpenes (i.e., α-pinene, terpinen-4-ol, citronellol, linalool, linalyl acetate, limonene, terpinolene, 1,8 cineole) was studied, both the skin layers and the receptor fluid were first extracted with methanol prior to GC analysis. Similarly, Schmitt *et al*. [45] investigated the *in vitro* permeation and the permeability coefficients of some monoterpenes and phenylpropanoids (i.e., β-myrcene, limonene, α-pinene, β-pinene, linalool, geraniol, citronellol, and isomenthone) and the compound were recovered from the receptor fluid by extraction with n-hexane/ tert-butyl methyl ether (1:1) before GC analysis. In 2005 Brain *et al.* [46] studied the *in vitro* human skin penetration of radio-labeled geranyl nitrile and recovered the investigated analyte from the residual vehicle and the skin layer by extraction with acetonitrile before liquid scintillation counting (LSC). A similar strategy was adopted by Hewitt *et al.*[47] who tested *in vitro* the skin absorption of 56 relevant cosmetic chemicals, including essential oil components such as geraniol, *trans*-cinnamaldehyde, isoeugenol, eugenol, cinnamyl alcohol, and anisyl alcohol.

Relatively fewer studies have adopted solvent-free sample preparation techniques that exploit the volatile nature of EO constituents, which can be online combined with the GC analysis. In 2009, Gabbani *et al*. [33] determined the permeability coefficient of 8 selected terpenes (camphor, carvone, 1,8-cineole, linalool, menthol, α-thujone, menthone, *trans*-anethole) through the reconstructed human epidermis. They sampled and quantified the investigated markers in the receptor phase by Headspace Solid-Phase Micro-Extraction (HS-SPME) online combined with GC-Mass Spectrometry (MS) analysis. They adopted the latter analytical platform for quantifying the investigate makers in the receptor fluid only and not in other compartments of the system as they aimed to determine the permeability coefficient of the investigated markers and not their overall distribution. In 2019 Rafael *et al.* [35] recovered the investigated markers accumulated in the receptor phase by dynamic headspace analysis (DHS) followed by GC analysis. The skin sample was

first extracted with methanol, and the resulting extract was then sampled by DHS-GC analysis to determine the cutaneous accumulation of the investigated markers.

3.9 References

[1] Scientific Committee on Consumer Products SCCP OPINION ON Tea tree oil, (2008). http://ec.europa.eu/health/ph_risk/risk_en.htm (accessed May 11, 2022).

[2] T. Byford, Environmental Health Criteria 235: Dermal Absorption, Int. J. Environ. Stud. 66 (2009) 662–663. https://doi.org/10.1080/00207230802361240.

[3] Zsikó, Csányi, Kovács, Budai-Szűcs, Gácsi, Berkó, Methods to Evaluate Skin Penetration In Vitro, Sci. Pharm. 87 (2019) 19. https://doi.org/10.3390/scipharm87030019.

[4] E.G. Samaras, J.E. Riviere, T. Ghafourian, The effect of formulations and experimental conditions on in vitro human skin permeation—Data from updated EDETOX database, Int. J. Pharm. 434 (2012) 280–291. https://doi.org/10.1016/j.ijpharm.2012.05.012.

[5] HSE - Skin at work: Work-related skin disease – Skin structure and function, (n.d.). https://www.hse.gov.uk/skin/professional/causes/structure.htm (accessed February 21, 2022).

[6] A. Pagliara, M. Reist, S. Geinoz, P.-A. Carrupt, B. Testa, Evaluation and Prediction of Drug Permeation, J. Pharm. Pharmacol. 51 (2010) 1339–1357. https://doi.org/10.1211/0022357991777164.

[7] Robert L. Wilbur, The Difference Between Topical and Transdermal Medications - Gensco Pharma, Gensco Pharma. (2017) 1–2. https://genscopharma.com/difference-topical-transdermal-medications/.

[8] H. Zhai, H.I. Maibach, Effects of Skin Occlusion on Percutaneous Absorption: An Overview, Skin Pharmacol. Physiol. 14 (2001) 1–10. https://doi.org/10.1159/000056328.

[9] D. Selzer, M.M.A. Abdel-Mottaleb, T. Hahn, U.F. Schaefer, D. Neumann, Finite and infinite dosing: Difficulties in measurements, evaluations and predictions, Adv. Drug Deliv. Rev. 65 (2013) 278–294. https://doi.org/10.1016/j.addr.2012.06.010.

[10] B. Desmedt, P. Courselle, J.O. De Beer, V. Rogiers, M. Grosber, E. Deconinck, K. De Paepe, Overview of skin whitening agents with an insight into the illegal cosmetic market in Europe, J. Eur. Acad. Dermatology Venereol. 30 (2016) 943–950. https://doi.org/10.1111/jdv.13595.

[11] J.S. Barbieri, K. Wanat, J. Seykora, Skin: Basic Structure and Function, in: Pathobiol. Hum. Dis., Elsevier, 2014: pp. 1134–1144. https://doi.org/10.1016/B978-0-12-386456-7.03501-2.

[12] L.T. Fox, M. Gerber, J. Du Plessis, J.H. Hamman, Transdermal Drug Delivery Enhancement by Compounds of Natural Origin, Molecules. 16 (2011) 10507–10540. https://doi.org/10.3390/molecules161210507.

[13] J.P. Skelly, V.P. Shah, H.I. Maibach, FDA and AAPS report of the workshop on principles and practices of in vitro percutaneous penetration studies: Relevance to bioavailability and bioequivalence, Pharm. Res. 4 (1987) 265–267. https://doi.org/https://doi.org/10.1023/A:1016428716506.

[14] A.M. Barbero, H.F. Frasch, Pig and guinea pig skin as surrogates for human in vitro penetration studies: A quantitative review, Toxicol. Vitr. 23 (2009) 1–13. https://doi.org/10.1016/j.tiv.2008.10.008.

[15] K. Sugibayashi, ed., Skin Permeation and Disposition of Therapeutic and Cosmeceutical Compounds, Springer Japan, Tokyo, 2017. https://doi.org/10.1007/978-4-431-56526-0.

[16] A. Dal Pozzo, E. Liggeri, C. Delucca, G. Calabrese, Prediction of skin permeation of highly lipophilic compounds; in vitro model with a modified receptor phase, Int. J. Pharm. 70 (1991) 219–223. https://doi.org/10.1016/0378-5173(91)90285-V.

[17] R.H. Guy, Predicting the Rate and Extent of Fragrance Chemical Absorption into and through the Skin, Chem. Res. Toxicol. 23 (2010) 864–870. https://doi.org/10.1021/tx9004105.

[18] S. Mitragotri, M.E. Johnson, D. Blankschtein, R. Langer, An Analysis of the Size Selectivity of Solute Partitioning, Diffusion, and Permeation across Lipid Bilayers, (1999).

[19] B.D. Anderson, P. V Raykar, Solute Structure-Permeability Relationships in Human Stratum Corneum, J. Invest. Dermatol. 93 (1989) 280–286. https://doi.org/10.1111/1523-1747.ep12277592.

[20] R.O. Potts, R.H. Guy, Predicting skin permeability., Pharm. Res. 9 (1992) 663–9. https://doi.org/10.1023/a:1015810312465.

[21] OECD, OECD Guideline for testing of chemicals. Skin Absorption: in vitro Method (427), Test. (2004) 1–8. http://www.oecd-ilibrary.org/docserver/download/9742801e.pdf?expires=1455016488&id=id&accname=guest&checksum=A084AE65CC5B740E047613C22407B0B9.

[22] Scientific Committee on Consumer Safety, Basic criteria for the in vitro assessment of dermal absorption of cosmetic ingredients, Eur. Comm. SCCS/1358 (2010) 1–14. https://doi.org/https://data.europa.eu/doi/10.2772/25843.
[23] H. Buist, P. Craig, I. Dewhurst, S. Hougaard Bennekou, C. Kneuer, K. Machera, C. Pieper, D. Court Marques, G. Guillot, F. Ruffo, A. Chiusolo, Guidance on dermal absorption, EFSA J. 15 (2017). https://doi.org/10.2903/j.efsa.2017.4873.
[24] Test No. 427: Skin Absorption: In Vivo Method, OECD, 2004. https://doi.org/10.1787/9789264071063-en.
[25] Test No. 428: Skin Absorption: In Vitro Method, OECD, 2004. https://doi.org/10.1787/9789264071087-en.
[26] Guidance Document for the Conduct of Skin Absorption Studies, OECD, 2004. https://doi.org/10.1787/9789264078796-en.
[27] J. Kielhorn, S. Melching-Kollmuß, I. Mangelsdorf, Environmental Health Criteria 235 DERMAL ABSORPTION First draft prepared by Drs, (2006).
[28] SCIENTIFIC COMMITTEE ON CONSUMER PRODUCTS (SCCP) Opinion on BASIC CRITERIA FOR THE IN VITRO ASSESSMENT OF DERMAL ABSORPTION OF COSMETIC INGREDIENTS, (n.d.).
[29] Monograph 020 - Percutaneous Absorption - ECETOC, (n.d.). https://www.ecetoc.org/publication/monograph-020-percutaneous-absorption/ (accessed May 10, 2022).
[30] Dermal Exposure Assessment: A Summary of EPA Approaches | Risk Assessment Portal | US EPA, (n.d.). https://cfpub.epa.gov/ncea/risk/recordisplay.cfm?deid=183584 (accessed May 10, 2022).
[31] T.J. Franz, Percutaneous absorption on the relevance of in vitro data, J. Invest. Dermatol. 64 (1975) 190–195. https://doi.org/10.1111/1523-1747.EP12533356.
[32] R.L. Bronaugh' And, R.F. Stewart, Methods for In Vitro Percutaneous Absorption Studies IV: the Flow-Through Diffusion Cell, (1985). https://doi.org/10.1002/jps.2600740117.
[33] S. Gabbanini, E. Lucchi, M. Carli, E. Berlini, A. Minghetti, L. Valgimigli, In vitro evaluation of the permeation through reconstructed human epidermis of essentials oils from cosmetic formulations, J. Pharm. Biomed. Anal. 50 (2009) 370–376. https://doi.org/10.1016/j.jpba.2009.05.018.
[34] A. Herman, A.P. Herman, Essential oils and their constituents as skin penetration enhancer for transdermal drug delivery: a review, J. Pharm. Pharmacol. 67 (2015) 473–485. https://doi.org/10.1111/jphp.12334.
[35] R.N. Almeida, P. Costa, J. Pereira, E. Cassel, A.E. Rodrigues, Evaporation and Permeation of Fragrance Applied to the Skin, Ind. Eng. Chem. Res. 58 (2019) 9644–9650. https://doi.org/10.1021/acs.iecr.9b01004.
[36] A. Olejnik, J. Goscianska, I. Nowak, Active compounds release from semisolid dosage forms, J. Pharm. Sci. 101 (2012) 4032–4045. https://doi.org/10.1002/jps.23289.
[37] E. Medicines Agency, Draft guideline on quality and equivalence of topical products, (n.d.). www.ema.europa.eu/contact (accessed March 31, 2022).
[38] U.S. Department of Health and Human Services, FDA-SUPAC-SS. Guidance for Industry, Non-Sterile Semisolid Dos. Forms. Scale-up Postapproval Chang. Chem. Manuf. Control. Vitr. Release Test. Vivo Bioequivalence Doc. (1997) 19–24. https://www.fda.gov/downloads/drugs/guidances/ucm070930.pdf.
[39] A.C. Williams, B.W. Barry, Essential oils as novel human skin penetration enhancers, Int. J. Pharm. 57 (1989) R7–R9. https://doi.org/10.1016/0378-5173(89)90310-4.
[40] Q. Jiang, Y. Wu, H. Zhang, P. Liu, J. Yao, P. Yao, J. Chen, J. Duan, Development of essential oils as skin permeation enhancers: penetration enhancement effect and mechanism of action, Pharm. Biol. 55 (2017) 1592–1600. https://doi.org/10.1080/13880209.2017.1312464.
[41] K. Cal, Skin Penetration of Terpenes from Essential Oils and Topical Vehicles, Planta Med. 72 (2006) 311–316. https://doi.org/10.1055/s-2005-916230.
[42] K. Cal, S. Janicki, M. Sznitowska, In vitro studies on penetration of terpenes from matrix-type transdermal systems through human skin, Int. J. Pharm. 224 (2001) 81–88. https://doi.org/10.1016/S0378-5173(01)00744-X.
[43] K. Cal, M. Sznitowska, Cutaneous absorption and elimination of three acyclic terpenes—in vitro studies, J. Control. Release. 93 (2003) 369–376. https://doi.org/10.1016/j.jconrel.2003.09.002.

[44] S. Schmitt, U. Schaefer, L. Doebler, J. Reichling, Cooperative Interaction of Monoterpenes and Phenylpropanoids on the in vitro Human Skin Permeation of Complex Composed Essential Oils, Planta Med. 75 (2009) 1381–1385. https://doi.org/10.1055/s-0029-1185744.
[45] S. Schmitt, U. Schaefer, F. Sporer, J. Reichling, Comparative study on the in vitro human skin permeation of monoterpenes and phenylpropanoids applied in rose oil and in form of neat single compounds., Pharmazie. 65 (2010) 102–5. https://doi.org/https://doi.org/10.1691/ph.2010.9716.
[46] K.R. Brain, D.M. Green, J. Lalko, A.M. Api, In-vitro human skin penetration of the fragrance material geranyl nitrile, Toxicol. Vitr. 21 (2007) 133–138. https://doi.org/10.1016/j.tiv.2006.08.005.
[47] N.J. Hewitt, S. Grégoire, R. Cubberley, H. Duplan, J. Eilstein, C. Ellison, C. Lester, E. Fabian, J. Fernandez, C. Géniès, C. Jacques-Jamin, M. Klaric, H. Rothe, I. Sorrell, D. Lange, A. Schepky, Measurement of the penetration of 56 cosmetic relevant chemicals into and through human skin using a standardized protocol, J. Appl. Toxicol. 40 (2020) 403–415. https://doi.org/10.1002/jat.3913.

3.10 Research projects

3.10.1 Tea Tree (*Melaleuca Alternifolia*) Essential Oil: Evaluation of Skin Permeation and Distribution from Topical Formulations with a Solvent-Free Analytical Method

Francesca Capetti[1], Barbara Sgorbini[1*], Cecilia Cagliero[1], Monica Argenziano[1], Roberta Cavalli[1], Luisella Milano[2], Carlo Bicchi[1], Patrizia Rubiolo[1]

Affiliation
[1]Dipartimento di Scienza e Tecnologia del Farmaco, Università degli Studi di Torino, Turin, Italy
[2]Dipartimento di Neuroscienze Rita Levi-Montalcini, Università degli Studi di Torino, Turin, Italy

*Corresponding author
Prof. Dr. Barbara Sgorbini, Dipartimento di Scienza e Tecnologia del Farmaco, Università degli Studi di Torino, Via Pietro Giuria 9, I-10125, Turin, Italy. E-mail: barbara.sgorbini@unito.it. Phone: +39 011 6707135 Fax: +39 011 670

Received: October 18, 2019
Revised: December 29, 2019
Accepted: January 31, 2020

Bibliography
Planta Medica 2020; 86(06): 442-450
DOI: 10.1055/a-1115-4848

3.10.1.1 Abstract

Melaleuca alternifolia essential oil (Tea Tree Oil, TTO) is widely used as an ingredient in skin-care products because of its recognized biological activities. The European Scientific Committee on Consumer Products (SCCP) constantly promotes research and collection of data on both skin distribution and systemic exposure to TTO components after the application of topical formulations. This study quantitatively evaluates permeation, skin-layer distribution (stratum corneum, epidermis and dermis) and release into the surrounding environment of bioactive TTO markers (i.e., α-pinene, β-pinene, α-terpinene, 1,8-cineole, γ-terpinene, 4-terpineol, α-terpineol) when a 5% TTO formulation is applied at a finite dosing regimen. Permeation kinetics were studied *in vitro* on pig-ear skin using conventional static glass Franz diffusion cells and cells ad hoc modified to monitor the release of markers into the atmosphere. Formulation, receiving phases and skin-layers were analyzed using a fully automatic and solvent-free method based on Headspace Solid Phase Microextraction/Gas Chromatography-Mass Spectrometry. This approach affords for the first time to quantify TTO markers in the different skin layers while avoiding using solvents and overcoming the existing methods based on solvent extraction.

The skin-layers contained less than 1% of each TTO marker in total. Only oxygenated terpenes significantly permeated across the skin, while hydrocarbons were only absorbed at trace level. Substantial amounts of markers were released into the atmosphere.

Keywords: *Melaleuca alternifolia*; Mirtaceae; tea tree oil; headspace solid phase microextraction; GC-MS; in vitro permeation kinetics; skin-layer distribution

3.10.1.2 Introduction

Interest in the skin permeation of the volatile bioactive components in topical formulations is constantly increasing, not only from scientists, but also from regulatory authorities and, thereby, industries of the field [1]. This interest has resulted in the 2003 EU directive that sets the no-declaration limits at 10 ppm for leave-on and at 100 ppm for rinse-off products for 24 volatile allergens in perfumes and cosmetics [2]. In 2011, the Scientific Committee on Consumer Safety (SCCS) proposed to extend the list of "established contact allergens in humans" to 54 chemicals and 28 natural extracts [3].

Tea tree essential oil (TTO) is widely used because of its recognized biological activities [4-6], in particular as ingredient in formulations to treat skin diseases, including acne, seborrheic dermatitis [7], scabies [8], and dandruff. It is obtained through steam distillation of the aerial parts of *Melaleuca alternifolia* (Maiden & Betche) Cheel, *Melaleuca dissitiflora* F. Muell. and *Melaleuca linariifolia* Sm. [9] (Myrtaceae family), TTO has been the object of interest from the European Scientific Committee on Consumer Products (SCCP), which remarked that the correct evaluation of both skin distribution and systemic exposure to its markers after treatment with topical formulations is not possible because of the limited number and inadequate nature of TTO dermal-penetration studies [10]. The SCCP thereby hoped that this lack of data on TTO would be quickly resolved, especially because some of its monoterpenoid markers are on the list of allergens updated in 2011 [3].

To the best of the authors' knowledge, only a few studies are available on TTO permeation [11-13], all of them investigating markers accumulated in the skin by solvent extraction. In 2006, Reichling et al. [6], compared several formulations, and studied the permeation of the major TTO component, i.e., 4-terpineol, without measuring its distribution in the skin layers. In 2008, Cross et al. [11] studied the epidermal retention of neat TTO and of a 20% TTO solution in ethanol by submitting skin layers to extraction with acetonitrile. In 2016, Sgorbini *et al.* studied the influence of both the formulation and partition coefficient of TTO bioactive components on their permeation at an "infinite dosing regimen" on pig-ear skin slices in an occluded system to evaluate both their systemic and overall skin bioavailability [14].

The present study reports the results of a project carried out on pig-ear skin slices and aimed to exhaustively investigate the distribution over time of seven bioactive TTO components (α-pinene, β-pinene, α-terpinene, 1,8-cineole, γ-terpinene, 4-terpineol, α-terpineol) in all "compartments" of the *in vitro* system (i.e., receiving phase, skin layers, residual amount in the formulation, amount released into the environment). The study focused on three main steps: 1) the application of a fully automated and solvent-free HS-SPME-GC-MS method to analyse and quantify TTO components in both the receiving phase and skin layers; 2) the evaluation of the distribution of bioactive components in the stratum corneum, epidermis, dermis and receiving phase when a 5% TTO model formulation is applied in a "finite dosing regimen" and in a non-occluded system mimicking the normal use of a topical formulation; and 3) the determination of the loss of TTO volatile bioactive components via spontaneous evaporation using an ad hoc modified static Franz cell to evaluate the "indicative" amount effectively undergoing the permeation process. The method was validated by measuring precision (repeatability and intermediate precision), linearity, LOD and LOQ values.

3.10.1.3 Materials and Methods

Chemicals and samples

Tea tree essential oil (TTO) was supplied by Witt. Its composition, reported in Table 1, complies with the ISO norms [16] and with European Pharmacopoeia [9].

The formulation was a 5% TTO oil/water emulsion, whose components were obtained from Merck-Sigma Aldrich and are reported in **Table 1**.

Table 1: Composition of the topic O/W formulation used for in vitro permeation studies

Component	% in the formulation
Deionized water	84.5
Glycerin	4.6
PEG 400	0.6
Disodium EDTA	0.1
Carbomer 341	0.4
Mineral oil	3.6
Cetyl alcohol	0.2
Triethylamine	0.3
Dimethicone	0.5
Methyl paraben	0.2
Tea Tree (*Melaleuca alternifolia*) essential oil	5.0

Pure α-pinene, β-pinene, α-terpinene, 1,8-cineole, γ-terpinene, 4-terpineol, α-terpineol solvents (acetone, cyclohexane), phosphate saline buffer, sodium dodecyl sulfate and ammonium chloride were obtained from Merck-Sigma Aldrich.

In vitro permeation tests

TTO permeation tests were carried out in agreement with the SCCP guidelines [17] using: 1) conventional static glass Franz diffusion cells to monitor the permeation kinetics and 2) an ad hoc modified static glass Franz diffusion cell to monitor the loss of volatiles into the headspace during the permeation tests (Figure 1). Both cells were magnetically stirred. The study was carried out on pig-ear skin slices, belonging to different individuals, purchased from a local slaughterhouse and isolated with a dermatome (thickness 1 mm). The permeation tests were performed on 12 mg of the formulation ("finite dosing regimen"), at 32°C under constant stirring (1000 rpm). The donor compartment was kept open during the permeation test to mimic everyday use. A phosphate saline buffer 0.05M (pH 5.5) containing sodium dodecyl sulphate 0.1% was selected as the receiving phase, in accordance with previous studies [14, 18]. Generally, the receiving phase is used at physiological pH (7.4) to study transdermal formulations. In this case, a 5.5 pH coherent with the skin value was adopted.

Sampling was carried out at seven different times after the beginning of the experiment; 1, 2, 4, 8, 10, 24, 27 hours. At each time point, the receiving phase (6 mL) was withdrawn and immediately replaced with the same volume of fresh buffer. The stability of the formulation was verified by analysis before and after the *in vitro* test along the whole working period. Each experiment was repeated three times.

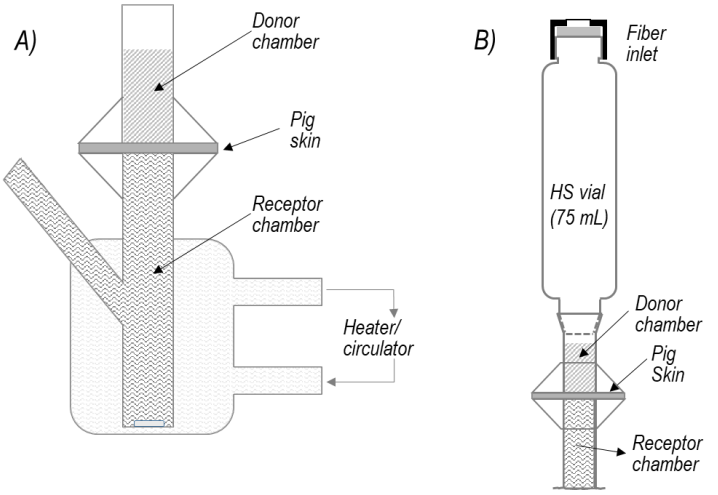

Figure 1, Scheme of the two different types of static Franz diffusion cells used for the in vitro permeation tests: conventional static Franz cells (Figure 1A) and modified static Franz cell (Figure 1B)

Skin layer separation

The *stratum corneum* was completely removed using the tape stripping procedure (25 times) with an adhesive film (Scotch Booktape, 3M).

Skin layers were separated using three different methods: 1) by immersing the skin in 1.8 mL of a 0.22 M ammonium chloride solution (pH = 9.5) for 15 min at room temperature [modified from 19]; 2) via thermal-shock (i.e., immersion of the skin in 1.8 mL of water at 60°C for 30s, immediately followed by cooling in ice at 0°C for 5 min) [19]; and 3) via mechanical separation with a cryostat (Cryostat Leica CM 1900) [19].

SPME fibers

Carboxen/divinylbenzene/PDMS (CAR/DVB/PDMS) SPME fibers were obtained from Supelco Co. and conditioned before use as recommended by the manufacturer. Three fibers were tested by analysing a set of standard solutions, at different concentrations of the target TTO components, in the receiving phase. ANOVA was carried out to confirm the homogeneity of fiber performance and to discard those with different sampling behaviour. The consistency of fiber performance was checked every 50 analyses using an in-fiber external standardization approach and a standard mixture of hydrocarbons (C9-C25) in cyclohexane (1 µL of a 0.1 mg/mL solution) [20,21].

Sampling conditions

Receiving phase: 1.8 mL of the receiving phase withdrawn at each time point and spiked with 3 µL of a 1.0 mg/mL tridecane (C13) solution in acetone, used as an internal standard, was sampled using HS-SPME with a CAR/DVB/PDMS fiber in a 20 mL headspace vial for 30 minutes at 35°C. The components below LOQ/LOD (i.e., α-pinene, β-pinene, α-terpinene and γ-terpinene) were quantified as the total amount involved in the permeation experiment by combining the total receiving phase withdrawn over 27 hours, and sampling 5.6 mL in a 20 mL sealed vial under the above conditions.

Formulation and skin: 5 mg of diluted formulation (1:50 with the same formulation without TTO) and suitable amounts of skin were sampled separately before and after permeation tests by HS-SPME in a 20 mL headspace vial under the above conditions.

Headspace release: seven *in vitro* permeation experiments were carried out separately in the *ad hoc* modified Franz cell. Each experiment was stopped at a different time point (i.e., 1, 2, 4, 8, 10, 24, 27

hours). The TTO markers accumulated in the HS vial at the different times were sampled by HS-SPME and analysed by GC-MS.
Each analysis was repeated three times. Blank runs did not show any carry-over effects.

Analysis conditions

Analyses were carried out using a MPS-2 multipurpose sampler (Gerstel) installed on a Shimadzu 2010 GC unit coupled to a Shimadzu QP2010 Mass spectrometer.
GC conditions: injector temperature: 280°C, injection mode: split; ratio: 1/20; carrier gas: helium; flow rate: 1 mL/min; fiber desorption time: 5 min; column: Mega SE52 (95% polydimethylsiloxane, 5% phenyl) 25 m×0.25 mm dc×0.25 µm df, from MEGA. Temperature program: from 50°C (1 min) to 125°C (0 min) at 3°C/min, then to 250°C (5 min) at 20°C/min.
MSD conditions: MS operated in EI mode (70 eV), scan range: 35-350 amu; dwell time: 40 ms, ion-source temperature: 230°C; quadrupole temperature: 150°C; transfer line temperature: 280°C. Marker compounds were identified by comparing their mass spectra and linear retention indices to those of authentic standards.

Quantitation

Receiving phase quantitation: a stock standard mixture of the markers to be quantified was prepared at 0.2 mg/mL of each pure standard in receiving phase. Suitably diluted solutions of the stock standard mixture were then prepared and renewed weekly. The resulting solutions (both stock and diluted) were stored at 4°C. Calibration curves were built up by analysing, in triplicate, 1.8 mL of nine diluted mixtures in the 0.5-100 µg/mL concentration ranges using HS-SPME-GC-MS under the conditions reported above.
The calibration curves of α-pinene, β-pinene, α-terpinene and γ-terpinene were built up by analysing, in triplicate, 5.6 mL of nine diluted mixtures in the 0.9-9 µg/mL concentration range using HS-SPME-GC-MS under the above conditions.
Formulation and skin quantitation: a stock standard mixture of each TTO marker was prepared in cyclohexane at a concentration of 10 mg/mL. Suitably diluted solutions of the stock standard mixture were then prepared and renewed weekly and stored at 4°C. Calibration curves were built by analyzing, in triplicate, nine diluted mixtures in the 5 µg/mL-10 mg/mL concentration range using HS-SPME-GC-MS in multiple headspace extraction (MHE) mode under the above conditions.

Method validation

Method validation was run on a six-week protocol, over six-months; the following parameters were characterized: precision, linearity, Limit of Detection (LOD) and Limit of Quantitation (LOQ). Repeatability was evaluated via the HS-SPME-GC-MS analyses of one of the calibration levels in the receiving phase five times, over five consecutive days. Intermediate precision (inter-week precision) was measured on the internal standard contained in 1.8 mL of receiving phase at a concentration of 1.7 µg/mL once a week, over six months. Linearity was assessed using linear-regression analyses within the working range, over at least nine different concentration levels.
The Limit of Quantification (LOQ) was experimentally determined by analyzing decreasing concentrations of TTO in the receiving phase, and in the formulation, using HS-SPME-GC-MS. LOQ was the lowest concentration for which the instrumental response integration reported an RSD% below 20% across replicate analyses. The LOD of each analyte was calculated from the average "peak to peak" noise values sampled in its region of elution in the chromatogram, with a coverage factor of 3. Each analysis was repeated three times.

3.10.1.4 Results and discussion

A list of the TTO markers is reported in **Table 2,** together with their partition coefficients (Log P), vapour pressures, the selected diagnostic ions used for their quantitation and their abundance (normalized relative % area) in the investigated essential oil.

Table 2, List of the TTO markers together with their partition coefficients (Log P) and vapour pressure values, the selected diagnostic ions used for their quantitation and their abundance in the investigated essential oil (expressed as relative % area).

Compounds	m/z	Log P*	Vapour pressure (mm Hg)*	Area %
α-pinene	93	4.37	4.75	4.9
β-pinene	93	4.16	2.93	0.3
1,8-cineole	43	2.82	1.56	5.2
α-terpinene	93	4.25	1.67	7.1
γ-terpinene	93	4.36	1.65	16.4
4-terpineol	71	2.99	0.0427	41.9
α-terpineol	59	2.79	0.0196	7.0

* Episuite database

In quantitative terms, TTO markers permeated in the receiving phase during the *in vitro* permeation tests can be divided into two groups: i) those present above their LOD/LOQ (4-terpineol, α-terpineol, 1,8-cineole) that were therefore quantified in each aliquot at each time, and ii) those present below their LOD/LOQ (α-pinene, β-pinene, α-terpinene, γ-terpinene) that were quantified as total amounts over the 27 hours as combined aliquots.

Two different types of static Franz diffusion cells were used for the *in vitro* permeation tests (Figure 1). Conventional static Franz cells (Figure 1A) were adopted to evaluate both the TTO components that permeated and distributed in ear pig skin layers (area surface 2.54 cm2); the donor compartment was kept open to mimic everyday use. Moreover, the static Franz cell was modified (Figure 1B) to measure the amounts of components vaporized during the permeation tests. The modified static Franz cell included a hermetically sealed glass vessel (75 mL) connected on-line to a donor compartment to collect the TTO components released by the formulation (i.e., the component(s) released into the environment during everyday use). The size of the glass vessel (75 mL) was selected to achieve the best compromise between a correct headspace/donor compartment ratio (data not shown) and a satisfactory analytical sensitivity.

Stratum corneum was removed from the skin after each in vitro permeation study using the tape stripping approach. An average of 25 adhesive strips were used to ensure its complete elimination. The removed *stratum corneum* was then submitted to HS-SPME-GC-MS analysis to evaluate the presence of TTO markers. The *stratum corneum* headspace only contained α-pinene at trace levels, although, in any case, below its LOQ.

Three approaches were investigated to split dermis from epidermis: the cryostat method was preferred as reference method because it provided well-separated skin layers ready for a direct HS sampling. The resulting epidermis/dermis ratio was around 1:30, deriving from the average weight of epidermis (6.7±1.5 mg) and dermis (189±45.5 mg).

The thermal shock method provided quite satisfactory results with relatively low TTO-marker losses (i.e., below 15%) while the ammonium chloride method was abandoned because of the high solubility of 4-terpineol and α-terpineol resulting in losses above 70 and 50 % respectively.
The amount of each TTO marker permeating into the receiving phase (expressed as μg/cm²) was quantitatively determined by HS-SPME-GC-MS with external standard calibration. The different calibration levels were directly prepared in an appropriate volume of receiving phase to overcome the matrix effect. **Table 3** reports the linearity range, the equations of the calibration curves and the correlation coefficients (r) of each quantifiable marker.

Table 3, Linearity range, equations of the calibration curves and correlation coefficients (r) for 1,8-cineole, 4-terpineol and α-terpineol.

Compound	linearity range (µg/mL)	slope	intercept	r	LOQ (µg/mL)	LOD (µg/mL)
1,8 cineole	0.1-1.0	1.28E-01	7.10E-03	0.9918	0.0034	0.0010
	2.5-75.0	4.19E-02	1.05E-01	0.9993		
4-terpineol	0.1-1.0	5.39E-02	-8.00E-04	0.9996	0.0174	0.0053
	2.5-75.0	3.58E-02	4.35E-02	0.9996		
α-terpineol	0.3-1.5	1.45E-02	9.00E-04	0.9990	0.0540	0.0164
	3.1-46.3	1.75E-02	-1.59E-02	0.9988		
Compound	**linearity range (ng/mL)**	**slope**	**intercept**	**r**	**LOQ (ng/mL)**	**LOD (ng/mL)**
α-pinene	0.9-9	8.98E+04	-4.39E+03	0.9932	0.45	0.14
β-pinene	0.9-9	8.19E+04	-1.11E+03	0.9952	0.48	0.15
α-terpinene	0.9-9	3.86E+04	-9.51E+03	0.9948	0.65	0.20
γ-terpinene	0.9-9	8.49E+04	-2.02E+03	0.9969	0.33	0.10

The most permeated compounds were oxygenated monoterpenes: 4-terpineol, α-terpineol and 1,8-cineole. **Figure 2** reports the *in vitro* kinetic permeation profiles obtained for 4-terpineol and α-terpineol (Figure 2A), and 1,8-cineole (Figure 2B), by applying zero-order kinetics (i.e., cumulative amount per unit surface area (µg/cm²) plotted versus time).

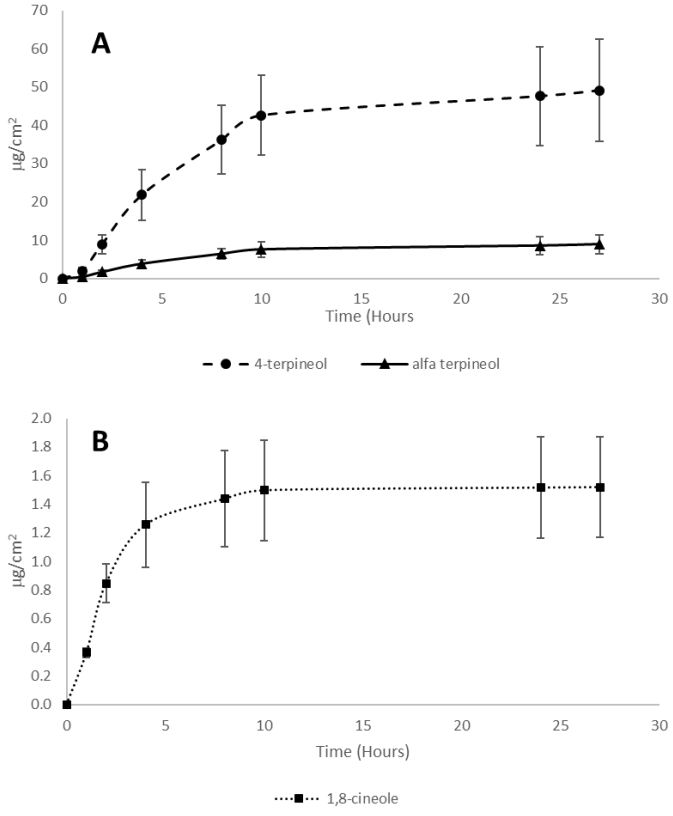

Figure 2 In vitro kinetic permeation profiles for 4-terpineol and α-terpineol (Figure 2A) and 1,8-cineole (Figure 2B), obtained by applying a zero-order kinetics (i.e., cumulative amount per unit surface area (µg/cm2) plotted versus time).

The reported data derive from twelve *in vitro* permeation tests carried out using skin samples belonging to different pig individuals. Kinetics are similar for all the oxygenated markers, although permeation rates differed quantitatively. The amounts over 27 hours were 49.1 µg/cm² for 4-terpineol, 8.90 µg/cm² for α-terpineol and 3.85 µg/cm² for 1,8-cineole. The kinetic permeation data

of the other TTO markers (i.e., α-pinene, β-pinene, α-terpinene, γ-terpinene) could not be measured because of the very low amounts permeated at each time. These amounts were below their LOD and LOQs, probably because of their high hydrophobicity. The total permeated amount of these components was measured over the entire *in vitro* permeation test, by quantifying them in an appropriate volume of the receiving phases collected over 27 hours combined (i.e., 5.6 mL). **Table 3** reports the calibration-curve equations and correlation coefficients (r) for α-pinene, β-pinene, α-terpinene and γ-terpinene. The total amount of permeated hydrocarbons was far lower than that of oxygenated monoterpenes, ranging from 0.0063 for β-pinene to 0.017 μg/cm^2 for α-pinene.

The higher permeation rate of the oxygenated compounds compared to that of the hydrocarbons is probably due to their higher relative abundance in the formulation (and in the TTO), and their better compatibility with the receiving phase (lower logP values). Conversely, the lower hydrocarbon permeation may also be due to their relatively high volatility responsible for a significant release from the formulation to the surrounding environment.

The amounts of TTO markers retained by the total skin, and by epidermis and dermis, were quantified by HS-SPME-GC-MS using the Multiple Headspace Extraction (MHE) approach [15 and references cited therein], which affords to bypass the strong skin matrix effect. **Table 4** reports the regression equations of the calibration curves, the linearity range and the correlation coefficient for each quantified component.

Table 5 reports the average total amount (expressed as μg) of each TTO marker in whole skin and in the epidermis and dermis, separated using the cryostat method.

Table 4 Regression equations of the calibration curves, linearity range, correlation coefficient for each quantified component obtained by HS-SPME-GC-MS with the Multiple Headspace Extraction approach.

Compound	linearity range (μg)	slope	intercept	r	LOQ (μg)	LOD (μg)
α-pinene	**10 -1.0**	1.00E+08	-8.00E+07	0.993	0.0025	0.0008
	0.50-0.05	3.00E+07	-7.99E+05	0.999		
	0.05-0.005	8.00E+06	7.18E+04	0.997		
β-pinene	**5.0 - 0.5**	3.00E+07	-5.00E+06	1.000	0.0020	0.0006
	0.50 - 0.05	2.00E+07	-4.65E+05	0.998		
	0.05-0.005	5.00E+06	65456	0.9963		
α-terpinene	**10.0 - 1.0**	8.00E+06	2.00E+06	0.991	0.0012	0.0004
	0.50 - 0.05	6.00E+06	-5.18E+04	0.987		
	0.05 - 0.005	2.00E+06	2.15E+04	0.997		
1,8-cineole	**5.0 - 0.05**	2.00E+07	-5.84E+05	1.000	0.0010	0.0003
	0.01 - 0.001	9.00E+06	7.61E+04	0.984		
γ-terpinene	**5.0 - 0.1**	2.00E+07	7.16E+05	0.999	0.0008	0.0002
	0.01 - 0.001	1.00E+07	1.76E+04	0.999		
4-terpineol	**5.0 - 0.5**	2.00E+07	1.00E+06	1.000	0.0016	0.0005
	0.5 - 0.05	3.00E+07	-3.18E+05	1.000		
	0.05-0.005	2.00E+07	7.00E+00	1.000		
α-terpineol	**3.0 - 0.01**	2.00E+07	-2.87E+05	1.000	0.0050	0.0015

In general, all TTO compounds were retained by the (whole) skin, although each one to a different extent; ranging from 0.031 μg for β-pinene and 1.3 μg for 4-terpineol. The two separated layers (epidermis and dermis) retained all TTO markers with the exception of β-pinene, which was exclusively found in the dermis (0.043 μg). Moreover, the absolute amounts of TTO components were found to be much higher in the dermis than in the epidermis, with a dermis/epidermis ratio corresponding to 7 for α-pinene and 1,8-cineole, about 30 for γ-terpinene, 4-terpineol and α-terpineol, and 170 for α-terpinene. The greater accumulation in the dermis is probably due to its higher abundance compared to epidermis (about 1:30 w/w). When the content of TTO markers is normalized to the weight of the skin-layer, the distribution between epidermis and dermis was comparable, in particular for γ-terpinene, 4-terpineol and α-terpineol dermis/epidermis ratio ranging from 0.8 to 1.3. Epidermis contained four-times more α-pinene and 1,8-cineole than dermis, while dermis accumulated more α-terpinene than epidermis (dermis/epidermis ratio of about 5).
Figure 3 shows the marker % distribution in each compartment (i.e., receiving phase, epidermis, dermis and headspace/ambient, residual formulation after the permeation test) in relation to their lipophilicity and volatility. TTO components were almost absent in the residual formulation after the permeation experiment, from, as expected, since it was applied at a finite dosing regimen in a non-occluded system.

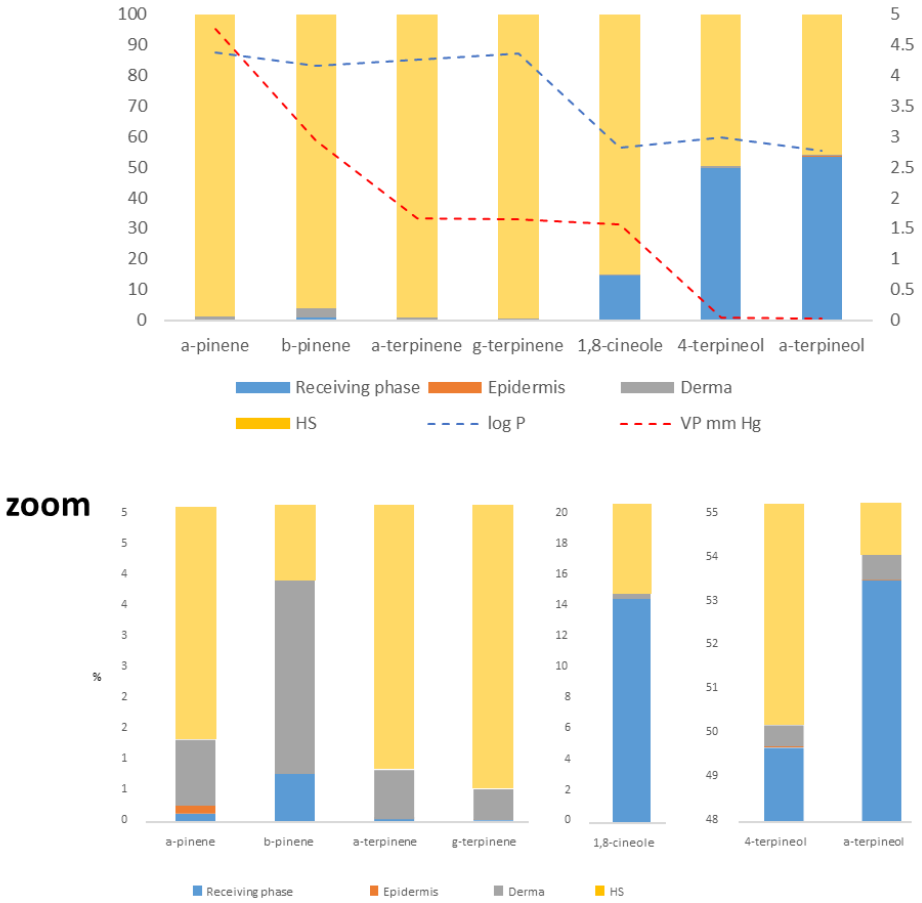

Figure 3 Marker % distribution in each compartment (i.e., receiving phase, epidermis, dermis and headspace/ambient, residual formulation after permeation test) related to lipophilicity (logP) and volatility (VP).

TTO markers were retained in the skin layers in very low percentages, in general below 1%.
Hydrocarbons were poorly retained (always around 1%) and transferred to the receiving phases (always below 0.2% with the exception of β-pinene, 0.8%). Conversely, oxygenated compounds were transferred into the receiving phase at a high rate, ranging from about 12% for 1,8 cineole to about 50% of the total content for 4-terpineol and α-terpineol. The distribution of TTO markers was in good agreement with their physicochemical characteristics.
When working with volatiles, the evaluation of their release/loss into the surrounding environment during an in vitro test performed in a non-occluded system is a useful way to define the effective quantities involved in the permeation process. The headspace amount is conditioned by two simultaneous equilibria: i) the release of formulation components into the headspace; and ii) their permeation through the skin into the receiving phase.
TTO markers behaved differently depending on their polarity and volatility (vapour pressure).
The highest percentage of oxygenated compounds (i.e., 1,8-cineole, 4-terpineol, α-terpineol) was released into the headspace within the first hour These results confirmed the data observed in the *in vitro* permeation kinetic studies (**Table 5**). They are in agreement with those obtained with the mass balance, i.e., the summed amount of each analyte present in the skin layers, in the receiving phase and the residue in the formulation. **Figure 4** shows the percentage distribution of the oxygenated components in the three systems involved in the *in vitro* study: headspace, formulation and receiving phase. 4-Terpineol and α-terpineol behave similarly as about 40-45% was released into the headspace. The value for 1,8-cineole was about 90% likely because of its relatively high volatility (1,8-cineole vapor pressure is about 30 times higher than that of 4-terpineol). After 2 hours, the release decreased, most probably because the equilibrium between formulation/ receiving phase became predominant. This equilibrium becomes prevalent in this closed system, possibly due

to the relatively high water solubility of TTO oxygenated compounds inducing their redistribution accordingly.
The opposite is true for hydrocarbons (i.e., α- and β-pinene, α- and γ-terpinene), which are highly hydrophobic and whose percentages of release into the headspace were constant over the entire experiment (i.e. 27 hours), indicating a prevalent formulation/headspace equilibrium. The results show that about 80% of the hydrocarbons was already released in the headspace after the first hour, and the remaining 20% was in the formulation. The hydrocarbons were not quantifiable in the receiving phases at this time because below the LOD/LOQ of the method.
The optimized HS-SPME-GC-MS method was validated by its precision (repeatability and intermediate precision), linearity, regression equation error, LOD and LOQ.
The method showed very good precision (repeatability), as the average RSD% for each TTO marker was always below 5.8%. The intermediate precision was equally satisfactory with the RSD% calculated on the internal standard (in the receiving phase for 143 analyses within a timeframe of six months) never exceeding 13.6%.
Tables 2 and **3** report the LOD and LOQ values for all TTO markers, determined in HS-SPME-GC-MS and MHE-SPME-GC-MS. In the former case, the LOD values ranged from 0.1 ng/mL for γ-terpinene to 16.4 ng/mL for α-terpineol, and the LOQs varied from 0.33 ng/mL to 54.0 ng/mL respectively. In the latter case (MHE mode), the LOD values ranged from 0.2 ng for γ-terpinene to 1.5 ng for α-terpineol, while the LOQs ranged from 0.8 ng to 5.0 ng, respectively
In summary, these results show that the *in vitro* permeation kinetics and distribution of TTO bioactive markers in a model formulation and at a finite dosing regimen can be monitored with a fully automated solvent-free method.
To the best of the authors' knowledge, this is the first time that: 1) a solvent-free method has been applied to monitor quantitatively the distribution of TTO components in skin layers, and their residual amounts in the formulation in an *in vitro* permeation test; 2) a modified static Franz cell has been used to evaluate the evaporation of TTO components from the formulation during the permeation process. The method has shown itself to be highly reliable and sensitive for permeation experiments, demonstrating high repeatability and intermediate precision.
The permeation results indicated that TTO component behaviour changed as a function of chemical structure; hydrocarbons did not pass the skin barrier (or only as traces), while oxygenated compounds permeated at percentages ranging from 12% (1,8-cineole) to 53.3% (α-terpineol).
This model study allows to evaluate for the first time the effect of the skin barrier on the permeation of volatile bioactive compounds of differing nature in a topical formulation, while also determining the true amount(s) of each that: 1) overcome the natural protective barrier (whole skin, its separated layers and pH) and; 2) can potentially be absorbed, and/or lost because of evaporation.
More generally, these model studies provide data useful to design topical formulations containing volatile bioactive compounds in amounts not only sufficient for their biological activity, but also within the limits fixed by regulatory authorities.

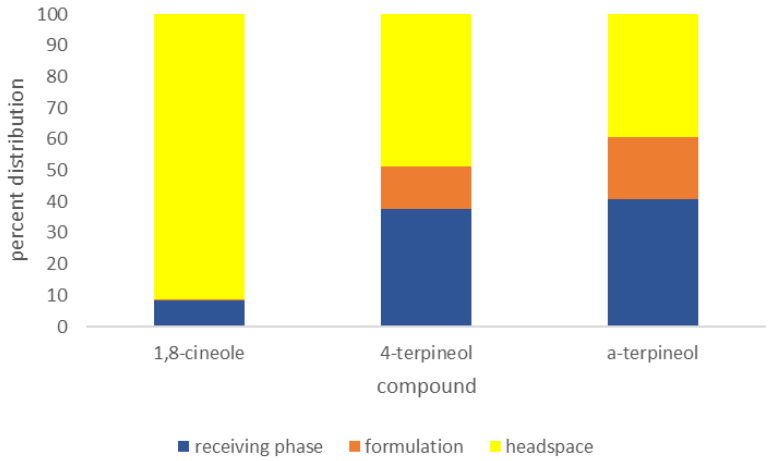

Figure 4 Percentage distribution of oxygenated components in the three systems in the in vitro study (i.e., headspace, formulation, receiving phase).

Table 5 Average total amount (expressed as µg) of each TTO marker in whole skin and in epidermis and dermis separated with the cryostat method, in receiving phase, in the remaining formulation after the in vitro permeation test and in the surrounding environment.

	α-pinene			β-pinene			α-terpinene			1,8-cineole			γ-terpinene			4-terpineol			α-terpineol		
Total amount in formulation (µg)	29.1			2.0			42.3			31.1			98.5			251			42.2		
	µg	σ	**% of the total**	µg	σ	**% of the total**	µg	σ	**% of the total**	µg	σ	**% of the total**	µg	σ	**% of the total**	µg	σ	**% of the total**	µg	σ	**% of the total**
Epidermis	0.042	0.007	**0.14**	< LOD		**-**	< LOD			0.013	0.007	**0.04**	0.016	0.002	**0.01**	0.035	0.003	**0.01**	0.012	0.002	**0.03**
Dermis	0.311	0.122	**1.07**	0.031	0.008	**1.55**	0.344	0.072	**0.80**	0.089	0.068	**0.29**	0.501	0.085	**0.51**	1.260	0.452	**0.50**	0.263	0.053	**0.62**
Total skin*	0.353	0.129	**1.21**	0.031	0.008	**1.55**	0.346	0.075	**0.82**	0.102	0.075	**0.33**	0.517	0.087	**0.52**	1.295	0.455	**0.51**	0.275	0.055	0.65
Receiving phase	0.042	0.008	**0.14**	0.016	0.005	**0.80**	0.027	0.004	**0.06**	3.85	0.89	**12.39**	0.031	0.005	**0.03**	124.80	33.83	**49.68**	22.61	6.45	**53.50**
Remaining amount in formulation	0.200	0.031	**0.69**	0.016	0.001	**0.80**	0.061	0.006	**0.14**	0.000	0.000	**0.00**	0.072	0.013	**0.07**	0.034	0.015	**0.01**	0.016	0.005	**0.04**

3.10.1.5 References

[1] World Health Organization. International Programme on Chemical Safety (IPCS). Dermal exposure. 2014

[2] Directive 2003/15/Ec of The European Parliament and of the Council of 27 February 2003

[3] Scientific Committee on Consumer Safety. Opinion on Fragrance allergens in cosmetic products. 2011 [May 1st, 2016]

[4] Carson CF, Hammer KA, Rileya TV. Melaleuca alternifolia (tea tree) oil: a review of antimicrobial and other medicinal properties. Clin Microbiol Rev 2006; 19: 50-62.

[5] Hammer KA, Carson CF, Rileya TV. Effect of Melaleuca alternifolia (tea tree) essential oil and the major component terpinen-4-ol on the development of single – and multistep antibiotic resistance and antimicrobial susceptibility. Antimicrob Agents Chemother 2012; 56: 909-915

[6] Reichling J, Landvatter U, Wagner H, Kostka KH. U.F. Schaefer, In vitro studies on release and human skin permeation of Australian tea tree oil (TTO) from topical formulations. Eur J Pharm Biopharm 2006; 64: 222-228

[7] Pazyar N, Yaghoobi R, Bagherani N, Kazerouni A. A review of applications of tea tree oil in dermatology. Int J Dermatol 2013; 52: 784-790

[8] Thomas J, Carson CF, Peterson GM, Walton SF, Hammer KA, Naunton M, Davey RC, Spelman T, Dettwiller P, Kyle G, Cooper GM, Baby KE. Therapeutic potential of Tea Tree Oil for scabies. Am J Trop Med Hyg 2016; 94: 258-266

[9] European Pharmacopoeia, 8th Edition, 2016

[10] SCCP Opinion on Tea Tree Oil, 2008, European Commission – Health and Consumer Protection Directorate General, SCCP/1155/08

[11] Cross SE, Russell M, Southwell I, Roberts MS. Human skin penetration of the major components of Australian tea tree oil applied in its pure form and as a 20% solution in vitro. Eur J Pharm Biopharm 2008; 69: 214-222

[12] Sinha P, Srivastava S, Mishra N, Kumar Singh D, Luqman S, Chanda D, Prasad YadavaSinh N. Development, optimization, and characterization of a novel tea tree oil nanogel using response surface methodology. Ind Pharm 2016; 42: 1434-1445

[13] Dong L, Liu C, Cun D, Fang L. The effect of rheological behavior and microstructure of the emulgels on the release and permeation profiles of Terpinen-4-ol. Eur J Pharm Biopharm 2015; 78: 140-150

[14] Sgorbini B, Cagliero C, Argenziano M, Cavalli R, Bicchi C, Rubiolo P. In vitro release and permeation kinetics of Melaleuca alternifolia (tea tree) essential oil bioactive compounds from topical formulations. Flav Fragr J 2017; 32: 354-361

[15] Sgorbini B, Bicchi C, Cagliero C, Cordero C, Liberto E, Rubiolo P. Herbs and spices: Characterization and quantitation of biologically-active markers for routine quality control by multiple headspace solid-phase microextraction combined with separative or non-separative analysis. J Chromatogr A 2015; 1376: 9-17

[16] ISO norm 4730:2017, Essential oil of melaleuca, terpinen-4-ol type (tea tree oil)

[17] Basic criteria for the in vitro assessment of dermal absorption of cosmetic ingredients - updated March 2006, Scientific Committee On Consumer Products

[18] Argenziano M, Haimhoffer A, Bastiancich C, Jicsinszky L, Caldera F, Trotta F. In vitro enhanced skin permeation and retention of imiquimod loaded in β-cyclodextrin nanosponge hydrogel. Pharmaceutics 2019; 11: 138

[19] Wilkinson DI, Walsh JT. Effect of various methods of epidermal-dermal separation on the distribution of 14c-acetate-labeled polyunsaturated fatty acids in skin compartments. J Investig Dermatol 1974; 62: 517–521

[20] Wang Y, O'Reilly J, Chen Y, Pawliszyn J. Equilibrium in-fibre standardisation technique for solid-phase microextraction. J Chromatogr A 2005; 1072: 13-17

[21] Bicchi C, Cordero C, Liberto E, Sgorbini B, Rubiolo P. Reliability of fibres in Solid Phase Microextraction for routine analysis of the headspace of aromatic and medicinal plants. J Chromatogr A 2007; 1152: 138-149

3.10.2 Investigation of the Dermal Absorption Profile of Tyrosinase Inhibitors Released from Topical Formulations Containing a Bioactive Mixture of Three Essential Oils: *Litsea Cubeba* (Lour.) Pers, *Pinus Mugo* Turra, *Cymbopogon Winterianus* Jowitt Ex Bor

Francesca Capetti[1], Barbara Sgorbini[1*], Cecilia Cagliero[1], Monica Argenziano[1], Roberta Cavalli[1], Carlo Bicchi[1], Patrizia Rubiolo[1]

Affiliation
[1]Dipartimento di Scienza e Tecnologia del Farmaco, Università degli Studi di Torino, Turin, Italy

*Corresponding author
Prof. Dr. Barbara Sgorbini, Dipartimento di Scienza e Tecnologia del Farmaco, Università degli Studi di Torino, Via Pietro Giuria 9, I-10125, Turin, Italy. E-mail: barbara.sgorbini@unito.it. Phone: +39 011 6707135 Fax: +39 011 670

In submission to Planta Medica

3.10.2.1 Abstract

Tyrosinase is the key enzyme in the biosynthesis of melanin pigments, and its downregulation is a general approach to treating hyperpigmentation disorders. In human skin, tyrosinase is contained within melanocytes which are dendritic cells located in the epidermis basal cell layer (i.e., *the stratum germinativum*). This study investigated the potential tyrosinase inhibitory activity of a mixture of three essential oils (EOs) (i.e., *Litsea cubeba* (Lour.) Pers, *Pinus mugo* Turra, *Cymbopogon winterianus* Jowitt ex Bor EOs). It evaluated the dermal absorption profile of the mixture bioactive constituents to establish whether their achievable concentration in the viable skin is sufficient to determine a discrete tyrosinase inhibition. The biological activity of the mixture was assessed *in vitro* using a colorimetric readout-based enzyme assay. *In vitro* release studies on static glass Franz diffusion were performed to select the optimal dermatological vehicle displaying the best compound release rate while minimising their evaporative loss. The dermal absorption profile of the active compounds was also investigated *in vitro* on a static glass Franz diffusion cell using pig-ear skin. The dermatological vehicles both containing the EO mixture at a concentration of 5% were tested under non-occlusive and semi-occlusive conditions. The results suggest that by employing an oil/water emulsion as a vehicle and under semi-occlusive conditions, the achievable concentration of the bioactive markers in the viable skin is very likely to be sufficient to significantly inhibit tyrosinase and reduce hyperpigmentation.

3.10.2.2 Introduction

Tyrosinase, being a key enzyme in the biosynthesis of melanin pigments, is a widespread target to be downregulated in order to reduce excessive melanin production and to avoid typical aging-related skin disorders [1]. For this reason, the research for tyrosinase inhibitors as skin-whitening agents has a particular impact in the cosmetic field, not only in terms of single molecules but also as mixtures of bioactive compounds. Essential oils (EOs) are complex mixtures of potentially bioactive compounds, mainly belonging to the terpenoid group. Among the limited number of investigated terpenoids able to inhibit tyrosinase, citral (i.e., neral and geranial) and β-myrcene have been proven to block the enzymatic activity of mushroom tyrosinase [2,3].

Citral is a fragrance ingredient characteristic of different EOs, including lemon balm, citronella, verbena, and litsea [4]. In 2021, Capetti *et al*. evaluated the possible synergistic and/or additive effect of the above EOs minor compounds on citral activity by using a bioassay-guided fractionation approach [2]. The study demonstrates the advantages of using mixtures of compounds/essential oils rather than individual molecules and highlights the additive and synergic effect of β-myrcene and citronellal on citral inhibitory activity, respectively.

Despite Citral being listed among the 26 fragrance substances introduced into Annex III of the Cosmetics Directive by the 7th amendment (2003/15/EC) based on the SCCNFP opinion (SCCNFP/0017/98) it can be used safely to formulate topic formulation at a level not expected to induce skin sensitization, as evident from the several products with EOs containing citral commercially-available.

The aim of this work is the evaluation of two different formulations (an oil/water emulsion and an oil solution) containing a mixture of EOs (i.e., *Litsea cubeba*, *Pinus mugo*, *Cymbopogon winterianus*) applied to the skin both in a non-occlusive and partially occlusive application. The study investigates the dermal delivery amount of citral, and other EO bioactive compounds (β-myrcene, citronellal) in the function of the type of formulation and of the application adopted.

Origin and chemical characterization of the employed essential oils

Litsea cubeba (Lour.) Pers, *Pinus mugo* Turra, *Cymbopogon winterianus* Jowitt ex Bor EOs were obtained by steam distillation and supplied by Erboristeria Magentina, Poirino, Italy. A mixture of 45% of *L. cubeba* EO, 45 % of *P. mugo* EO and 10 % *C. winterianus* EO was prepared by mixing a suitable amount of each component. The chemical composition of the essential oils used to prepare the mixture and that of the mixture itself were determined by GC-MS, analysing 5 mg/mL solutions in cyclohexane of each sample. The absolute amount of citronellal, geranial (i.e., *trans*-citral), β-myrcene, neral (i.e., *cis*-citral) in the EO mixture was assessed using the multilevel external calibration method. Pure standards of citronellal, geranial, β-myrcene, neral as well as cyclohexane and acetone solvents were provided by Merck, Darmstadt, Germany. A stock solution containing all the above-mentioned markers at a concentration of 10 mg/mL was prepared in cyclohexane. Suitable calibration levels spanning the range 5.0 – 0.01 mg/mL were prepared from the stock solution and analysed by GC-MS.

Analyses were carried out on a MPS-2 multipurpose sampler (Gerstel, Mülheim a/d Ruhr, Germany) installed on a Shimadzu GC-FID-MS system consisting of a Shimadzu GC 2010 system, equipped with FID, in parallel with a Shimadzu QP2010-PLUS GC–MS mass spectrometer (Shimadzu, Milan, Italy). A narrow bore MEGA-5 95% methyl-polysiloxane 5%-phenyl (MEGA, Legnano, MI, Italy) column was employed. Column geometry was the following 15 m × 0.18 mm dc, 0.18 µm df.

Analyses were carried out in triplicate under the following conditions. Temperatures: injector: 250°C, transfer line: 270°C, ion source: 200°C; carrier gas: He; flow control mode: constant linear velocity; flow rate: 0.72 mL min^{-1}; injection mode: split; split ratio: 1:20. The MS was operated in electron ionisation mode (EI) at 70 eV, scan rate: 666 u/s, mass range: 35–350 m/z. Temperature program: 50°C (30 s) //7.2°C/min// 250°C (2 min). The chromatographic conditions for the narrow bore columns were obtained by translating the method parameters through the Agilent method translator software [5]. Identification was performed via comparisons of linear retention indices and mass spectra either with those of authentic standards or with data stored in commercial [6] and in-house libraries.

Data was processed with the ChemStation Version E.02.02.1431 data processing system (Agilent Technologies, Santa Clara, CA).

Tyrosinase inhibitory activity of the essential oils and corresponding mixture

The tyrosinase inhibitory activities of the EOs and the resulting mixture were investigated *in vitro* using a colorimetric readout-based enzyme assay that was optimised in our previous work [2]. Mushroom tyrosinase from *Agaricus bisporus* (J.E. Lange) Imbach and kojic acid as positive control inhibitor were selected for this study. Photo-spectroscopy measurements were performed on a Thermo Spectronic Genesys 6. The solutions of the investigated essential oils and mixture were prepared in DMSO at a concentration of 50 mg/mL. The mushroom tyrosinase solution 200 U/ml (27.9 µg/mL) was prepared in sodium phosphate buffer (pH 6.8), and aliquots of 9 ml were stored at -18 °C and thawed just before the assays. Tyrosine solution 0.1 mg/ml was prepared in sodium phosphate buffer (pH 6.8) and renewed daily. The reaction mixture components were placed in the vial in the following order: 1 ml of mushroom tyrosinase solution 200 U/ml; 1 mL of sodium phosphate buffer solution; 10 µl of EO mixture, kojic acid solution, and, finally, 1 ml of tyrosine solution 0.1 mg/ml. The final DMSO percentage in the reaction mixture was 0.3 %, while the final EOs/ mixture concentration in the reaction mixture was 166.7 µg/mL. The assays were performed in sealed 4 ml vials to avoid the loss of any EO components into the surrounding environment and to

minimize their release into the headspace above the reaction mixture. The reaction mixture was incubated in a thermostatic water bath at 25 °C for 6 minutes. Subsequently, the absorbance at 475 nm was registered, as this wavelength allows the identification of dopachrome. The absorbance corresponding to 100% of tyrosinase activity was measured by replacing the EO/EO mixture solution with 10 µL of pure DMSO. Blank solutions were prepared as follows: 2 ml of sodium phosphate buffer solution, 10 µL of EO/ EO mixture/kojic acid/DMSO solution, and 1 ml of tyrosine solution 0.1 mg/ml. The percentage of tyrosinase inhibition was measured according to the equation below:

% Inhibition= ΔA (Control)- ΔA (Sample) / ΔA (Control) ×100
ΔA (Control) or (Sample)= A_{475} (Control) or (Sample)- A_{475} (Control Blank) or (Sample Blank)

Vehicle formulation

The EOs mixture was incorporated into two different dermatological vehicles, an o/w emulsion and an oily solution (almond oil) in both cases at a concentration (w/w) of 5%. The o/w emulsion consisted of (w/w %): deionized water (84.6 %), glycerine (4.6 %), PEG 400 (0.6 %), disodium EDTA (0.1 %), carbomer 341 (0.4%), mineral oil (3.6%), cetyl alcohol (0.2 %), triethylamine (0.3 %), dimethicone (0.5 %), methyl paraben (0.2 %), EOs mixture (5 %). All the components of the formulation were purchased from Merck, Darmstadt, Germany.

In vitro release studies

Dialysis tubing Membra cell ™cellulose (Spectrapore, cut-off = 14000 Da) was employed for the *in vitro* release studies. A static Franz cell diffusion system with a 6 mL volume receiving chamber and a surface area of 2.54 cm^2 was used. The receiving phase consisted of a 50 mM phosphate buffer solution (pH 5.5) containing sodium dodecyl sulphate (SDS) 0.1 % as solubilising agents to allow for achieving sink conditions. The vehicle was dispensed by means of transferpette; the exact amount of vehicle delivered was evaluated by weighting the transferpette tip when loaded with the vehicle and after it had been delivered onto the skin. The average amount of vehicle applied was 12 ± 1.6 mg. The *in vitro* release test temperature was set at 32± 0.5°C to reflect the usual skin temperature. The test lasted 24 hours; at specific sampling intervals (i.e., 0.5h, 1h, 2h, 4h, 8h, 24h) 6 mL of the receptor phase were withdrawn, replaced with a fresh new solution, and analysed to determine the concentration of each marker. At the end of the test, the cell was disassembled and the membrane was properly analysed to measure the residual amount of the selected markers remaining in the vehicle.

In vitro permeation studies

Pig ear skin was employed for the *in vitro* permeation tests. The pig ears were purchased from a local slaughterhouse within few hours post-mortem. No ethical approval from the animal committee was required as the animals were not slaughtered for the purpose of the study. The ears were first washed with water, then any visible hair was trimmed with scissors, and finally, a full-thickness layer 1 mm thick was sliced from the dorsal ear side by using a dermatome. The samples were stored in aluminum foil at -20 °C. Barrier integrity was measured before each experiment. The same static Franz diffusion cell system and the same receiving phase differing only in pH (i.e., 7.4 in the case of *in vitro* permeation studies) as those described for the *in vitro* release studies were adopted. The skin sample was placed in between the donor and receiving chamber, with the stratum corneum facing the donor chamber. The receptor chamber was set at 37.0 °C ± 0.5 °C, which ensured that the skin surface temperature was at 32.0 °C ± 1 °C. The vehicle containing the formulation was applied in a finite dose regimen to mimic the expected in-use conditions. The average amount of vehicle applied

was 12 ± 3.2 mg to remain under finite dose conditions (i.e., below 10 mg/ cm^2[7]) considering the surface area of the employed static Franz cell (i.e., 2.54 cm^2). The vehicle was applied with the same procedure as that described for the *in vitro* release test. The skin sample was exposed to the vehicle for 27 hours. At specific sampling intervals (i.e., 1h, 2h, 4h, 8h, 24h and 27h) 6 mL of the receptor phase were withdrawn, replaced with a fresh new solution and analysed to determine the concentration of each marker. The *in vitro* permeation tests were performed under both semi-occluded and non-occluded conditions. Under semi-occluded conditions, the skin surface area was covered by a foil disk. At the end of the exposure time, the skin sample was taken out from the system; the residual vehicle was isolated by a gentle mechanical removal using absorbent paper. To isolate the *stratum corneum* from the viable epidermis and dermis, adhesive tape (Scotch Book Tape, 3 M) was pressed onto the skin sample and then firmly torn off. The procedure was repeated 20 times, each time with a new piece of adhesive tape. The tape samples as well as the residual epidermis and dermis, were analysed to define both the localisation and the concentration of the investigated marker compounds within the skin, as required by the aims of the study.

The downstream analytical platform for *in vitro* release and permeation studies

At the end of the permeation and release tests, the amounts of citronellal, geranial, β-myrcene, and neral were determined in all the system compartments, including the receiving phase (both release and permeation tests), the *stratum corneum*, the viable epidermis + dermis (*in vitro* permeation studies), membrane (*in vitro* release studies). The quantitative analysis was performed employing an analytical protocol based on HS-SPME online combined with fast GC-MS analysis. GC-MS instrument and analysis conditions were identical to those previously reported.

HS-SPME conditions were the following*:* Divinylbenzene/carboxen/polydimethylsiloxane (DVB/CAR/PDMS) 50/30 µm (2 cm length) fibers were employed for the experiments. The fibers were purchased from Merck KGaA, Darmstadt, Germany, and conditioned following the manufacturer's instructions. Three fibers were tested by analysing a set of standard solutions at different concentrations of the target compounds in the receiving phase. ANOVA was carried out to confirm the homogeneity of fiber performance and to discard those with different sampling behaviour. The consistency of fiber performance was checked every 50 analyses using an in-fiber external standardization approach and a standard mixture of hydrocarbons (C9-C25) in cyclohexane (1 µL of a 0.1 mg mL-1 solution) [8,9]. Sampling conditions: temperature 35°C, time 30 minutes, vial volume 20 mL.

Receiving phase: For each sampling time, 1.8 mL of the collected receptor fluid were spiked with 3.0 µL of 1.0 mg/mL tridecane (C_{13}) solution in acetone and finally sampled by HS-SPME for 30 minutes at 35 °C. After the sampling, the fiber was withdrawn, and the SPME device moved to the GC-MS system for analysis. GC desorption lasted 10 minutes to minimise carry-over. Suitable calibration levels in the range 5.0 – 0.01 mg/mL were prepared in 50 mM phosphate buffer solution (pH 5.5 and 7.4) containing sodium dodecyl sulphate (SDS) 0.1 % and 1.8 mL of each calibration level were sampled in triplicates by HS-SPME online combined to GC-MS analysis following the procedure described above. GC-MS conditions were identical to those previously reported.

Stratum corneum, viable epidermis + dermis, (in vitro permeation studies) membrane (in vitro release studies): The investigated markers were extracted from the listed matrices by HS-SPME under the MHE method and subsequently analysed by GC-MS analysis. The HS-SPME sampling parameters were the same as those employed for the receiving phase. For the quantitative evaluation of MHE experiments, simple vapour standards (10 to 0.01 µg) were prepared in the vial using the total vaporization technique and were extracted by HS-SPME under the MHE and subsequently analysed by GC-MS analysis.

3.10.2.4 Results and discussion

Tyrosinase inhibitory activity of the essential oils mixture

Both *Litsea cubeba* and *Pinus mugo* EOs proved promising *in vitro* tyrosinase inhibitory activities. When tested at a concentration of 166.7 µg/mL, the observed inhibitory activities were 59 ± 6 and 40 ± 3, respectively. As regards *L. cubeba* EO, it contains three bioactive constituents, namely *cis* and *trans*-3,7-dimethyl-2-6-octadienal (i.e., neral and geranial) and β-myrcene. Neral and geranial are the EO most abundant constituents, and they are responsible for the majority of its bioactivity. β-Myrcene contributes as well to the EO tyrosinase inhibitory potential despite being present only at trace levels in the EO as it proved a ten times more potent inhibitory activity compared to neral and geranial [2]. *Pinus mugo* EO is among the available EOs with the highest level of β-myrcene (i.e., 12 %), which explains its interesting inhibitory activity. In light of this fact, a mixture containing 45% of *L. cubeba* EO, 45 % of *P. mugo* EO, and 10 % *C. winterianus* EO was formulated and tested in terms of tyrosinase inhibitory activity. *C. winterianus* EO was included in the mixture in reason of its high content in citronellal, which proved to enhance neral and geranial activity [2]. When tested at the same concentration as that of the individual EOs, the mixture inhibited the enzyme activity to a similar extent (i.e., 48 ± 10), while the concentrations of *Litsea cubeba* and *Pinus mugo* EO were halved. In light of potential use as active ingredients in a dermatological formulation, the advantages of employing the formulated mixture instead of the individual EOs are the following. As regards *L. cubeba EO*, the benefit is related to the possibility of halving neral and geranial concentration while maintaining the same inhibitory activity and reducing the risk of developing contact dermatitis. As previously mentioned, citral is one of 26 fragrance materials identified as a suspected cause of allergic contact dermatitis by the European Commission's advisory committee, with a pretty high No Observed Effect Level (NOEL) of 1400 µg/cm^2 [10]. On the other hand, compared to *Pinus mugo EO,* the mixture is very likely to display improved sensory characteristics exploiting the pleasant scent of citral while preserving the same tyrosinase inhibitory activity.

Chemical characterization of the mixture of the essential oils

The qualitative chemical composition of the investigated EO mixture is reported in Table 1, along with the normalised relative percentage abundance of each constituent. The absolute quantitative analysis of β-myrcene, citronellal, neral, and geranial in the essential oil mixture was assessed. Table 2 reports the absolute amount of the investigated markers together with their physicochemical properties.

Table 1 Normalized percentage abundance of the compounds identified in the essential oil mixture under investigation

Compound	**I^t_s Lit.**	**I^t_s Exp. (MEGA-5 NB)**	**Relative % Abundance**
α-Thujene	931	922	0.10
α-Pinene	939	929	11.31
Camphene	953	940	0.51
Sabinene + β-Pinene	976-980	967	6.79
β-Myrcene	991	983	5.49
α-Phellandrene	1005	992	0.34
δ-3-Carene	1011	1000	8.37
α-Terpinene	1018	1005	0.21
p-Cimene	1026	1008	1.06
β-Phellandrene	1031	1016	5.53
Limonene	1031	1019	9.66
cis-Ocimene	1040	1028	0.10

Compound	I^t_s Lit.	I^t_s Exp. (MEGA-5 NB)	Relative % Abundance
trans-Ocimene	1050	1039	0.10
γ-Terpinene	1062	1047	0.14
α-Terpinolene	1088	1076	0.62
Linalool	1098	1084	0.77
Citronellal	1153	1131	4.77
4-Terpineol	1177	1157	0.17
α-Terpineol	1189	1168	0.35
Neral	1240	1212	13.90
trans-Geraniol	1255	1238	2.87
Geranial	1270	1244	16.18
Bornyl acetate	1285	1264	1.64
Citronellyl acetate	1354	1336	0.30
Geranyl acetate	1383	1362	0.53
β-Elemene	1391	1378	0.24
trans-β-Caryophyllene	1418	1401	2.98
α-Humuulene	1454	1435	0.24
Germacrene D	1480	1461	0.40
δ-Cadinene	1524	1503	0.30
Caryophyllene oxide	1583	1551	0.34

Table 2 Molecular formula, molecular weight and main physicochemical properties ($LogK_{ow}$, boiling point and vapour pressure) of the investigated bioactive compounds along with their absolute amount in the EO mixture

Compound	Molecular Weight*	$LogK_{ow}$*	Boiling Point (°C) 760mmHg*	Vapour pressure (mmHg) 25°C*	Water solubility 25 °C (mg/L)*	% w/w
β-Myrcene	136	4.17	156	2.40E+00	6.923	6.82 ± 0.78
Citronellal	154	3.83	205.07	2.54E-01	38.94	7.50 ± 0.45
Neral	152	3.45	217.44	9.13E-02	84.71	19.97 ± 0.64
Geranial	152	3.45	217.44	9.13E-02	84.71	21.71 ± 0.80

*EPI SuiteTM-Estimation Program Interface | US EPA, Downloaded Oct. 2021. (n.d.). https://www.epa.gov/tsca-screening-tools/epi-suitetm-estimation-program-interface (accessed February 2, 2022)

In vitro release studies

Monoterpenes' volatility represents probably the biggest challenge in using them as active ingredients in a topical or transdermal formulation, as it may lead to their significant evaporative loss before they are dermally absorbed. The fraction that is lost because of vaporisation depends on different factors, including, among others, the interaction of the active compound with the vehicle ingredients [11,12]. In the current study, *in vitro* release testing was performed on two dermatological vehicles, namely an oily solution (i.e., almond oil base) and O/W emulsion, to define the best vehicle that minimises the evaporative loss of the selected markers. The vehicle was applied under non-occluded conditions, and its amount was chosen to mimic the expected in-use conditions (12 ± 1.6 mg). **Figure 1** displays the *in vitro* kinetic release profiles of the investigated markers obtained applying Higuchian Model [13,14] (i.e., cumulative amount per unit surface area (μg/cm^2) plotted *versus* the square root of time, expressed as hour).**Table 3** and **Table 4** report the mass balance of the investigated markers, meaning the distribution of the different investigated markers in all the compartments of the system at the end of the *in vitro* release study (i.e., the amount

released in the receptor phase, the residual amount detected on the membrane and the percent evaporative loss, measured knowing the initial amount of each marker applied to the system and that recovered at the end of the experiments).

Among the investigated markers, β-myrcene and citronellal experienced the highest evaporative loss irrespective of the type of vehicle. In the case of the oily solution, their evaporative loss accounted for 99.91 ± 0.01 % and 90.19 ± 2.45%, respectively; the residual amount was recovered from the vehicle at the end of the release test, while only trace levels (i.e., below the LOQ) of the compounds were detected in the receptor phase irrespective of the sampling time. In the case of the O/W emulsion, β-myrcene and citronellal evaporative losses were slightly reduced, and respectively 1.17 ± 0.24 % and 18.75 ± 7.05 % of the applied doses were released in the receiving phase at the end of the test. Irrespective of the vehicle nature, neral, and geranial evaporative loss was less significant, as was expected from the compounds' lower vapour pressures. The markers' release rate was higher from the O/W emulsion compared to the oily solution, as proved by the steepest slopes of the linear proportion of their kinetic release profiles reported in **Figure 1**. The overall amount of neral and geranial released in the receiving phase was, on average, three times higher in the case of the O/W emulsion compared to the oily solution.

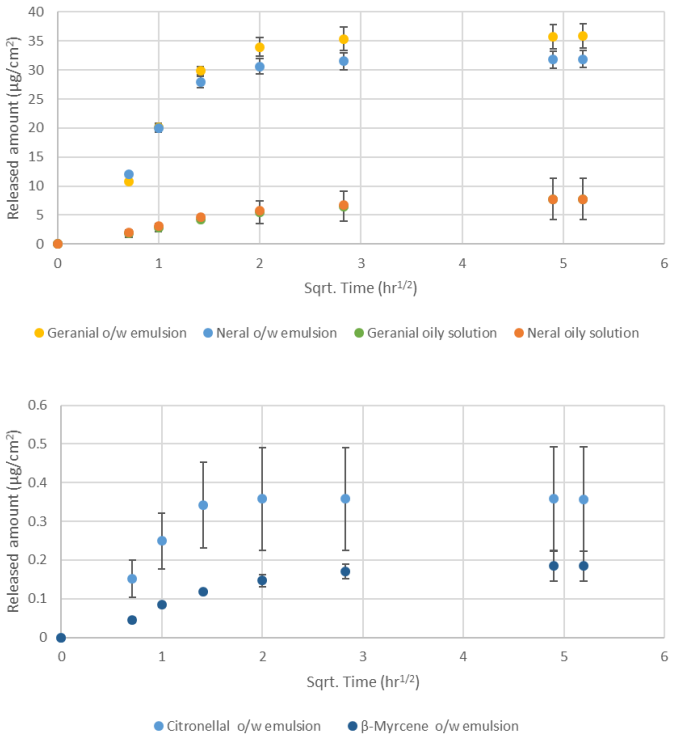

Figure 8 in vitro kinetic release profiles of the investigated markers obtained applying Higuchian Model

Table 3 ***o/w emulsion****: mass balance of the investigated markers (i.e., the amount released in the receptor phase, residual amount detected on the membrane, and the percent evaporative loss*

Compound	**Released amount (µg) (i.e. receiving phase)**	**Residual amount on the membrane (µg)**	**% Amount detected in the system**
b-Myrcene	0.479 ± 0.098	0.013 ± 0.004	1.203 ± 0.249
Citronellal	0.929 ± 0.349	0.690 ± 0.128	32.675 ± 4.469
Neral	82.605 ± 3.774	0.063 ± 0.002	76.691 ± 3.476
Geranial	93.170 ± 5.145	0.099 ± 0.006	71.604 ± 3.955

Table 4 ***oily solution****: mass balance of the investigated markers (i.e., the amount released in the receptor phase, residual amount detected on the membrane, and the percent evaporative loss*

Compound	Released amount (µg) (i.e. receiving phase)	Residual amount on the membrane (µg)	% Amount detected in the system
β-Myrcene	n.d	0.037 ± 0.003	0.090 ± 0.007
Citronellal	n.d	0.486 ± 0.122	9.805 ± 2.454
Neral	24.828 ± 6.199	1.051 ± 0.091	24.008 ± 5.836
Geranial	25.273 ± 7.259	1.214 ± 0.030	20.335 ± 5.595

In vitro permeation studies

Tyrosinase is contained within melanocytes which are dendritic cells located in the epidermis basal cell layer (i.e., the *stratum germinativum*). *In vitro* permeation studies were carried out to define the actual amount of the bioactive compounds (i.e., β-myrcene, citronellal, neral, and geranial) that could reach their biological target (i.e., tyrosinase) and unfold their inhibitory activity. The amount of the investigated markers that were considered potentially available to interact with the enzyme tyrosinase was that detected in the receiving phase (i.e., dermally absorbed) and that accumulated within the viable epidermis and the dermis. Therefore, *the stratum corneum* was removed from the sample at the end of the exposure time before quantitation of the compounds in the viable skin. To postulate whether this amount could be sufficient for an effective inhibitory activity, two types of data were considered: 1) literature data on kojic acid dermal absorption profile obtained under similar *in vitro* conditions; 2) the results obtained in our previous work in which β-myrcene and citral proved inhibitory activities respectively 10 and 100 times lower than that of kojic acid suggesting that for these compounds the bioavailable amount should be at least 10 and 100 times greater than that observed for kojic acid in order to expect a significant inhibitory activity.

According to a study reported in the European Scientific Committee on Consumer Safety opinion on kojic acid [15], the mean amount of kojic acid that penetrated over the entire exposure period of 24 hours was 0.142 ± 0.265 µg/cm². The *in vitro* percutaneous absorption of kojic acid was determined in human dermatomed skin by using a leave-on skin care formulation containing 1% of kojic acid applied in finite dose conditions. In the current study, a similar experimental setup was employed: *in vitro* permeation studies were performed applying a finite amount of vehicles under both non-occluded and semi-occluded conditions. Under semi-occluded conditions, the entire skin surface was covered with an aluminum foil without leaving any head space in between the skin sample and the cover. The system was defined as semi-occluded as it was not hermetically sealed, and an evaporative loss, albeit a reduced one compared to non-occluded condition, could still take place. The selected vehicle for the *in vitro* permeation test was the O/W emulsion which proved to minimise the markers' evaporative loss compared to the oily solution according to the *in vitro* release tests.

Under non-occluded conditions, the percutaneous absorption (i.e., the overall amount of the investigated markers that reached the receiving phase) of all the investigated markers was

negligible. In the receptor phase, the compounds were not detected, or they were only at trace levels (i.e., below LOQ) irrespective of the sampling time. A very small fraction of the applied dose was recovered from the viable skin (See **Table 5**), which was however considered too low to exert any inhibitory activity against tyrosinase. To exclude the possibility that the low dermal absorption was due to the barrier function of the stratum corneum, which was however very unlikely considering the physicochemical properties of the investigated markers, the amount of the investigated marker in the removed *stratum corneum* was investigated. The stratum corneum was free from the investigated markers with the only exception of β-myrcene whose abundance did not exceed 0.006 % of the applied dose, suggesting that the low dermal absorption was ascribed to significant evaporative loss.

Under semi-occluded conditions, the results were more promising. **Figure 2** displays the *in vitro* permeation kinetics of the monitored markers, while **Table 5** reports the absolute amount of each compound remaining in the viable skin and that dermally absorbed (i.e., the percent amount recovered in the receiving phase). For citronellal, neral, and geranial, 58.4%, 45.5%, and 48.3% of the applied dose were detected in the receiving phase, while 1.04, 0.67, and 0.72 %, respectively, were retained by the viable skin. The hydrocarbon β-myrcene was poorly dermally absorbed after 27 hours of exposure as only 0.43% of the applied dose was recovered from the receiving phase; however, its viable skin retention increased up to 2.12 % of the applied dose. The overall bioavailability (i.e., amount of the compound recovered from the receiving phase and the detected in the viable skin layers) of the investigated markers was considerably higher than that reported for kojic acid (i.e., 0.142 ± 0.265 µg/cm²), and it accounted to 0.4 ± 0.11 µg/ cm², 19.14 ± 4.37 and 25.54 ± 5.60 µg/ cm² for β-myrcene, neral, and geranial respectively. These results suggest that significant inhibition of tyrosinase may occur after the application of the investigated formulation under-semi occluded conditions, provided that the *in vitro* inhibitory activities observed for the investigated markers reflect *in vivo* conditions on human tyrosinase.

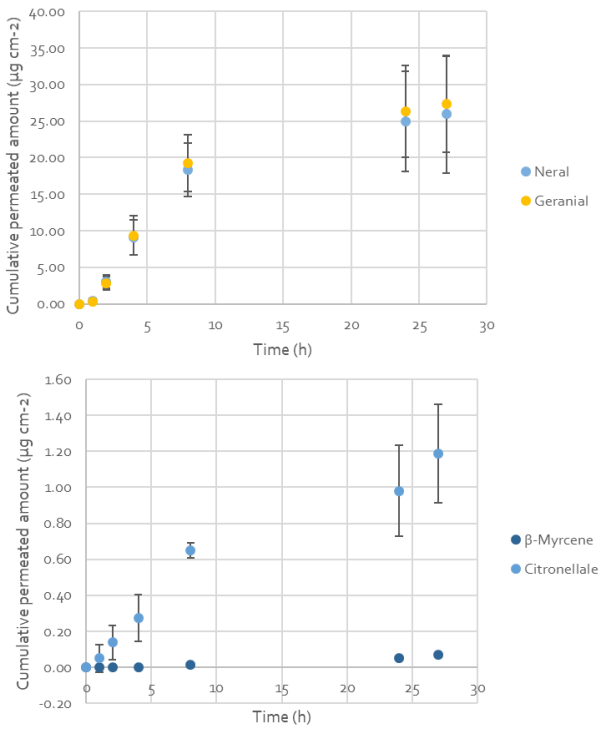

Figure 9 In vitro kinetic permeation profiles for the investigated markers following the application of the o/w emulsion under semi-occluded conditions. The permeation profiles were obtained by applying a zero-order kinetics (i.e., cumulative amount per unit surface area (µg/cm2) plotted versus time).

Table 5 Absolute amounts of each investigated compound remaining in the viable skin and dermally absorbed (i.e., amount detected in the receptor phase)

	Non-occluded condition		**Semi-occluded** condition	
Compound	Epidermis + Dermis (μg/cm²)	Dermally absorbed (μg/cm²)	Epidermis + Dermis (μg/cm²)	Dermally absorbed (μg/cm²)
β-Myrcene	0.029 ± 0.008	n.d.	0.334 ± 0.106	0.068 ± 0.003
Citronellal	0.024 ± 0.012	n.d.	0.399 ± 0.143	1.114 ± 0.202
Neral	0.022 ± 0.009	n.d.	0.280 ± 0.073	18.858 ± 4.292
Geranial	0.028 ± 0.011	n.d.	0.358 ± 0.094	24.177 ± 5.503

3.10.2.5 Conclusions

The aim of this study was to highlight the potential tyrosinase inhibitory activity of a mixture of three EOs, namely *Litsea cubeba*, *Pinus mugo*, and *Cymbopogon winterianus,* and to study the dermal absorption profile of the terpenoid derivatives responsible for the observed inhibitory activity (i.e., citral, β-Myrcene, and citronellal). The *in vitro* release rates of the investigated markers from two different vehicles were asses and the results proved that an oil/water emulsion should be preferred over an oily solution as it releases faster the active compounds and minimises their evaporative loss caused by the relatively high vapour pressures of the compounds under investigation. *In vitro* dermal absorption, studies proved that the investigated markers easily penetrate the *stratum corneum*; however, semi-occluded conditions are required to prevent evaporation from occurring faster than dermal absorption resulting in limited availability of the compounds in the viable skin even when an oil/water emulsion is employed as the vehicle.

To conclude, the results of this study suggest that significant inhibition of tyrosinase is likely to occur after the application of the investigated EOs mixture under-semi occluded conditions, provided that the *in vitro* inhibitory activities observed for the investigated markers reflect *in vivo* conditions on human tyrosinase.

3.10.2.6 References

[1] B. Desmedt, P. Courselle, J.O. De Beer, V. Rogiers, M. Grosber, E. Deconinck, K. De Paepe, Overview of skin whitening agents with an insight into the illegal cosmetic market in Europe, J. Eur. Acad. Dermatology Venereol. 30 (2016) 943–950. https://doi.org/10.1111/jdv.13595.

[2] F. Capetti, M. Tacchini, A. Marengo, C. Cagliero, C. Bicchi, P. Rubiolo, B. Sgorbini, Citral-Containing Essential Oils as Potential Tyrosinase Inhibitors: A Bio-Guided Fractionation Approach, Plants 2021, Vol. 10, Page 969. 10 (2021) 969. https://doi.org/10.3390/PLANTS10050969.

[3] R. Matsuura, H. Ukeda, M. Sawamura, Tyrosinase inhibitory activity of citrus essential oils, J. Agric. Food Chem. 54 (2006) 2309–2313. https://doi.org/10.1021/jf051682i.

[4] X.-W. Huang, Y.-C. Feng, Y. Huang, H.-L. Li, Potential cosmetic application of essential oil extracted from Litsea cubeba fruits from China, J. Essent. Oil Res. 25 (2013) 112–119. https://doi.org/10.1080/10412905.2012.755479.

[5] GC Calculators and Method Translation Software | Agilent, (n.d.). https://www.agilent.com/en/support/gas-chromatography/gccalculators (accessed January 29, 2022).

[6] NIST Chemistry WebBook, (n.d.). https://webbook.nist.gov/chemistry/ (accessed January 29, 2022).

[7] SCCS Scientific committee on Consumer Safety, the Sccs Notes of Guidance for the Testing of Cosmetic Ingredients and Their Safety Evaluation 10 Th Revision - Sccs/1602/18, 2018. https://ec.europa.eu/health/sites/health/files/scientific_committees/consumer_safety/docs/sccs_o_224.pdf.

[8] C. Bicchi, C. Cordero, E. Liberto, B. Sgorbini, P. Rubiolo, Reliability of fibres in solid-phase microextraction for routine analysis of the headspace of aromatic and medicinal plants, J. Chromatogr. A. 1152 (2007) 138–149. https://doi.org/10.1016/j.chroma.2007.02.011.
[9] Y. Wang, J. O'Reilly, Y. Chen, J. Pawliszyn, Equilibrium in-fibre standardisation technique for solid-phase microextraction, J. Chromatogr. A. 1072 (2005) 13–17. https://doi.org/10.1016/j.chroma.2004.12.084.
[10] J. Lalko, A.M. Api, Citral: Identifying a threshold for induction of dermal sensitization, Regul. Toxicol. Pharmacol. 52 (2008) 62–73. https://doi.org/10.1016/j.yrtph.2008.01.006.
[11] N.J. Hewitt, S. Grégoire, R. Cubberley, H. Duplan, J. Eilstein, C. Ellison, C. Lester, E. Fabian, J. Fernandez, C. Géniès, C. Jacques-Jamin, M. Klaric, H. Rothe, I. Sorrell, D. Lange, A. Schepky, Measurement of the penetration of 56 cosmetic relevant chemicals into and through human skin using a standardized protocol, J. Appl. Toxicol. 40 (2020) 403–415. https://doi.org/10.1002/jat.3913.
[12] R.N. Almeida, P. Costa, J. Pereira, E. Cassel, A.E. Rodrigues, Evaporation and Permeation of Fragrance Applied to the Skin, Ind. Eng. Chem. Res. 58 (2019) 9644–9650. https://doi.org/10.1021/acs.iecr.9b01004.
[13] A. Olejnik, J. Goscianska, I. Nowak, Active compounds release from semisolid dosage forms, J. Pharm. Sci. 101 (2012) 4032–4045. https://doi.org/10.1002/jps.23289.
[14] T. HIGUCHI, Rate of release of medicaments from ointment bases containing drugs in suspension., J. Pharm. Sci. 50 (1961) 874–5. https://doi.org/10.1002/jps.2600501018.
[15] K. Karin, Scientific Committee on Consumer Safety, opinion on kojic acid; Scientific Committee on Consumer Safety, opinion on kojic acid, (2012). https://doi.org/10.2772/8334.

Conclusions

As emerged from **Chapter 1**, fraud and counterfeiting is not uncommon among commercially available essential oils and their respective plant raw materials, putting at risk the safe use of those EOs with promising biological activities for humans. In chapter 1, the analytical strategies based on GC-MS analysis required to detect EO adulteration are presented, and their effectiveness is demonstrated. In addition, a relatively new sample preparation technique, namely "Vacuum-assisted Headspace Solid-Phase microextraction" has been explored for the fast characterisation of both the volatile and semivolatile fractions of plant raw materials bearing EOs. Vacuum proved to be a very promising parameter during HS-SPME samplings devoted to the quality assessment of essential oil plant raw materials, especially when diagnostic markers belong to the matrix semi-volatile fraction.

As regards the second line of research followed in this project, both the study of citral-containing essential oils as tyrosinase inhibitors and the screening of a larger number (i.e., 47 samples) of EOs as sources of skin whitening agents (**Chapter 2**) have identified β-myrcene as a new promising tyrosinase inhibitor in addition to those EOs constituents for which tyrosinase inhibitory activity had already been established (i.e., citral, cinnamaldehyde, eugenol, *trans*-anethole, thymol, and carvacrol). In the past, β-myrcene had been investigated as a potential tyrosinase inhibitor; however, it was then neglected as experimental data described it either as a negligible inhibitor or as an inactive compound. The results of this study proved quite the opposite, and β-Myrcene showed *in vitro* inhibitory activities not far from those of a well-known skin whitening agent: kojic acid. It is very likely that these differing results are ascribable to the investigated tyrosinase inhibitory activity. In literature data where no or negligible activity was observed, the β-myrcene effect on tyrosinase diphenolase activity only was assessed. In this thesis, the *in vitro* assay was optimised to detect both monophenolasic and diphenolosic inhibitors, suggesting thus that β-myrcene has a greater influence on tyrosinase monophenolasic activity. Limonene is another example of a terpenoid derivative for which, up to now, it was not clear whether it inhibits tyrosinase enzyme or not. This study confirmed no inhibitory activity for both limonene enantiomers. Finally, the study entitled "citral-containing essential oils as tyrosinase inhibitors" demonstrates once again the advantages of using mixtures of compounds/EOs rather than individual molecules as it suggests plausible additive and synergic effect of β-myrcene and citronellal on citral inhibitory activity, respectively. More in-depth studies based on a dose-response matrix design, should be performed to properly claim the synergistic and additive interaction in between citral and citronellal and in between citral and β-myrcene, respectively. In addition, to provide further evidence of the promising potentials of β-myrcene, citral and citronellal as agents to treat hyperpigmentation disorders, similar investigations should be performed on relevant cellular systems such as melanoma cell line, B16F10.

The *in vitro* dermal absorption studies of EO components released from topic formulations (**Chapter 3**) provided useful insights into the different behaviours (i.e., evaporative loss and dermal absorption profile) of EOs constituents when applied to the skin according to their physicochemical properties. Under finite dose and non-occlusive conditions, for those monoterpenoids presenting an alcoholic functional group (i.e., 4-terpineol and α-terpineol) that leads to relatively lower vapour pressure, skin penetration and dermal absorption still occur to quite a significant extent, despite evaporation. The latter observation is not true for monoterpene hydrocarbons, aldehydes, and ethers (i.e., β-myrcene, citral and citronellal, and 1,8-cineole), for which the evaporative loss rapidly depletes the formulation leaving a few to negligible amounts available for skin absorption under non-occlusive conditions. However, provided that evaporative loss is minimised, EOs components can easily

penetrate the skin barrier. Under semi-occluded conditions, the tyrosinase inhibitors citral and β-myrcene reach a bioavailability with the viable skin, which is likely to significantly reduce melanin formation provided that the *in vitro* inhibitory activities observed for the investigated markers reflect *in vivo* conditions on human tyrosinase. Future studies should focus on developing nanostructure delivery systems (i.e., polymeric, lipidic, or molecular complexes) that minimise the evaporative loss even under non-occlusive conditions, which are certainly more pleasant under practical usage.

Scientific Pubblications

F. Capetti, B. Sgorbini, C. Cagliero, M. Argenziano, R. Cavalli, L. Milano, C. Bicchi, P. Rubiolo, *Melaleuca alternifolia* Essential Oil: Evaluation of Skin Permeation and Distribution from Topical Formulations with a Solvent-Free Analytical Method, Planta Med. 86 (**2020**) 442–450. https://doi.org/10.1055/a-1115-4848.

F. Capetti, P. Rubiolo, C. Bicchi, A. Marengo, B. Sgorbini, C. Cagliero, Exploiting the versatility of vacuum-assisted headspace solid-phase microextraction in combination with the selectivity of ionic liquid-based GC stationary phases to discriminate *Boswellia* spp. resins through their volatile and semivolatile fractions, J. Sep. Sci. 43 (**2020**) 1879–1889. https://doi.org/10.1002/jssc.202000084.

F. Capetti, C. Cagliero, A. Marengo, C. Bicchi, P. Rubiolo, B. Sgorbini, Bio-guided fractionation driven by in vitro α-amylase inhibition assays of essential oils bearing specialized metabolites with potential hypoglycemic activity, Plants. 9 (**2020**) 1–17. https://doi.org/10.3390/plants9091242.

F. Capetti, M. Tacchini, A. Marengo, C. Cagliero, C. Bicchi, P. Rubiolo, B. Sgorbini, Citral-Containing Essential Oils as Potential Tyrosinase Inhibitors: A Bio-Guided Fractionation Approach, Plants. 10 (**2021**) 969. https://doi.org/10.3390/plants10050969.

K. Calvopiña, O. Malagón, **F. Capetti**, B. Sgorbini, V. Verdugo, G. Gilardoni, A New Sesquiterpene Essential Oil from the Native Andean Species Jungia rugosa Less (Asteraceae): Chemical Analysis, Enantiomeric Evaluation, and Cholinergic Activity, Plants. 10 (**2021**) 2102. https://doi.org/10.3390/plants10102102.

F. Capetti, A. Marengo, C. Cagliero, E. Liberto, C. Bicchi, P. Rubiolo, B. Sgorbini, Adulteration of Essential Oils: A Multitask Issue for Quality Control. Three Case Studies: *Lavandula angustifolia* Mill., *Citrus limon* (L.) Osbeck and *Melaleuca alternifolia* (Maiden & Betche) Cheel, Molecules. 26 (**2021**) 5610. https://doi.org/10.3390/molecules26185610.

G. Mastellone, A. Marengo, B. Sgorbini, F. Scaglia, **F. Capetti**, F. Gai, P.G. Peiretti, P. Rubiolo, C. Cagliero, Characterization and Biological Activity of Fiber-Type *Cannabis sativa* L. Aerial Parts at Different Growth Stages, Plants. 11 (**2022**) 419. https://doi.org/10.3390/plants11030419.

F. Capetti, P. Rubiolo, G. Mastellone, A. Marengo, B. Sgorbini, C. Cagliero, A sustainable approach for the reliable and simultaneous determination of terpenoids and cannabinoids in hemp inflorescences by vacuum assisted headspace solid-phase microextraction, Adv. Sample Prep. 2 (**2022**) 100014. https://doi.org/10.1016/j.sampre.2022.100014.

Oral contributions to congresses

F. Capetti, B. Sgorbini, C. Cagliero, S. Battaglino, M. Argenziano, R. Cavalli, C. Bicchi, P. Rubiolo. *In vitro* permeation kinetics, skin layers distribution and emission in the surrounding environment of biologically active *Melaleuca alternifolia* (Tea Tree) essential oil components from topic formulations. *50th International Symposium on Essential Oils, (ISEO) Vienna, Austria, September 9 - 11, 2019*

F. Capetti, C. Cagliero, A. Marengo, P. Rubiolo, C. Bicchi, B. Sgorbini. Composti volatili del metabolismo secondario vegetale: oli essenziali contenenti citrale come potenziali inibitori della tirosinasi. *115° Congresso della Società Botanica, online, September 9-11, 2020*

F. Capetti, C. Cagliero, A. Marengo, C. Bicchi, P. Rubiolo, B. Sgorbini. Oli essenziali contenenti citrale come potenziali inibitori della tirosinasi. *XXVIII Congresso Nazionale di Fitoterapia, May 21- 23, 2021*

F. Capetti, G. Mastellone, P. Rubiolo, C. Bicchi, A. Marengo, B. Sgorbini, E. Psillakis, C. Cagliero. Application of vacuum-assisted headspace solid phase microextraction to characterize the volatile and semi-volatile fractions of complex solid plant matrices. *XXIII INTERNATIONAL SYMPOSIUM ON ADVANCES IN EXTRACTION TECHNOLOGIES, Alicante, Spain, June 30- July 2, 2021*

Poster contribution to congresses

B. Sgorbini, **F. Capetti**, C. Cagliero, A. Marengo, S. Acquadro, C. Bicchi, P. Rubiolo. Essential oils and hypoglycemic activity: bio-guided fractionation approach looking for plant bioactive secondary metabolites with a-amylase inhibition capacity. *50th International Symposium on Essential Oils, (ISEO) Vienna, Austria, September 9 - 11,* ***2019***

B. Sgorbini, **F. Capetti**, C. Cagliero, A. Marengo, M. Argenziano, R. Cavalli, S. Acquadro, P. Rubiolo, C. Bicchi. *In vitro* permeation, skin-layers distribution and environmental emission of bioactive Tea Tree essential oil components from topic formulations. *67th International Congress and Annual Meeting of the Society for Medicinal Plant and Natural Product Research, Innsbruck, Austria, September 1-5,* ***2019***

B. Sgorbini, **F. Capetti**, C. Cagliero, A. Marengo, S. Acquadro, C. Bicchi, P. Rubiolo. Bio-guided fractionation of essential oils looking for plant bioactive secondary metabolites with potential hypoglycemic activity. *67th International Congress and Annual Meeting of the Society for Medicinal Plant and Natural Product Research, Innsbruck, Austria, September 1-5,* ***2019***

F. Capetti, C. Cagliero, A. Marengo, C. Bicchi, P. Rubiolo, B. Sgorbini.Plant Volatile secondary metabolites: citral containing essential oils as potential tyrosinase inhibitors. *PSE E-CONGRESS 2020 PLANT DERIVED NATURAL PRODUCTS AS PHARMACOLOGICAL AND NUTRACEUTICAL TOOLS September 15-18-22-25, October 6-9-13-16,* ***2020***

F. Capetti, C. Cagliero, A. Marengo, G. Mastellone, C. Bicchi, P. Rubiolo, B. Sgorbini. Essential oils bearing specialized metabolites with potential tyrosinase inhibitory. *69th International Congress and Annual Meeting of the Society for Medicinal Plant and Natural Product Research (GA). September 6-8,* ***2021***

B. Sgorbini, ***F. Capetti****, C. Cagliero, A. Marengo, G. Mastellone, C. Bicchi, P. Rubiolo. Citral Containing Essential Oils as Potential Tyrosinase Inhibitors: a bio-guided fractionation approach to investigate the additive and/or synergistic contribution of minor compounds. 69th International Congress and Annual Meeting of the Society for Medicinal Plant and Natural Product Research (GA). September 6-8,* ***2021***

F. Capetti, A. Corgiat-Mecio, C. Cagliero, A. Marengo, G. Mastellone, C. Bicchi, P. Rubiolo, B. Sgorbini. Essential oils bearing specialized metabolites with potential acetylcholinesterase inhibitory activity*. 16th Annual Congress of the Italian Botanical Society (VII International Plant Science Conference), Settembre, 8 – 10* ***2021***

F. Capetti, P. Rubiolo, G. Mastellone, A. Marengo, B. Sgorbini, C. Cagliero. Vacuum assisted headspace solid-phase microextraction for the simultaneous, reliable and sustainable characterization of the terpenoid and cannabinoid fractions of hemp inflorescences. *2nd European Sample Preparation e-Conference and the 1st Green and Sustainable Analytical Chemistry e-Conference, online event s March 14 – 16,* ***2022****.*